The role of the p38 MAP kinase substrate, MAPKAPK-2 in proinflammatory cytokine signalling

Thesis

UNRESTRICTED

The role of the p38 MAP kinase substrate, MAPKAPK-2 in proinflammatory cytokine signalling

Simon Lumb

A thesis submitted in partial fulfilment of the requirements of the Open University for the degree of Doctor of Philosophy

April 2000

Department of Lead Discovery
Celltech Chiroscience,
216, Bath Road , Slough, Berkshire, UK.

DATE OF SUBMISSION : 8 MAY 2000
DATE OF AWARD : 11 MARCH 2001

ProQuest LLC.
789 East Eisenhower Parkway
P.O. Box 1346
Ann Arbor, MI 48106 – 1346

Abstract

The pro-inflammatory cytokine IL-1 induces the synthesis of many genes during inflammation. The signalling mechanisms triggered by IL-1 include activation of several distinct parallel MAP kinase pathways. The p38 MAP kinase pathway is activated particularly strongly by this cytokine. MAPKAP kinase-2 (MAPKAPK-2) is one of several p38 substrates that are regulated by direct phosphorylation. Few MAPKAPK-2 substrates are known. One of these, the small heat shock protein 27 (Hsp27), is rapidly phosphorylated following MAPKAPK-2 activation. In an attempt to delineate the role of MAPKAPK-2 in IL-1 signalling, IL-1α induced MAPKAPK-2 activity was inhibited by stable overexpression of dominant negative (MAPKAPK-2 K93R) and MAPKAPK-2 anti-sense RNA (MAPKAPK-2 A/S) in HeLa cells. IL-1α strongly induced COX-2 protein in empty vector transfected cells. In contrast MAPKAPK-2 K93R and MAPKAPK-2 A/S overexpressing cells strongly inhibited COX-2 protein and mRNA. In addition IL-1α induced IL-6 synthesis was also strongly inhibited by MAPKAPK-2 A/S. These results suggest that MAPKAPK-2 may act as an effector molecule involved in IL-1α induced COX-2 and IL-6 synthesis. In an attempt to identify new MAPKAPK-2 substrates, yeast two-hybrid screening of a human leukocyte cDNA library identified a novel protein interaction between MAPKAPK-2 K93R and a close homologue of the human polyhomeotic 2 (HPH2) protein.

Acknowledgements

I would like to thank my supervisor at Celltech, Dr. Ray Owens, for his advice, ideas and encouragement for over what has seemed at times to be like an eternity. I would also like to thank my external supervisor Prof. Jerry Saklatvala at the Kennedy Institute for his advice and discussion.

As is usual with a project of this nature there are many people who I would like to thank for their technical advice and assistance. In particular, I am indebted to Jean Delgado for her help with the kinase assays, Dr. Andrew Clark for his help with the RPA assays, Steve 'Ski' (and soon to be doctor) Rapecki for help with the cytokine ELISAs.

Finally, I would like to thank Ines for her support and understanding and for not divorcing me when at times we have been like ships that didn't even pass in the night. I would also like to promise my two sons Richard and Marcos that I will spend less time in the lab looking at 'Daddy's cells' and more time at home.

Abbreviations

aa	amino acid
AP-1	activating protein-1
A/S	antisense
AREs	AUUUA repeat elements
ATF-1,-2	activating transcription factor –1,-2
ATP	adenosine 5' triphosphate
β-gal	β-galactosidase
BSA	bovine serum albumin
cAMP	cyclic adenosine 3',5' monophosphate
cDNA	complementary DNA
COX-1,-2	cyclooxygenase-1,-2
CREB	cAMP response element binding protein
CRE	cAMP response element
DNA	deoxyribonucleic acid
DMSO	dimethyl sulphoxide
DTT	dithiothreitol
DMEM	Dulbeccos Modified Eagles Medium
DMF	dimethyl formamide
dNTPs	deoxynucleotide triphosphates
ERK	extracellular regulated kinase
EGF	epidermal growth factor
ECL	enhanced chemiluminescence
EDTA	ethylenediaminetetra acetic acid
ELISA	enzyme linked immunosorbent assay
FCS	foetal calf serum
GM-CSF	granulocyte macrophage-colony stimulting factor
GST	glutathione S-transferase

GAL4 BD	GAL4 binding domain
GAL4 AD	GAL4 activation domain
GAPDH	glyceraldehyde-3-phophosphate dehydrogenase
HOG-1	high-osmolarity glycerol-1
Hsp27	heat shock protein 27
HRP	horseradish peroxidase
IL-1,-2,-6,-8	interleukin-1,-2,-6,-8
IFN	interferon
ICAM-1	intercellular adhesion molecule-1
IL-1Ra	interleukin-1 receptor antagonist
IL-1RI,-II	interleukin-1 receptor I,-II
iNOS	inducible nitric oxide synthase
ICE	interleukin-1 converting enzyme
IPTG	isopropyl-β-D thiogalactoside
IRAK	IL-1 receptor-associated kinase
IκB	inhibitory subunit of NF-κB
IKK	IκB kinase
kDa	kilo Dalton
LSP-1	lymphocyte-specific protein-1
LPS	lipopolysaccharide
JNK	jun N-terminal kinase
MCP-1	myocyte chemoattractant protein-1
MAPK	mitogen activated protein kinase
MAPKK	mitogen activated protein kinase kinase
MAPKKK	mitogen activated protein kinase kinase kinase
MAPKAPK-1,-2,-3	mitogen activated protein kinase activated protein kinase-1,-2,-3
μCi	micro Curie
MKK	MAPK kinase
MLK	mixed lineage kinase
MEF2	myocyte-enhancer factor 2

MNK	MAP kinase signal-integrating kinase
MSK1	mitogen-and stress activated protein kinase 1
MMPs	matrix metalloproteinases
mRNA	messenger RNA
NIK	NF-κB-inducing kinase
NSAIDs	non-steroidal anti-inflammatory drugs
NGF	nerve growth factor
NF-κB	nuclear factor-κB
PCR	polymerase chain reaction
PDGF	platelet derived growth factor
PLA_2	phospholipase A_2
PGE_2	prostaglandin E_2
PAK	p21-activated kinase
PRAK	p38-regulated/activated kinase
PBS	phosphate buffered saline
PAGE	polyacrylamide gel electrophoresis
RIP	receptor interacting protein
RPA	ribonuclease protection assay
RNA	ribonucleic acid
SAPKs	stress activated protein kinases
SDS	sodium dodecyl sulphate
SD	synthetic dropout
TNF	tumour necrosis factor
TACE	TNFα converting enzyme
TCF	ternary complex factor
TNFRI,-II	tumour necrosis factor receptor I,-II
TCF	ternary complex factor
TAK1	TGFβ activated kinase
TAE	Tris-acetate EDTA
TE	Tris-EDTA
TMB	3,3',5,5'-tetramethylbenzidine

TRADD	TNF receptor associated death domain
TRAF	TNF receptor associated factor
UV	ultra-violet
UAS	upstream activating sequences
3'-UTR	3'-untranslated region
VCAM-1	vascular cell adhesion molecule-1

Contents

List of Figures

List of Tables

Chapter 1

Introduction

1.1 General Introduction

Following injury, trauma or infection of a tissue, the host organism initiates a complex series of reactions in an effort to prevent ongoing tissue damage, to isolate and destroy the infective agent and to activate the repair processes that are necessary to return the organism to normal function. This cumulative homeostatic process is known as inflammation. The characteristics of the inflammatory response are that the area is reddened, swollen, hot and painful and that there is loss of function. The redness and heat are due to vasodilation and increased blood flow. The swelling is due to increased vascular permeability with leakage of fluid into the tissue and accumulation of inflammatory cells. The pain is due to stimulation of afferent nerves by chemical mediators and also the pressure from increased tension. The restriction of movement in an inflamed joint or the narrowing of the airways with resulting breathing difficulties are examples of loss of function.

1.1.1 Initiation of the inflammatory response

The macroscopic inflammatory effects described above, are the result of an early and immediate set of reactions at the site of infection or trauma, which lead to the release of soluble mediators, including cytokines, that mobilise the metabolic response of the whole organism. The cells responsible for initiating the inflammatory and acute phase response are activated monocytes or tissue macrophages (reviewed by Baumann and Gauldie, 1994), which release the primary pro-inflammatory cytokines, interleukin-1

(IL-1) and tumour necrosis factor (TNF). These pro-inflammatory cytokines are released in response to stimuli which may be exogenous such as, bacterial endotoxin (LPS) and other bacterial products or mixtures of cytokines such as IL-2, IL-1, TNF, interferon-γ and granulocyte-monocyte colony stimulating factor (reviewed by Dinarello, 1994). Both IL-1 and TNF have pleiotropic activity and may act individually or synergistically to trigger both local and systemic inflammatory processes. Locally, IL-1 and TNF act upon many cell types, such as epithelial cells and fibroblasts, which are stimulated to further produce IL-1 and TNF. These cell types are also responsible for the production of secondary pro-inflammatory cytokines, such as IL-6 and IL-8 and monocyte chemoattractant protein -1 (MCP-1). IL-6 regulates most of the acute phase plasma proteins from hepatocytes (reviewed by Baumann and Gauldie, 1994), whilst IL-8 and MCP-1 are highly chemotactic for neutrophils and mononuclear cells respectively (reviewed by Matsushima and Oppenheim, 1989) see Figure 1.1.

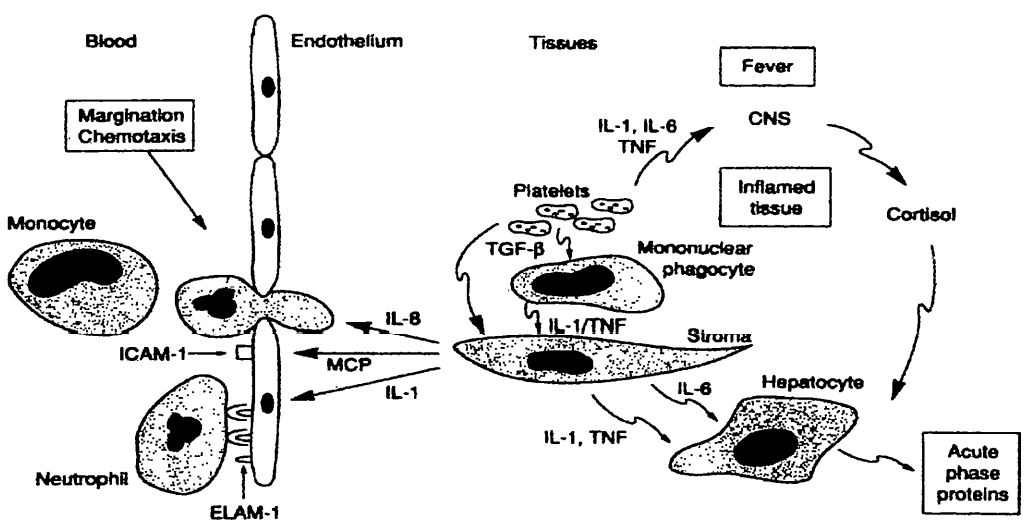

Figure 1.1. Diagram illustrating cell and cytokine interactions in the inflammatory response (reviewed by Baumann and Gauldie, 1994).

Interleukin-1 and TNF have a similar, broad range of physiological effects and provide crucial signals by which activated mononuclear phagocytes control functions of other cells. The most notable biological difference between them is that TNF has cytotoxic properties whereas IL-1 does not.

The activated endothelium plays a critical role in the communication between the site of inflammation and circulating leukocytes. Leukocytes can be selectively attracted to the inflammatory site to defend the host against invading pathogens or remove cellular debris. Stimulation by IL-1 and TNF induces the surface expression of adhesion molecules such, as intercellular adhesion molecule-1 (ICAM-1), endothelial leukocyte adhesion molecule -1 (ELAM-1), E-selectin and P-selectin.

Neutrophils appear early in the course of inflammation and are removed from the circulation by attaching to surface adhesion molecules. At first they interact weakly through L-selectin binding to carbohydrates on endothelial glycoprotein receptors. Following further stimulation by chemokines the neutrophils adhere tightly through integrin and endothelial adhesion molecule interactions (reviewed by Proost *et al.*, 1996). Finally the cells migrate through the endothelial layer in response to a chemokine gradient and infiltrate the tissues by a process known as diapedesis. Neutrophil infiltration is usually followed by an influx of macrophages and together these cells release a wide range of pro-inflammatory substances including proteases, low molecular-weight reactive oxygen species and lipid mediators as well as IL-1 and TNF. These low molecular weight mediators, prostaglandins, leukotrienes and thromboxanes, are the products of arachidonic acid metabolism by 5-lipoxygenase and cyclooxygenase enzymes.

1.1.2 Cyclooxygenase enzymes and prostaglandin synthesis

As indicated above cyclooxygenase enzymes are responsible for the production of highly potent pro-inflammatory intermediates that prolong the actions of IL-1/TNF long after activation. Two cyclooxygenases, COX-1 and COX-2, also known as prostaglandin synthases (PGHS) 1 and 2 have been identified in humans. The enzymes, which are encoded by separate genes on different chromosomes, share 60% amino acid homology (DeWitt and Smith, 1988; Xie *et al.*, 1991; Kujubu *et al.*, 1991). Both are haem-containing, 66 kDa homodimers that are heavily glycosylated, which results in the proteins migrating with an apparent molecular mass of 72 kDa (Sirois and Richards, 1992). Although structurally COX-1 and COX-2 are very similar, the crystal structures are virtually superimposable and the active sites differ by only a single amino acid (COX-2 V509/ COX-1 I509), the enzymes differ substantially in their patterns of expression and biology. COX-1 is constitutively expressed in most tissues and appears to be responsible for the production of prostaglandins that mediate normal physiological functions such as renal and vascular homeostasis (reviewed by Smith *et al.*, 1996; reviewed by Smith and DeWitt, 1995). The regulation of COX-1 expression is poorly understood. However, like most other developmentally regulated housekeeping genes COX-1 lacks a TATA box, which is a characteristic feature of most inducible genes (Kraemer *et al.*, 1992). In contrast to COX-1, COX-2 is not detectable in most mammalian tissues, but its expression can be induced rapidly (2-6 hr) by pro-inflammatory cytokines (Maier *et al.*, 1990), tumour promoters (Kujubu *et al.*, 1991), growth factors (Habenicht *et al.*, 1985) and oncogenes (Han *et al.*, 1990). The rapid induction of COX-2 mRNA, which can be

superinduced by cycloheximide, mirrors the induction of immediate early genes such, as *c-fos* and has therefore resulted in COX-2 being classified as such.

Cyclooxygenases are bifunctional enzymes that catalyse the rate limiting step in prostaglandin synthesis. This reaction occurs in two stages; in the first, arachidonate is released from cellular membrane phospholipids by the action of phospholipase A_2 and converted by the cyclooxygenase activity to prostaglandin G_2 (PGG_2); secondly, PGG_2 is reduced by the peroxidase activity of the enzyme to prostaglandin H_2 (PGH_2) (see Figure 1.2). Once activated the levels of COX-2 protein within the cell remain elevated for several hours and large amounts of prostaglandins are synthesized, in particular PGE_2. In fact, many of the biological effects of IL-1 are due to increased PGE_2, which can increase vasodilation resulting in leakage from the blood vessels, particularly at the post-capillary venules, resulting in swelling and in some cases redness. In addition prostaglandins can act synergistically with IL-1 to enhance the transcription of secondary pro-inflammatory cytokines such as IL-8, IL-6 and also IL-1 itself (Vannier and Dinarello, 1993; Vannier and Dinarello, 1994).

Ten chemical classes of prostaglandins have been recognised (PGA to PGJ) of which PGH_2 acts as a common precursor. Different cell types produce different prostaglandins and the conversion of PGH_2 to the end product is dependent upon which specific synthase is present in the cell. PGE_2 is produced mainly by macrophages, fibroblasts, monocytes and chondrocytes whilst, PGD_2 and PGI_2 (prostacyclin) are produced mainly by mast cells and endothelial cells respectively (reviewed by DeWitt and Smith, 1995).

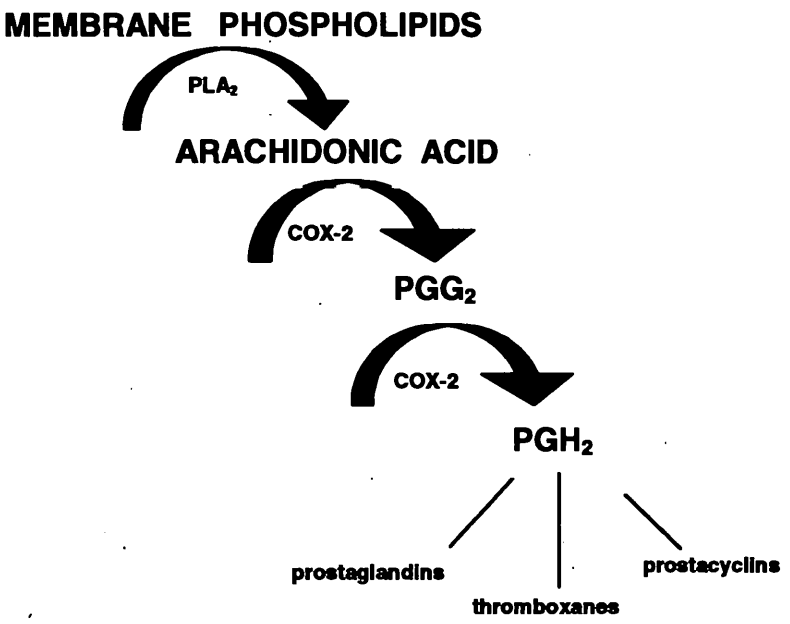

Figure 1.2: Diagram illustrating the bifunctional enzymatic properties of COX-2.

The role of COX-2 in inflammation and pain has been demonstrated and COX-2 is now regarded as an important therapeutic target (Seibert *et al.*, 1994). Elevated prostaglandin levels have been linked to chronic and acute inflammatory disease (reviewed by Smith and DeWitt, 1996; Lipsky and Isakson, 1997) and colon cancer (reviewed by Marnett, 1992; Rao *et al.*, 1995). The importance of inhibiting COX-2 for anticancer therapy has been supported following a recent study, which demonstrated that selective inhibition of COX-2 caused nearly complete suppression of azoxymethane-induced colon cancer (Kawamori *et al.*, 1998).

1.1.3 Inhibitors of cyclooxygenase enzymes

Cyclooxygenases are the main therapeutic target for non-steroidal anti-inflammatory drugs (NSAIDs) (reviewed by Smith *et al.*, 1994). The most notable of these, being

acetylsalicylic acid (aspirin), which permanently inactivates COX-1 by acetylating serine 530 at the cyclooxygenase active site (Loll *et al.*, 1995). The unique long-lived effect of aspirin on platelet thromboxane A_2 formation, is a combined result of the covalent modification of COX-1 within these cells and that circulating platelets, unlike other cells, do not synthesize new COX-1. Other NSAIDs include ibuprofen, indomethacin, flurbiprofen and meclofenamate, which behave as competitive reversible inhibitors of arachidonate (Laneuville *et al.*, 1994; reviewed by Smith and DeWitt, 1996).

Until recently all available NSAIDs inhibited both COX-1 and COX-2 by competing with arachidonate for binding to the cyclooxygenase active site. However, although these compounds are effective anti-inflammatory agents they have the particular disadvantage of gastrointestinal toxicity, caused by the inhibition of cytoprotective prostaglandins in the stomach and gut. The discovery that COX-2 is the relevant enzyme in inflammation (Seibert *et al.*, 1994) and that COX-1 and not COX-2 is present in the stomach (Isakson P *et al.*, 1995) has led to the development of COX-2 specific inhibitors such as celecoxib (SC58635) and MK966 (L745337), which are active in animal models of inflammatory disease (Reitz *et al.*, 1995; Penning *et al.*, 1997). Recently, a novel class of pyridinyl imidazole compounds have been shown to inhibit PGE_2 production in IL-1 stimulated human fibroblasts (Ridley *et al.*, 1997), in LPS stimulated monocytes (Pouliot *et al.*, 1997) and in IL-1 stimulated mesanglial cells (Guan *et al.*, 1997). Prostaglandin E_2 production in these studies has been shown to be due to decreased COX-2 synthesis and not inhibition of COX-2 activity. The biological target of these compounds is p38 MAP kinase an enzyme that is strongly activated by pro-inflammatory cytokines (Freshney *et al.*, 1994; Raingeaud *et al.*,

1995). The mechanism of p38 MAPK activation, inhibition and the role of p38 MAPK in the regulation of COX-2 synthesis are discussed in later sections.

1.1.4 Interleukin -1 and tumour necrosis factor in disease states

As discussed in section 1.1.1, IL-1 and TNF play a key role in both the initiation and the progression of the inflammatory response. However, in some cases the inflammatory response occurs in an uncontrolled manner, resulting in the overproduction of either IL-1 or TNF. Consequently, much attention has been focused on these cytokines because of their critical role in the pathogenesis of inflammatory diseases. Both are implicated in acute and chronic inflammatory diseases, such as rheumatoid arthritis, osteoarthritis, inflammatory bowel disease and toxic shock syndrome and many of the pathological features observed in these disease states can be reproduced by infusion of IL-1 and TNF (reviewed by Dinarello, 1996). In humans IL-1 and TNF added intravenously mimic the systemic inflammatory symptoms of septic shock (Smith *et al.*, 1992) and in rabbits the symptoms can be potentiated by co-infusion of both cytokines (Okusawa *et al.*, 1988; Tredget *et al.*, 1988). Infusion of IL-1 and TNF into joint space produces cellular and destructive changes indicative of acute arthritis, whilst elevated levels of both cytokines have been detected in the joint fluids in patients with rheumatoid arthritis (Miyasaka *et al.*, 1988). Limiting or reducing the production of these cytokines has provided further evidence for IL-1 and TNF in such disease states. Antibodies to TNF have been given with success to patients with rheumatoid arthritis (Elliott *et al.*, 1994; Elliott and Maini, 1995) and Crohns disease (van Dullemen *et al.*, 1995). Whilst naturally occurring specific inhibitors of IL-1 such as the interleukin-1 receptor antagonist (IL-1Ra) have demonstrated therapeutic efficacy in clinical trials with patients with rheumatoid

arthritis (Breshihan *et al.*, 1996). Recently, inhibitors of p38 MAP kinase an enzyme that is involved in pro-inflammatory cytokine synthesis and signalling (Freshney *et al.*, 1994; Lee *et al.*, 1994) have, in animal models, demonstrated therapeutic benefit in some of the conditions described above (Badger *et al.*, 1996).

1.2 Interleukin-1 and Tumour Necrosis Factor

1.2.1 Interleukin-1 family

The IL-1 gene family is composed of three members: IL-1α, IL-1β (March *et al.*, 1985) and the IL-1 receptor antagonist (IL-1Ra) (Eisenberg *et al.*, 1990; Carter *et al.*, 1990). The biological effects of IL-1 are mediated by IL-1α and IL-1β whilst the IL-1Ra acts as true antagonist of IL-1α and IL-1β. IL-1α and IL-1β are first translated as 31 kDa pro-forms (proIL-1α/β) that lack leader sequences. Unlike proIL-1β, proIL-1α is biologically active and a percentage of this (10-15%) is myristoylated on specific lysine residues within the pro-piece and transported to the cell membrane where it is referred to as membrane IL-1. ProIL-1β is also myristoylated, but is not transported to the membrane (Stevenson *et al.*, 1993).

ProIL-1α is proteolytically cleaved to produce mature IL-1α (17 kDa) and a 16 kDa pro-piece, by activation of a calcium-dependent, membrane- associated cysteine protease called calpain (Kobayashi *et al.*, 1990). ProIL-1β is cleaved by the interleukin-1 converting enzyme (ICE) to produce mature, biologically active IL-1β (17 kDa) and a 16 kDa pro-piece (Thornberry *et al.*, 1992; Cerretti *et al.*, 1992). Mature IL-1β is transported out of the cell through a putative membrane channel,

whilst mature IL-1α remains cytosolic and is not found in the circulation except in severe disease states, in which it may be released from dying cells or by proteolytic cleavage by calpains (Watanabe and Kobayashi, 1994). The exact role of IL-1α is unclear although evidence suggests that it may function as an autocrine intracellular messenger since IL-1α and IL-1 receptor complexes have been identified inside the nucleus with a resulting increase in signal transduction (Curtis *et al.*, 1990).

The third member of the IL-1 family is the IL-1 receptor antagonist (IL-1Ra). Two forms of the IL-1Ra exist, secreted IL-1RA (sIL-1Ra) and intracellular IL-1Ra (icIL-1Ra) which are transcribed from alternate promoters (Haskill *et al.*, 1991; Muzio *et al.*, 1995). After stimulation by bacterial endotoxin, monocytes initially express pro(s)IL-1Ra from the sIL-1Ra promoter, which is translated in the endoplasmic reticulum and transported to the Golgi. After removal of the leader sequence, sIL-1Ra is secreted from the cell. After 24 hours the cell switches to the icIL-1Ra promoter and icIL-1Ra becomes the major transcript, which lacks a leader sequence and remains intracellular (Andersson *et al.*, 1992).

1.2.2 Interleukin-1 receptor family

The IL-1 receptor family consists of two principal members: IL-1RI (Sims *et al.*, 1989) and IL-1RII (McMahan *et al.*, 1991). Evidence suggests that IL-1RI binds IL-1α with a higher affinity whereas IL-1RII binds IL-1β with higher affinity (Scapigliati *et al.*, 1989). IL-1RI is a heavily glycosylated 80 kDa protein, constitutively expressed at low levels and expressed on most cell types. IL-1RII (68 kDa) is also heavily glycosylated and is expressed primarily on neutrophils, monocytes and B-lymphocytes. Both receptors have three extracellular Ig-like domains that are 26-28%

homologous and they both contain a single transmembrane domain. However, the cytoplasmic domains of each receptor are very different. IL-1Rl has a cytosolic domain of 213 amino acids, whilst that of IL-1Rll is only 29 amino acids (Sims *et al.*, 1989; McMahan *et al.*, 1991). It is therefore not surprising that most of the biological effects of IL-1 are mediated by IL-1Rl, with IL-1Rll acting as a decoy receptor, which sequesters and binds IL-1β tightly thus preventing it binding and signalling through IL-1Rl (Colotta *et al.*, 1993).

The cytosolic domain of IL-1Rl shares 45% homology with the cytosolic domain of the *Drosophila* protein Toll (Gay and Keith, 1991). Recently, Toll has been identified in a signalling pathway that is critical for anti-microbial peptide production in adult flies (Lemaitre *et al.*, 1996). Like Toll, the other components of this pathway share significant homology with their mammalian counterparts in the IL-1 signalling pathway, therefore implying that this signalling system is conserved between insects and mammals (reviewed by O'Neill and Greene, 1998).

1.2.3 IL-1 signalling

For IL-1RI to signal it must form a complex with the IL-1 receptor accessory protein (IL-1AcP) (Greenfeder *et al.*, 1995). The IL-1AcP is essential for signalling since cells lacking this protein do not respond to IL-1 (Wesche *et al.*, 1997b). Binding of IL-1 to the IL-1RI receptor induces heterodimerization with IL-1AcP resulting in a change from low to high affinity binding of IL-1, which may be the result of a conformational change within the complex (Greenfeder *et al.*, 1995). IL-1AcP then recruits MyD88, an adapter protein that functions to mediate interactions between the cytoplasmic domain of the receptor and a serine threonine kinase called, IL-1 receptor

associated kinase (IRAK) (Cao *et al.*, 1996a; Wesche *et al.*, 1997a). MyD88 contains an N-terminal death domain, related to those found within the cytoplasmic domains of TNFRSF members and a C-terminal Toll domain similar to that found in Toll/IL-1-like receptors. MyD88 coimmunoprecipitates with the IL-1RI complex in an IL-1 dependent manner (Burns *et al.*, 1998). IRAK has been shown to complex with the IL-1AcP, but not IL-1RI (Huang *et al.*, 1997; Volpe *et al.*, 1997). IRAK then dissociates from the complex and interacts with TRAF6 (Cao *et al.*, 1996b).

TRAF6 is a member of the TNF-receptor associated factors (TRAFs), but which paradoxically is not involved in TNF signalling. Members of this family of proteins are characterised by a conserved carboxyl-terminal TRAF-C domain of ~170 amino acids, a α-helical TRAF-N domain and with the exception of TRAF1, an amino terminal RING finger (Rothe *et al.*, 1994). Immunoprecipitation studies have demonstrated that TRAF6 does not associate with IL-1RI, but with IRAK, implying that IRAK recruits TRAF6. This interaction is entirely dependent upon stimulation with IL-1 (Cao *et al.*, 1996b). Cotransfection studies using dominant negative mutants of IRAK and TRAF6 have demonstrated that both are critical intermediates in the pathways leading to IL-1 induced NFκB and JNK/p38 MAP kinase activation (Cao *et al.*, 1996b; Baud *et al.*, 1999). In addition over-expression of TRAF6 (or TRAF2, see section 1.2.6) is sufficient to activate signalling pathways leading to NF-κB and AP-1 in the absence of extracellular stimuli (Cao *et al.*, 1996b). This latter observation may be explained by a recent study which has demonstrated using TRAF chimeras, that a critical event in TRAF-mediated IL-1 (TNF) signalling is ligand- induced TRAF oligomerisation (Baud *et al.*, 1999). In this study the amino terminal halves of the TRAF proteins were fused to a threefold repeat of the immunophilin FKBP12 and

oligomerised by incubating with the dimeric ligand FK1012. Once oligomerised, the TRAF-FKBP12 chimeras were able to induce the same set of genes that are normally induced by IL-1 (TNF). Oligomerisation of the TRAF amino terminal domains appears to facilitate binding to other effector molecules, such as MEKK which is a member of the MAPKKK family (Baud *et al.*, 1999).

Recently, it has been demonstrated that TRAF6 interacts with TAK1 (TGFβ activated kinase), which is also a member of the MAPKKK family (Ninomiya-Tsuji *et al.*, 1999). TAK1 requires TAB1 (TAK binding protein) for activation (Shibuya *et al.*, 1996) and both interact with TRAF6 in a process that is IL-1 dependent. TAK1 phosphorylates and activates NIK (NF-κB inducing kinase), a critical component of the complex leading to NF-κB activation (Malinin *et al.*, 1997). NF-κB dependent reporter gene assays linked to luciferase have demonstrated that NIK lies downstream of TAB1/TAK1, since dominant negative NIK is able to block TAB1/TAK1 induced NF-κB activation. Inactive TAK1 also inhibits IL-1 induced NF-κB activation in a dose dependent manner, but it has no effect on NIK induced activation. Dominant negative TAK1 is able to block IL-1 induced JNK and p38 MAPK activation. However dominant negative NIK did not inhibit IL-1 or TAK1/TAB1 induced activation, indicating that bifurcation of the IL-1 signalling pathway occurs at TAK1 (Ninomiya-Tsuji *et al.*, 1999).

NIK, which also shares sequence similarity with MAPKKK members, was identified in a yeast two-hybrid study using TRAF2 a component of the TNF signalling pathway as bait (Malinin *et al.*, 1997). NIK appears to represent a crucial convergence point for both the IL-1 pathway via TRAF6 (as described above) and the TNF pathway via

TRAF2 (see section 1.2.6). NIK activates NF-κB when over-expressed and kinase inactive mutants of NIK can act as dominant negative inhibitors of TNF and IL-1 mediated NF-κB activation, indicating that this enzyme is essential for IL-1 and TNF induced activation of NF-κB (Malinin *et al.*, 1997).

1.2.4 Tumour necrosis factors

The tumour necrosis factors comprise of two closely related proteins, TNFα (also known as cachectin) and TNFβ (also known as lymphotoxin). TNFα is produced by a variety of cell types including, neutrophils, activated lymphocytes, macrophages, NK cells, endothelial cells, astrocytes and some transformed cells. TNFβ is produced by lymphocytes. The two proteins share about 30% amino acid homology and bind to the same cell surface receptors to elicit a wide range of similar, but not identical biological responses (Vilcek and Lee, 1991). Human TNFα can exist as a membrane bound pro-form (26 kDa) or soluble (17 kDa) form. Both forms have biological activity although the soluble form is more potent (Decoster *et al.*, 1995). Membrane bound proTNFα is cleaved to release soluble TNFα by a membrane bound protease called TNFα converting enzyme (TACE) (Black *et al.*, 1997; Moss *et al.*, 1997). TNFβ possesses a signal peptide sequence and is processed and secreted in the same manner as other secretory proteins. TNFβ has a molecular weight of 25 kDa .The higher apparent molecular mass of TNFβ is a result of extra amino acids at the amino terminus and *N*- glycosylation which are absent in TNFα (Vilcek and Lee, 1991). In their biologically active native forms TNFα and TNFβ are found as tightly packed trimers (Jones *et al.*, 1989; Eck *et al.*, 1992).

1.2.5 The TNF receptor family

TNF mediates its effects through two distinct receptors, TNFRI and TNFRII. TNFRI is a 55 kDa (455 aa) transmembrane glycoprotein that is present on the surface of virtually all nucleated cell types (Loetscher *et al.*, 1990). Soluble TNFα and TNFβ are able to bind to TNFRI with K_d values of 20-60 pM and 650 pM respectively (Marsters *et al.*, 1992). The extracellular domain of TNFRI is 190 aa residues and contains four cysteine-rich motifs that are believed to be involved in binding (Marsters *et al.*, 1992). The transmembrane domain is 25 aa residues with the remaining 240 aa residues comprising the cytoplasmic domain (Loetscher *et al.*, 1990). Within the cytoplasmic domain there is an 80 aa residue "death domain" that can recruit accessory proteins to trigger either an apoptotic signal, anti-viral activity or induction of general inflammatory responses (Tartaglia *et al.*, 1993a). Death domain motifs facilitate protein interactions and are a common feature of proteins involved in receptor mediated apoptosis. TNFRI is also able to transduce signals that lead to NF-κB activation although the mechanism determining the choice of pathways is not clear.

TNFRII is a 75 kDa (461 aa) transmembrane glycoprotein whose exact function is unclear (Smith *et al.*, 1990). TNFRII is expressed on many cell types such as macrophages, monocytes and endothelial cells. TNFRII does have a biological role since TNFα binding to TNFRII is able to induce apoptosis in skeletal muscle tumour cells and cell migration in Langerhan cells (Medvedev *et al.*, 1994; Wang *et al.*, 1996). Another possible role for TNFRII, is that it may act as a co-receptor that presents TNF for binding to TNFRI (Tartaglia *et al.*, 1993b). Although most biological responses are mediated through TNFRI, including activation of the transcription factors AP-1 and NF-κB, recent evidence suggests that this receptor may

be most important for circulating TNFα, while TNFRII is more important for membrane bound TNFα (Grell, 1996). Since most of the biological properties of TNF are mediated through TNFRI, including activation of the transcription factors AP-1 and NF-κB, only signalling events initiated from this receptor will be discussed below.

1.2.6 TNF signalling

Binding of trimeric TNF to TNFRI induces receptor clustering and catalyses the recruitment of several downstream signal-transducing proteins to the cytoplasmic domains of the receptors (reviewed by Darnay and Aggarwal, 1997). TRADD (TNF receptor associated death domain) (Hsu *et al.*, 1995) is the first protein to be recruited to the TNFRI receptor. TRADD is a 34 kDa protein containing a C-terminus death domain that is essential for binding to TNFRI via its own cytoplasmic death domain. TRADD is able to serve as a platform and recruit at least three other proteins that mediate both the apoptotic signal as well as TNF induced AP-1 and NF-κB activation (Hsu *et al.*, 1996). TRADD recruits a protein called RIP (receptor-interacting protein), which was identified by yeast two-hybrid screening using TRADD as bait (Hsu *et al.*, 1996). RIP binds to TRADD through death domain interactions and like TRADD is essential for activation of NF-κB and apoptosis. The TRADD-RIP complex is then able to recruit and bind either of two proteins, FADD (Fas associated death domain) or TRAF2 (Chinnaiyan *et al.*, 1995; Rothe *et al.*, 1994). FADD binding signals to apoptosis following binding of caspase-8 (FLICE) which initiates a proteolytic cascade of caspases (Boldin *et al.*, 1996). TRAF2 binds NIK and signals to NF-κB activation via the IKK complex. In addition TRAF2 is also part of an NIK-independent signal transduction pathway that results in the activation of AP-1 through

the JNK and p38 MAP kinase cascades (Natoli *et al.*, 1997; Carpentier *et al.*, 1998). The signal transduction events from TRAF2 leading to AP-1 activation have not yet been elucidated although MEKK can interact with TRAF2 and induce TNF and IL-1 responsive genes (Baud *et al.*, 1999).

1.2.7 IL-1 and TNF signalling leading to AP-1 and NF- κB activation

Most of the pleiotropic effects of IL-1 and TNF are due to their unique abilities to increase the expression of a wide variety of genes in a multitude of target cells (Table 1.1). This induction may be the result of either increased transcriptional activity or increased half-life (stabilisation) or both of the mRNA (reviewed by Dinarello, 1996; reviewed by Vilcek and Lee, 1991).

IL-1 and TNF activate several transcription factors. Of these, nuclear factor κB (NF-κB) and activating protein-1 (AP-1) are two of the most significant. Both transcription factors regulate the induction of many genes critical for the progression of normal immune and inflammatory responses (Table 1.1). NF-κB belongs to the Rel family of transcriptional activators and is composed of one RelA (p65) and one p50 subunit (reviewed by Huguet *et al.*, 1997). The early intracellular events leading to the activation of AP-1 and NF-κB following IL-1 and TNF stimulation are illustrated in Figure 1.3.

cytokines:	IL-6, IFN, IL-8, IL-2, IL-1Ra, TNF, IL-1and GM-CSF
growth factors:	PDGF, NGF
proinflammatory mediators:	cyclooxygenase-2, cytosolic secretory phospholipase A2, iNOS
oncogenes:	c-jun, c-fos, c-myc
tissue remodeling:	collagenase-1, gelatinases, elastase stromelysin
adhesion molecules:	ICAM-1, ELAM-1 VCAM-1, lymphocyte L-selectin

Table1.1: Examples of genes whose expression is increased by IL-1 and TNF (modified from a review article by Dinarello, 1996).

In addition to increasing the transcriptional activity of NF-κB, IL-1 and TNF also simultaneously activate the JNK and p38 MAP kinase families (Figure 1.3), also known as stress activated protein kinases (SAPKs) (Kyriakis *et al.*, 1994; Raingeaud *et al.*, 1995). Both JNK and p38 MAP kinases contribute to the activation of AP-1 by activating the transcription factors (c-jun, ATF-2 and Elk-1) that induce c-*jun* and c-*fos* genes, the products of which form the AP-1 complex (reviewed Karin, 1995; reviewed Karin *et al.*, 1997). The integral role of p38 MAP kinase in pro-inflammatory cytokine signalling has became apparent with the aid of the highly specific inhibitor, SB 203580 (Figure 1.5). SB 203580 has demonstrated that p38 MAP kinase activity is rate limiting for a number of IL-1 and TNF responsive genes (Lee *et al.*, 1994; Beyaert *et al.*, 1996; Ridley *et al.*, 1997; Pietersma *et al.*, 1997).

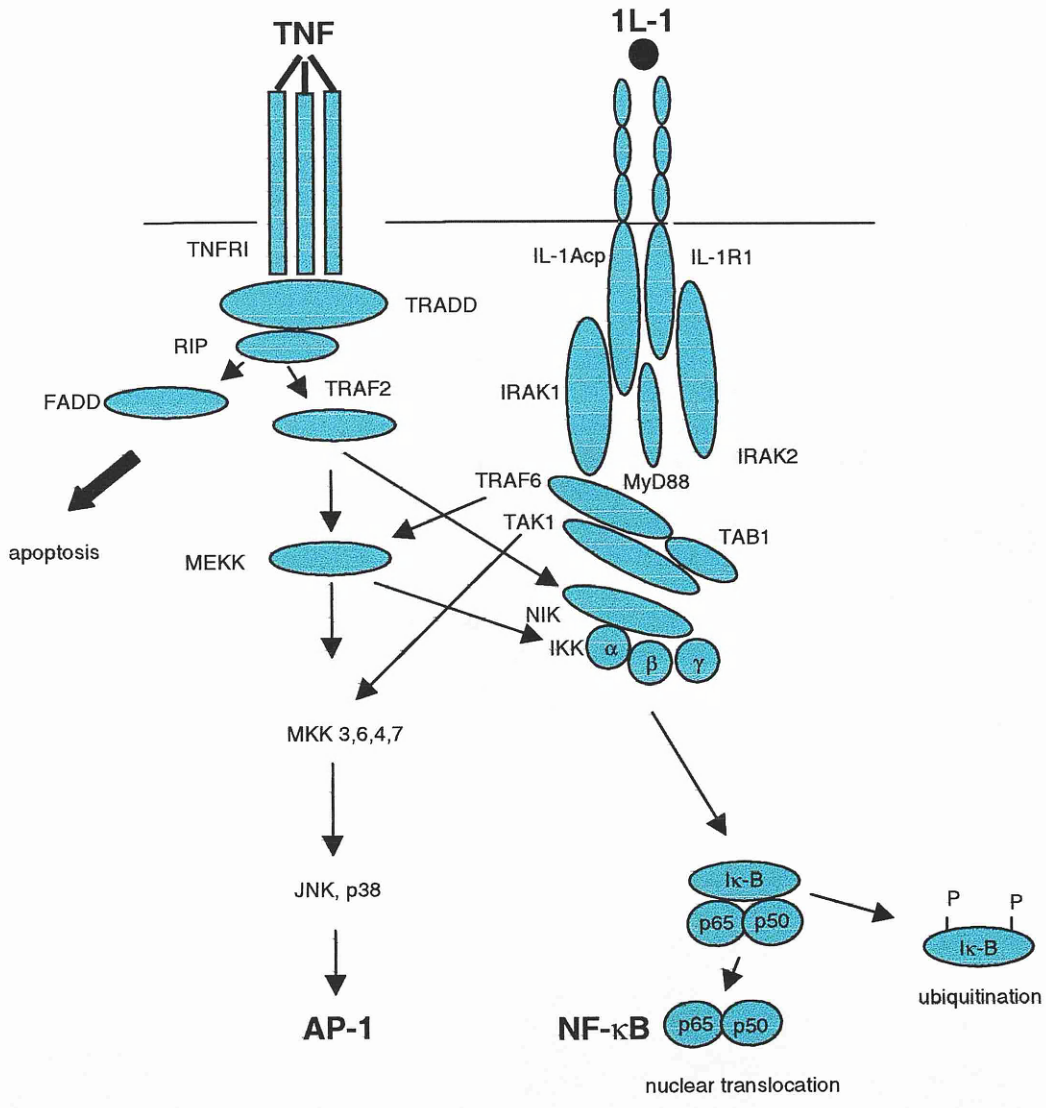

Figure 1.3: Schematic diagram illustrating the key protein interactions involved in IL-1 and TNF signalling leading to NF-κB and AP-1 activation. This figure is a modified version of an illustration in a review article by O'Neill and Greene, 1998.

1.3 Mitogen activated protein kinase cascades

Mitogen activated protein kinase (MAPK) cascades are important mediators of signal transduction from the cell surface to the nucleus. MAPK pathways have been identified in yeast and in mammalian cells and exhibit a high degree of conservation (reviewed by Blumer and Johnson, 1994). These pathways are typically characterised by a MAPK module consisting of a MAPK kinase kinase (MAPKKK), a MAPK kinase (MAPKK) and a MAPK. The specificity of MAPK responses to given stimuli is achieved by activation of specific MAPKKK- MAPKK-MAPK modules. There is now emerging evidence that the specificity is achieved, in part, by the use of scaffolding or anchoring proteins that sequester and hold these modular components together (reviewed by Garrington and Johnson, 1999). Activation of MAPK cascades results in the sequential phosphorylation and activation of each of these components, culminating in the phosphorylation of the MAPK by a dual specificity kinase (MAPKK) (Figure 1.4). In mammalian cells three parallel MAPK pathways have been extensively studied. The MAPK members from each of these pathways are discussed below. However, for the purpose of this project emphasis will be given to the p38 MAP kinase family and its substrate MAP kinase activated protein kinase-2 (MAPKAPK-2). The role of the p38 MAP kinase pathway in pro-inflammatory cytokine signalling and the biological effects of specifically inhibiting p38 MAP kinase will be discussed. Finally the potential of identifying other therapeutic targets within this pathway will be reviewed.

1.3.1 ERK (p42/p44) MAP kinases

The ERK kinases, also known as p42 (ERK1) and p44 (ERK2) were the first members of the MAPK family to be characterised and cloned (Boulton *et al.*, 1990;

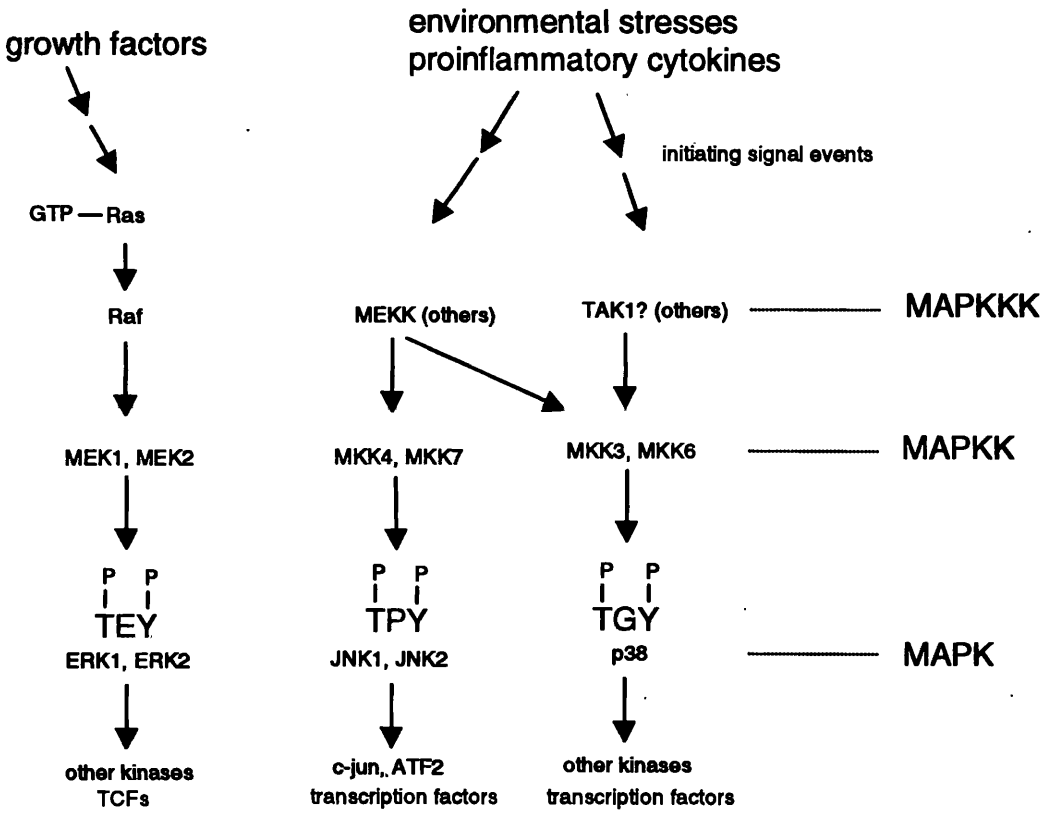

Figure 1.4: Diagram illustrating the sequential activation of the ERK, JNK and p38 MAP kinases by mitogenic stimuli and cellular stresses respectively. As described in the text activation occurs following phosphorylation of threonine and tyrosine residues at the specific TXY motif.

Boulton *et al.*, 1991). ERK kinases are activated following phosphorylation of the threonine and tyrosine residues at the T-E-Y activation motif (Figure 1.4) in response to mitogenic stimuli including; NGF in PC12 cells (Boulton *et al.*, 1991), EGF in hepatocytes (Liu *et al.*, 1996) and PDGF in smooth muscle cells (Graves *et al.*, 1996). However in certain cell types they can also be activated by pro-inflammatory cytokines (IL-1 and TNF) (Saklatvala *et al.*, 1993). Of the three principal MAP kinase pathways, the events leading to the activation of the ERK kinases are the best understood. Growth factors acting through tyrosine kinase receptors or seven transmembrane receptor coupled to G-proteins induce ERK activation via Ras GTPase/Raf/MAPK kinase (MEK) (Figure 1.4) (reviewed by Waskiewicz and Cooper, 1995). Several substrates for ERK1/2 have been identified including protein kinases, MAPKAPK-1 or ribosomal S6 kinase ($p90^{rsk}$) (Sturgill and Wu, 1991) and MAPKAPK-2 *in-vitro* (Stokoe *et al.*, 1992). Members of the ternary complex factor (TCF) sub-family of ETS-domain transcription factors, Sap-1 (Price *et al.*, 1996), Elk-1 (Janknecht *et al.*, 1993; Marais *et al.*, 1993), are also phosphorylated by ERKs. Other proteins include $cPLA_2$ (Lin *et al.*, 1993), cMyc (Gupta and Davis, 1994). Recently, several new ERK members, ERK3 (Cheng *et al.*, 1996), ERK4 (Peng *et al.*, 1996) and ERK5 have been identified and with the exception of ERK3, which contains an S-E-G motif, all contain the characteristic T-E-Y activation motif. To date little is known about the physiological roles of these proteins.

1.3.2 JNK MAP kinases

The second MAP kinase family are the JNKs or SAPKs (stress activated protein kinases) which are predominantly activated by cellular insults such as, UV light, pro-inflammatory cytokines (IL-1 and TNF), sodium arsenite and hyperosmolarity

(Derijard *et al.*, 1994; Kyriakis *et al.*, 1994). Activation occurs following phosphorylation of the threonine and tyrosine residues at the T-P-Y activation motif (Figure 1.4). The first member of the SAPK family, called p54, was isolated from livers of rats injected with cycloheximide (Kyriakis and Avruch, 1990). Tryptic peptide sequences of p54 were used to design oligonucleotides and the subsequent amplification of a cDNA probe. Screening of a rat brain cDNA library isolated four classes of p54 cDNAs (αI, αII, β and γ) which were highly homologous proteins (85-90%) of 54 kDa and 45 kDa (Kyriakis *et al.*, 1994). Independently, JNK1 (jun N-terminal kinase 1) which is identical to the 45 kDa SAPKγ protein and JNK2 which is identical to 54 kDa SAPKαII were cloned (Derijard *et al.*, 1994). Recently a third member of the JNK (SAPK) family has been identified that also contains the long (54 kDa) and short (46 kDa) forms (Gupta *et al.*, 1996). To date, three distinct genes in humans (JNK1, 2 and 3), which can give rise to ten variants, have been identified (Gupta *et al.*, 1996).

The precise upstream mechanisms that lead to JNK activation are not yet fully elucidated. In response to cellular stress two major JNK kinases have been identified, MKK4 (Derijard *et al.*, 1995), also called SEK1 (Sanchez *et al.*, 1994) or JNKK (Lin *et al.*, 1995) and MKK7 (Moriguchi *et al.*, 1997; Tournier *et al.*, 1997; Yao *et al.*, 1997). Of these only MKK7 is specific for JNK and was found to be the only IL-1-induced JNK activator in rabbit liver (Finch *et al.*, 1997). The specificity of MKK4 is unclear. In COS cells MKK4 does not co-precipitate with p38 MAP kinase but does with JNK. In addition, overexpressed MEKK which is a strong MKK4 activator results in JNK but not p38 MAP kinase phosphorylation (Zanke *et al.*, 1996). Contrary to these data Guan *et al.* (1998) demonstrated that catalytically inactive

MKK4 permanently expressed in rat mesangial cells inhibited IL-1β-induced phosphorylation of p38 MAP kinase.

Several transcription factors, c-jun (Derijard *et al.*, 1994), ATF-2 (Gupta *et al.*, 1995), Elk-1 (Yang *et al.*, 1998) have been identified as JNK substrates. Elk-1 is also a substrate of the ERK kinases and recent data suggests that ERK and JNK MAP kinases target over-lapping yet specific domains (Yang *et al.*, 1998).

1.3.3 p38 MAP kinases

p38 MAPK is the archetypal member of the third MAPK-related pathway. Activation occurs after phosphorylation of the threonine and tyrosine residues at the activation motif, T-G-Y, following cellular insults including; pro-inflammatory cytokines, UV, chemical and osmotic shock (Figure 1.4) (Freshney *et al.*, 1994; Raingeaud *et al.*, 1995; Rouse *et al.*, 1994). However in certain cell types p38 MAP kinase can be activated by other stimuli including; N-formyl-Met-Leu-Phe in neutrophils (Krump *et al.*, 1997), thrombin/collagen in platelets (Saklatvala *et al.*, 1996), IL-2 and IL-7 in T-cells (Crawley *et al.*, 1997) and IL-10 (Foey *et al.*, 1998). The details describing the characterisation and cloning of p38 MAP kinase are described in Chapter 3. To date four p38 MAP kinase isoforms p38α (p38/CSBP), β, γ and δ, encoded by separate genes have been identified (Lee *et al.*, 1994; Jiang *et al.*, 1996; Li *et al.*, 1996; Kumar *et al.*, 1997). The sequence of p38 MAP kinase shares extensive homology with the yeast *Saccharomyces cerevisiae* high-osmolarity glycerol 1 (*hog1*) gene (Brewster *et al.*, 1993). HOG1 is required by yeast to enable them to survive in hyperosmotic conditions. The mammalian homologue of HOG1, p38 MAP kinase (and JNK), was able to complement this enzyme by allowing growth in hyperosmotic conditions in a

hog1 deleted yeast strain (Han *et al.*, 1994; Lee *et al.*, 1994; Kumar *et al.*, 1995; Galcheva-Gargova *et al.*, 1994). This result led to the assumption that the HOG1 MAP kinase kinase, PBS2, may be a homologue of the physiological MAP kinase kinase that activates p38 MAP kinase. With this aim Derijard *et al.* (1995) used the sequence of PBS2 to design degenerate oligonucleotides and subsequently amplified a cDNA probe. Screening of a human foetal brain cDNA library isolated two activators of p38 MAP kinase, MKK3 (also termed SAPKK2) and MKK4 (see JNK MAP kinases). Another p38 MAPK activator, MKK6 (also termed SAPKK3), has also been identified (Han *et al.*, 1996; Moriguchi *et al.*, 1996; Cuenda *et al.*, 1996). Whilst both MKK3 and MKK6 have been shown to be specific for p38 MAPK activation (Raingeaud *et al.*, 1996; Meier *et al.*, 1996) the predominant activator of p38 MAPK by pro-inflammatory cytokines in epithelial cells and monocytes is MKK6 (Cuenda *et al.*, 1996). The exact mechanisms leading to the activation of MKK3 and MKK6 following pro-inflammatory cytokine stimulation are still unclear. However, the protein interactions illustrated in Figure 1.3 may explain some of the early signalling events that lead to the activation of potential MKK3 and MKK6 activators including; TAK1 (TGFβ activated kinase) (Moriguchi *et al.*, 1996), PAK (p21-activated kinase) (Frost *et al.*, 1996) and MLK3 (mixed lineage kinase-3) (Tibbles *et al.*, 1996).

Several substrates of p38 MAP kinase have been identified based on the results of overexpression studies, *in-vitro* kinase assays, reporter gene assay and selective inhibition of p38 MAP kinase. Among these are several protein kinases and transcription factors. Potential nuclear targets include members of the ETS-domain family of transcription factor Elk-1 (Raingeaud *et al.*, 1996; Yang *et al.*, 1998) and Sap1-a (Janknecht and Hunter, 1997) which interact and complex with the serum

response factor and bind the serum response element in genes such as *c-fos*. MEF2-C, which is member of the myocyte-enhancer factor 2 group of transcription factors (Han *et al.*, 1997), ATF-2 (Derijard *et al.*, 1995; Raingeaud *et al.*, 1996) and CHOP (Wang and Ron, 1996) have also been proposed as potential nuclear targets. Potential protein kinase substrates include PRAK (New *et al.*, 1998), MNK1/2 (Fukunaga and Hunter, 1997; Waskiewicz *et al.*, 1997), MAPKAPK-3 (mitogen activated protein kinase activated protein kinase -3) (McLaughlin *et al.*, 1996), MAPKAPK-2 (Rouse *et al.*, 1994; Freshney *et al.*, 1994) and MSK1 (Deak *et al.*, 1998). Although the exact physiological relevance of most of these substrates with regards to the biological activities p38 MAPK have yet to be defined some such as MAPKAPK-2 have been well characterised.

MAPKAPK-2 is a recognised physiological substrate of p38 MAPK that can also be phosphorylated *in-vitro* by p42/p44 MAPK (Stokoe *et al.*, 1992). However, stimuli that strongly activate MAPKAPK-2 *in-vivo* such as pro-inflammatory cytokines and cellular stresses do not activate p42/p44 MAPK (Freshney *et al.*, 1994; Rouse *et al.*, 1994). The first reported association of increased MAPKAPK-2 activity with pro-inflammatory cytokine signalling was made by Freshney *et al.* (1994). In this study, which also identified and associated p38 MAPK (termed p40) with IL-1 signalling, MAPKAPK-2 (termed p50) was purified to near homogeneity and its activity could be increased following incubation with purified fractions of IL-1 activated p40. MAPKAPK-2 was phosphorylated by p38 MAPK on threonine and serine residues and increased activity was associated with increased phosphorylation of the small heat shock protein 27 (Hsp27) (Freshney *et al.*, 1994). The physiological relevance of Hsp27 phosphorylation by activation of the p38 MAPK pathway is unclear. Hsp27 is

a cytoplasmic protein homologous to α-crystallin. Two main roles of Hsp27 have been proposed. The first is that of a molecular chaperone aiding the correct folding of proteins (Jakob *et al.*, 1993) and the second is to preserve the structural integrity of the cell by inhibiting actin polymerization (Lavoie *et al.*, 1993). In unstressed cells Hsp27 forms large aggregates which dissociate upon phosphorylation after heat shock or other cellular stresses (Kato *et al.*, 1994). Recent data in transfected L929 cells suggests that Hsp27 aggregates are necessary for chaperone action and protection against oxidative stress/TNF. Further phosphorylation of these complexes down-regulates these protective properties (Rogalla *et al.*, 1999). Activated MAPKAPK-2 has also been shown to phosphorylate lymphocyte-specific protein 1, LSP1 (Huang *et al.*, 1997), cAMP response element-binding protein (CREB) and ATF-1 (Tan *et al.*, 1996).

1.4 Inhibitors of p38 MAPK

The prototype p38 MAPK inhibitor, SK&F 86002, was identified from a series of dual 5-lipooxygenase/cyclooxygenase inhibitors which also blocked the production of IL-1 and TNF both *in-vitro* and *in-vivo* (Lee *et al.*, 1993). Recognition that the anti-inflammatory properties of SK&F 86002 were independent of its inhibition of arachidonate metabolism led to the search for the molecular targets for this compound. Lee *et al.* (1994) designed a drug-binding assay using a radiolabelled derivative of SK&F 86002, SB 202190, and partially purified an enzyme from the cytosol of THP.1 cells that tightly bound this compound. Tryptic peptide sequences were used to design redundant oligonucleotides, which were then used to screen a GM-CSF stimulated human monocyte library and isolate p38 MAPK. Subsequent

work using p38 MAPK inhibitors has been carried out using SB 203580 (Figure 1.5) which is a more potent analogue of SB 202190.

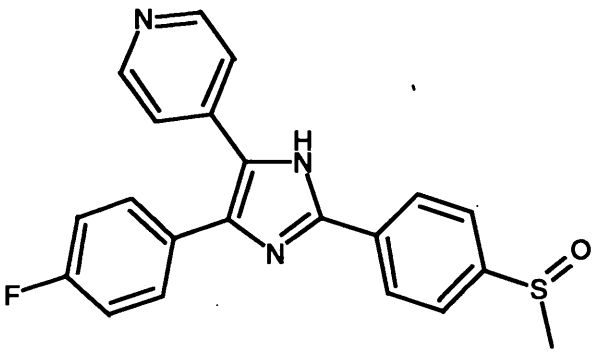

Figure 1.5: SB 203580

Recently, the biochemical and structural basis by which SB 203580 interacts and inhibits p38 MAPK activity has been elucidated. In competition assays, using GST-ATF2 as substrate with SB 203580 and a related tritiated pyridinyl imidazole SB202190, Frantz *et al.* (1998) showed that p38 MAPK had a particularly high K_M value for ATP (25 μM). SB 203580 competed with ATP for the active site of p38 MAPK and inhibited LPS and TNF induced p38 MAPK activation in THP.1 cells with an IC_{50} value comparable to the IC_{50} (50-100 nM) for inhibition of cytokine induction. Furthermore, SB 203580 was able to bind to the active and inactive forms of p38 MAPK with equal affinity, whilst ATP only competed with the tritiated inhibitor for binding to the active form. Together these results suggest that under physiological conditions p38 MAPK is not bound to ATP but upon activation its affinity for ATP is increased (Frantz *et al.*, 1998).

Several groups have now published the crystal structure of p38 MAPK complexed with or without inhibitors (Wilson *et al.*, 1996; Wang *et al.*, 1997; Tong *et al.*, 1997;

Wilson *et al.*, 1997). These data support the biochemical results described above and reveal that pyridinyl imidazole compounds do bind to the ATP pocket of the inactive enzyme in a manner that resembles ATP binding. Site directed mutagenesis studies of amino acid residues within the ATP binding pocket have identified Met 109 and Thr 106 as crucial for the potency and specificity of these compounds. Mutating Met 109 to alanine results in a 6-fold drop in potency of SB 203580 (Lisnock *et al.*, 1998) whilst Thr 106 associates with the fluorophenyl moiety of the inhibitor and induces a local conformational change in the enzyme (Wang *et al.*, 1998). This interaction is crucial for conferring selectivity as has been demonstrated by mutagenesis studies. Of the four p38 MAPK isoforms that exist (α,β,δ and γ) only the p38 MAPKα and β isoforms are sensitive to SB 203580 (Kumar *et al.*, 1997) and a comparison of the nucleotide sequences of these isoforms reveals that Thr 106 is conserved. Significantly, mutating Thr 106 to the corresponding residue of the p38 MAPKγ and δ isoforms (Met 106) results in complete loss of inhibition. Conversely, mutation of Met 106 in the p38 MAPKγ and δ isoforms to Thr 106 confers sensitivity to the inhibitor (Gum *et al.*, 1998). The change in sensitivity to inhibition is not solely restricted to p38 MAPK family members since a similar mutation in JNK1 can also confer a degree of susceptibility to inhibition by pyridinyl imidazole inhibitors (Gum *et al.*, 1998; Eyers *et al.*, 1998). Although the high degree of specificity of SB 203580 towards p38 MAPK can be explained by structural differences, a degree of caution must still be exercised when interpreting data suggesting a biological role for p38 MAPK in which chemical inhibitors have been used. Recently, it has been shown that certain isoforms of JNK, notably JNK1β and JNK2β (Clerk and Sugden, 1998) and c-Raf (Hall-Jackson *et al.*, 1999) are sensitive to SB 203580.

1.4.1 Pharmacological activity of p38 MAPK inhibitors

Inhibitors of p38 MAPK have been shown to inhibit pro-inflammatory cytokine production from LPS-stimulated human monocytes (Lee *et al.*,1994). In addition pro-inflammatory cytokine inhibition with concomitant beneficial effects has been demonstrated in animal models of inflammation. In a collagen-induced arthritis model in DBA/1 LACJ mice, SB 203580 (50 mg/kg p.o., b.i.d.) possessed significant therapeutic activity as determined by reduced paw inflammation and serum amyloid protein levels. Evidence for disease modifying activity was indicated by improved bone mineral density as determined by foetal rat long bone assay and histological evaluation. In the foetal rat long bone assay, SB 203580 inhibited radiolabelled calcium release from pre-radiolabelled foetal long bones with an IC_{50} of 0.6 μM (Badger *et al.*, 1996). It has previously been demonstrated using anti-TNF and anti-IL-1 antibodies that in this model of arthritis IL-1 and TNF contribute to the pathophysiology of disease (Williams *et al.*, 1992; van de Berg *et al.*, 1994). Thus the efficacy of p38 MAPK inhibitors in this disease model is entirely consistent with the regulation of IL-1 and TNF signalling by p38 MAPK.

The commercial availability of SB 203580 has meant that the role of p38 MAPK in response to pro-inflammatory cytokine signalling has been extensively studied in a variety of cell systems. These results have contributed greatly to our understanding of the underlying mechanisms by which p38 MAPK inhibitors, in particular SB 203580, may be efficacious in animal models of inflammation. In addition to the original observation that SB 203580 inhibited IL-1 and TNF production in human monocytes (Lee *et al.*, 1994) it has also been shown to inhibit the synthesis of secondary pro-inflammatory cytokines such as IL-6 (Ridley *et al.*, 1997; Beyaert *et al.*, 1996) and

IL-8 (Hashimoto *et al.*, 1999). Both of these cytokines are involved in augmenting the inflammatory response (see section 1.1.1). Inhibition of matrix metalloproteinases (MMPs), collagenase-1 (MMP1) and stromelysin-1 (MMP3) by SB 203580 has also been noted (Ridley *et al.*, 1997). Recently several reports have also shown that p38 MAPK inhibitors can modulate the synthesis of prostaglandins in IL-1-induced fibroblasts (Ridley *et al.*, 1997) and in LPS, IL-1, TNF and zymosan treated monocytes (Pouliot *et al.*, 1997; Dean *et al.*, 1999). As described in section 1.1.2, prostaglandins are potent pro-inflammatory mediators synthesised by cyclooxygenases from arachidonate. In the studies described above decreased prostaglandin production was shown to be due to direct effect of p38 MAPK inhibitors on COX-2 protein synthesis and not a result of blocking cytokine production *per se*, thus implicating p38 MAPK in the regulation of COX-2.

1.5 Molecular mechanisms

The exact role of p38 MAP kinase in the regulation of pro-inflammatory cytokine and IL-1 inducible gene synthesis, such as COX-2, is still unclear. Gene expression is controlled at many levels and there is evidence for the involvement of p38 MAP kinase in transcription (possibly by activation of transcription factors), mRNA stabilisation or translational regulation. With the aid of specific p38 MAPK inhibitors the level(s) of regulation at which p38 MAPK can modulate the expression of some of the genes described above have been determined (Table 1.2). From this table it can be seen that p38 MAPK regulates the expression of different genes at different levels depending upon the cell type and the nature of the stimuli.

Gene	Agonist	Cell Type	Regulatory Mechanisms	Reference
IL-1	LPS	monocytes	translational	Lee *et al.*, 1994
TNF	LPS	monocytes	translational	Lee *et al.*, 1994
IL-6	TNF	murine L929	decreased mRNA (transcription and/or mRNA stability?)	Bayaert *et al.*, 1996
IL-8	IL-1/TNF	endothelial cells	decreased mRNA (transcription and/or mRNA stability?)	Hashimoto *et al.*, 1999
COX-2	IL-1	HeLa	mRNA stability	Ridley *et al.*,1998
COX-2	LPS	monocytes	transcription and mRNA stability	Dean *et al.*, 1999
COX-2	LPS, IL-1 zymosan	monocytes	decreased mRNA (transcription and/or mRNA stability	Pouliot *et al.*, 1997
MMP-1	IL-1	dermal fibroblasts	decreased mRNA (transcription and/or mRNA stability	Ridley *et al.*, 1997
IL-6	IL-1	synoviocytes	mRNA stability	Miyazawa *et al.*, 1998

Table 1.2: Regulation of gene expression by p38 MAPK as determined using specific inhibitors.

1.5.1 Transcriptional regulation

Although several transcription factors have been identified as potential p38 MAPK substrates (see section 1.3.3) the physiological relevance of many of these remains to be determined. For instance ATF-2 can be phosphorylated by p38 MAPK *in-vitro* and ATF-2-dependent gene transcription can be increased by cotransfection with MKK3 and MKK6 (Raingeaud *et al.*, 1996). However SB 203580 does not inhibit ATF-2 phosphorylation *in-vivo* when cells are stimulated with agonists that activate p38 MAPK, therefore indicating that p38 MAPK is not rate-limiting for this process (Hazzalin *et al.*, 1996). ETS domain transcription factors, Elk-1 and Sap1-a, have also been identified as potential p38 MAPK substrates that can be phosphorylated *in-vitro*

and stimulate a *c-fos* SRE-driven luciferase reporter gene (Janknecht and Hunter, 1997). These transcription factors bind together with the serum response factor to the serum response element (SRE) in immediate early genes such as *c-fos*. Fos is then able to form a heterodimer with c-Jun and form the AP-1 complex (see section 1.2.7). In a recent report a role for p38 MAPK in *c-fos* induction has been demonstrated using SB 203580 at concentrations similar to the IC_{50} value for the inhibition of p38 MAPK enzyme activity. However in this study *c-fos* was induced by UV radiation and not by pro-inflammatory cytokines (Hazzalin *et el.*, 1996). MEF2C, a member of the myocyte-enhancer factor (MEF2) group of transcription factors, has also been identified as a substrate of p38 MAPK (Han *et al.*, 1997). In monocytes stimulated with LPS the transactivation activity of MEF2C is increased through p38 MAPK catalysed phosphorylation. A consequence of MEF2C activation is increased *c-jun* gene transcription and evidence suggests that p38 MAPK may regulate the levels of c-Jun during infection of inflammation. Another possible mechanism for transcriptional control may be mediated by the p38 MAPK substrates, MAPKAPK-2 and MSK1 which have been shown to phosphorylate CREB (cAMP-responsive element binding protein) which binds to the cAMP response element (CRE) within target genes (Deak *et al.*, 1998; Tan *et al.*, 1996).

From the evidence described above it can be proposed that p38 MAPK may regulate gene transcription at several levels. At one level p38 MAPK may phosphorylate and increase the activity of transcription factors that directly induce the target gene such as COX-2, which contains putative binding sites for members of the Ets/TCF, CRE and MEF2 families. At another level p38 MAPK may regulate the induction of early immediate genes such as *c-fos* and *c-jun* whose gene products form the dimeric

transcription factor complexes, such as AP-1, that regulate the transcription of many IL-1 inducible genes (see section 1.2.7) (reviewed by Eder, 1997).

1.5.2 Post-transcriptional

There is now a large body of evidence to support a role for p38 MAPK activity in the stabilization of mRNAs from a number of different genes within different cell types (Ridley *et al.*, 1998; Dean *et al.*, 1999; Miyazawa *et al.*, 1998). Regulation of mRNA stability is often mediated by repeat AUUUA sequence motifs located within the 3' untranslated region (3' UTR) of numerous induced cytokines and protooncogenes (Caput *et al.*, 1986; Chen and Shyu, 1994; Chen and Shyu, 1995). The COX-2 gene produces two major mRNA transcripts, COX-2 (4.6 kb) and COX-2 (2.8 kb), which are derived by alternative polyadenylation site usage (Newton *et al.*, 1997). In the 3' UTR of the most abundant COX-2 transcript, COX-2 (4.6 kb), there are 22 AU-rich elements (AREs) that have been recognised as important determinants of mRNA stability (Ristimaki *et al.*, 1996). In the case of TNF mRNA, AREs present in the 3' UTR have also been claimed to regulate translation (Han *et al.*, 1990). Recently, tristetraprolin (TTP) the prototype of a class of zinc finger proteins has been shown to inhibit TNFα production by destabilizing its mRNA. This effect appeared to result from direct binding of TTP to the AU-rich element of the TNFα mRNA (Carballo *et al.*, 1998). Several other *trans*-activating factors including AUF1 (DeMaria and Brewer, 1996) and AUBF (Rajagopalan and Malter, 1994) have also been identified that bind to AREs. At present it is still unclear how AREs regulate mRNA stability and/or translational inhibition or how ARE binding proteins mediate selective mRNA degradation or protection.

1.6 Aim of this project

As discussed above specific p38 MAPK inhibitors have implicated p38 MAPK activity in the regulation of several IL-1 inducible genes most notably COX-2 (Dean *et al.*, 1999; Ridley *et al.*, 1998; Pouliot *et al.*, 1997) (Table 1.2). In addition, the level of regulation at which p38 MAPK modulates gene expression appears to be dependent on the cell type and stimulus. In view of this, it is highly likely that the effects of p38 MAPK are mediated by several downstream substrates (some of which may have not yet been identified). Therefore the aim of this investigation was to try and identify a novel protein substrate or protein interaction that could add to our current understanding of pro-inflammatory cytokine signalling and gene regulation by the p38 MAPK pathway. To do this p38 MAP kinase and its substrate MAPKAPK-2 were used as bait in a yeast two-hybrid screen. This method has been previously used successfully to identify many of the components involved in the early signalling events of IL-1 and TNF (see Figure 1.3). In addition an investigation was also carried out to determine the role of MAPKAPK-2 in pro-inflammatory cytokine signalling and gene induction. To achieve this HeLa cells were stably transfected with a kinase inactive MAPKAPK-2 mutant and MAPKAPK-2 anti-sense RNA. HeLa cells were chosen for study because of their responsiveness to IL-1 stimulation. Dominant negative and anti-sense methods to target and specifically reduce endogenous kinase activities have previously been described in the ERK (p42/p44) and JNK MAP kinase pathways (Pages *et al.*, 1993; Krause *et al.*, 1998).

Chapter 2

Materials and Methods

2.1 Materials

2.1.1 General chemicals and materials

General laboratory chemicals were purchased from Sigma Chemical Co. Ltd. (Poole, Dorset, UK) or BDH Ltd., (Poole, Dorset, UK) unless otherwise stated. Ethanol was obtained from Hayman Ltd. (Witham Essex, UK), Biophenol / Tris from Camlab Ltd. (Cambridge, UK), Bacto-tryptone, bacto-agar and yeast extract were obtained from Difco Ltd., (Detroit, Michigan, USA).

Radiolabelled chemicals [γ-^{32}P]-ATP, [^{32}P]-orthophosphate and [^{35}S]- methionine were supplied by Amersham Pharmacia Biotech Ltd (Bucks., UK)

Tissue culture media and supplements were obtained from Gibco-BRL (Paisley, Scotland). Tissue culture plastics were supplied by Falcon™ (NJ., USA).

Restriction enzymes, T4 DNA ligase, and calf intestinal phosphatase were purchased from Boehringer Manheim Ltd., (Lewes, East Sussex, UK) or New England Biolabs (Beverly, MA., USA).

For the construction of epitope-tagged proteins, the mammalian expression vector pcDNA3 (Invitrogen BV, Netherlands) was used. For routine non-expression cloning and sub-cloning the vector pSP73 (Promega Ltd., Southampton, UK) was used. For

the construction of GST-fusion proteins, pGEX-3X from Pharmacia (St., Albans, Herts., UK) was used.

The FireLite™ Dual Firefly and Renilla Luciferase Reporter Gene Assay Kit was provided by Packard Bioscience (Netherlands) and the Prostaglandin E_2 Monoclonal Enzyme Immunoassay Kit was supplied by Cayman Chemical (US).

QIAGEN plasmid Maxi / Midi Kits and SuperFect™ Transfection Reagent were obtained from QIAGEN Ltd. (Crawley, UK).

DNA Sequence Kit™ (Big Dye Terminator Cycle Sequencing Ready Reaction) and AmpliTaq DNA Polymerase was obtained from PE Applied Biosystems (Foster City, CA., USA). Sequence reactions were carried out in a Biometra™ Trio-Thermoblock complete with Biometra™ heated lid (Anachem Ltd, Luton, UK) and analysed on a 373A DNASequencer (PE Applied Biosystems, Foster City, CA., USA). All other PCR reactions were done in a Perkin Elmer TC1 machine (PE Applied Biosystems, Foster City, CA., USA).

Protein gels / Western blot apparatus and See Blue™ pre-stained protein markers were obtained from Novex Experimental Technology (San Diego, CA., USA). Immobilon™ PVDF transfer membrane was supplied by Millipore Corp. (Bedford, MA., USA).

Horizontal gel electrophoresis equipment was supplied by Bethesda Research Laboratories Inc., (Maryland, USA). DNA molecular weight markers (100 bp /1 kb ladders) were obtained from Gibco-BRL (Paisley, Scotland).

The gene pulser, pulse controller and electroporation cuvettes were obtained from BIO-RAD (Hemel Hempstead, Hertfordshire, UK).

Small scale centrifugation was carried out using a benchtop microfuge (Anderman centrifuge 5414). Large scale centrifugation was carried out using a Sorvall® RC3B or RC5B refrigerated centrifuge.

Gammabind G Sepharose beads were obtained from Pharmacia Biotech (St.Albans, Herts., UK).

2.1.2 Microbiological media

YPD broth	2%(w/v) Bacto-peptone, 1%(w/v) Bacto-yeast extract, 2% dextrose (added separately as 40% stock)
YPD agar	2%(w/v) Bacto-peptone, 1%(w/v) Bacto-yeast extract, 2% dextrose (added separately as 40% stock), 2% (w/v) Bacto-agar
SD broth	0.67%(w/v) yeast nitrogen base without amino acids, 2% dextrose (added separately as 40% stock), pH 5.8

SD agar	0.67%(w/v) yeast nitrogen base without amino acids, 2% dextrose (added separately as 40% stock), 2% (w/v) Bacto-agar, pH 5.8
LB agar	1%(w/v) Bacto-tryptone, 0.5%(w/v) Bacto-yeast extract, 171 mM NaCl, 1.5%(w/v) Bacto-agar
2X TY broth	2%(w/v) Bacto-tryptone, 1%(w/v) Bacto-yeast extract, 171 mM NaCl, pH 7.0
SOC	2%(w/v) Bacto-tryptone, 0.5%(w/v) Bacto-yeast extract, 10 mM NaCl, 25 mM KCl, 10 mM $MgCl_2$, 10 mM $MgSO_4$, 20 mM glucose

2.1.3 Solution and buffer formulations

5X M9 salts	230 mM $Na_2HPO_4 \cdot 7H_2O$, 110 mM KH_2PO_4, 42 mM NaCl, 93 mM NH_4Cl
PBS	120 mM NaCl, 2.7 mM KCl, 10 mM phosphate buffered salts
TE	10 mM Tris-HCl pH 7.5, 1 mM EDTA
TAE	40 mM Tris-acetate pH 8.0, 1 mM EDTA

X-gal stock	50 mg/ml X-gal (5-bromo-4-chloro-3- indolyl-β-D-galactopyranoside in N,N- dimethylformamide
10X LiAc	1 M lithium acetate (adjust to pH 7.5 with acetic acid and autoclave)
10X PCR buffer	500 mM KCl,100 mM Tris-HCl pH 8.0,150 mM $MgCl_2$
Z-buffer	60 mM $Na_2HPO_4 \cdot 7H_2O$, 40 mM $NaH_2PO_4 \cdot H_2O$, 10 mM KCl, $MgSO_4 \cdot 7H_2O$ (adjust to pH 7.0 and autoclave)
5X ligation buffer	5 mM ATP, 100 mM DTT, 50 mM $MgCl_2$, 250 mM Tris-HCl pH 7.4

Z-buffer/Xgal solution

100 ml	Z-buffer
0.27 ml	β-mercaptoethanol
1.67 ml	X-gal stock (50 mg/ml)

5X DNA sample loading buffer

glycerol	25%
EDTA	100 mM
Bromophenol blue	0.1%

yeast lysis solution

2% Triton X-100

1% SDS

100 mM NaCl

10 mM Tris pH 8.0

1.0 mM EDTA

5X protein sample buffer

β-mercaptoethanol	5%
SDS	10%
Glycerol	50%
Tris-HCl pH 6.8	100 mM
Bromophenol blue	0.2%

PEG/LiAc solution

	Final Conc.	To prepare 10 ml
PEG 4000	40%	8 ml of 50% PEG
TE Buffer	1X	1 ml of 10X TE
LiAc	1X	1 ml of 10X LiAc

10X kinase buffer

	Final Conc.	To prepare 10 ml
β-glycerophosphate	25 mM	2.5 ml of a 1 M stock
$MgCl_2$	25 mM	2.5 ml of a 1 M stock
Hepes pH 7.4	25 mM	2.5 ml of a 1 M stock

DTT	2 mM	0.4 ml of a 0.5 M stock
Na_3VO_4	100 µM	10 µl of a 1 M stock

mammalian cell lysis buffer

	Final Conc.	To prepare 10 ml
NP40	1%	1 ml of a 10% stock
EDTA	10 mM	0.4 ml of a 0.25 mM stock
NaCl	0.15 M	1 ml of a 1.5 M stock
Tris-HCl pH 7.5	10 mM	0.1 ml of a 1 M stock
NaF	50 mM	1 ml of a 0.5 M stock
Na_3VO_4	1 mM	0.1 ml of a 0.1 M stock
$Na_4P_2O_7$	20 mM	0.4 ml of a 0.5 M stock
H_2O		6.0 ml

protease inhibitor tablet*

* Complete™ Mini protease inhibitor cocktail tablet (Boehringer)

QIAGEN plasmid purification buffers

Buffer P1 (Resuspension Buffer)	50 mM Tris-HCl pH 8.0, 10 mM EDTA, 100 µg/ml RNAse A
Buffer P2 (Lysis Buffer)	200 mM NaOH, 1% SDS
Buffer P3 (Neutralization Buffer)	3.0 M potassium acetate pH 5.5
Buffer QBT (Equilibration Buffer)	750 mM NaCl, 50 mM MOPS pH 7.0, 15% isopropanol, 0.15% Triton X-100
Buffer QC (Wash Buffer)	1.0 M NaCl, 50 mM MOPS pH 7.0, 15% isopropanol

Buffer QF (Elution Buffer)	1.25 M NaCl, 50 mM Tris-HCl pH 8.5, 15% isopropanol
Buffer N3* (Neutralization Buffer)	contains chaotropic salt
Buffer PB* (Optional Wash Buffer)	contains chaotropic salt
Buffer PE* (Wash Buffer)	

* The ingredients to the QIAprep Spin buffers N3, PB, PE are withheld at the manufacturers' discretion

2.1.4 cDNA and vector sources

Human peripheral blood mononuclear cell (cPBMC) and skeletal muscle cDNA were kindly provided by Dr. Patrick Slocombe (Celltech). The human COX-2 promoter (-2309 to +37) cloned into the pGL3b *Firefly* luciferase reporter vector (Promega, Southampton,UK) was kindly provided by Dr Andrew Clark (Kennedy Institute of Rheumatology, London). The E-selectin promoter (-170 to +52) cloned into the pGL3b *Firefly* luciferase reporter vector was kindly provided by Dr. Breda Twomey (Celltech). The pRL-CMV *Renilla* luciferase reporter vector was also obtained from Promega.

2.1.5 Bacterial strains

For the routine propagation of recombinant plasmids and for the purification of recombinant glutathione S-transferase (GST) fusion proteins, ultra competent Epicurian Coli XL-1 Blue cells (*rec*A1 *end*A1 *gyr*A96 *thi*-1 *hsd*R17 *sup*E44 *rel*A1 *lac*[F' *pro*AB *lacI*^{q} ZΔM15 Tn10(Tet^{r})]), were used (Stratagene Ltd., Cambridge, UK).

To select for Leu^+, Amp^r transformants in the yeast two-hybrid experiments, electrocompetent *E.coli* HB101 cells, a strain carrying a LeuB mutation (F^- *hsd* S20 (r_B^- m_B^-) *sup*E44 *ara*14 *gal*K2 *lac*Y1 *pro*A *rps*L20 (Str^R) *xyl*-5 *mtl*-1 *rec*A13 *mcr*B *thi*-1 *leu*B6) were used.

2.1.6 Antibodies and recombinant proteins

The anti-human Hsp27 and anti-MAPKAPK-2 (anti-p50) antibodies and the murine GST-cleaved MAPKAPK-2 protein were kindly donated by Professor J. Saklatvala (Kennedy Institute of Rheumatology, London). Anti-human c-Myc antibodies were obtained from UBI. Anti-human COX-2 was obtained from Oxford Biomedical Research. GAL4 BD and GAL4 AD monoclonal antibodies were purchased from Clontech and the murine anti-FLAG monoclonal antibody was obtained from Kodak Scientific Imaging Systems. Anti-human actin was purchased from Santa Cruz Biotechnology and the anti-human IL-6, IL-8 and detection antibodies used in the IL-6 and IL-8 ELISA were obtained from PharMingen, UK. Anti- MAPKAPK-2 antibodies were obtained from various sources and are discussed in detail in Chapter 6.

2.1.7 Yeast two-hybrid reagents

An oligo (dT) + random primed human leucocyte MATCHMAKER cDNA library in the vector pGAD10 was purchased from Clontech (Hants, UK).

Yeast growth media and amino acid dropout supplements (Leu^-,Trp^-,His^-, Leu^-/Trp^-, Leu^-/Trp^-/His^- DO) and all other reagents required for the Matchmaker Two-Hybrid System were also purchased from Clontech.

2.1.8 Yeast strains

Strain	Genotype	Reporters	Transformation Markers
SFY526	MATa, *ura* 3-52, *his* 3-200, *ade* 2-101, *lys* 2-801, *trp* 1-901, *leu* 2-3, 112, *can*^{r}, *gal* 4-542, *gal* 80-538, URA3::GAL1-*lacZ*	*lacZ*	*trp1*, *leu2*
HF7z	MATa, *ura* 3-52, *his* 3-200, *lys* 2-801, *ade* 2-101, *trp* 1-901, *leu* 2-3, 112, *gal* 4-542, *gal* 80-538 LYS2::GAL1-HIS3, URA3::(GAL4 17mers)$_3$-CYC1-*lacZ*	HIS3, *lacZ*	*trp1*, *leu2*

Table 2.1: Yeast strains used in the two-hybrid study

2.1.9 Vectors

The cloning and control vectors provided with the MATCHMAKER system used in the yeast two-hybrid screen (Chapter 5) and are shown in Table 2.2 below.

Plasmid	Description	Selection on SD medium	References
pAS2-1	$GAL4_{(1-147)}$ DNA-BD, TRP1,amp^r, CYHS2	Trp-	Harper *et al.*, 1993
pGAD10	$GAL4_{(768-881)}$AD, LEU2,amp^r	Leu-	Bartel *et al.*, 1993
pGAD424	$GAL4_{(768-881)}$AD, LEU2,amp^r	Leu-	Bartel *et al.*, 1993
pCL-1	wild-type full-length GAL4 gene, LEU2, amp^r	Leu-	Fields & Song 1989
pVA3	murine $p53_{(72-390)}$, TRP1, amp^r	Trp-	Iwabuchi *et al.*, 1993
pTD1	SV40 large T-$antigen_{(84-708)}$ LEU2, amp^r	Leu-	Li & Fields 1993

Table 2.2: Cloning vectors used in the yeast two-hybrid study

2.1.10 Oligonucleotides

Oligonucleotides were designed from the database sequences (accession numbers indicated below). Only the oligonucleotides that were used for PCR cloning, PCR mutagenesis, RT-PCR and DNA/riboprobe amplification are indicated below. Sequencing and vector specific oligonucleotides are not shown.

CSBP2/p38MAP kinase oligonucleotides: (Accession No. L35264)

N5378 (forward)

5' - GCG GGA TCC AAA ATG GAC TAC AAG GAC GAC GAT GAC AAG TCT CAG GAG AGG

Bam HI Start FLAG epitope

CCC ACG TTC TAC CGG CAG G - 3'

N0465 (reverse)

5' - CAG GGA TCC CCT CAC AGT GAA GTG GGA TC - 3'

Bam HI

27019 (reverse)

5' - TGG TCT GGA GAG CTT CCT CAC TGC C - 3'

K53R

27020 (forward)

5' - CGT GTG GCA GTG AGG AAG CTC TCC AG - 3'

K53R

27021 (reverse)

5' - CAC CAG ATA CAC ATC ATT GAA TTC CTC C - 3'

Eco RI

W0988 (forward)

5' - CCG GGG ATC CGT ATG TCT CAG GAG AGG CCC ACG TTC TAC C - 3'

Bam HI

MAPKAPK-2 oligonucleotides: (Genbank Accession No. U12779)

N3257 (forward)

5' - GCG GGA TCC ACC ATG CTG TCC AAC TCC CAG GG - 3'

Bam HI

N3258 (reverse)

5'- GAG GCC CGG GGT CGA CGG ACA GGA ACA CAG AAT CCT CTG CTC ACA A - 3'

Sma I / Sal I

P0324 (reverse)

5'- GAG GCC CGG GGT CGA CGG TGG CTC AGT GGG CCA GAG CCT CCA GGG - 3'

Sma I / Sal I

W0989 (forward)

5' - CCG GGG ATC CGT CCG CAG CAG TTC CCG CAG TTC CAC - 3'

Bam HI

W9760 (forward)

5' - GGC AAA GTT TTG CAG ATC TTC AAC AAG AGG ACC CAG GAG AAA TTC GCC CTC

Bgl II

AGA ATG CTT CAG - 3'

K93R

A0488 (forward)

5' - GCG GAA TTC **ATG** CTG TCC AAC TCC CAG GGC CAG AGC CCG CCC ACC CCT GCC

Eco RI

CTG CCG CAC CCC CCG GCG CAG CCG CCG CCG CCG CCC CCG CAG CAG TTC - 3'

N3256 (reverse)

5' - GAG ATT CTC AGG CTT GAC ATC C - 3'

B5640 (reverse)

5' - ATA GCC AAG CTT TCT AGA TTA ATT CAA GTC CTC TTC A AAT GAG CTT TTG CTC

Hind III /Xba I c-Myc epitope

CAT GTG GGC CAG AGC CGC AGC CTC CAG GGC CCG AGC - 3'

MAPKAPK-2 RT-PCR anti-sense

F6070 (forward)

5' - GTC CTC TTC AGA AAT GAG CTT TTG CTC CAT GTG G - 3'

c-Myc epitope

F6071 (reverse)

5' - CGC CAT CCT GAA ACT CAC TGA CTT TGG - 3'

MAPK Kinase 6 oligonucleotides: (Genbank Accession No. U39657)

W0990 (forward)

5' - ATC CGT CGA CCT ATG TCT CAG TCG AAA GGC AAG AAG CG - 3'

Sal I

V6483 (reverse)

5' - GCG ATA GTC GAC TTA GTC TCC AAG AAT CAG TTT TAC AAA AGA TG - 3'

Sal I

Human Heat Shock Protein 27 oligonucleotides: (Genbank Accession No. X54079)

N3984 (forward)

5' - GAG GGA TCC AGC ATG ACC GAG CGC CGC GTC CCC TT - 3'

Bam HI

N3985 (reverse)

5' - CTG GGA TCC GGG CTA AGG CTT TAC TTG G - 3'

Bam HI

Human polyhomeotic 2 homologue (HPH2) oligonucleotides: (Genbank Accession No. U89278)

C4045 (forward)

5' - GCG AAG CTT **ATG** GAC TAC AAG GAC GAC GAT GAC AAG CAG GCC ATT GTG

Hind III Start FLAG epitope

AAA CCC CAA ATC CTG ACG CAT GTT ATC - 3'

C4047 (reverse)

5' - GCG GGA TCC GCC CTA GGA GTC CTT GAG CAT GCT GAT - 3'

Bam HI

D5865 (forward)

5' - GCG GAT CCA GGC CAT TGT GAA ACC CCA AAT CCT G - 3'

Bam HI

2.1.11 Cell Lines

Human HeLa cells and COS-1 cells were obtained from the European Collection of Animal Cell Cultures, ECACC Nos 85060701 and CRL1650 respectively.

2.2 DNA and RNA Methods

2.2.1 PCR amplification of DNA fragments

Typically, PCR reactions were carried out in 50 µl total reaction volumes comprising of: 50-200 ng of cDNA or plasmid DNA template, 10 pmoles of each oligonucleotide, 5 units of AmpliTaq DNA polymerase, 2 µl DMSO, 5 µl 10X PCR buffer, 5 µl of a 2.5 mM dNTP mix (dATP,dTTP,dCTP and dGTP) and sterile dH_2O. The reaction mixture was overlayed with 2 drops of paraffin oil and amplified for 30 cycles under the following conditions 95°C/1 min, 60°C/1 min, 72°C/1 minute. Oligonucleotides were usually designed to have a melting temperature (Tm) of > 60°C. Samples were then analysed by agarose gel electrophoresis.

2.2.2 Analysis of DNA fragments by gel electrophoresis

Horizontal, submerged gel electrophoresis was typically carried out on 1 % (w/v) agarose gels in TAE buffer containing 25 µg/ml ethidium bromide and electrophoresed at 100 V/cm. The DNA bands were visualised under UV light at

254_{nm}. Agarose gel electrophoresis was used analytically and preparatively, the latter for purification of DNA fragments for cloning.

2.2.3 Purification of DNA fragments from agarose gels

DNA fragments were purified from agarose gels using Geneclean II (Bio 101 Inc, CA., USA) following the manufacturers instructions. In brief, the desired DNA bands were excised from the agarose and incubated for 10 min with 2.5 volumes of sodium iodide at 55°C. To each sample, glass milk (5 µl/µg of DNA) was added and mixed by rotation at room temperature for 5 min before spinning at 13,000 rpm for 5 seconds. The supernatant was discarded and the glassmilk pellet with bound DNA was washed three times with 1 ml NEW wash buffer (Bio101 Inc.) and spun at 13,000 rpm for 5 seconds between each wash. After the supernatant from the final wash was removed, the pellet was air dried for 5 min to remove any traces of ethanol. The DNA was then eluted from the glass beads by resuspending the pellet in 30 µl of distilled water and incubating at 55°C for 5 minutes. After a final spin at 13,000 rpm for 1 minute the eluted DNA solution was carefully removed.

2.2.4 Analysis of of DNA fragments by restriction enzyme

For general restriction enzyme analysis, 1-2 µg of DNA was incubated in the appropriate enzyme buffer with 10 units of restriction enzyme at 37°C* for 1-2 hours. Digestions were stopped by adding sample loading buffer and the bands were resolved by agarose gel electrophoresis. In cases where the DNA was to be used in subsequent sub-cloning procedures the amounts of DNA and enzyme were scaled up to 10 µg and 20 units respectively and incubated for a period of 2-4 hours.

* Sma I digestions for the construction of GST-ΔMAPKAPK-2 were carried out at 25 °C.

2.2.5 Alkaline phosphatase treatment of DNA fragments

Prior to sub-cloning DNA fragments cut with a single restriction enzyme, either the vector or the fragment were treated with alkaline phosphatase to prevent self-ligation of the fragments or re-ligation of the vector. The reaction was carried out by adding alkaline phosphatase (10 U /μg DNA) to an appropriate volume containing 10X phosphatase buffer. After incubating at 37°C for 45 min, the DNA was purified once by phenol /chloroform/isoamyl alcohol (24:24:1) extraction, followed by a single chloroform extraction. The DNA was then precipitated by adding 2.5 volumes of 100% ethanol and 1/10 volume of 3 M sodium acetate (pH 4.6) and incubated at -20 °C for 1 hour, followed by micro-centrifugation at maximum speed for 15 minutes. The DNA pellet was then washed once in 70% ethanol and resuspended in an appropriate volume of water.

2.2.6 DNA ligations

DNA fragments were ligated using bacteriophage T4 DNA ligase in a total reaction volume of 20 μl comprising: 4 μl of 5X ligation buffer, 2 units of T4 DNA ligase, 100 ng of vector DNA and a 3 Molar excess of insert fragment. Control ligations containing only the vector were routinely carried out to determine the transformation efficiency. Ligations were incubated at room temperature for a minimum of one hour, before transformation into the appropriate competent cells.

2.2.7 Transformation of competent *E.coli* cells

Epicurian® *E.coli* XL-1 Blue competent cells were transformed following the manufacturer instructions. Briefly, 1.7 µl of β-mercaptoethanol was added to 100 µl of competent cells and incubated on ice for 10 min. 0.1-50 ng of DNA was added and incubated for a further 30 min on ice. Each sample was heat shocked at 42°C for 45 seconds and chilled on ice for 2 minutes before the addition of 0.9 ml pre-warmed SOC medium and incubated at 37°C for 1 hr with constant shaking. 200 µl of each sample was plated out onto the appropriate antibiotic plates and incubated at 37°C overnight.

Electro-transformation of HB101 cells was carried out in 0.2 cm electroporation cuvettes using a Bio-Rad gene pulser and pulse controller. In brief, 40 µl of electrocompetent *E.coli* HB101 cells and 1 µl of plasmid (1-20 ng) in TE buffer were mixed and incubated on ice for 1 minute. The gene pulser apparatus was set at 25 µF and 2.5 kV and the pulse controller was set at 200 Ω. The mixture was then transferred into a pre-chilled electroporation cuvette and pulsed. The cuvette was removed and 1 ml of SOC medium was immediately added to resuspend the cells. The cell suspension was transferred to a sterile 15 ml polypropylene tube and allowed to recover at 37°C for 1 hr with constant shaking. 200 µl of each transformation were plated onto appropriate antibiotic plates and incubated at 37°C overnight.

2.2.8 Isolation of plasmid DNA (Maxi Protocol)

Large scale preparation of plasmid DNA from 100-200 ml of overnight culture (2XTY medium containing 100 µg/ml of ampicillin), was carried out using a QIAGEN-tip 500 following the manufacturers instructions. In brief, the cells were

pelleted by centrifugation at 5,000 rpm for 10 minutes and resuspended in 10 ml of buffer P1. 10 ml of buffer P2 was added mixed gently and then incubated at room temperature for 5 min. 10 ml of chilled buffer P3 was then added and incubated on ice for 20 min. The cell lysate was cleared by centrifugation at 12,000 rpm at 4°C for 30 min. The supernatant was added to an equilibrated QIAGEN-tip 500 (equilibrated by adding 10 ml of buffer QBT) and allowed to flow through by gravity pressure only. Following this, the QIAGEN-tip was washed with 2 X 30 ml of buffer QC. The DNA was then eluted with 15 ml of buffer QF, mixed with 0.7 volumes of isopropanol (10.5 ml) and centrifuged at 7,000 rpm 4°C for 30 minutes. The DNA pellet was air dried and resuspended in TE buffer.

2.2.9 Isolation of plasmid using QIAprep spin columns (mini-preps)

Plasmid mini-preps using Qiagen spin columns were used to rapidly purify plasmid DNA from recombinant colonies for restriction enzyme analysis following the manufacturers instructions. In this method all the centrifugation steps were carried out in a bench top centrifuge at maximum speed (13,000 rpm). In brief, 1.5 ml of culture was centrifuged for 5 min and the cell pellet was resuspended in 250 µl of buffer P1. To this, 250 µl of lysis buffer P2 was added and mixed by gentle inversion. The solution was then neutralised by adding 350 µl of buffer P3 and mixing immediately. The cell lysate was centrifuged for 10 minutes and the cleared supernatant was added to a QIAspin column. The column was placed in a 2 ml collection tube and spun for 60 sec. The flow through was discarded and 0.5 ml of wash buffer (PB) was added and spun for 60 seconds. The column was then washed with 0.75 ml of buffer PE and centrifuged for 60 seconds. Finally, the DNA was eluted by adding 50 µl of H_2O to

the column which was then allowed to stand at room temperature for 1 min. Centrifuging for a further minute eluted the DNA solution.

2.2.10 Optical density measurement of DNA

The concentration of DNA was determined by optical density measurement in a quartz cuvette at 260 nm, using a Unicam 5625 UV/VIS spectrometer, assuming an $OD_{260\,nm}$ of 1.0 represents a concentration of 50 μg/ml.

2.2.11 Analysis of transformed recombinant colonies by PCR screening

This method was used to rapidly screen colonies for cloned inserts and to determine the correct orientation when non-directional cloning was carried out. Individual colonies were picked using sterile inoculating needles and mixed with 20 μl of PCR reaction mix (see section 2.2.1). To enable the correct orientation of the inserts to be determined, the reaction mix contained a sense oligonucleotide complementary to vector sequence flanking the multiple cloning sites and an anti-sense oligonucleotide designed from the gene sequence. The reaction was overlayed with paraffin oil and amplified for 30 cycles under the following conditions 94°C/1 min, 55°C/1 min and 72°C/3 min.

2.2.12 DNA sequencing

DNA sequencing reactions were carried out in 0.5ml thin-bottomed Eppendorf tubes. Each reaction comprised of; 3.2 pmol sequencing primers, 0.5-1.0 μg plasmid DNA, 4 μl sequencing buffer and 4 μl of reaction premix (Big Dye Terminator Reaction Ready, Applied Biosystems). Distilled water was added to a final volume of 20 μl. The reactions were then thermo-cycled in a Biometra™ Trio-Thermoblock with

heated lid, for 25 cycles under the following conditions 96°C/30 sec, 50°C/15 sec, 60°C/4 min. The DNA was precipitated by adding 2 µl of 3 M sodium acetate, pH 4.6 and 50 µl of 95% ethanol. The samples were incubated on ice for 10 min and then centrifuged at maximum speed on a bench top centrifuge for 15 minutes. The ethanol was removed and the pellet was allowed to air dry before resuspending in sample loading buffer. Sequence reactions were run on a 373A automated DNA sequencer (Applied Biosystems).

2.2.13 Isolation of mRNA

To isolate polyA$^+$ mRNA from HeLa cells the Micro-FastTrack^{TM} Kit (Invitrogen) was used. Briefly, cells (1X10^6) were lysed in a detergent based buffer containing RNase/Protein degrader, incubated at 45°C for 15 minutes and then applied directly to an oligo (dT) cellulose spin column. DNA, degraded proteins and cellular debris were washed off the resin with a high salt buffer (0.5 M). Non-polyadenylated RNAs were washed off with a low salt buffer (0.25 M) and polyA$^+$ mRNA is then eluted in the absence of salt (10 mM Tris-Cl, pH 7.5).

2.2.14 Synthesis of first-strand cDNA for RT-PCR

First-strand cDNA from mRNA was generated using the cDNA Cycle® Kit (Invitrogen). Briefly, 0.01-1 µg of mRNA was mixed with random primers (1 µg), heated at 65°C for 10 minutes and then allowed to anneal at room temperature for 2 minutes. First-strand cDNA was transcribed in a 20 µl reaction volume comprising of: AMV reverse transcriptase (5U), 5 X RT buffer, 1 µl of dNTPs (100 mM) and 1 µl of 80 mM sodium pyrophosphate. The mixture was then incubated at 42°C for 1 hour. RNA-cDNA hybrids were denatured by heating at 95°C and cooled rapidly on ice. To

carry out gene specific PCR amplifications, 2-5 µl of the reverse transcriptase mixture was used as template under the conditions described in section 2.2.1.

2.2.15 Ribonuclease protection assays

Ribonuclease protection assays (RPA) were carried out using the Direct Protect™-lysate RPA system (Ambion). This method allows direct detection and quantitation of target RNA in crude lysates of solid tissue or cultured cells. In brief, cells (1.5×10^6) were seeded into 60 mm tissue culture plates and allowed to recover for 5-6 hours. Following pre-treatment with inhibitor (2 hrs) and IL-1 (20 ng/ml) for 8 hours the cells were lysed in 150 µl of guanidine thiocyanate buffer (GuSCN). Cellular debris was pelleted by spinning for 10 minutes at maximum speed in a refrigerated microfuge. The supernatant was removed and stored at -20°C until required.

The COX-2 riboprobe was transcribed using T7 polymerase from a 256 bp Cla I (1549)/ Bst YI (1805) COX-2 restriction enzyme fragment, cloned into pBluescript (kindly provided by Dr. A.Clark, Kennedy Institute of Rheumatology, London). Pharmingen supplied the hGAPDH housekeeping control template used for *in-vitro* transcription. *In-vitro* transcription reactions were typically carried out in a total volume of 20 µl comprising: 2 µl of DTT (100 mM), 2 µl of T7 transcription buffer (10X), 1 µl RNasin (40U/µl), 1 µl template DNA (0.1-1.0 µg/µl), 5 µl [α-^{32}P] UTP (~800Ci/mmol), 4 µl of ATP, GTP, CTP (2.5 mM each), 2.5 µl of UTP (100 µM) and 1 µl of T7 polymerase (15U/µl). The reaction was incubated at 37°C for 1 hour followed by the addition of 1 µl of RNase-free DNase I and incubated at 37°C for a further 30 minutes. Spin columns removed unincorporated nucleotides and the reaction was purified once by phenol-chloroform extraction and ethanol precipitated.

The RNA pellet was resuspended in 100 µl of TE buffer from which a 1 µl aliquot was removed and counted. 5 µl of labelled probe (10^5 cpm/µl) was hybridised overnight with 45 µl of lysate. For each probe two control tubes containing 5 µl of probe + 45 µl of lysis buffer were also set up. One tube acted as a control to ensure RNase digestion was complete and the other as a minus RNase control. Single-strand specific ribonuclease cocktail (440 µl H_2O, 50 µl buffer, 10 µl RNase cocktail) was added to digest unprotected RNA and incubated at 37°C for 30 minutes. 10 µl of Proteinase K (20 mg/ml) and 10 µl of 10% sodium sarcosyl were added and incubated for 30 minutes at 37°C. Protected fragments were precipitated with isopropanol and resuspended in 10 µl of loading buffer. Samples were heated for 5 minutes at 95°C, resolved by electrophoresis on a 6% polyacrylamide gel and analysed on a phosphorimager.

2.3 Cell Culture and Cell Biology Methods

2.3.1 General cell culture

HeLa and COS-1 cell lines were cultured in DMEM (Dulbeccos Modified Eagles Medium) supplemented with 10% (v/v) heat-inactivated foetal calf serum, 2 mM glutamine, 50 µg/ml penicillin and 50 mg/ml streptomycin. Stable cell lines were maintained in the above medium containing G418 antibiotic at 500 µg/ml. Both HeLa and COS-1 are adherent cells and were routinely passaged in T175 flasks. To remove the cell monolayers 5 ml of trypsin /EDTA in Pucks modified saline solution (GIBCO) was added and the cells were incubated at 37°C in 5% CO_2 for 5 min. A further 5 ml of serum-containing DMEM was added, 1 ml of this was then removed

and added to 50 ml of fresh serum-containing DMEM. The flask was then incubated at 37°C in 5% CO_2 for 3-4 days before passaging again. For long term storage, pelleted cells (~2.5 x 10^6) were resuspended in medium containing 10% (v/v) DMSO, aliquoted into freezing vials and stored in liquid nitrogen.

2.3.2 Transient transfection of COS-1 and HeLa Cells

The expression of recombinant proteins in mammalian cells was tested by transiently transfecting either COS-1 or HeLa cells. COS-1 cells were transfected as described by (Whittle *et al.*, 1987), which is an adaptation of the procedure set out by (Lopata *et al.*, 1984). Cells cultured in DMEM, 10% FCS, 2 mM glutamine, 50 ug/ml penicillin and 50 mg/ml streptomycin were plated out into 24 well tissue culture plates at a density of 2 x 10^5 cells/ml and allowed to adhere overnight. Cells were washed twice with serum-free DMEM and incubated for 6-8 hours at 37°C with a DNA-dextran mixture consisting of 1-3 µg DNA in serum-free DMEM buffered with 50 mM Tris-HCl pH 7.5 and 0.2 mg/ml DEAE dextran (Pharmacia) prepared in TBS (25 mM Tris-HCl pH 7.4, 38 mM NaCl, 5 mM KCl, 0.5 mM $MgCl_2$, 0.7 mM $CaCl_2$, 0.6 mM Na_2HPO_4). The DNA-dextran complex was removed and the cells were shocked by adding 10% (v/v) dimethyl sulphoxide (DMSO) in Hepes buffered saline pH 7.4 (138 mM NaCl, 5 mM KCl, 6 mM glucose, 0.7 mM Na_2HPO_4, 21 mM Hepes) and incubating at room temperature for 3 minutes. Cells were washed once with serum-free DMEM before adding 1 ml of fresh serum-containing medium and incubating at 37°C in 5% CO_2. Two days after transfection the cells were harvested in mammalian cell lysis buffer and assayed for protein expression by Western immunoblotting (see section 2.4.4).

HeLa cells were transiently transfected using SuperFect™ Transfection Reagent (QIAGEN) following the manufacturers protocol with minor modifications. Briefly, the cells were seeded at 2 x 10^5 /ml in a 24 well tissue culture plate and incubated overnight to 40-80% confluency. Plasmid DNA (1-3 μg) was diluted in serum-free DMEM to give a total volume of 60 μl (in co-transfection experiments 1-1.5 μg of each plasmid was added). SuperFect™ transfection Reagent (5 μl/μg DNA) was added and mixed by vortexing. The mixture was then allowed to stand at room temperature for 10 minutes to allow the formation of transfection complexes. During this time the cells were washed once with 1 ml of PBS. Serum-containing DMEM (350 μl) was added to the reaction tubes containing the transfection complexes, mixed by pipetting and added immediately to the cells, which were then incubated for 2-3 hr at 37°C in 5% CO_2. The transfection medium was removed and the cells were washed once with PBS. Fresh medium (1 ml) was added and the cells were incubated at 37°C in 5% CO_2 for 2-3 days.

2.3.3 Large scale transient transfection of COS-1 cells

In some cases, such as for the p38 MAP kinase assays, a larger yield of protein material was required. To achieve this a confluent T175 tissue culture flasks was transiently transfected as described in section 2.3.2, with the following modifications. T175 flasks were seeded with 50 ml of medium containing 2 X 10^5 cells/ml, 100 μg of DNA was added in 10 ml of transfection buffer (serum-free DMEM+DEAE dextran in TBS), the cells were shocked by adding 10 ml of 10% DMSO in HBS buffer. Finally, the cells were washed twice with PBS and 50 ml of fresh medium was added.

2.3.4 Generation of stable cell lines

HeLa cell lines stably expressing c-Myc-tagged MAPKAPK-2 and MAPKAPK-2 anti-sense message were generated as follows. Cells were transfected as described in section 2.3.2, with the following modifications. Cells ($2x10^5$) were seeded in 60 mm plates such that they were only 20-40% confluent on the day of transfection. Plasmid DNA (5 μg) was diluted in serum-free DMEM to give a total volume of 150 μl, into which 20 μl of SuperFect™ reagent was added and mixed by vortexing. After the formation of transfection complexes (5-10 min) serum-containing DMEM (1 ml) was added and the cells were incubated for 2-3 hr. The transfection mixture was then removed and the cells were washed 3-4 times with 4 ml of PBS. Fresh medium (3 ml) was then added and the cells were incubated at 37°C in 5% CO_2. After 48 hours the cells were washed twice with PBS and harvested by trypsinisation. The cells were counted and diluted to a density of 5,000 cells/ml in medium containing G418 (500 μg/ml) and then seeded into 20 x 96-well plates (200 μl/well) and incubated at 37°C in 5% CO_2. After 2-3 weeks the plates were examined for wells containing only a single G418 resistant colony. Colonies were removed by trypsinisation and inoculated into 1 ml of medium containing G418 (500 μg/ml) in 24 well plates and incubated until confluent. The colonies were then expanded up into T175 tissue culture flask. Isolated clones were screened by Western blotting using an anti-c-Myc polyclonal antibody for epitope-tagged MAPKAPK-2 expression (see section 2.4.4) or by RT-PCR for MAPKAPK-2 anti-sense message (see section 2.2.14). A G418 resistant HeLa control cell line transfected with empty pcDNA3 was also generated as described above.

2.3.5 COX-2 reporter gene assays

Cells from the G418 resistant HeLa control cell line (pcDNA3 transfected) were seeded at a density of 20,000 cells/well into a 96-well tissue culture plate and incubated overnight at 37°C in 5% CO_2. The following day the cells were washed once in PBS and transiently transfected using Superfect™ transfection reagent following the manufacturers protocol. Briefly, 550 ng of plasmid DNA (comprising of 500 ng of either COX-2 or E-selectin promoter firefly luciferase reporter gene vectors and 50 ng of renilla luciferase reporter gene vector) and 2.5 µl of transfection reagent were diluted in 20 µl and 30 µl of serum-free medium respectively. The two mixtures were added together and incubated for 5-10 min at room temperature. Serum-containing medium (150 µl) was then added and the mixture was added to the washed cells and incubated at 37°C in 5% CO_2 for 3 hours. The transfection medium was then removed and the cells were washed once in PBS before adding 200 µl fresh serum-containing medium and incubating for 16 hours. The amounts and volumes described above are those required for a single transfection. In all experiments carried out a master transfection mix using these amounts and volumes was made and then aliquoted accordingly.

The following day the medium was removed and replaced with 100 µl of phenol red free medium with or without IL-1α (20 ng/ml) and the cells were incubated for a further 8 hours. 100 µL of reconstituted LucLite substrate (Packard) was then added and incubated for 10 min with gentle agitation. The plate was counted on a TopCount™ Microplate Scintillation and Luminescence Counter. To each well 50 µl of RenLite substrate was then added and incubated for 30 min before counting again.

2.3.6 IL-6 and IL-8 ELISA

ELISA assays were carried out to measure the concentration of IL-6 and IL-8 secreted into the overlaying tissue culture medium following stimulation of stably transfected HeLa cells (10^6) with IL-1α (20 ng/ml) for 16 hours. In this experiment and also in the PGE_2 ELISA (see section 2.3.7) some of the samples were pre-treated for 2 hours with SB 203580 (1 μM) prior to stimulation.

Purified anti-cytokine antibodies were diluted to 1μg/ml in binding solution (0.1 M Na_2IIPO_4, adjusted to to pH 9.0 with 0.1 M NaH_2PO4), 50 μl was added to the wells of an enhanced protein-binding ELISA plate (Nunc Maxisorb) and incubated overnight at 4°C. The plates were then blocked by adding 200 μl/well of blocking buffer (filtered PBS containing 10% foetal calf serum) and incubated at room temperature for 2 hours. The plates were then washed three times in PBS +0.05% Tween-20. IL-6 and IL-8 standards and the samples (prepared by diluting in serum-free DMEM in doubling dilutions) were added at 100 μl/well and incubated at room temperature for 3 hours. The plates were then washed 4 times with PBS +0.05% Tween-20. Biotinylated anti-IL6/IL-8 detection antibodies (Pharmingen) were diluted to 1 μg/ml in blocking buffer and added at 100 μl/well. The plates were incubated for 1 hour at room temperature and then washed 4 times with PBS +0.05% Tween-20. AMDEX™ streptavidin-horseradish peroxidase (HRP) conjugate (Amersham Pharmacia Biotech, UK) was diluted (1:2500) in blocking buffer and added at 100 μl/well and incubated at room temperature for 30 minutes. The plates were washed 4 times with PBS +0.05% Tween-20 and 100 μl/well of TMB* substrate was added and incubated at room temperature for colour development (10-80 minutes). The optical

density for each well was determined by reading at 405 nm on a Microplate Autoreader.

*To make TMB substrate 2 L of β-cyclodextrin buffer (3.3 g sodium acetate, 0.77 ml acetic acid, 40 g β-cyclodextrin, 20 ml DMSO and 66.8 µl of hydrogen peroxide) was mixed with 20 ml of TMB (0.63 g, 21 ml DMSO).

2.3.7 Prostaglandin E_2 determination

Prostaglandin E_2 (PGE_2) levels were measured in the overlaying culture medium following activation of the cells with IL-1α using a PGE_2 Immunoassay Kit (Caymen, US). The assay is based on the competition between PGE_2 and a PGE_2-acetylcholinesterase conjugate (PGE_2 tracer) for a limited amount of PGE_2 monoclonal antibody. Because the concentration of the PGE_2 tracer is held constant while the concentration of PGE_2 varies, the amount of PGE_2 tracer that is able to bind to the PGE_2 monoclonal antibody will be inversely proportional to the concentration of PGE_2 in the well. The antibody-PGE_2 complex then binds to a goat anti-mouse polyclonal antibody on pre-coated plates. The assay conditions and final PGE_2 concentrations were carried out following the manufacturers protocol. The standards and samples were diluted in culture medium.

2.4 Protein methods

2.4.1 Immunoprecipitation of epitope-tagged and endogenous proteins

Epitope-tagged and endogenous proteins were immunoprecipitated from either transiently or stably transfected cells as follows. Cells were typically lysed in 1 ml of

ice-cold mammalian cell lysis buffer and cellular debris was pelleted by microcentrifugation at 13,000 rpm for 10 min at 4°C. The supernatants were removed and pre-cleared by adding 50 µl of a 50% slurry of washed Gammabind G sepharose and incubated at 4°C for 1 hour with constant rotation. The samples were centrifuged at maximum speed for 15 seconds and the supernatant was carefully removed and added to fresh Eppendorf tubes. Antibody was added at the concentration recommended by the manufacturer (anti- FLAG (3 µg/ml), anti-c-Myc (5 µg/ml), anti-rabbit MAPKAPK-2 (5 µg/ml) or anti-Hsp27(10 µl serum)) and incubated overnight at 4°C with gentle rotation. To precipitate the immune complexes, 50 µl of a 50% slurry of Gammabind G Sepharose was added and mixed by rotating slowly at 4°C for 4 hours. The sepharose beads were pelleted by centrifugation at maximum speed for 15 seconds and the supernatant was carefully removed. The beads were washed once in lysis buffer supplemented to 0.5M NaCl, once in lysis buffer containing 0.1% SDS and once in TE containing 0.1% NP40. After the final wash the beads were resuspended in the desired volume and 5X sample loading buffer was added. Immunoprecipitated proteins used for kinase assays were not resuspended in loading buffer, but instead the beads were additionally washed twice and resuspended to a 50% slurry in kinase buffer.

2.4.2 Batch purification of epitope-tagged protein

FLAG-tagged p38 MAP kinase used for the SB 203580 titration assay was batch purified from transiently transfected COS-1 cells grown in a T175 tissue culture flask (see section 2.3.3). The cells were lysed in 25 ml of mammalian cell lysis buffer and centrifuged (7000 rpm for 15 min at 4 °C) to precipitate the cellular debris. The supernatant was removed and pre-cleared by adding 1250 µl of a 50% slurry of

Gammabind G sepharose and incubated at 4 °C with constant rotation for 1 hour. The beads were then precipitated by centrifugation (3000 rpm for 5 min at 4 °C) and the supernatant removed. Anti-FLAG antibody (75 µg) was added and incubated for a minimum of 4 hours with constant rotation at 4 °C. The immune complexes were precipitated by adding 1250 µl of a 50% slurry of Gammabind G sepharose and incubated at 4 °C with constant rotation for 2 hours. The beads were pelleted by centrifugation (3000 rpm for 5 min at 4 °C), washed twice in lysis buffer and twice in kinase buffer and resuspended to 50% before aliquoting into equal volumes.

2.4.3 Preparation of GST-fusion proteins

To prepare GST-ΔMAPKAPK-2wt, GST-ΔMAPKAPK-2 K93R, GST-Hsp27 and GST-HPH2 fusion proteins, 10 ng of each construct was transformed into ultra competent Epicurian Coli XL-1 Blue cells. The transformation mixtures were plated onto LB agar plates containing ampicillin (100 µg/ml) and incubated overnight. Single colonies from each transformed clone were then picked and used to inoculate 20 ml of 2XTY broth containing ampicillin (100 µg/ml) and incubated overnight. The following day 500 ml of pre-warmed 2XTY broth containing antibiotic were inoculated with the 20 ml of overnight culture and incubated at 30°C with constant shaking (200 rpm), until an OD_{600nm} = 0.6 - 0.7. Isopropyl-β-D-thiogalactoside (IPTG) was added to 0.2 mM and the cells were incubated for a further 4 hours. The cells were then pelleted by centrifugation (5000 rpm for 10 min) and resuspended in 10 ml of PBS supplemented with 1 mM DTT and a Complete™ protease inhibitor cocktail tablet. The cells were snap frozen in liquid nitrogen and then thawed at 42 °C. The suspension was then sonicated (4X20 seconds) and 0.1% Brij 35 was added. Cellular debris was removed by centrifugation (15,000 rpm for 30 min at 4 °C) and

the supernatant was carefully removed and loaded onto a packed glutathione sepharose column (Pharmacia Biotech). The column was washed and GST-fusion proteins eluted as described in the manufacturers protocol.

2.4.4 Immunological detection of proteins (Western blotting)

Whole cell lysates (pre-spun to remove cellular debris) or immunoprecipitated proteins bound to sepharose beads were mixed with 5X sample loading buffer, heated at 95 °C for 5 minutes and centrifuged at 13,000 rpm for 1 minute. Typically, between 10-35 µl of each sample was loaded onto either a 10% or 4-20% pre-cast Tris-glycine polyacrylamide gel (Novex). Gels were subjected to electrophoresis with appropriate molecular weight markers at 100 V/50 mA until the bromophenol blue dye front reached the bottom of the gel. Samples were transferred onto Millipore nylon membrane, pre-wetted in methanol, using Novex blotting apparatus in Tris-glycine buffer for 2 hours at 30 V/200 mA. The success of the transfer could be demonstrated by using pre-stained molecular weight markers. The membrane was washed twice in water and then blocked in PBS containing 5% Marvel for 1 hour at room temperature with constant agitation. The membrane was then incubated with the primary antibody diluted in blocking buffer according to the manufacturers instructions. Following incubation with primary antibody the membrane was washed three times for 5 minutes each in PBS and then incubated with the appropriate conjugated secondary antibody diluted in blocking buffer according to the manufacturers instructions. Finally, the membranes were washed three times for 5 minutes each in PBS+0.05% Tween-20 at room temperature followed by rinsing in 3-4 changes of distilled water. Proteins were detected using the Peirce enhanced chemiluminescence system and the signal was visualised by exposure to X-ray film.

2.4.5 Immune complex kinase assays

Kinase assays were typically carried out in 50 µl reaction volumes of which 30 µl comprised of a 50% slurry of sepharose beads complexed with epitope-tagged protein (either c-MycMAPKAPK-2 or FLAGp38 MAP kinase). The remaining volume comprised: 2-5 µg of GST-fusion protein substrate(s), radiolabelled [γ^{32}P]ATP (5 µC*i*), unlabelled ATP (20 µM) and 10X kinase buffer. In the reactions containing SB 203580, the inhibitor was diluted in DMSO and added in a volume that did not exceed 1% of the total reaction volume. The reactions were incubated at 37°C for 25 minutes and then stopped by the addition of 5X protein loading buffer. The samples transferred to nylon membranes (as described in section 2.4.4) and visualised by autoradiography.

2.4.6 Metabolic labelling of cells with ^{32}P-orthophosphate

Cells (1X 10^6) were seeded into 6-well tissue culture plates and incubated overnight. The following day the medium was removed and the cells were washed twice in serum-free, phosphate-free DMEM. The cells were then incubated in phosphate-free DMEM containing 10% dialysed foetal calf serum and 100µCi/ml ^{32}P-orthophosphate. After 5 hours the medium was removed and the cells were washed twice in PBS and then lysed in 1 ml of mammalian cell lysis buffer. Endogenous Hsp27 was immunoprecipitated using an anti-Hsp27 antibody complexed to Gammabind G sepharose as described in section 2.4.1. The samples were transferred to nylon membrane as described in section 2.4.4 and phosphorylated Hsp27 was visualised by autoradiography. In this experiment, cells were treated with or without IL-1α (20ng/ml) and SB 203580 (1 µm), which were added 20 minutes and 2 hours respectively before lysis.

2.5 Yeast Two-Hybrid Methods

2.5.1 Plasmid library titering

Prior to screening the human leucocyte MATCHMAKER cDNA library, it was amplified to obtain sufficient plasmid for large scale yeast transformations. The high titre library stock was thawed and 1 µl was added to 1 ml of pre-warmed LB broth to give a 10^3 dilution. This was then repeated to give a dilution of 10^6. From each dilution, 1 µl was removed and added to 50 µl of LB broth and spread onto prewarmed LB+Amp (100 µg/ml) agar plates. The plates were incubated overnight at 37 °C and the number of colonies on each plate were counted. The titer of the library (cfu/ml) was determined for each dilution factor and an average value of $7.4x10^9$ cfu/ml was calculated. Using this value the *E.coli* transformants were plated to obtain at least 2-3X the number of independent clones in the library (~ $2X10^6$).

2.5.2 Library amplification

Cells were plated onto 30 X (243 x 243 mm) sterile bioassay plates (Nunc) containing selective medium (LB+Amp 100 µg/ml) at a density of 70,000 colonies/plate and incubated overnight at 37 °C. The following day the colonies were harvested by scraping and the plates were washed with LB+Amp. The suspension was incubated at 37 °C for 2-4 hr with shaking. The cells were then pelleted and plasmid DNA was purified using Qiagen 500 columns as described in section 2.2.8.

2.5.3 Transformation of plasmid(s) into competent yeast cells

The LiAc method for preparing yeast competent cells was done following the method of (Gietz *et al.*, 1992). The human leucocyte library (GAL4 AD/library 'hybrid') was co-transformed with the GAL4 BD/MAPKAPK-2 K93R 'hybrid' as detailed below

(the volumes indicated in parenthesis are for small scale yeast transformations with either singularly transfected or co-transfected plasmids).

Several colonies of yeast HF7z cells, 2-3 mm in diameter, were inoculated into 1 ml of YPD broth and vortexed vigorously to disperse the clumps. The suspension was then transferred into a flask containing 100 ml (50 ml) of YPD and incubated at 30 °C for 16-18 hr with shaking at 250 rpm to stationary phase (OD_{600}> 1.5). The culture was then diluted into a new flask containing 1 L (300 ml) of YPD to produce an OD_{600}= 0.2-0.3 and incubated for 4 hr at 30 °C with shaking at 230 rpm. The cells were then pelleted by centrifugation at 4000 rpm for 5 min at room temperature and washed in 500 ml (50 ml) of sterile water. The cells were pelleted once again by centrifugation and resuspended in 8 ml (1.5 ml) of 1X TE/LiAc.

The library DNA and pAS2.1/BDMAPKAPK-2 K93R, 500 μg each (0.1 μg), were then mixed with 20 mg (0.1 mg) of herring testes carrier DNA and added to 8 ml (0.1 ml) of competent yeast cells. Sterile PEG/LiAc solution, 60 ml (0.6 ml), was added and mixed by vortexing and the suspension was incubated at 30 °C for 30 min with shaking at 200 rpm. The cells were then shocked by adding 7 ml (70 μl) of DMSO and mixed by gentle inversion. After incubating the cells at 42 °C for 15 min, they were chilled on ice for 5 min, pelleted by centrifugation and resuspended in 10 ml (0.5 ml) of TE buffer. 200 μl of cells were spread onto sterile, 135 mm plates (X50) containing SD/Trp^-/Leu^-/His^- and incubated at 30 °C for 7-8 days (for reactions involving only single plasmid transformations, the appropriate SD plates were prepared). To determine the efficiency of transformation and hence the number of colonies screened 10 μl of the transformation mixture was plated onto SD/Trp^-/Leu^-

plates. To check that the co-transformants that survived the *HIS3* growth selection from the library screening were indeed true His^+ colonies, they were picked using sterile inoculating needles and the phenotype was verified again by gridding the colonies onto a freshly made SD/Trp^-/Leu^-/His^- master plate.

2.5.4 β-galactosidase colony lift filter assays

Colony lift β-galactosidase filter assays were done on the isolated co-transformants growing on the SD/Trp^-/Leu^-/His^- master plate (no more than 2 days old). Cells were picked using a sterile inoculating needle and resuspended into 20 µl of TE buffer. 10 µl of this suspension was then spotted onto a 125 mm sterile filter disk (Whatman) overlayed on top of a 135 mm SD/Trp^-/Leu^-/His^- plate and incubated for 48 hours at 30 °C. The cells were permeabilized by lifting the filter and plunging it into liquid nitrogen for 30 sec. The filter was then removed, thawed at room temperature and placed on top of another filter paper that had been pre-soaked in Z-buffer/X-gal solution. Both filters were placed inside a large 135 mm petri dish and incubated at room temperature for a maximum for 8 hours. The plate was checked periodically for the appearance of blue ($LacZ^+$) signals.

2.5.5 Plasmid isolation from yeast cells

Because transformed yeast may take up several plasmids it was important to isolate and check each GAL4AD/library plasmid from each potential HIS^+, $lacZ^+$ positive transformant. Plasmids were isolated from the yeast cells following a procedure based on the methods of (Kaiser and Auer, 1993). This method yields plasmid DNA that is suitable for *E.coli* transformation by electroporation.

Using a single yeast colony, 2 ml of YPD broth were inoculated and incubated at 30 °C until the culture was saturated (~16 hr). The cells were then pelleted by centrifugation at 14,000 rpm for 5 sec at room temperature. The supernatant was removed and the cells were resuspended in 200 µl of lysis solution and vortexed, followed by the addition of 200 µl of phenol:chloroform:isoamyl alcohol (24:24:1) and 0.3 g of 425-600 µm glass-beads (Sigma). The mixture was vortexed for 2 min and then centrifuged at 14,000 rpm for 5 min at room temperature. The aqueous layer was removed and the plasmid(s) were precipitated by adding1/10 volume 3 M NaOAc, pH 5.2 and 2.5 volumes of ethanol. The DNA pellet was washed with 70% ethanol and air-dried before resuspending in 20 µl of TE buffer.

To isolate the library component of the heterogenous plasmid preparation, the mixture was electroporated into *E.coli* HB101 cells and the AD/library plasmid was selected using its *LEU2* selectable marker gene to complement the *leuB* mutation in this *E.coli* strain. The cells were electroporated as described in section 2.2.7 and plated onto SD/Leu$^-$, M9 minimal medium plates containing 50 µg/ml ampicillin, 40 µg/ml proline and 1 mM thiamine-HCl and incubated overnight at 37 °C. To determine if the clone from which the plasmid DNA was prepared contained more than one AD/library plasmids, the transformants were PCR screened as described in section 2.2.11, using oligonucleotides designed to specific vector (pGAD10) sequences flanking the multiple cloning sites. Ten colonies were picked from each transformation and the insert sizes were determined. Plasmid DNA was prepared as described in section 2.2.9 and sequenced from colonies containing different insert sizes.

Chapter 3

Cloning and vector construction

3.1 Introduction

This chapter describes the cloning and construction of epitope-tagged, FLAG-p38 MAP kinase wild type (wt) and kinase dead mutant (K53R), cMyc-MAPKAP kinase-2 (wt) and kinase dead mutant (K93R) and the GST- fusion proteins, Hsp27 and truncated (Δ) MAPKAP kinase-2 (wt) and (K93R) mutant. Epitope-tagged p38 MAP kinase and MAPKAP kinase-2 were constructed in the mammalian expression vector, pcDNA3 (Figure 3.1). GST- fusion proteins were constructed in pGEX-3X (Figure 3.6) vector and expressed in bacteria. The GST-fusion proteins were used as substrates in the kinase assays described in Chapter 4, whilst the kinase dead mutants of p38 MAP kinase and MAPKAPK-2 were used to generate GAL4 binding domain (BD) and activation domain (AD) fusion proteins, used in the yeast two-hybrid study described in Chapter 5. In addition the MAPKAPK-2 constructs were also used to generate stable cell lines described in Chapter 6.

At the time of starting this work the human nucleotide sequence of p38 MAP kinase had only recently been described (Lee *et al.*, 1994). The enzyme encoded by this sequence was found to be the target of a series of compounds that inhibited the production of IL-1 and TNF *in-vivo*. The gene was cloned from a GM-CSF-stimulated monocyte library, using degenerate oligonucleotides designed from peptide sequences following tryptic digestion of the purified enzyme. Two cDNAs, that were identical except for a small sequence of 25 amino acids between residues 230-255 (Figure 3.2) were isolated and named CSBP1 and CSBP2 (cytokine suppressor binding proteins).

CSBP2 differed by only 2 amino acids from the murine homologue (p38), which had previously been described and shown to be rapidly tyrosine phosphorylated by hyperosmotic stress and endotoxin (LPS) stimulation of a murine pre-B cell line, 70Z/3, transfected with the LPS receptor CD14 (Han *et al.*, 1993).

MAP kinase activated protein kinase-2 (MAPKAP kinase-2/MAPKAPK-2) is a serine/threonine protein kinase that was first purified from rabbit skeletal muscle. It was originally identified as an enyzme that could be activated *in-vitro* by the p42 and p44 MAP kinase isoforms and inactivated *in-vitro* by protein phosphatase 2A (PP2A). The nucleotide sequence of rabbit MAPKAP kinase-2 was determined using degenerate oligonucleotides derived from peptide sequences of the purified enzyme (Stokoe *et al.*, 1992).

The first reported human nucleotide sequence of MAPKAP kinase-2, was obtained by screening a human skeletal muscle cDNA library with rabbit cDNA fragments generated by PCR amplification using degenerate oligonucleotides designed from the rabbit peptide sequences. The largest clone obtained from this library was then subsequently used to probe a human teratocarcinoma cDNA library, from which a longer clone was isolated. However, the lack of an initiating methionine residue and the aberrant molecular weight of this clone when expressed, led to the conclusion that it was not a full-length clone (Stokoe *et al.*, 1993). The first full-length clone of MAPKAP kinase-2 was isolated from a human HL60 cDNA library also using a rabbit DNA probe (Zu *et al.*, 1994). However, although this clone had an initiating methionine at the N- terminal, it differed significantly at the C-terminal from the clone described by Stokoe *et al.* (1993) (Figure 3.8). The two isoforms, MAPKAPK-2

a (Stokoe *et al.*, 1993) and MAPKAPK-2b (Zu *et al.*, 1994), are the products of an alternate splicing event at the C-terminus of the same gene and are expressed in high levels in both heart and skeletal muscle tissues (Zu *et al.*, 1997).

Mammalian MAPKAP kinase-2 enzymes contain a proline-rich N-terminal domain, a catalytic domain, the sequence of which is most closely related to the family of calmodulin dependent kinases and a C-terminal domain which contains a putative nuclear localization signal (NLS) (Engel *et al.*, 1993; Stokoe *et al.*, 1993). This signal motif (-K-R-R-K-K-) is absent in the C-terminal of the shorter splice variant described by Zu *et al.* (1994). In transfected cells, MAPKAPK-2 is predominantly located in the nucleus. However, upon cellular stress the protein is rapidly translocated to the cytoplasm. This translocation which can be blocked by treatment with SB 203580 and leptomycin B appears to be regulated and induced by phosphorylation (Engel *et al.*, 1998). In mammalian MAPKAPK-2 enzymes, the sequence immediately N-terminal to the catalytic domain contains two potential proline rich, SH3-binding domain (-P-P-P-X-P-P-) regions (Stokoe *et al.*, 1993; Engel *et al.*, 1993), which are absent in the in the *Drosophila* homologue, Dm MAPKAPK-2 (Larochelle and Suter, 1995). By possessing these binding sites MAPKAP kinase-2 may interact with proteins that contain SH3 domain(s).

The human small heat shock protein (Hsp27) is a metabolically stable protein present at low levels in all cells and tissues. Following stimulation by cellular insults such as heat shock, UV-irradiation, arsenite and pro-inflammatory cytokines (Rouse *et al.*, 1994; Freshney *et al.*, 1994) Hsp27 is rapidly phosphorylated at three serines, the major one being Ser 82 and two minor ones Ser 15 and Ser 78 (Landry *et al.*,1992).

The sequence and organisation of human Hsp27 has been described. Hsp27 is a 205 amino acid polypeptide that shows striking similarity with mammalian α-crystallin (Hickey *et al.*, 1986; Carper *et al.*, 1990). The amino acid sequence of human Hsp27 is homologous to the reported sequences of the small heat shock proteins from other mammals (Gaestel *et al.*, 1989; Lavoie *et al.*, 1990).

3.2 Results

3.2.1 Cloning of FLAG-tagged p38 MAP kinase

To clone p38 MAP kinase (CSBP2) the following oligonucleotide primers were designed, N5378 and N0465, complementary to the terminal 5' and 3' sequences respectively of p38 MAP kinase. The 5' oligonucleotide, N5378, contained the FLAG epitope (-DYKDDDD-) inserted between codons 1 and 2 of the enzyme as well as a Bam HI restriction enzyme site to facilitate cloning. N0465 also contained a Bam HI restriction site. CSBP2 was amplified by PCR from a human peripheral blood mononuclear cell (PBMC) cDNA library. An amplified fragment of ~1143 bp was gel purified, digested with Bam HI and ligated into the mammalian expression vector pcDNA3 (Figure 3.1). Transformed colonies were screened by PCR to determine the correct orientation using a forward, vector specific oligonucleotide (T7) and a reverse p38 MAP kinase specific oligonucleotide. A single clone was sequenced in its entirety on both strands using oligonucleotides designed from the published sequence. In addition, T7 and SP6 vector specific oligonucleotides were used to sequence the 5' and 3' ends respectively. The sequence obtained from this clone was the same as that described by Lee *et al.* (1994) and the clone was named pcDNA3/FLAGp38wt (Figure 3.2). Because CSBP1 and CSBP2 have identical 5' and 3' terminal sequences and therefore either enyzme could be potentially amplified, four additional clones

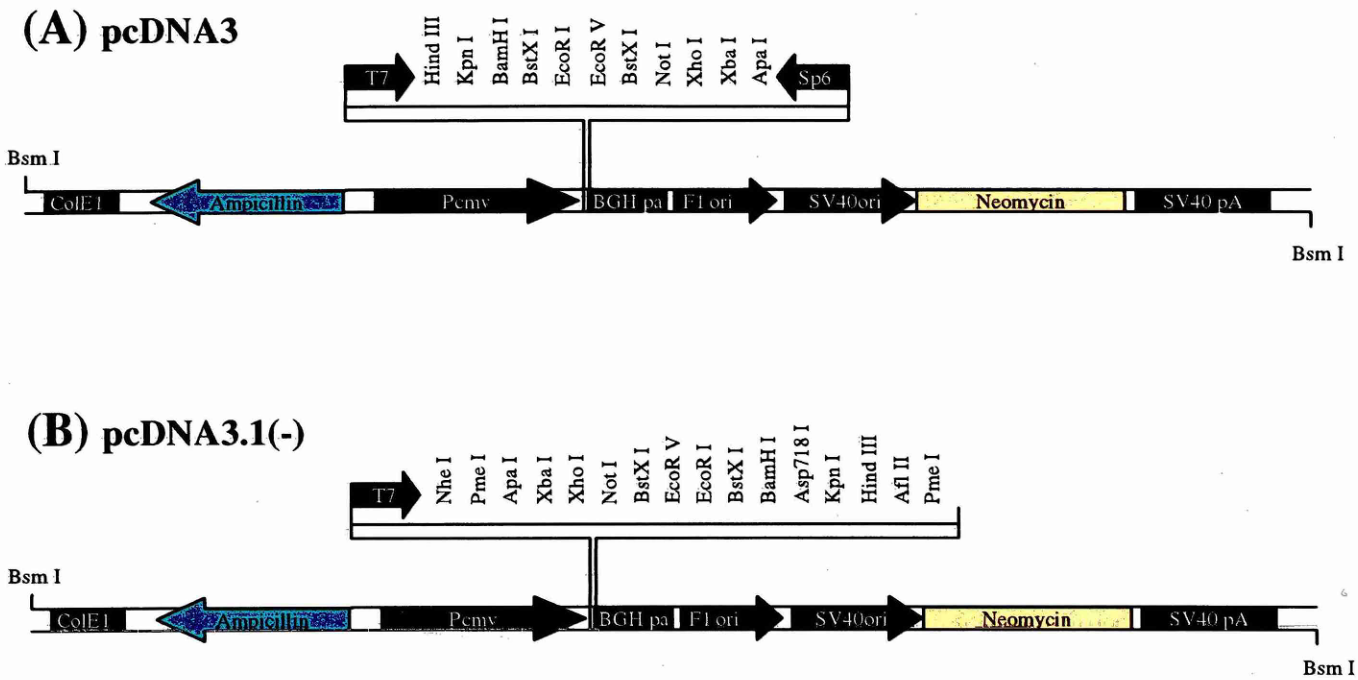

Figure 3.1: Schematic diagram of the mammalian expression vectors pcDNA3 (A) and pcDNA3.1(-) (B). Both vectors are approx. 5.4 kb in size and are identical except, pcDNA3.1 (-) lacks the SP6 promoter and contains a more extensive and inverted multiple cloning site (MCS). The essential features of both plasmids include: CMV (human cytomegalovirus) major intermediate early promoter/enhancer region to drive expression of cloned genes; F1 origin of replication; SV40 origin for transient episomal replication in cells expressing SV40 large T antigen; Neomycin resistance marker, expressed from the SV40 early promoter for the selection of stable transformants in the presence of G418; Bovine growth hormone (BGH) polyadenylation signal for polyadenylation of transcribed mRNAs; β-lactamase gene to confer ampicillin resistance; ColE1 origin of replication from pUC19 for high copy number.

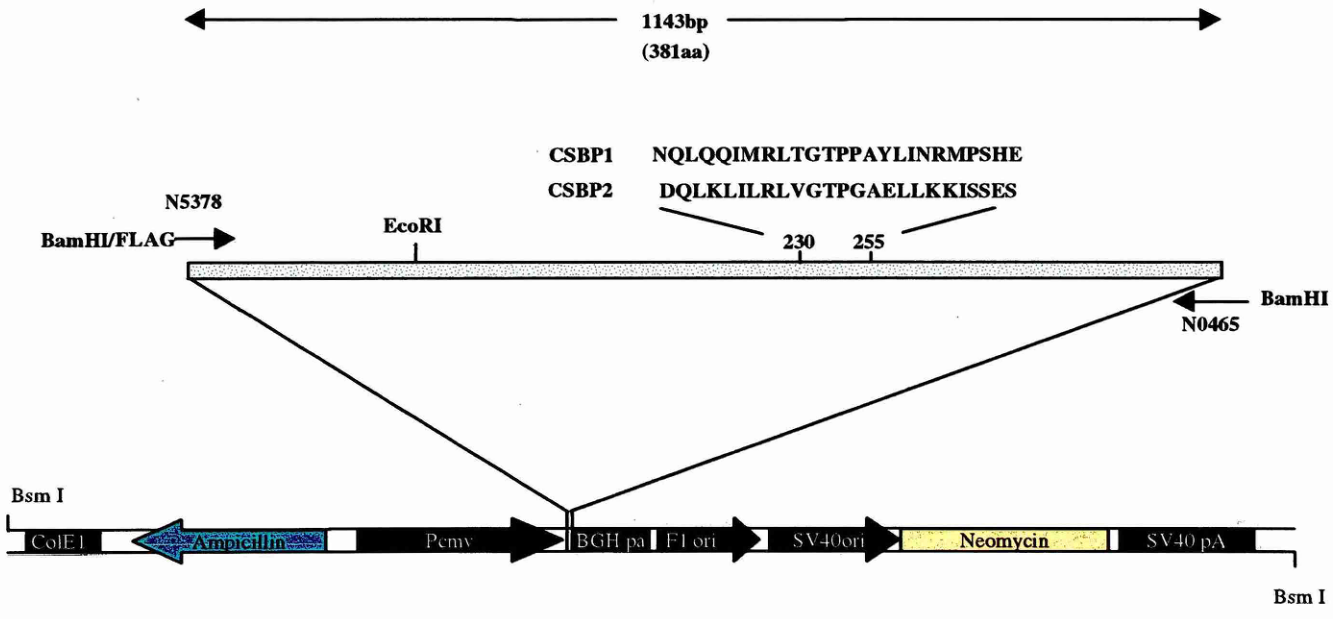

Figure 3.2: Construction of pcDNA3/FLAGp38wt. CSBP2/p38 MAPK was amplified from a human peripheral blood mononuclear cell cDNA library using the 5' oligonucleotide N5378, containing the FLAG epitope DYKDDDD, and the 3' oligonucleotide, N0465. The fragment was digested with Bam HI restriction enzyme and cloned into pcDNA3. The above figure indicates the amino acid differences between CSBP1 and CSBP2. A unique Eco RI restriction site located within the gene is shown above. This site was used to facilitate construction of the kinase dead construct.

were sequenced across the small variable amino acid region (between residues 230-255) previously described (Figure 3.2). The sequences of all four clones were identical to CSBP2.

3.2.2 Generation of FLAG-tagged p38 kinase dead mutant

To generate a p38 MAP kinase mutant the lysine residue critical for ATP binding was mutated by PCR mutagenesis. This residue appears to be invariable at the ATP binding sites of protein kinases (Hanks *et al.*, 1988) and has been shown in structural studies of p42 MAPK (ERK2) to be essential for ATP binding (Zhang *et al.*, 1994).

To construct a kinase dead clone, PCR mutagenesis was used. Two complementary oligonucleotides, 27020 (forward) and 27019 (reverse), were designed, across the ATP binding site. Both oligonucleotides contained the necessary base modifications to mutate lysine-53 (K53) to an arginine (R) residue (K53R). In addition, a further oligonucleotide, 27021 (reverse), was designed across a unique Eco RI restriction enzyme site located within the p38 MAP kinase sequence. Two primary PCR reactions were carried out using pcDNA3/FLAGp38wt as template. The first reaction involved oligonucleotides N5378 and 27019 to generate a fragment of approximately 150 bp. The second PCR reaction involved the oligonucleotides 27020 and 27021 to generate a similar size fragment. Both PCR products were electrophoresed on a 2 % agarose gel and purified to remove any unincorporated oligonucleotides. A secondary PCR reaction was then carried out by mixing equimolar amounts (50 ng) of each fragment with the oligonucleotides N5378 and 27021 (Figure 3.3). A single fragment of 318 bp was amplified, resolved by electrophoresis, purified and digested with Bam HI and Eco RI.

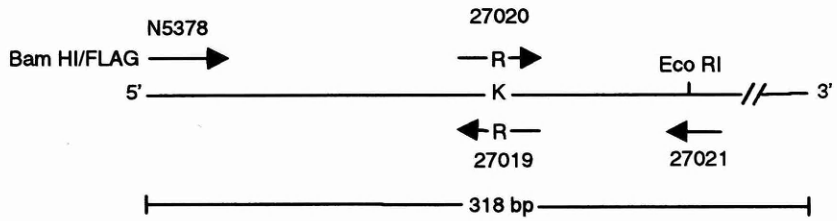

Figure 3.3: Mutation of lysine 53 (K53) at the ATP binding site of p38 MAP kinase by PCR mutagenesis.

The fragment was then cloned into Bam HI/Eco RI digested pSP73 (Figure 3.4) to produce the intermediate construct pSP73/FLAGp38K53R 5' (Figure 3.5A). The mutation was confirmed by sequencing the fragment on both strands using vector and gene specific oligonucleotides.

The complete construct was then generated by 3-way ligation of the mutated fragment from pSP73/FLAGp38K53R 5' with the larger fragment from pcDNA3/FLAGp38wt (Figure 3.5B) into Bam HI digested pSP73 (Figure 3.5C). Transformed colonies were digested to confirm the integrity of the ligation and a single clone was sequenced on both strands using gene specific oligonucleotides. Vector specific oligonucleotides (SP6 and T7) were used to sequence the 5' and 3' terminal regions. This clone was then digested with Bam HI and the fragment was sub-cloned into Bam HI digested pcDNA3 to produce pcDNA3/FLAGp38K53R.

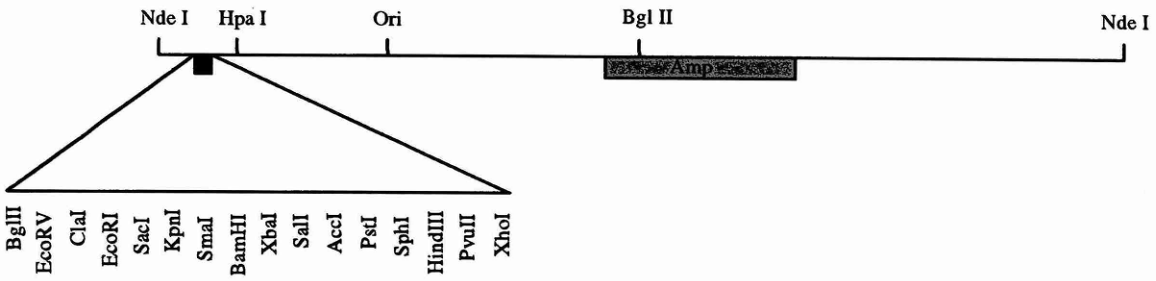

Figure 3.4: Schematic diagram of the cloning vector pSP73. pSP73 is a high copy cloning vector, 2464 base pairs in size. The essential features of the vector include: an *E.coli* origin of replication (Ori); an ampicillin resistance marker for selection in bacteria (Amp); an extensive multiple cloning site; SP6 and T7 promotors for *in-vitro* transcription of either strand (as indicated by arrows).

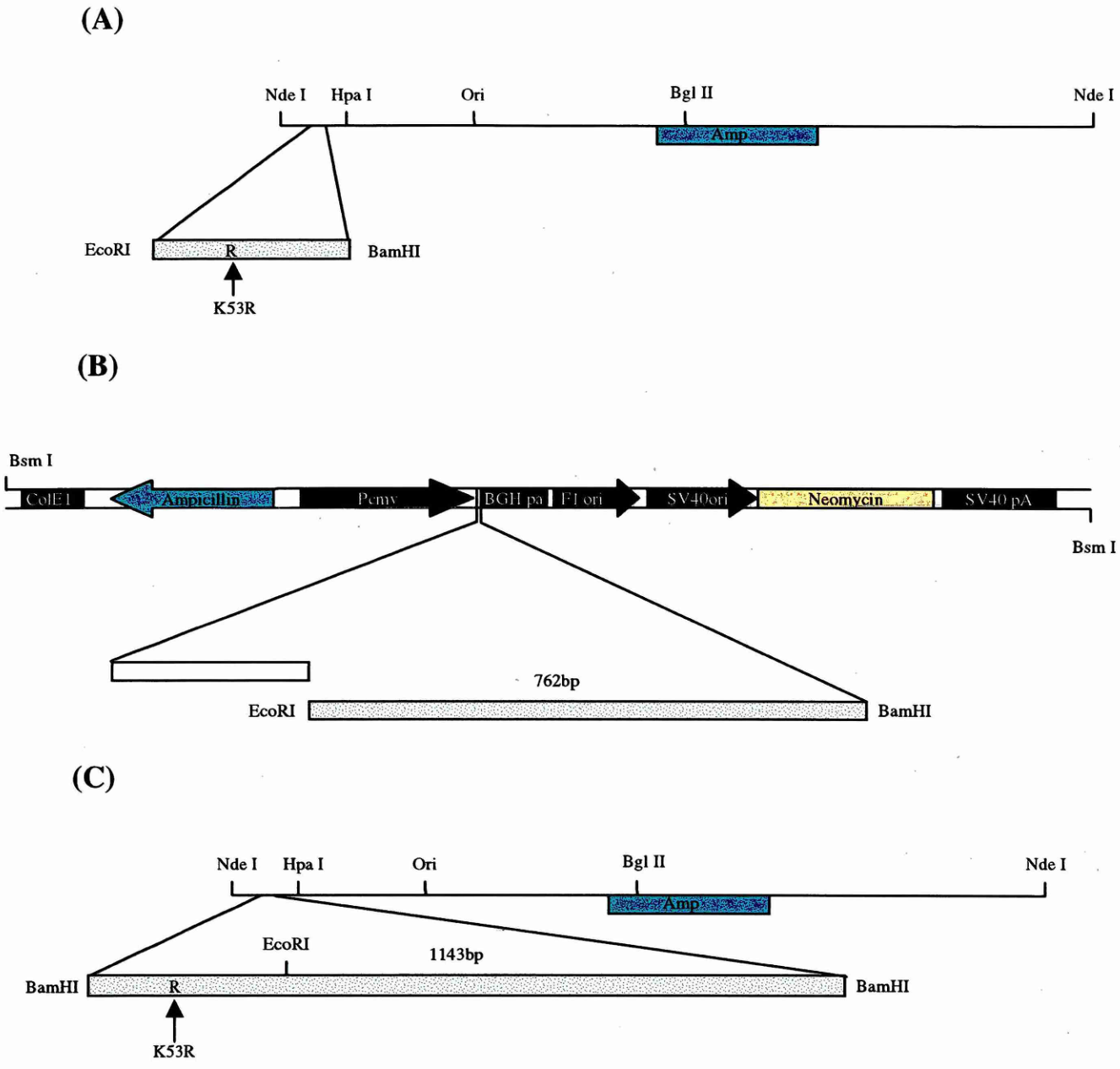

Figure 3.5: Schematic diagram illustrating the construction of kinase dead p38 MAP kinase in pSP73. To construct a p38 kinase dead mutant the Eco RI/Bam HI fragment of pSP73/FLAGp38K53R 5' **(A)** was excised and joined in a 3-way ligation with the Eco RI/Bam HI fragment of pcDNA3/FLAGp38wt **(B)** into Bam HI digested pSP73 to produce pSP73/FLAGp38K53R (C).

3.2.3 Cloning of truncated (Δ) MAPKAPK-2_{40-400} as a GST- fusion protein

ΔMAPKAP kinase-2 was built as a glutathione S-transferase (GST) fusion protein to act as a substrate to assess the kinase activities of pcDNA3/FLAGp38wt and pcDNA3/FLAGp38K53R (see Chapter 4). As discussed previously two 3' splice variants of MAPKAP kinase-2 have been identified (Stokoe *et al.*, 1993; Zu *et al.*, 1994). The oligonucleotide primers, P0324 and N3258, were designed to specifically bind to the 3' sequence of each splice variant. Both oligonucleotides contained Sal I and Sma I restriction enzyme sites to facilitate cloning. Initially, PCR reactions using skeletal muscle and PBMC cDNA as templates were carried out in an attempt to amplify a full-length MAPKAPK-2 clone. A common 5' oligonucleotide (N3257), designed across the initiating methionine was used in combination with each of the specific 3' oligonucleotides. Unfortunately, no full-length MAPKAPK-2 clone could be amplified in either PCR reaction or from either cDNA source.

In previous studies a truncated GST-MAPKAPK-2 fusion protein (GST-ΔMAPKAPK-2) had been shown to be active when incubated and assayed against a synthetic peptide designed from the N-terminus of glycogen synthase (Zu *et al.*, 1994; Ben-Levy *et al.*, 1995) and with murine Hsp25 (Engel *et al.*, 1995). Consequently further PCR reactions were then carried out in an attempt to amplify the largest catalytically active fragment. The oligonucleotide primer W0989, complementary to amino acids 40-47, was designed containing a Bam HI restriction enzyme site. PCR reactions were carried out using this oligonucleotide in combination with each of the specific 3' splice variant oligonucleotides (P0324 and N3258). Interestingly, only the PCR reactions that contained the 3'oligonucleotide (P0324), complementary to the MAPKAPK-2 sequence described by Stokoe *et al.* (1993), produced an amplified

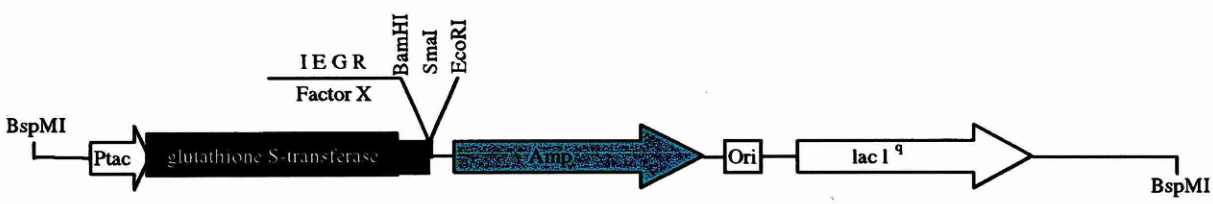

Figure 3.6: Schematic diagram of the glutathione S -transferase fusion vector pGEX-3X.
The important features of the vector are: a *tac* promotor for inducible, high level expression; an internal *lac* I^q gene for use in any *E.coli* host; a Factor X recognition site for cleavage of the desired protein from the fusion product.

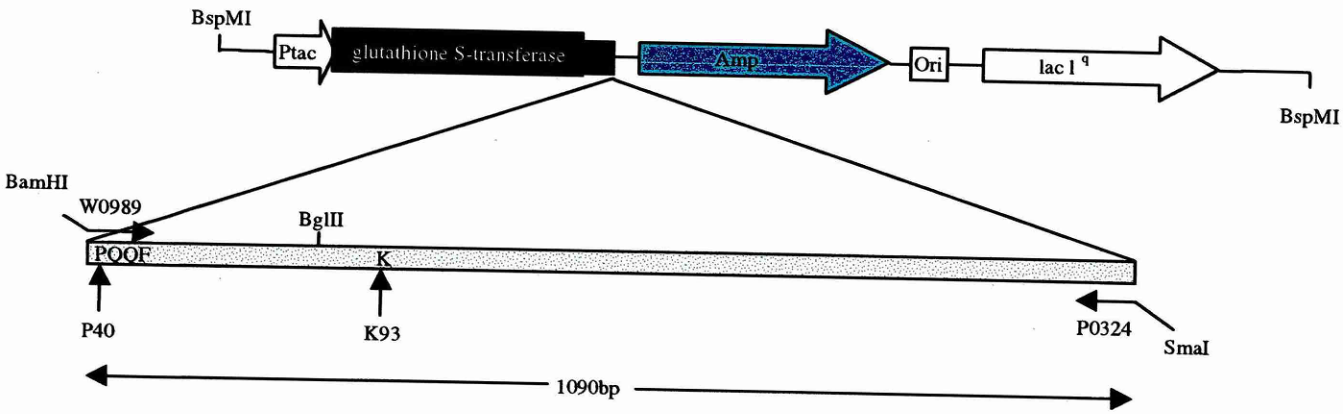

Figure 3.7: Construction of GST-ΔMAPKAPK-2 wt fusion protein (pGEX/GSTΔMAPKAPK-2wt). ΔMAPKAPK-2 was amplified from a human peripheral blood mononuclear cell cDNA library using the 5' oligonucleotide W0989 and the 3' oligonucleotide P0324. The fragment was digested with Bam HI and Sma I and cloned into pGEX-3X.The above figure indicates the amino acid residue (P40) at which ΔMAPKAPK-2 fuses with GST. The diagram also shows the relative position of the lysine residue (K93) at the ATP binding site, with respect to the the unique Bgl II restriction enzyme site which was used to facilitate construction of ΔMAPKAPK-2K93R.

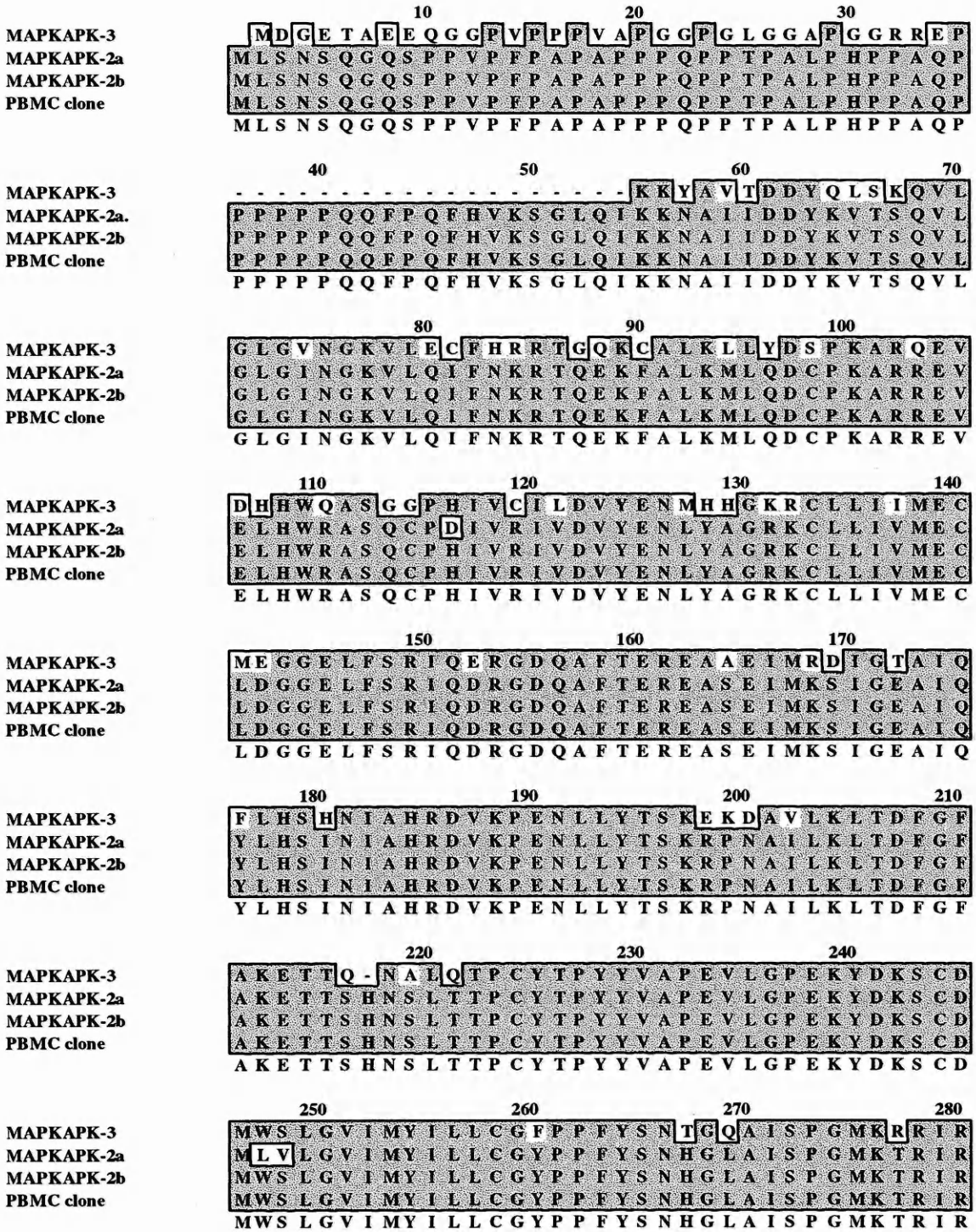
10 20 30
MAPKAPK-3 M D G E T A E E Q G G P V P P P V A P G G P G L G G A P G G R R E P
MAPKAPK-2a M L S N S Q G Q S P P V P F P A P A P P P Q P P T P A L P H P P A Q P
MAPKAPK-2b M L S N S Q G Q S P P V P F P A P A P P P Q P P T P A L P H P P A Q P
PBMC clone M L S N S Q G Q S P P V P F P A P A P P P Q P P T P A L P H P P A Q P
M L S N S Q G Q S P P V P F P A P A P P P Q P P T P A L P H P P A Q P
40 50 60 70
MAPKAPK-3 - - - - - - - - - - - - - - - - - - - K K Y A V T D D Y Q L S K Q V L
MAPKAPK-2a. P P P P P Q Q F P Q F H V K S G L Q I K K N A I I D D Y K V T S Q V L
MAPKAPK-2b P P P P P Q Q F P Q F H V K S G L Q I K K N A I I D D Y K V T S Q V L
PBMC clone P P P P P Q Q F P Q F H V K S G L Q I K K N A I I D D Y K V T S Q V L
P P P P P Q Q F P Q F H V K S G L Q I K K N A I I D D Y K V T S Q V L
80 90 100
MAPKAPK-3 G L G V N G K V L E C F H R R T G Q K C A L K L L Y D S P K A R Q E V
MAPKAPK-2a G L G I N G K V L Q I F N K R T Q E K F A L K M L Q D C P K A R R E V
MAPKAPK-2b G L G I N G K V L Q I F N K R T Q E K F A L K M L Q D C P K A R R E V
PBMC clone G L G I N G K V L Q I F N K R T Q E K F A L K M L Q D C P K A R R E V
G L G I N G K V L Q I F N K R T Q E K F A L K M L Q D C P K A R R E V
110 120 130 140
MAPKAPK-3 D H H W Q A S G G P H I V C I L D V Y E N M H H G K R C L L I I M E C
MAPKAPK-2a E L H W R A S Q C P D I V R I V D V Y E N L Y A G R K C L L I V M E C
MAPKAPK-2b E L H W R A S Q C P H I V R I V D V Y E N L Y A G R K C L L I V M E C
PBMC clone E L H W R A S Q C P H I V R I V D V Y E N L Y A G R K C L L I V M E C
E L H W R A S Q C P H I V R I V D V Y E N L Y A G R K C L L I V M E C
150 160 170
MAPKAPK-3 M E G G E L F S R I Q E R G D Q A F T E R E A A E I M R D I G T A I Q
MAPKAPK-2a L D G G E L F S R I Q D R G D Q A F T E R E A S E I M K S I G E A I Q
MAPKAPK-2b L D G G E L F S R I Q D R G D Q A F T E R E A S E I M K S I G E A I Q
PBMC clone L D G G E L F S R I Q D R G D Q A F T E R E A S E I M K S I G E A I Q
L D G G E L F S R I Q D R G D Q A F T E R E A S E I M K S I G E A I Q
180 190 200 210
MAPKAPK-3 F L H S H N I A H R D V K P E N L L Y T S K E K D A V L K L T D F G F
MAPKAPK-2a Y L H S I N I A H R D V K P E N L L Y T S K R P N A I L K L T D F G F
MAPKAPK-2b Y L H S I N I A H R D V K P E N L L Y T S K R P N A I L K L T D F G F
PBMC clone Y L H S I N I A H R D V K P E N L L Y T S K R P N A I L K L T D F G F
Y L H S I N I A H R D V K P E N L L Y T S K R P N A I L K L T D F G F
220 230 240
MAPKAPK-3 A K E T T Q - N A L Q T P C Y T P Y Y V A P E V L G P E K Y D K S C D
MAPKAPK-2a A K E T T S H N S L T T P C Y T P Y Y V A P E V L G P E K Y D K S C D
MAPKAPK-2b A K E T T S H N S L T T P C Y T P Y Y V A P E V L G P E K Y D K S C D
PBMC clone A K E T T S H N S L T T P C Y T P Y Y V A P E V L G P E K Y D K S C D
A K E T T S H N S L T T P C Y T P Y Y V A P E V L G P E K Y D K S C D
250 260 270 280
MAPKAPK-3 M W S L G V I M Y I L L C G F P P F Y S N T G Q A I S P G M K R R I R
MAPKAPK-2a M L V L G V I M Y I L L C G Y P P F Y S N H G L A I S P G M K T R I R
MAPKAPK-2b M W S L G V I M Y I L L C G Y P P F Y S N H G L A I S P G M K T R I R
PBMC clone M W S L G V I M Y I L L C G Y P P F Y S N H G L A I S P G M K T R I R
M W S L G V I M Y I L L C G Y P P F Y S N H G L A I S P G M K T R I R

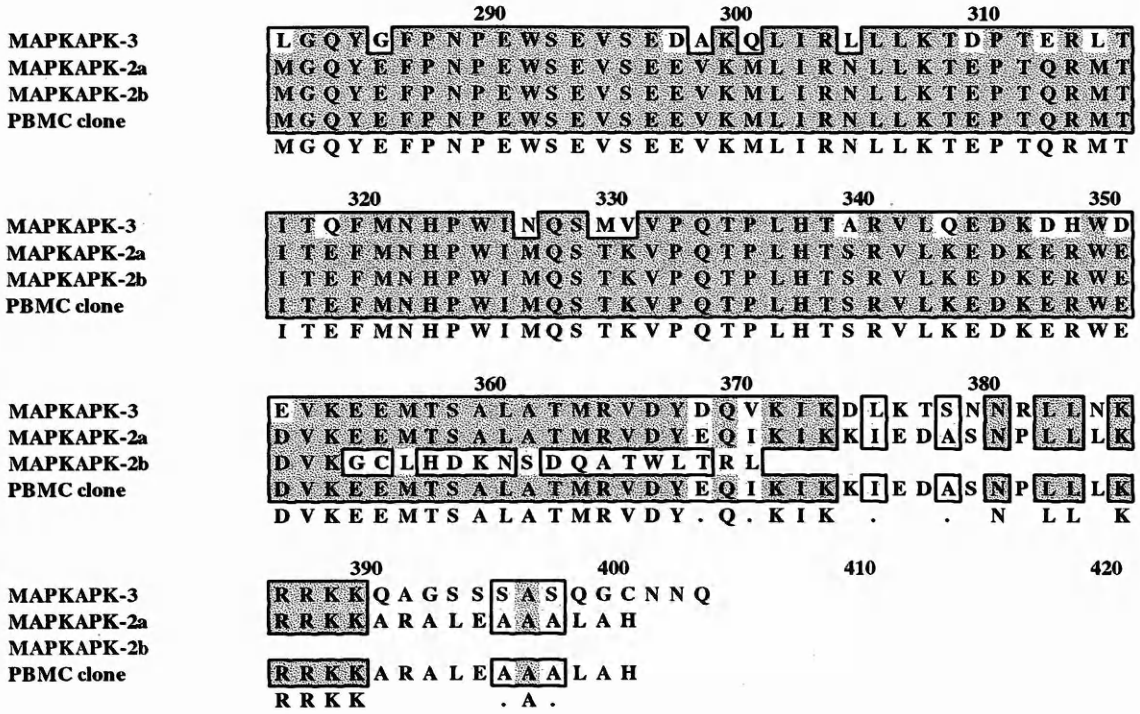

Figure 3.8: Sequence alignments of MAPKAPK-3 (McLaughlin *et al.*, 1996), MAPKAPK-2a (Stokoe *et al.*, 1993), MAPKAPK-2b (Zu *et al.*, 1994) and the PBMC clone isolated in this study.

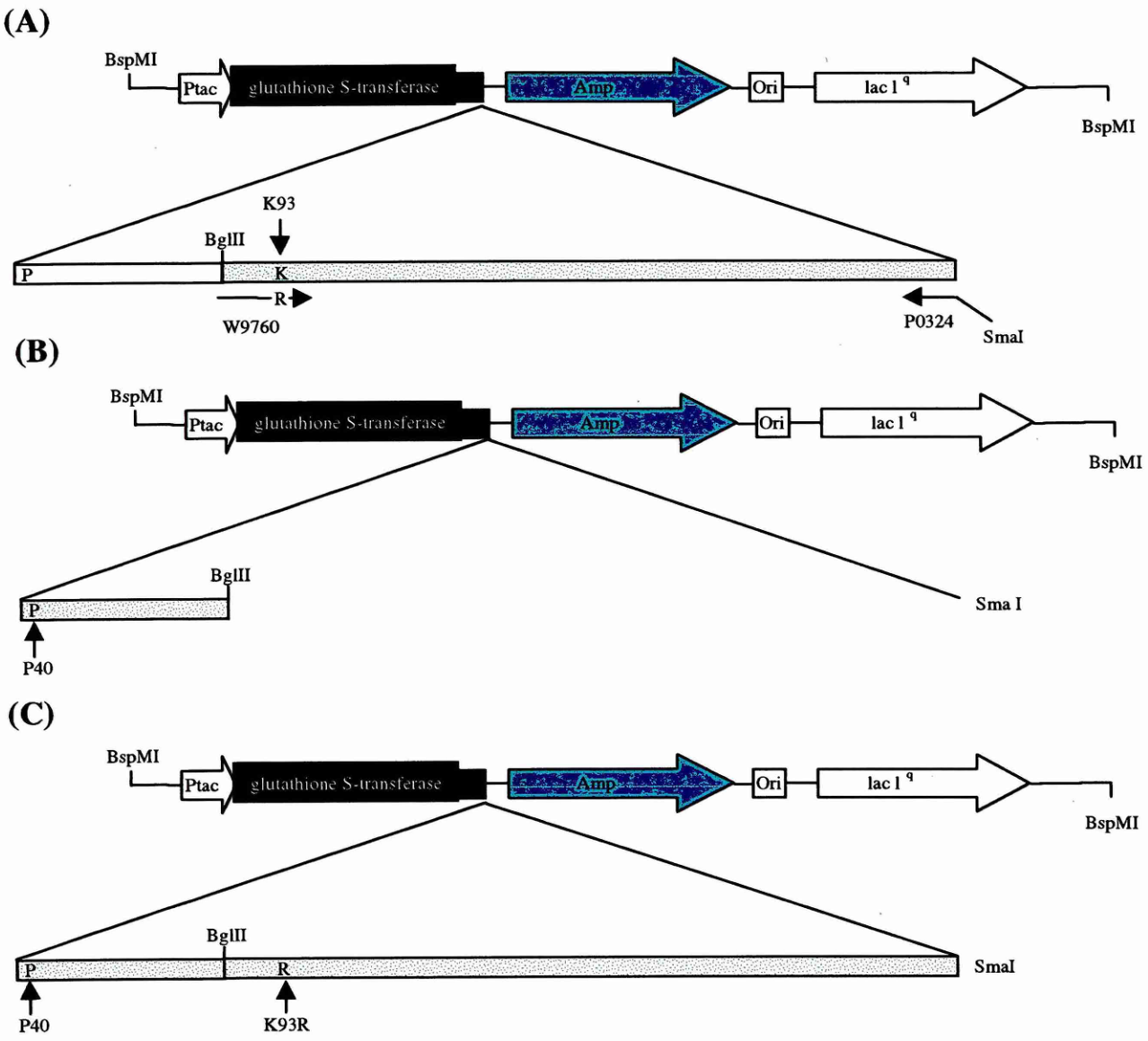

Figure 3.9: Schematic diagram outlining the construction of ΔMAPKAPK-2K93R. **(A)** Using the oligonucleotides, W9760 and P0324, pGEX/GSTΔMAPKAPK-2wt was used as a template to amplify a MAPKAPK-2 fragment containing a mutation at the ATP binding site (K93R). The oligonucleotide, W9760, contained the necessary nucleotide changes to incorporate this mutation. This oligonucleotide also extended upstream across a unique Bgl II site located within the MAPKAPK-2 gene which was used to facilitate cloning. **(B)** pGEX/GSTΔMAPKAPK-2wt was digested with Bgl II and Sma I to remove the equivalent wild-type fragment. **(C)** The amplified PCR fragment was digested with Bgl II/ Sma I and ligated into the Bgl II/Sma I digested pGEX/GSTΔMAPKAPK-2wt to generate pGEX/GSTΔMAPKAPK-2 K93R.

fragment. This result was the same from both of the cDNA library sources. The fragment was digested with Bam HI and Sma I restriction enzymes, purified and cloned into Bam HI/Sma I cut pGEX-3X vector (Figure 3.6). Four clones were sequenced in their entirety on both strands using oligonucleotides designed from the published sequence. Vector oligonucleotides were designed to sequence the 5' and 3' terminal regions. A single error free clone was named pGEX/GSTΔMAPKAPK-2wt (Figure 3.7).

The sequences of all four clones described above were identical to each other. However, they differed from the sequence described by Stokoe *et al.* (1993) at three amino acid positions (Figure 3.8). At amino acid position 116 there is an aspartic acid to histidine change (D116H), at position 247 there is a leucine to tryptophan change (L247W) and finally, at position 248 there is a valine to serine (V248S) change. All of the amino acid changes above are conserved in the MAPKAPK-2b sequence described by Zu *et al.* (1994). Interestingly, these changes are also conserved within the sequence of MAPKAPK-3/3pK, a recently identified homologue of MAPKAPK-2 (McLaughlin *et al.*, 1996; Sithanandam *et al.*, 1996).

3.2.4 Construction of truncated kinase dead ΔMAPKAPK-2_{40-400}

Ludwig *et al.* (1996), demonstrated that the kinase activity of 3pK/MAPKAPK-3 could be completely abolished by mutation of lysine-73 to methionine (K72M). An amino acid alignment of 3pK/MAPKAPK-3 vs MAPKAPK-2 revealed that this lysine residue is located at the putative ATP binding site and is conserved in both sequences. As a consequence of this an oligonucleotide (W9760) was designed containing the necessary nucleotide modifications to mutate the respective lysine of MAPKAPK-2 to

an arginine residue (K93R). MAPKAP kinase-2 contains a unique Bgl II restriction enzyme site upstream of the ATP binding site. Therefore the mutated oligonucleotide was extended over this site to facilitate cloning.

PCR reactions with W9760 and the 3' oligonucleotide P0324 were carried out using pGEX/GSTΔMAPKAPK-2wt as template (Figure 3.9A). The amplified fragment was gel purified and digested with Bgl II/Sma I. pGEX/GSTΔMAPKAPK-2wt was then digested with Bgl II and Sma I and gel purified to remove the equivalent wild type Bgl II/Sma I fragment (Figure 3.9B). The amplified mutated fragment was then cloned into this construct to produce pGEX/GSTΔMAPKAPK-2K93R (Figure 3.9C). A single clone was sequenced in its entirety on both strands to confirm the mutation and to check for any PCR errors. The activity of the truncated mutant expressed in *E.coli* was evaluated (see Chapter 4) and the mutation was found to completely abolish kinase activity. As a consequence of this result a full-length enzyme with this mutation was constructed.

3.2.5 Construction of the 5' terminus of MAPKAPK-2

As discussed above, initial attempts to clone full-length MAPKAPK-2 from a human PBMC cDNA library had been unsuccessful. However, PCR reactions using oligonucleotides designed around the 5' terminus of the gene did enable additional sequence upstream of the fusion point (P40) of GST-ΔMAPKAPK (described above) to be identified. Thus revealing that longer cDNA messages were present within the library. From this information a 'mega' 5' oligonucleotide primer (A0488) was constructed containing the initiating methionine and the missing residues of MAPKAPK-2 and which also overlapped with the 5' sequence of the longest message

identified in the PBMC cDNA library (Figure 3.10). To facilitate cloning the oligonucleotide was constructed with an Eco RI restriction enzyme site.

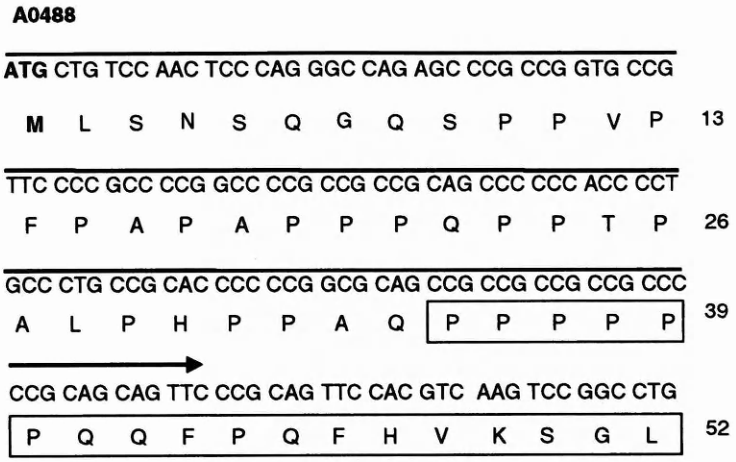

Figure 3.10: N-terminus of MAPKAPK-2 showing the abundant proline rich regions. The length of the oligonucleotide, A0488, used to artificially construct a full-length clone is indicated by the bold arrow. The 5' limit of the longest clone isolated from the PBMC cDNA library is indicated in the boxed area. The initiating methionine is shown in bold type.

To amplify the 5'-terminus of MAPKAPK-2, PCR reactions using oligonucleotides A0488 and N3256 were carried out using human PBMC cDNA as template. N3256 was designed downstream of the unique Bgl II restriction site that was used to construct the truncated MAPKAPK-2 GST-fusion proteins previously described (Figure 3.11).

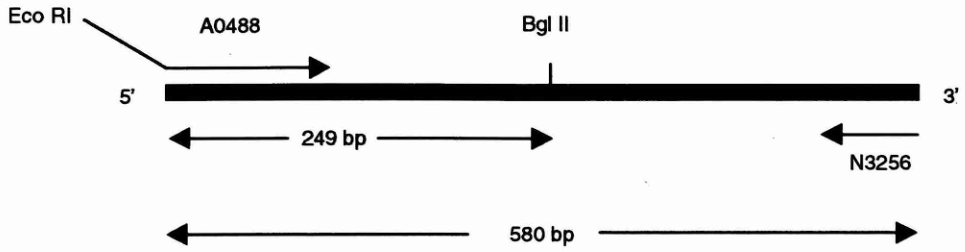

Figure 3.11: Construction of the 5' terminus of MAPKAPK-2 by PCR amplification.

A PCR product of ~580 bp was amplified and gel purified. The fragment was then digested with the restriction enzymes Eco RI and Bgl II to produce two fragments of 331 bp and 249 bp (Figure 3.11). Because the yield from this amplification was poor the two fragments were not purified, but instead the mixture was 'shotgun' cloned into Eco RI/Bgl II digested pSP73. This method captured only the 249 bp fragment that contained both the Eco RI and Bgl II sites. Three clones were then sequenced using gene and vector specific oligonucleotides. Two of the clones contained nucleotide errors located within the oligonucleotide (A0488) sequence, whilst the third clone was error free. This intermediate construct was recorded as pSP73/MAPKAPK-2 5' (Figure 3.12A).

3.2.6 Construction of full-length wild-type and kinase dead MAPKAPK-2

To construct the full-length wild type and kinase dead genes, pSP73/MAPKAPK-2 5' was digested with Eco RI and Bgl II to remove the MAPKAPK-2 5' fragment. pGEX/GSTΔMAPKAPK-2wt and pGEX/GSTΔMAPKAPK-2K93R were digested with Bgl II and Sal I to remove the remainder of the gene. The fragments were then

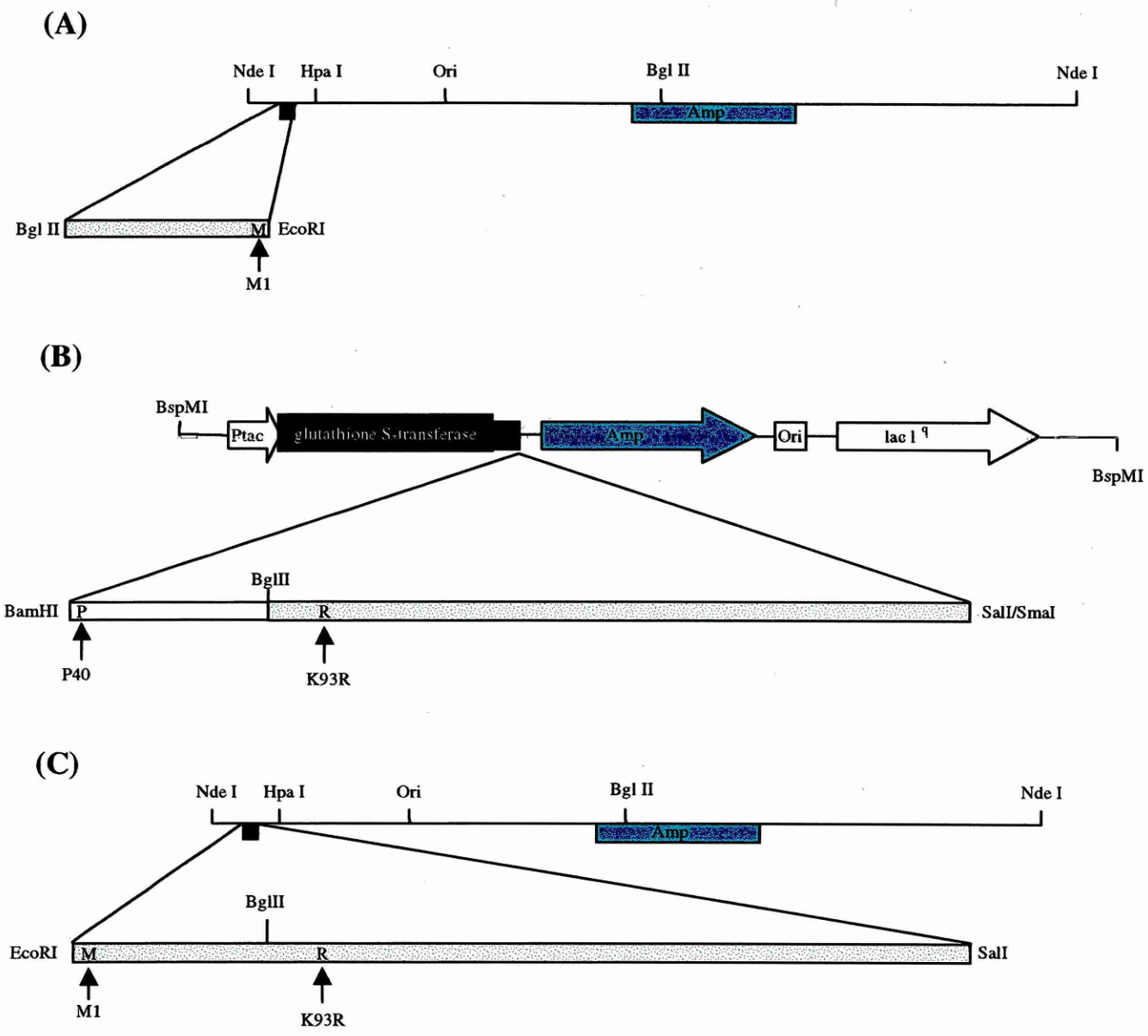

Figure 3.12: Schematic diagram illustrating the construction of full length MAPKAPK-2K93R into pSP73. Full length kinase dead MAPKAPK-2 was constructed by 3-way ligation involving the Eco RI/Bgl II fragment of pSP73/MAPKAPK-2 5' (**A**) and the Bgl II/Sal I fragment of pGEX/GSTΔMAPKAPK-2K93R (**B**) into Eco R1/Sal I digested pSP73 to generate pSP73/MAPKAPK-2K93R (**C**). As detailed in the text this method was also used to construct full-length MAPKAPK-2wt.

joined in a 3-way ligation with Eco RI/Sal I digested pSP73 to produce pSP73/MAPKAPK-2wt and pSP73/MAPKAPK-2K93R (Figure 3.12).

3.2.7 Construction of full-length cMyc-tagged wild-type (wt) and kinase dead (K93R) MAPKAPK-2

To detect MAPKAPK-2 expression in mammalian cells and to facilitate purification, a cMyc epitope tag (-MEQKLISEEDLN-) was incorporated into the 3' end of the sequence. Incorporation of the epitope at the 3' end of the gene avoided amplification of the GC-rich 5' terminus.

To construct cMyc-tagged wild type and kinase dead genes, PCR reactions using oligonucleotides, W0989 (forward) and B5640 (reverse) were carried out using pSP73/MAPKAPK-2wt and pSP73/MAPKAPK-2K93R as templates respectively. B5640 contained the restriction enzyme sites Xba I and Hind III as well as the cMyc epitope sequence. The amplified fragments were digested with Pst I (a unique MAPKAPK-2 restriction site downstream of the W0989 priming site) and Hind III. The fragments were purified and cloned into pSP73/MAPKAPK-2wt that had been digested with Pst I and Hind III to remove the equivalent fragment. Two wild type clones and two kinase dead clones were sequenced on both strands using gene and vector specific oligonucleotides. A single representative of each clone was designated pSP73/cMycMAPKAPK-2wt and pSP73/cMycMAPKAPK-2K93R (Figure 3.13).

The wild type and kinase dead fragments were then removed by digestion with Eco RI and Xba I and subcloned into Eco RI/Xba I digested pcDNA3 to generate the

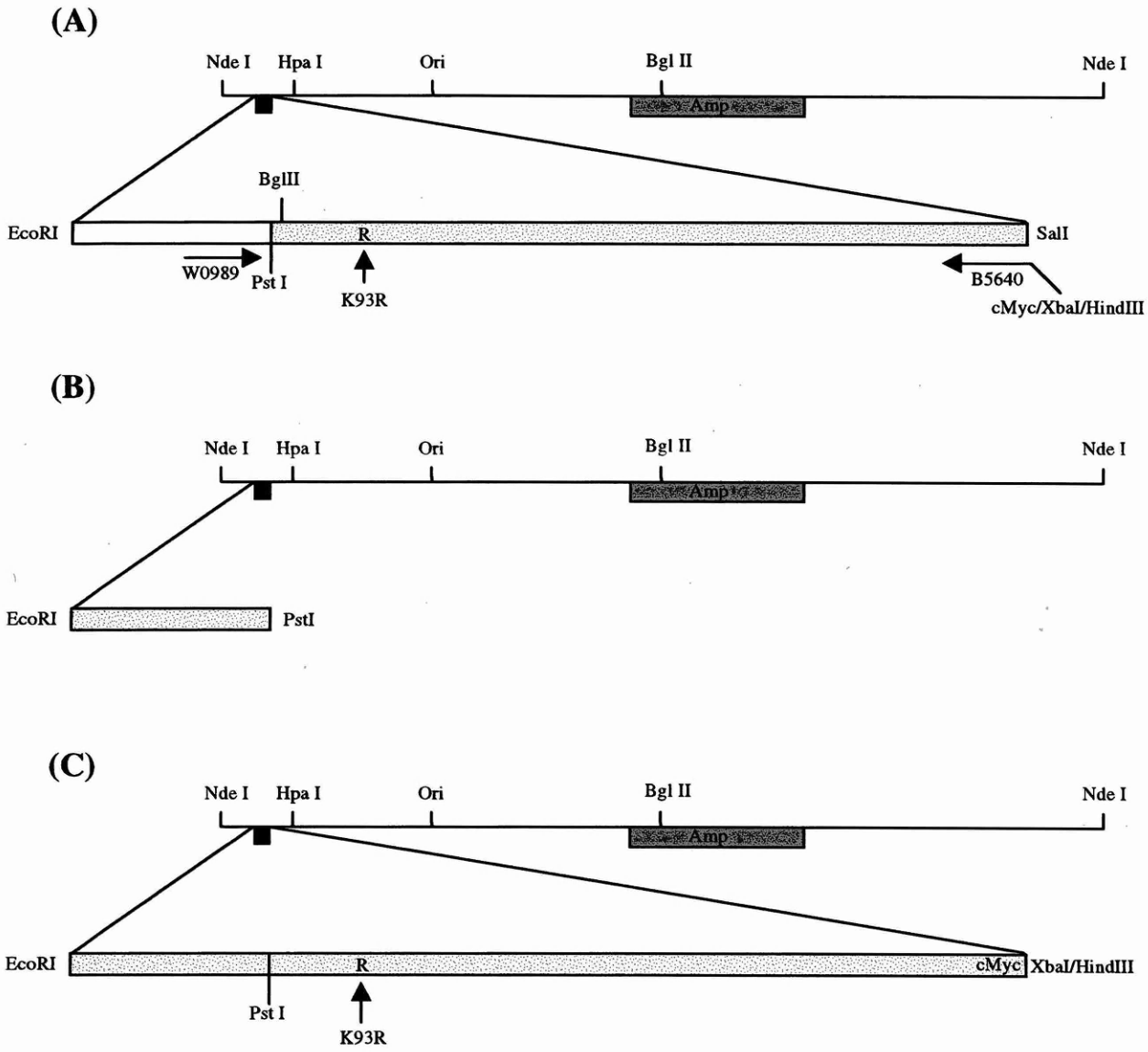

Figure 3.13: Construction of cMyc-tagged MAPKAPK-2 K93R. A C-terminal cMyc-tagged MAPKAPK-2K93R fragment was amplified by PCR using pSP73/MAPKAPK-2K93R as template (**A**). The fragment was digested with Pst I and Hind III. pSP73/MAPKAPK-2wt was also digested with Pst I and Hind III and the corresponding fragment was removed (**B**). The final construct was then assembled by ligation (**C**). As outlined in the text this method was also used to construct full-length cMycMAPKAPK-2wt.

(A)

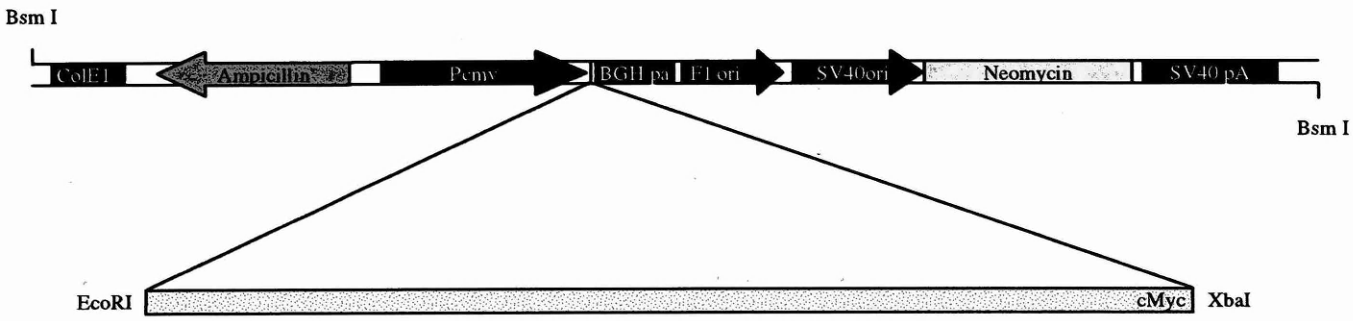

(B)

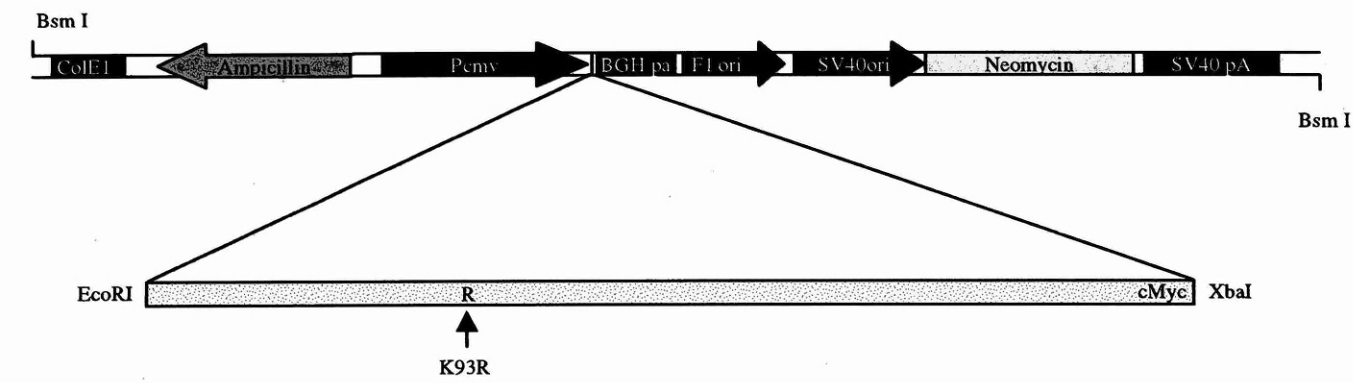

Figure 3.14: cMyc-tagged MAPKAPK-2 wt (A) and kinase dead (B) genes in the mammalian expression vector pcDNA3. pSP73/cMycMAPKAPK-2wt and pSP73/cMycMAPKAPK-2K93R were digested with Eco RI and Xba I and the fragments were subcloned into pcDNA3 as described in the text.

constructs pcDNA3/cMycMAPKAPK-2wt (Figure 3.14A) and pcDNA3/cMycMAPKAPK-2K93R (Figure 3.14B).

3.2.8 Construction of MAPKAPK-2 anti-sense (A/S) expressing vector

To construct a vector overexpressing MAPKAPK-2 anti-sense message, pcDNA3/cMycMAPKAPK-2wt was digested with Eco RI and Xba I and the fragment was purified. This was then cloned in the reverse orientation into Eco RI and Xba I digested pcDNA3.1 (Figure 3.1B). The integrity of the construct was checked by restriction enzyme digestion and sequenced at the 5' and 3' terminals using vector specific oligonucleotides. This was recorded as pcDNA3/cMycMAPKAPK-2 A/S.

3.2.9 Construction of GST-Hsp27 fusion protein

Hsp27 is an *in-vivo* substrate of MAPKAPK-2 and was constructed as a GST-fusion protein to facilitate purification for *in-vitro* kinase studies. The sequence of Hsp27 was obtained from the Genbank database and two oligonucleotide primers (N3984 and N3985), containing Bam HI restriction sites, were designed from the 5' and 3' ends of the gene respectively. PCR reactions were carried out using human PBMC cDNA as template and a fragment of the correct size (630 bp) was amplified and gel purified. This was then digested with Bam HI and cloned into Bam HI digested pGEX-3X. Recombinant colonies were screened by PCR to determine the correct orientation using vector specific and gene specific oligonucleotides. A single clone was sequenced in its entirety on both strands and was identical to that of the published sequence. This clone was named pGEX/GSTHsp27 (Figure 3.15).

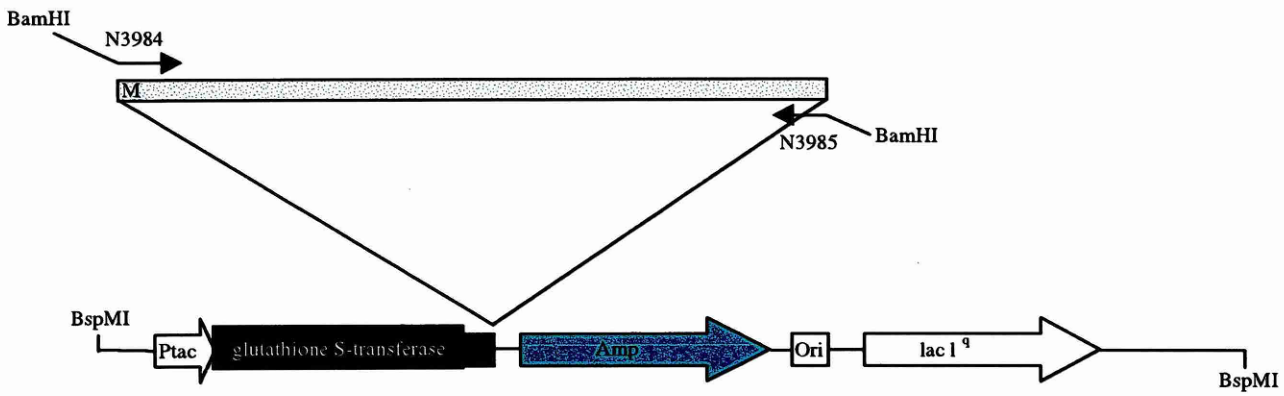

Figure 3.15: Construction of GST-Hsp27 (pGEX/GSTHsp27). GST-Hsp27 was amplified from a human PBMC cDNA library, digested with Bam HI and cloned into the correct reading frame of Bam HI digested pGEX-3X.

3.3 Discussion

The sequence of p38/CSBP2 amplified from the PBMC cDNA library was identical the sequence published by Lee *et al.* (1994). Interestingly, all four clones isolated and sequenced from this library all were identified as CSBP2 . This may imply that CSBP2 and not CSBP1, is the predominant isoform in these cell types. However, a greater number of clones would have to be analysed for this observation to have any statistical significance.

The sequences of two isoforms of human MAPKAPK-2 have been published (Stokoe *et al.*, 1993; Zu *et al.*, 1994). These two isoforms are produced by alternate splicing of the same gene and differ extensively at the C-terminals. The longer isoform, MAPKAPK-2a, described by Stokoe *et al.* (1993) contains a nuclear localization signal at the C- terminal which is absent in the shorter MAPKAPK-2b isoform. In addition to the gross sequence changes at the C-terminals the two clones also have three amino acid differences (a.a. positions 116, 247 and 248) within the conserved catalytic region of the enzyme.

The PBMC clone isolated in this chapter was identical at the C-terminus to that described by Stokoe *et al.* (1993). However, this clone had the same three amino acid residues changes at the positions indicated above, as those in the sequence described by Zu *et al.* (1994). The three amino acid residues (H116, W247 and S248) are also conserved in 3pK/MAPKAPK-3, a recently identified homologue of MAPKAPK-2 (Sithanandam *et al.*, 1996; McLaughlin *et al.*, 1996). These enzymes share 72% sequence identity at the nucleotide level and 75% at the amino acid level. None of the residues described above are crucial for MAPKAPK-2 activation and it is possible

that in the sequence described by Stokoe *et al.* (1993) these changes may be erroneous.

The reason for the failure to directly amplify full-length MAPKAPK-2 from either the skeletal muscle or PBMC cDNA libraries, is probably due to the absence of full-length MAPKAPK-2 clones within these libraries. This may be a result of the high GC-rich content at the 5'-end of the MAPKAPK-2 mRNA sequence. High GC-rich regions contain large regions of symmetry, which may then form stable secondary mRNA (hairpin) structures and thereby inhibit full-length first strand cDNA synthesis.

Chapter 4

Expression and Kinase Activities

4.1 Introduction

The p38 MAP kinase pathway is predominantly activated by cellular stresses such as: bacterial endotoxin (Han *et al.*, 1994; Lee *et al.*, 1994), chemical, heat and osmotic shock (Rouse *et al.*, 1994), pro-inflammatory cytokines (IL-1 and TNF) (Freshney *et al.*, 1994) and UV irradiation (Raingeaud *et al.*, 1995). Activation of p38 MAP kinase by any of the above stimuli leads to the rapid phosphorylation and activation of MAPKAPK-2, a physiological substrate of p38 MAP kinase, which in turn phosphorylates the small heat shock protein Hsp27 (Rouse *et al.*, 1994; Freshney *et al.*, 1994). Activation of MAPKAPK-2 and phosphorylation of Hsp27 can be blocked by the specific p38 MAP kinase inhibitor SB 203580 (Cuenda *et al.*, 1995).

The p38 MAP kinase and MAPKAPK-2 ATP binding mutants, described in Chapter 3, were designed to be used as bait in a yeast two-hybrid screen (see Chapter 5) and to generate stable cell lines (see Chapter 6). This chapter analyses the transient expression and the kinase activities of these constructs prior to their use in the studies described above. The FLAG and cMyc epitope-tags incorporated into the constructs facilitated purification for *in-vitro* kinase assays and for detection of expression by immunoblotting. In addition, the physiological pathway described above was reconstituted *in-vitro* by incubating immunoprecipitated p38 MAP kinase with GST-ΔMAPKAPK-2 and GST-Hsp27. The sensitivity of p38 MAPK to SB 203580 was determined by analysing the phosphorylation of MAPKAPK-2 and Hsp27.

4.2 Results

4.2.1 Expression of p38 and MAPKAPK-2 in HeLa cells

HeLa cells ($2x10^5$) were transiently transfected with FLAG-tagged p38wt, FLAG-tagged p38 K53R, cMyc-tagged MAPKAPK-2wt and cMyc-tagged MAPKAPK-2 K93R. After 48 hours, the cells were lysed and the relative levels of protein expression were investigated by immunoblotting with anti-FLAG or anti-cMyc antibodies.

The anti-FLAG antibody detected specific immunoreactive bands of ~42 kDa corresponding to the correct molecular masses of the FLAG-tagged p38 wild type and kinase dead proteins (Figure 4.1A, *lanes 1 and 2*). No non-specific binding was observed with this antibody as observed in the cells transfected with empty vector (Figure 4.1A, *lane 3*). Although the relative expression levels of both proteins were quite high, expression of the wild type protein was stronger. This relative difference in expression was observed in all transient transfection experiments carried out, suggesting that the difference was not merely due to the transfection efficiencies of each experiment.

The anti-cMyc antibody detected two equally expressed bands representing cMyc-tagged MAPKAPK-2 wild type and kinase dead (K93R) proteins (Figure 4.1B, *lanes 1 and 2*). Epitope-tagged MAPKAPK-2 proteins migrated with apparent molecular masses of ~50 kDa which differed slightly from the calculated molecular mass of ~45 kDa. No non-specific binding was observed with this antibody in the control reaction transfected with empty vector (Figure 4.1B, *lane 3*).

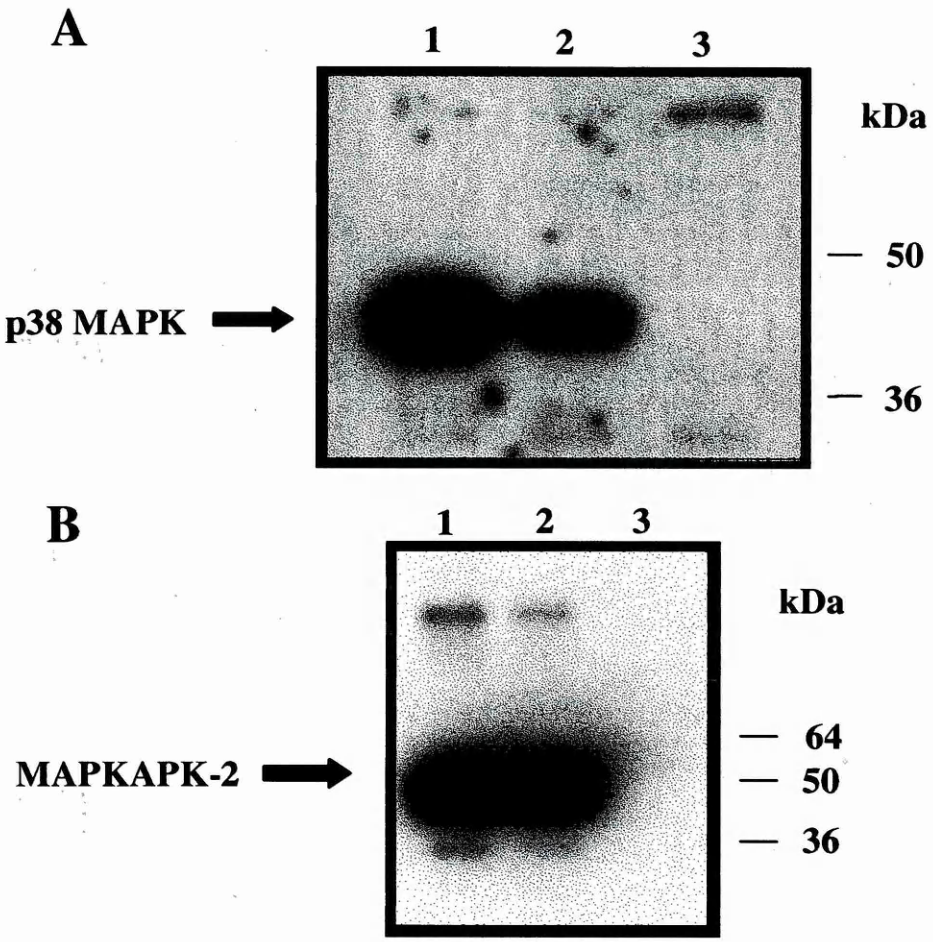

Figure 4.1: Expression of FLAG-tagged p38 wild type and K53R proteins (A) and cMyc-tagged MAPKAPK-2 wild type and K93R proteins in HeLa cells (B). HeLa cells ($2x10^5$) were transiently transfected with 1.5 μg of plasmid DNA. After 48 hours the cells were lysed in 100 μl of lysis buffer. Cellular debris was centrifuged and the supernatant removed. 5X sample buffer was added and the samples were boiled for 5 minutes.15 μl of sample was resolved by electrophoresis on a 4-20% polyacrylamide gel and transferred to nylon membranes.

Panel A: Probed with anti-FLAG murine monoclonal antibody (10 μg/ml).
***lane 1*:** p38 wt ***lane 2*:** p38 K53R ***lane 3*:** empty vector

Panel B: Probed with anti-cMyc rabbit polyclonal antibody (1 μg/ml)
***lane 1*:** MAPKAPK-2 wt ***lane 2*:** MAPKAPK-2 K93R ***lane 3*:** empty vector

Proteins were visualised with a secondary antibody linked to HRP and enhanced chemiluminescence. Arrows indicate the positions of the proteins.

4.2.2 Expression of GST-ΔMAPKAPK-2_{40-400} wt, GST-ΔMAPKAPK-2_{40-400} K93R and GST-Hsp27 in *E.coli*

Epicurian XL-1 blue *E.coli*, transformed with GST-ΔMAPKAPK-2wt, GST-ΔMAPKAPK-2 K93R and GST-Hsp27 were induced with 0.2 mM isopropyl-β-D-thiogalactoside (IPTG) for four hours at 30°C. The proteins were affinity purified using glutathione sepharose beads and samples of each protein were electrophoresed on a 4-20% polyacrylamide gel and visualised by Coomasie staining. To estimate the concentrations of each fusion protein, for subsequent kinase assays, titrated concentrations of bovine serum albumin (BSA) were also loaded onto the gel (Figure 4.2).

Truncated MAPKAPK-2 wild type and kinase dead GST-fusion proteins (residues 40-400) migrated as single bands with apparent molecular masses corresponding to their calculated molecular masses (~65 kDa) (Figure 4.2, *lanes 1 and 2 respectively).* GST-Hsp27 migrated with an apparent molecular mass of ~50 kDa, which corresponded closely to its calculated mass of 52 kDa (Figure 4.2, *lane 3*). The relative level of expression of GST-Hsp27 was weaker than that of GST-ΔMAPKAPK-2 and may be a consequence of the low solubility of GST-Hsp27 when expressed in *E.coli* (see Chapter 5, section 5.3.2). In *lanes 2 and 3,* the two low molecular weight bands probably represent cleaved GST and ΔMAPKAPK-2, whilst in *lane 1,* the low molecular weight band probably comprises of a doublet of cleaved GST and Hsp27 which have similar molecular weights.

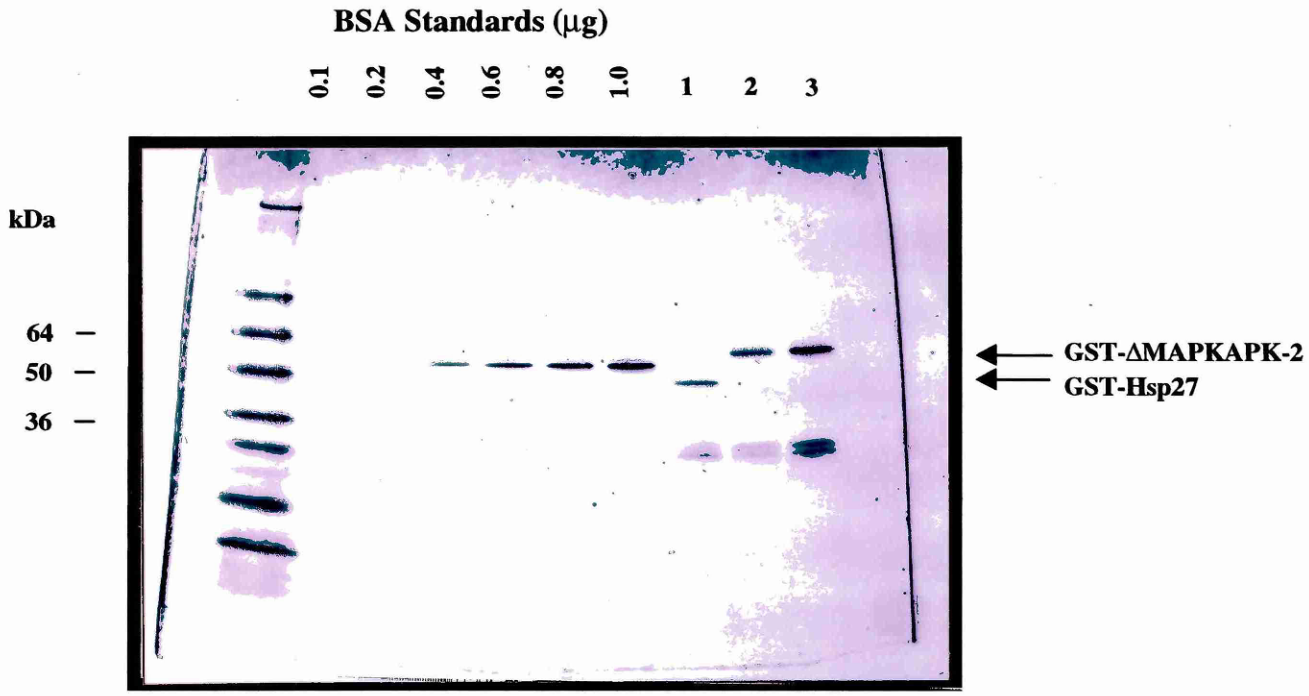

Figure 4.2: Affinity purification of GST-ΔMAPKAPK-2 and GST-Hsp27 fusion proteins. *E.coli* XL-1 blue cells expressing GST- ΔMAPKAPK-2 wt, GST- ΔMAPKAPK-2 K93R and GST-Hsp27 were induced with IPTG (0.2 mM) for 4 hr and then lysed. GST-fusion proteins were purified using glutathione sepharose. 3 µl of each purified sample was loaded and electrophoresed on a 4-20% Tris-glycine polyacrylamide gel. The concentrations of GST-Hsp27 (***lane 1***), GST- ΔMAPKAPK-2 wt (***lane 2***) and GST- ΔMAPKAPK-2 K93R (***lane 3***) were estimated by comparing the amount of protein loaded against titrated concentrations of BSA (0.1 -1.0 µg).

4.2.3 Evaluation of the ATP binding site mutation (K53R) in FLAG-tagged p38 MAPK

COS-1 cells were transiently transfected with FLAG-tagged p38wt, FLAG-tagged p38 K53R or empty vector. After 48 hours, the cells were osmotically stressed by the addition of sodium chloride (0.2 M) to the medium for 20 minutes. The cells were then lysed and the FLAG-tagged proteins were immunoprecipitated using Gammabind G sepharose beads coupled to an anti-FLAG M2 monoclonal antibody. The kinase activities were assayed in an immune complex protein kinase assay using purified GST-ΔMAPKAPK-2wt as substrate and analysed by autoradiography. Figures 4.3 A and 4.3 B show the results of the above kinase assays when the phosphorylated substrate was exposed to X-ray film for 4 hours and 19 hours respectively.

As shown in Figures 4.3A and 4.3B, mutation of the lysine residue (K53) at the ATP binding site of p38 MAP kinase dramatically reduces the kinase activity of this enzyme. After 4 hours exposure there was no visible phosphorylation of GST-ΔMAPKAPK-2wt by the mutated p38 enzyme isolated from stressed cells, whilst the wild type p38 protein isolated from stressed cells strongly phosphorylated GST-ΔMAPKAPK-2wt (Figure 4.3 A, *lanes 5 and 2 respectively*). After 19 hours exposure a weak signal was observed in the lane containing the mutated p38 enzyme isolated from stressed cells, however, this signal was also observed in the empty vector transfected samples and may therefore represent a small degree of autophosphorylation of the GST-ΔMAPKAPK-2wt substrate (Figure 4.3 B, *lanes 5, 4 and 1*). These results confirm that mutating lysine 53 to arginine within the ATP binding site of p38 MAP kinase inhibits the kinase activity of this enzyme.

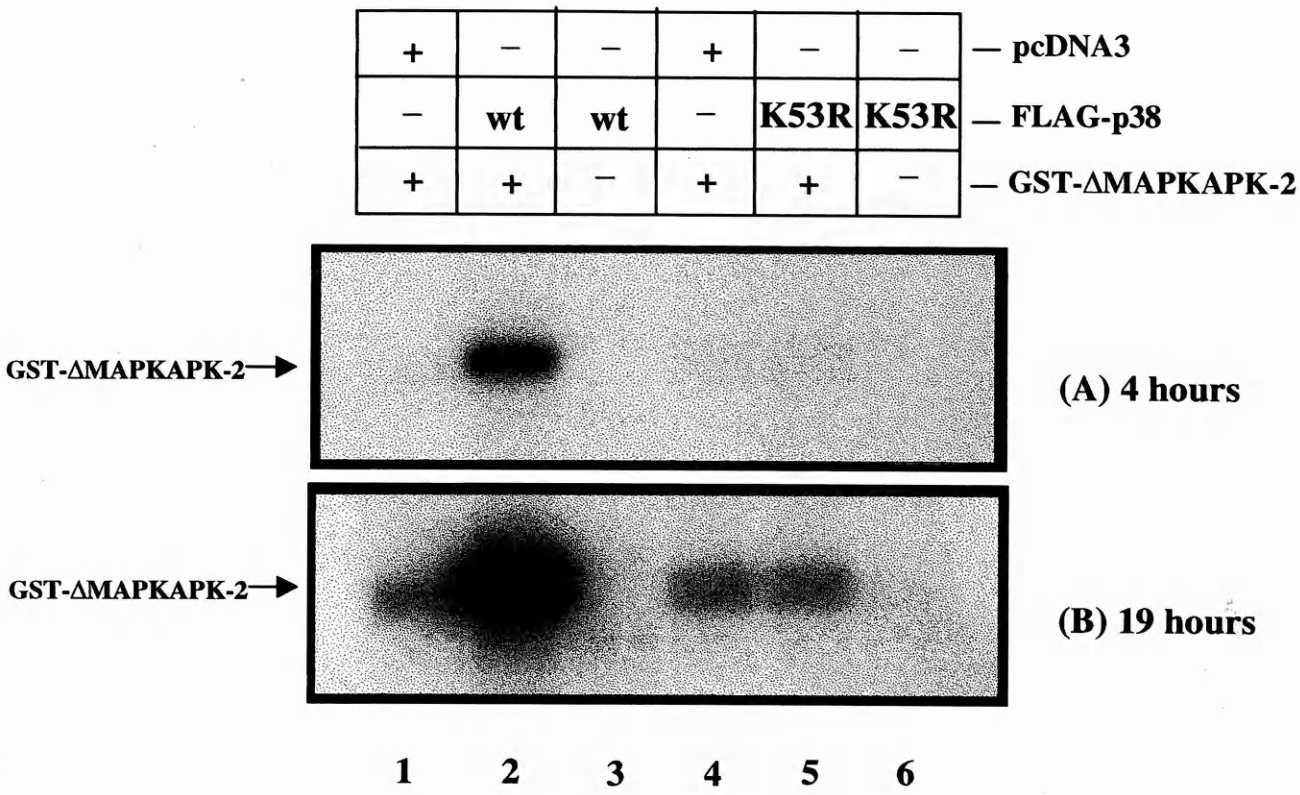

Figure 4.3: Evaluation of the ATP binding site mutation of FLAG-tagged p38 (K53R): COS-1 cells were transfected with 1.5 μg of either p38wt, p38 K53R mutant or empty vector. Epitope-tagged proteins were immunoprecipitated and incubated in an immune complex kinase assay with or without GST-ΔMAPKAPK-2wt (5 μg) . The reactions were stopped after 30 minutes by the addition of 5X sample loading buffer and analysed by SDS-PAGE. Substrate phosphorylation was detected by autoradiograpy at 4 hour **(A)** and 19 hour **(B)** time intervals.

4.2.4 Evaluation of the ATP binding site mutation (K93R) in full length cMyc-tagged MAPKAPK-2

HeLa cells were transiently transfected with cMyc-tagged MAPKAPK-2wt, cMyc-tagged MAPKAPK-2 K93R or empty vector. After 48 hours, the cells were osmotically stressed by the addition of sodium chloride (0.2 M) to the medium for 20 minutes. Control reactions in which sodium chloride was omitted were also carried out. The cells were then lysed and the cMyc-tagged proteins were immunoprecipitated using Gammabind G sepharose beads coupled to an anti-cMyc antibody. The kinase activities were assayed in an immune complex protein kinase assay using purified GST-Hsp27 as substrate and analysed by autoradiography. Figures 4.4 A and 4.4 B show the results of the above kinase assays when the phosphorylated substrate was exposed to X-ray film for 6 hours and 18 hours respectively.

It can be clearly seen, by the level of phosphorylation of GST-Hsp27, that the MAPKAPK-2 K93R mutant has significantly reduced kinase activity when compared to the wild- type enzyme (Figure 4.4 A, *lanes 1 and 2 respectively*). Surprisingly, there was still a small amount of Hsp27 phosphorylation when compared to the control sample transfected with empty vector, which could be due to the non-specific binding of kinases to the sepharose beads (Figure 4.4 A, *lane 4*).

The kinase activities of MAPKAPK-2wt recovered from stressed and unstressed cells (Figure 4.4 A, *lanes 1 and 5 respectively*), and MAPKAPK-2 K93R recovered from stressed and unstressed cells (Figure 4.4 A, *lanes 2 and 6 respectively*) were also compared. As expected, the kinase activity of the wild type enzyme, recovered from osmotically stressed cells was enhanced. Interestingly, the phosphorylation of GST-

Hsp27 incubated with MAPKAPK-2 K93R also increased when the cells were osmotically shocked. However, there is an increase in non-specific 'background' signals in the osmotically shocked control sample (Figure 4.4 B, *lane* 4). This clearly indicates that other osmotically induced kinases are non-specifically bound to the sepharose beads.

4.2.5 Inhibition of p38 MAP kinase activity by SB 203580

The sensitivity of FLAG-tagged p38 MAP kinase expressed in COS-1 cells to SB 203580 was investigated. FLAG- tagged p38 MAP kinase was batch purified from osmotically shocked cells, using Gammabind G sepharose coupled with anti-FLAG antibody. The physiological pathway described in the introduction of this chapter was reconstituted by the addition of GST-ΔMAPKAPK-2wt and GST-Hsp27 to the sepharose/FLAG-p38wt complex. SB 203580 was added at different concentrations and the sensitivity of p38 MAP kinase to SB 203580 was viewed by the inhibition of GST-Hsp27 phosphorylation by MAPKAPK-2 (Figure 4.5).

The results from this experiment clearly show that pre-incubation of FLAG-tagged p38 MAP kinase, *in-vitro,* with SB 203580 prevented the activation of GST-ΔMAPKAPK-2 and the subsequent phosphorylation of GST-Hsp27 in a dose dependent manner. SB 203580 (0.37 μM) strongly inhibited FLAG-tagged p38 MAP kinase activation as indicated by the reduced signal intensities of GST-ΔMAPKAPK-2 and GST-ΔHsp27 (Figure 4.5, *lane* 4). Although the results in this experiment are only qualitative, SB 203580 appears to inhibit p38 MAP kinase with an IC_{50} of 0.37-0.123 μM.

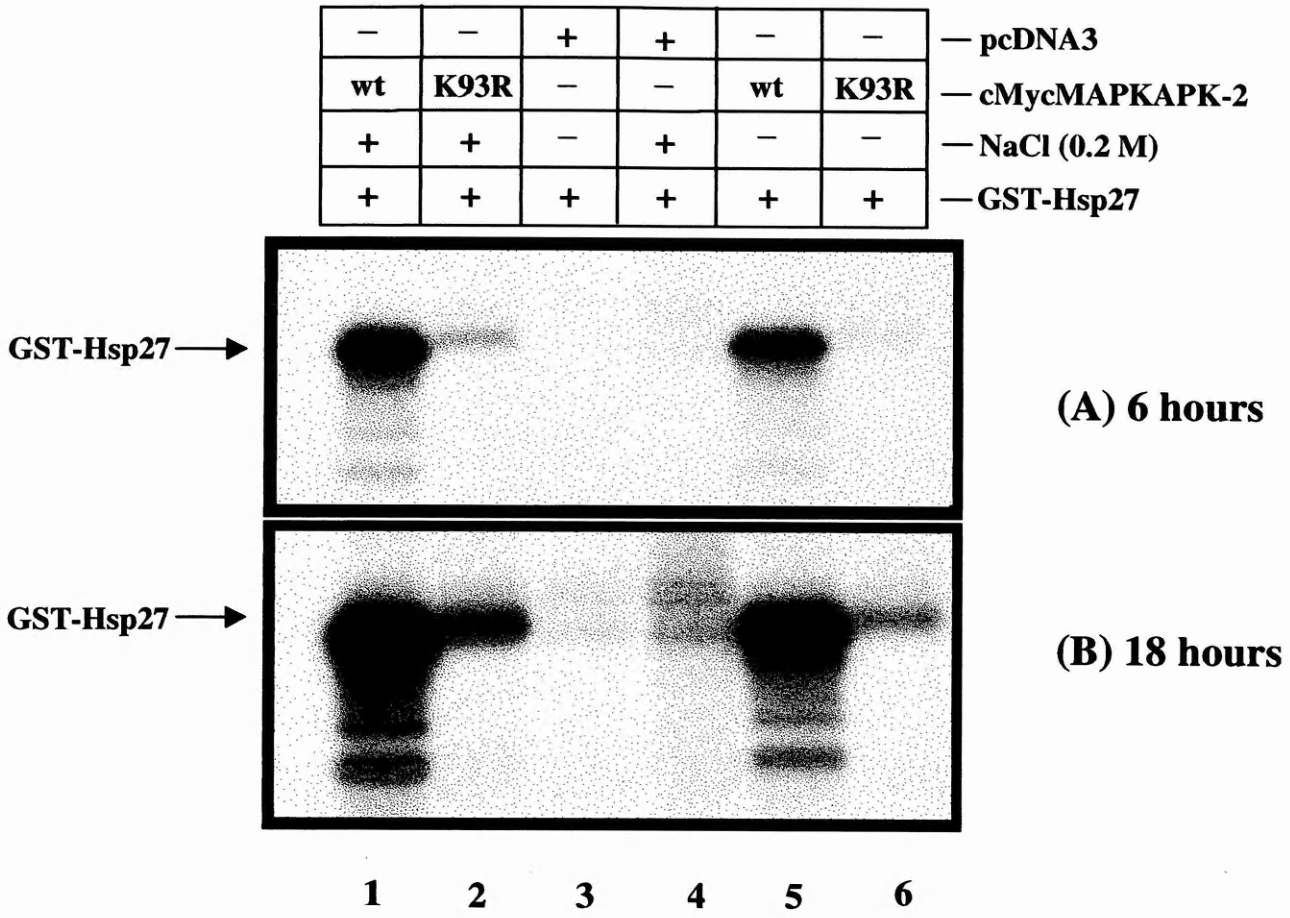

Figure 4.4: Evaluation of the ATP binding site mutation of cMyc-tagged MAPKAPK-2 (K93R): HeLa cells were transiently transfected with 1.5 µg of either cMycMAPKAPK-2wt, cMycMAPKAPK-2 K93R or empty vector. After 48 hours the cells were treated with or without NaCl (0.2 M) for 20 min. The cells were lysed and epitope-tagged protein was immunoprecipitated and incubated in an immune complex kinase assay with GST-Hsp27 (5 µg). After 30 minutes the reactions were stopped and analysed by SDS-PAGE. Substrate phosphorylation was visualised by autoradiography at 6 hour (**A**) and 18 hour (**B**) time intervals.

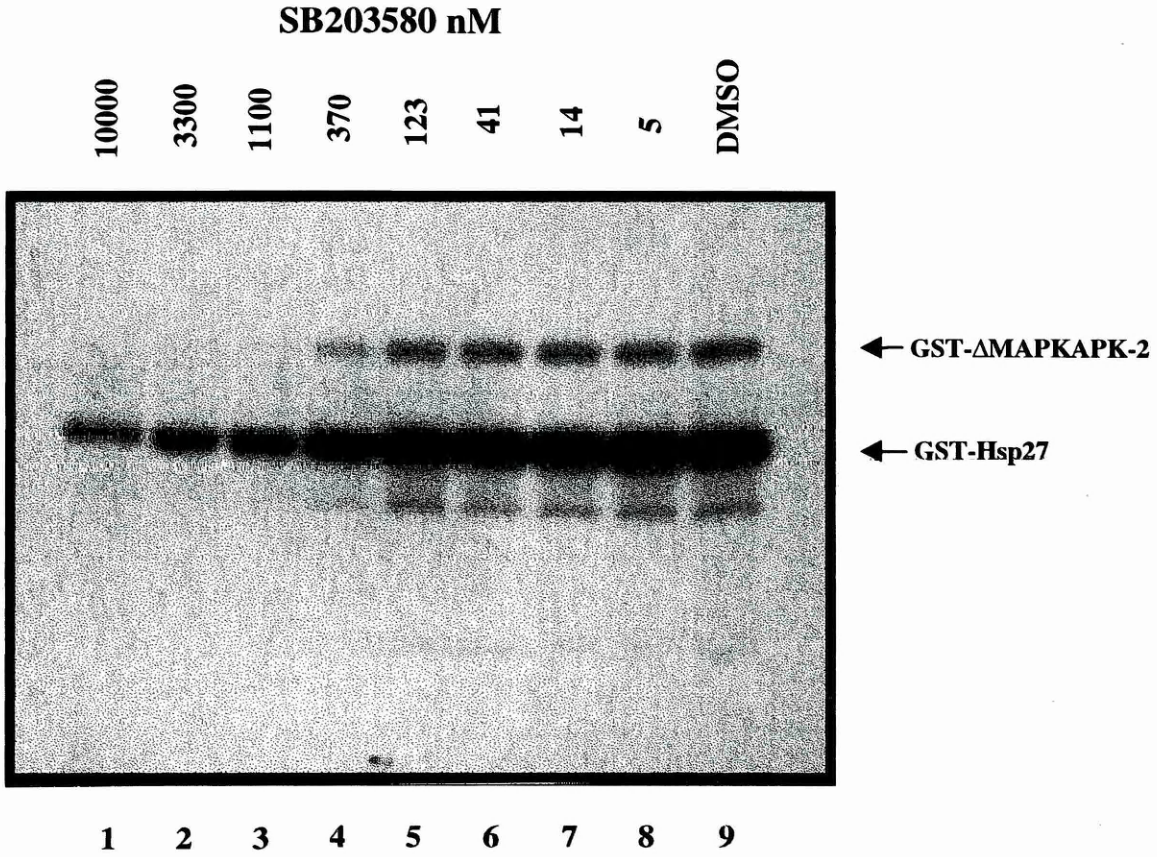

Figure 4.5: *In-vitro* inhibition of GST-Hsp27 phosphorylation by SB203580. FLAG-tagged p38 MAP kinase was transiently expressed and immunoprecipitated from osmotically shocked COS-1 cells. Immune complex protein kinase assays with GST-ΔMAPKAPK-2 and GST-Hsp27(5 μg each) were carried out containing SB203580 at concentrations ranging from 10000 - 5 nM (***lanes 1-8***). ***Lane 9*** represents the DMSO control.

4.3 Discussion

FLAG-tagged p38 MAP kinase and cMyc-tagged MAPKAPK-2 both expressed well in HeLa cells. MAPKAPK-2 migrated with an apparent molecular mass of ~50 kDa, corresponding to the apparent molecular mass of the Hsp27 kinase reported by Freshney *et al.* (1994) and endogenous MAPKAPK-2 in human PMN cells (Krump *et al.*, 1997). The apparent molecular mass of MAPKAPK-2 differs significantly from its calculated molecular mass of ~45 kDa. The reason for this discrepancy is unclear, but the proline rich N-terminal domain may retard the migration of this enzyme during electrophoresis. This hypothesis could be checked by expressing MAPKAPK-2 lacking the N-terminal domain.

Bacterially expressed wild-type and kinase dead GST-ΔMAPKAPK-2_{40-400} fusion proteins, lacking the N-terminal domain, migrated as single bands with the expected molecular masses (~65 kDa). However, Ben-Levy *et al.* (1995) reported two bands with apparent molecular masses of 65 and 62 kDa, when a GST- MAPKAPK-2_{46-400} fusion protein was expressed and purified from *E.coli*. Intriguingly, only the 65 kDa product could be phosphorylated by p38 MAP kinase. Both the 65 and 62 kDa products had the same N-terminal sequence, but the 62 kDa species was truncated at the C-terminus by 26 residues, suggesting that the terminal 26 amino acid residues may play an important role in permitting phosphorylation by p38 MAP kinase.

In this chapter the catalytically inactive p38 and MAPKAPK-2 enzymes described in Chapter 3 were analysed. Mutation of the lysine residues at the ATP binding sites of p38 and MAPKAPK-2, lysines 53 and 93 respectively, abolished the kinase activities of these enzymes as determined by *in-vitro* phosphorylation of their substrates.

In addition, in this chapter it has also been shown that components of the physiological p38 MAP kinase signalling pathway can be successfully reconstituted *in-vitro* using immunoprecipitated p38 MAP kinase with GST-ΔMAPKAPK-2wt and GST-Hsp27, thus confirming that the recombinant proteins share the same mechanisms of activation with the native enzymes. P38 kinase activity was inhibited by SB 203580 with an IC_{50} value of ~0.37-0.123 μM which corresponded to that obtained by Cuenda *et al.* (1995), who calculated an IC_{50} of ~0.6 μM, using bacterially expressed p38 MAP kinase with MAPKAPK-2 as substrate.

The results in this chapter show that both recombinant p38 MAP kinase and MAPKAPK-2 expressed strongly in HeLa cells and that mutation of the ATP binding sites of p38 and MAPKAPK-2 completely abolished the catalytic activities of these enzymes. In Chapter 5, the results of using these proteins as bait in a yeast two-hybrid screen are described, whilst in Chapter 6, the expression of these mutants and their effectiveness in producing a dominant effect, by blocking IL-1 signalling in stably transfected HeLa cells is investigated.

Chapter 5

Yeast Two-Hybrid Screen

5.1 Introduction

5.1.1 General Introduction and aim

With the development of the specific inhibitor, SB 203580, p38 MAP kinase has been identified as having a uniquely pivotal role in a number of inflammatory and immunomodulatory responses. The p38 MAP kinase pathway has been shown to be implicated in the production of IL-1 and TNF in LPS stimulated monocytes (Lee *et al.*, 1994), in IL-1 and TNF induced synthesis of IL-6 and granulocyte-macrophage colony stimulating factor in fibroblasts (Beyaert *et al.*, 1996; Ridley *et al.*, 1997), in collagen-induced platelet aggregation (Saklatvala *et al.*, 1996), in the transcription of interferon-γ (IFNγ) in $CD4^+$ Th1 cells (Rincon *et al.*, 1998), in IL-2 stimulated proliferation of T-cells (Crawley *et al.*, 1997) and in the transcription and translation of IL-1 induced collagenase (matrix metalloproteinase 1), stromelysin (matrix metalloproteinase 3) and cyclooxygenase-2 (COX-2) in fibroblasts (Ridley *et al.*, 1997).

The activation of p38 MAP kinase, with the concomitant biological effects, by the variety of different physiological stimuli described above suggests there may be many yet unidentified proximal and distal components within this pathway. Given the obvious therapeutic potential in inhibiting pro-inflammatory cytokine signalling, as demonstrated by SB 203580, the search for new activators and substrates within this pathway has intensified. With this aim, yeast two-hybrid methodology was employed

to try to identify a novel protein or interaction using integral members of the p38 MAP kinase pathway as "bait". Recent yeast two-hybrid studies have been successful in identifying MAPKAPK-3 from a human leucocyte cDNA library, using a catalytically inactive p38 MAP kinase mutant (D168A) as bait (McLaughlin *et al.*, 1996) and in identifying an interaction between p38 MAP kinase and the transcription factor MEF2C (Han *et al.*, 1997). In the latter study p38 MAP kinase was mutated at the dual phosphorylation site and used to screen a human foetal brain library.

In this study we describe the construction of MKK6B, p38 K53R and MAPKAPK-2 K93R as GAL4 binding domain fusion proteins. The screening of a human leucocyte cDNA library with p38 MAP kinase was unsuccessful in identifying any two-hybrid interactions. However, a potential two-hybrid interaction was identified using MAPKAPK-2 K93R as bait. The results of this screen and the attempts to validate this interaction are presented in this chapter.

5.1.2 Yeast two-hybrid methodology

The yeast two-hybrid system is a powerful and sensitive technique that allows protein interactions to be detected *in-vivo*. The technique was developed from the seminal suggestion by Fields and Song, (1989) that protein interactions could be detected if two potentially interacting proteins were expressed as hybrids. In their suggestion, the first protein contains a DNA binding domain and is bound to DNA upstream of a reporter gene, the second protein contains an activation domain (Figure 5.1). The concept was demonstrated using SNF1 and SNF4, two yeast proteins that interact *in-vivo*. They showed that SNF1 fused to a DNA binding domain and SNF4 fused to an activation domain could interact together and activate transcription of a reporter gene.

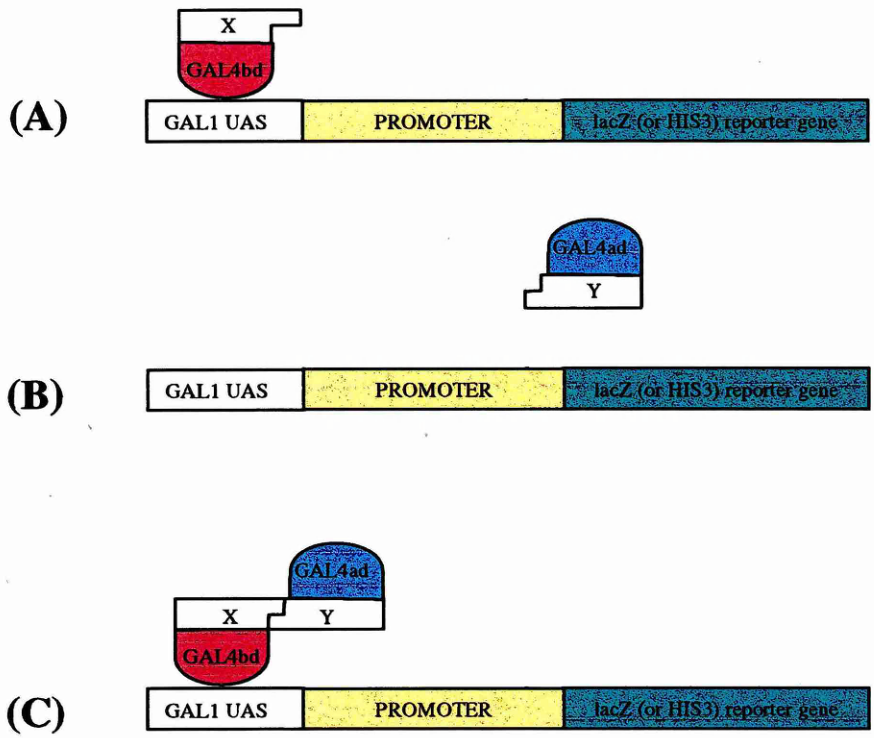

Figure 5.1: Schematic diagram demonstrating the basis of the two-hybrid system. **(A)** The hybrid of the GAL4 DNA-binding domain (bd) and protein X binds to the GAL1 UAS but can not activate transcription without the activation domain. **(B)** The hybrid of the GAL4-activation domain (ad) and protein Y cannot localise to the UAS and therefore no transcription occurs. **(C)** Interaction between the X and Y regions of the two hybrid proteins *in-vivo* reconstitutes GAL4 function and results in expression of the reporter genes.

This finding was of considerable significance since it demonstrated that transcription could be used as a tool to study interactions between proteins not involved in transcription.

The commercial development of the two-hybrid system has been facilitated by the versatility of yeast promoters and their *cis*-acting regulatory elements. All yeast structural genes are preceded by a region containing a loosely preserved TATA box, located approximately 25 bp upstream of the transcriptional start site. Many genes also contain *cis*-activating elements, regions of DNA that are recognized by transcription factors or other *trans*-acting regulatory proteins. In contrast to multicellular organisms yeast *cis*-activating elements tend to be closely associated with the TATA box (Yoccum, 1987). One type of *cis*-acting transcription element in yeast is upstream activating sequences (UAS) which are recognized by specific transcriptional activators that enhance transcription from adjacent downstream TATA regions (Giniger and Ptashne, 1988). The enhancing effect of UASs is generally independent of orientation and they can also be eliminated or modified to change the regulation of genes. In addition, there may be more than one copy of a UAS upstream of a coding region.

The 'mix and match' nature of yeast TATA boxes and upstream activating sequences has led to the creation of artificial promoters linked to reporter genes (Heslot and Gaillardin, 1992). In most cases, the reporter genes are under the control of a promoter comprising a TATA sequence and a UAS derived from a different gene. In some cases, both the TATA and UAS are derived from different genes. In this study the yeast strains HF7z (Feilotter *et al.*, 1994) and SFY526 (Harper *et al.*, 1993) were

used. Table 5.1 below shows the promoter constructs used to regulate reporter gene expression in these strains.

Strain	Reporter gene	Origin of UAS	UAS regulated by	Origin of TATA sequence
HF7z	HIS3	GAL1	GAL4	GAL1
	lacZ	$UAS_{G\ 17\text{-}mer(x3)}$	GAL4	CYC1
SFY526	*lacZ*	GAL1	GAL4	GAL1

Table 5.1: Promoter constructs of the yeast strains HF7z and SFY526 used in this study (Guthrie and Fink 1991).

5.1.3 Reporter genes under the control of GAL4-responsive elements

As shown in Table 5.1, the two-hybrid screen carried out in this study was GAL4 based (Heslot and Gaillardin, 1992). In yeast, the genes required for galactose metabolism are controlled by two regulatory proteins, GAL4 and GAL80, as well as by the carbon source in the medium (Guthrie and Fink, 1991). When galactose is present, GAL4 binds to the GAL4-responsive elements within the UASs of several genes involved in galactose metabolism, such as GAL1, GAL7 and GAL10 and activates transcription (Giniger *et al.*, 1985). In the absence of galactose, GAL80 binds to GAL4 and blocks transcriptional activation. In addition, the presence of glucose also represses transcription of the galactose genes (Johnston *et al.*, 1994). The

tight regulation of the GAL UASs by GAL4 have made it a valuable tool for manipulating the expression of reporter genes that are GAL4 DNA-binding domain (DNA-BD) dependent. However, the yeast host strain must carry deletions in both the *gal4* and *gal80* genes to avoid interference by endogenous GAL4 and GAL80 proteins. Mutations in both of these genes abolish glucose repression and induction unless a two-hybrid interaction occurs.

In the yeast strain, SFY526, the *lacZ* reporter gene is under the control of native GAL1 UAS and TATA sequences. In the yeast strain, HF7z, the *HIS3* reporter gene is also under the control of native GAL1 UAS and TATA sequences. However, the *lacZ* reporter gene in HF7z is controlled by a synthetic $UAS_{G\ 17\text{-}mer\ (x3)}$ consensus sequence and a TATA sequence derived from yeast cytochrome C1 (CYC1) gene (Table 5.1) (Guthrie and Fink, 1991). Consequently, plasmids encoding potential interacting proteins that are $LacZ^+$ in one yeast strain are then isolated and transformed into the other yeast strain. Since these two promoters share only GAL4 responsive elements in common (the rest of the promoter sequences differ significantly), any positive interactions observed in both strains are likely to require binding of the GAL4 DNA-binding domain specifically to the GAL4-responsive elements. Expression of *lacZ* from the synthetic promoter in HF7z cells is much weaker than the level of expression seen with the intact GAL1 promoter in SFY526 cells. The *HIS3* reporter gene in HF7z cells is also under the control of the entire GAL1 promoter, leading to tight regulation of the *HIS3* reporter (Feilotter *et al.*, 1994).

5.1.4 Reporter genes under the control of non-GAL4 responsive elements

The LexA- based two-hybrid system is the most common alternative to the GAL4 dependent system. In this system not only are the TATA sequences and the UAS are derived from different genes, but the LexA *cis*-acting regulatory elements are derived from *E.coli* (Ebina *et al.*, 1983). The 'bait' protein in this system is constructed as a fusion protein with the entire LexA protein. In *E.coli* LexA normally functions as a repressor of SOS genes when it binds to LexA *cis*-acting regulatory elements. In the two-hybrid system there is no repression because the LexA cis-acting motifs are integrated upstream of the TATA and coding region of the reporter genes (Estojak *et al.*, 1995).

5.1.5 Application of the yeast two-hybrid system

The sensitivity of the yeast two-hybrid system has made it an invaluable technique in all laboratories searching for novel protein interactions. During the last few years yeast two-hybrid technology has identified many new proteins and interactions including many of those, described in Chapter 1, involved in pro-inflammatory cytokine signalling such as; RIP (Hsu *et al.*, 1996), TRAF1/2 (Rothe *et al.*, 1994), NIK (Malinin *et al.*, 1997), TRADD (Hsu *et al.*, 1995) and IKKα (Regnier *et al.*, 1997). These findings have contributed greatly to our understanding of cell signalling from the receptor to the nucleus.

Yeast two-hybrid technology can also be used to delineate specific amino acid residues or protein domains involved in a given protein interaction. In yeast two-hybrid systems, the strength of the reporter gene activation generally correlates with

the strength of interaction between the two proteins. Using site specific mutagenesis and deletion mutants, the essential interacting regions of proteins may be identified.

5.2 Results

5.2.1 Construction of p38 K53R, MAPKAPK-2 K93R and MKK6B GAL4 binding domain fusion proteins

In the identification of MAPKAPK-3 by two-hybrid screening with a p38 D168A MAP kinase mutant, McLaughin *et al.* (1996) reported the autonomous activation of the HF7z *HIS3* reporter gene by a GAL4 BD/p38 wt fusion protein. This activation was presumed to be a consequence of the high basal kinase activity of this protein. Because of this a catalytically inactive mutant was produced that did not activate the HF7z reporter gene. Following a similar approach, a catalytically inactive p38 K53R mutant was constructed, as described in Chapter 3, section 3.2.2, to screen a human leucocyte cDNA library. To construct a GAL4 BD fusion protein and remove the FLAG epitope, pcDNA3/FLAGp38K53R was re-amplified using the oligonucleotide primers, W0988 and N0465. The amplified fragment was gel purified, digested with Bam HI and cloned into the correct reading frame of the yeast two hybrid cloning vector pAS2-1 (Figure 5.2B). Transformed colonies were PCR screened to determine the correct orientation of the cloned inserts. Two clones were sequenced in their entirety on both strands to check for any PCR errors. A single error free clone was designated pAS2-1/GAL4BDp38K53R (Figure 5.3).

A full-length MAPKAPK-2 kinase dead GAL4 BD fusion protein was constructed by digesting pSP73/MAPKAPK-2 K93R (see Chapter 3, section 3.2.6) with Eco RI and

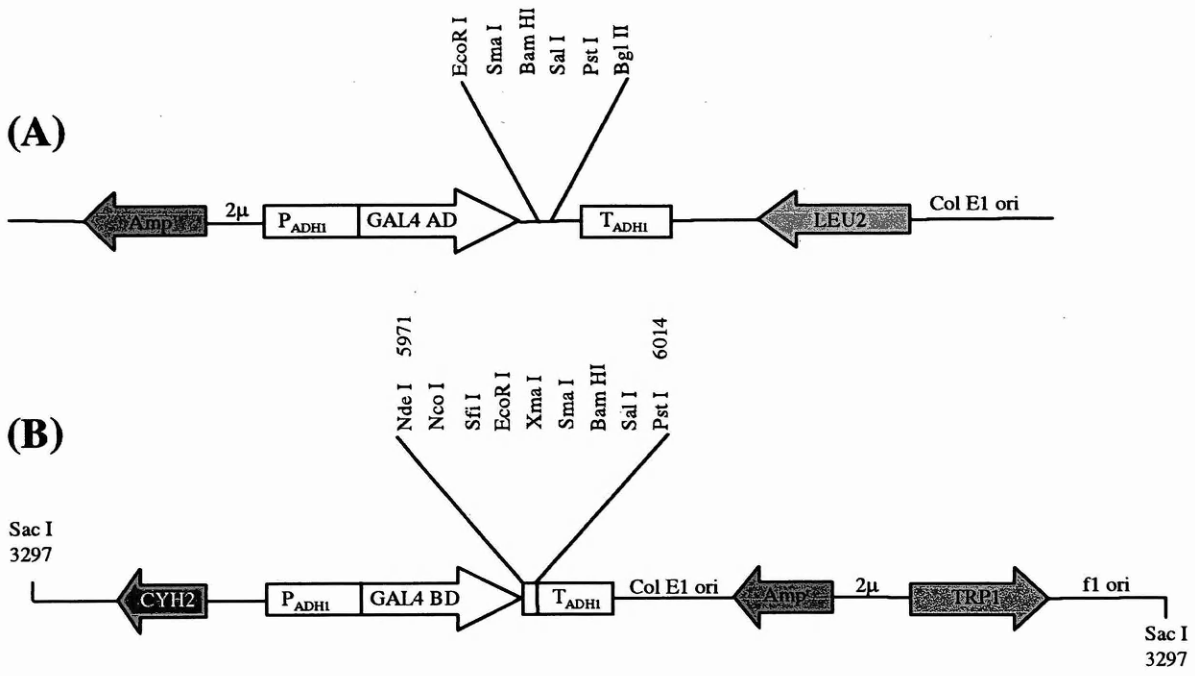

Figure 5.2 (A): pGAD424 DNA-Activation Domain Hybrid Cloning vector. pGAD424 is used to generate GAL4 activation domain fusion proteins. A Col E1 origin of replication and ampicillin resistance gene allow propagation and selection, respectively, in *E.coli;* the 2μ origin of replication allows propagation in yeast. The *LEU2* gene allows selection in yeast host strains which are deficient in leucine biosynthesis.

Figure 5.2 (B): pAS2-1 DNA-Binding Domain Hybrid Cloning Vector. pAS2-1 generates a GAL4 DNA-BD (amino acids 1-147) fusion when the protein of interest is cloned into the MCS in the correct orientation and reading frame. pAS2-1 carries the wild-type yeast CYH^S2, which confers sensitivity to cycloheximide (P); transcription is terminated at the ADH1 transcription termination signal (T) and targeted to the yeast nucleus by nuclear localization sequences. pAS2-1 is a shuttle vector that replicates autonomously in both *E.coli* and *S.cerevisiae,* and carries the *bla* gene, which confers ampicillin resisitance in *E.coli.* pAS2-1 also carries the *TRP1* nutritional gene that allows yeast auxotrophs to grow on limiting synthetic media.

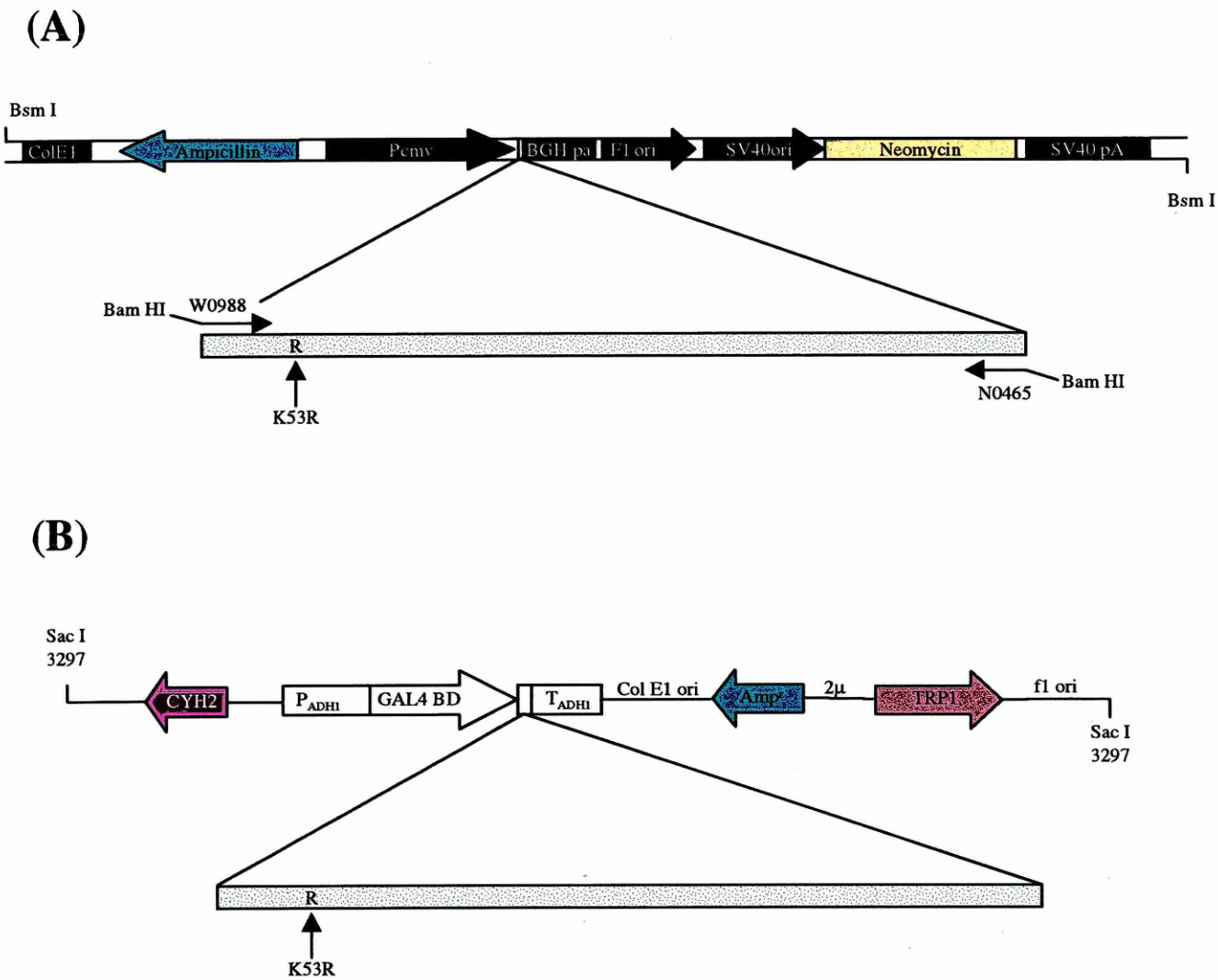

Figure 5.3: Construction of GAL4 BD/p38 K53R fusion protein. **(A)** pcDNA3/FLAGp38K53R was used as template and re-amplified using the oligonucleotides W0988 (forward) and N0465 (reverse). **(B)** The amplified fragment was digested with Bam HI and cloned into the correct reading frame of Bam HI digested pAS2-1.

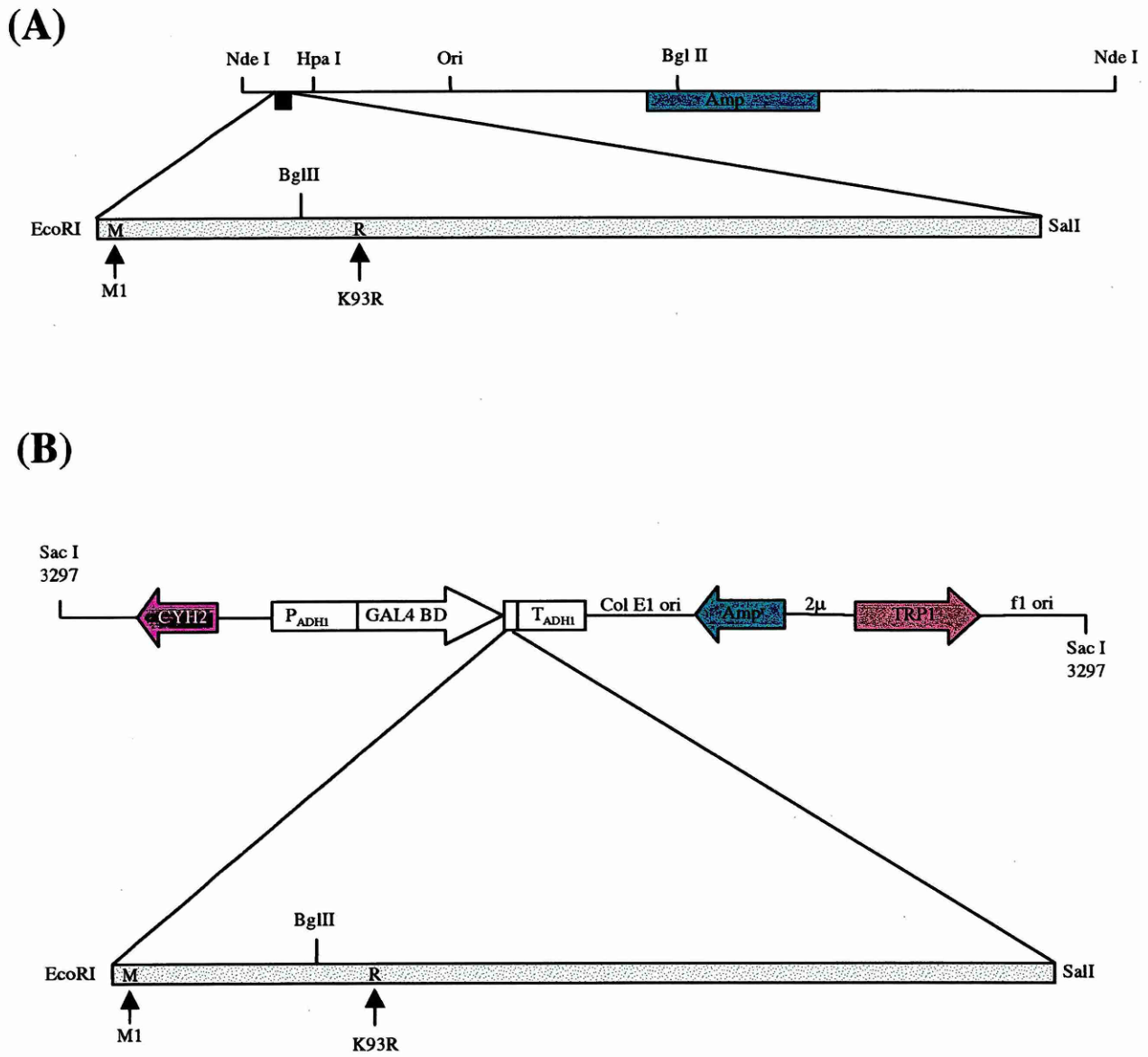

Figure 5.4: Construction of the GAL4 BD/MAPKAPK-2 K93R fusion protein. **(A)** pSP73/MAPKAPK-2K93R was digested with the Eco R1 and Sal I and cloned into the correct reading frame of Eco R1/Sal I cut pAS2-1 **(B).**

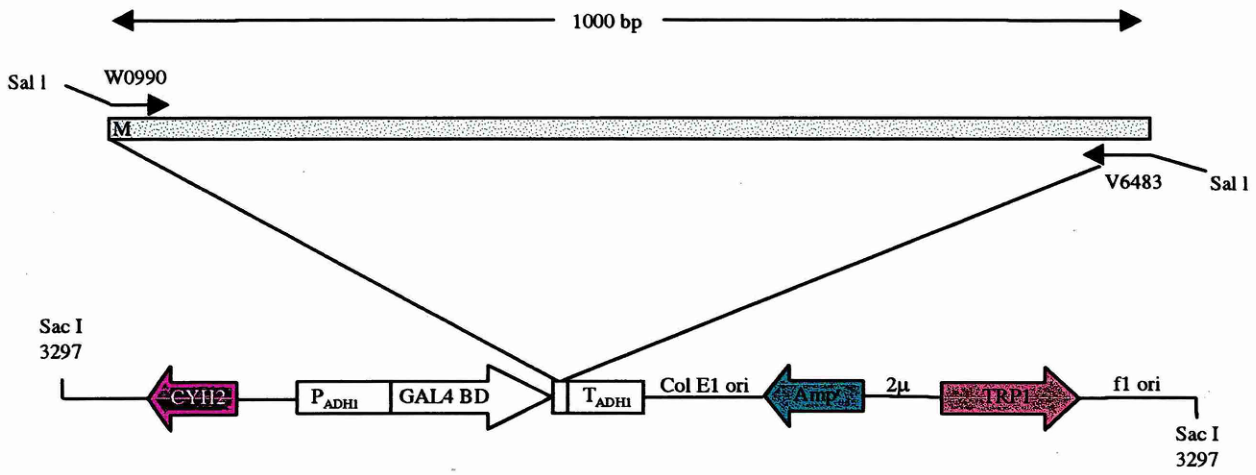

Figure 5.5: Construction of the GAL4 BD/MKK6B fusion protein. MKK6B was amplified from a human PBMC cDNA library using the oligonucleotides W0990 (forward) and V6483 (reverse). A fragment of ~1 kb was amplified, digested with Sal I and cloned into the correct reading frame of Sal I digested pAS2-1.

Sal I. The MAPKAPK-2 K93R fragment was then sub-cloned into pAS2-1 (Figure 5.4).

MKK6B was amplified from a human peripheral blood mononuclear cell cDNA library (PBMC cDNA) using oligonucleotide primers, W0990 and V6483, designed to the 5' and 3' terminals off the gene. Both oligonucleotides contained Sal I restriction enzyme sites to facilitate cloning. The MKK6B fragment was gel purified and cloned into the correct reading frame of pAS2-1. Transformed colonies were PCR screened using vector and gene specific oligonucleotides to determine the correct orientation of the cloned inserts. Two clones were sequenced in their entirety on both strands using oligonucleotides designed from the published sequence of MKK6B (Han *et al.*, 1996; Moriguchi *et al.*, 1996). A single error free clone was designated pAS2-1/GAL4BDMKK6 (Figure 5.5).

5.2.2 Construction of a GAL4 activation domain /p38 K53R fusion protein

The strength of activation of the *HIS3* and *LacZ* reporter genes in the yeast two-hybrid system are directly related to the strength of interaction between the two GAL4 BD and GAL4 AD fusion-proteins. The exact nature of the interaction between p38 MAP kinase and MKK6B is unknown. However, in a recent report evidence was provided of a physical interaction between p38 MAP kinase and MAPKAPK-2 *in-vivo* (Ben-Levy *et al.*, 1998). Because of this p38 K53R was cloned as a GAL4 activation domain fusion protein (GAL4 AD) to act as a positive control when co-transformed with either MKK6B or MAPKAPK-2 GAL4 BD fusion proteins.

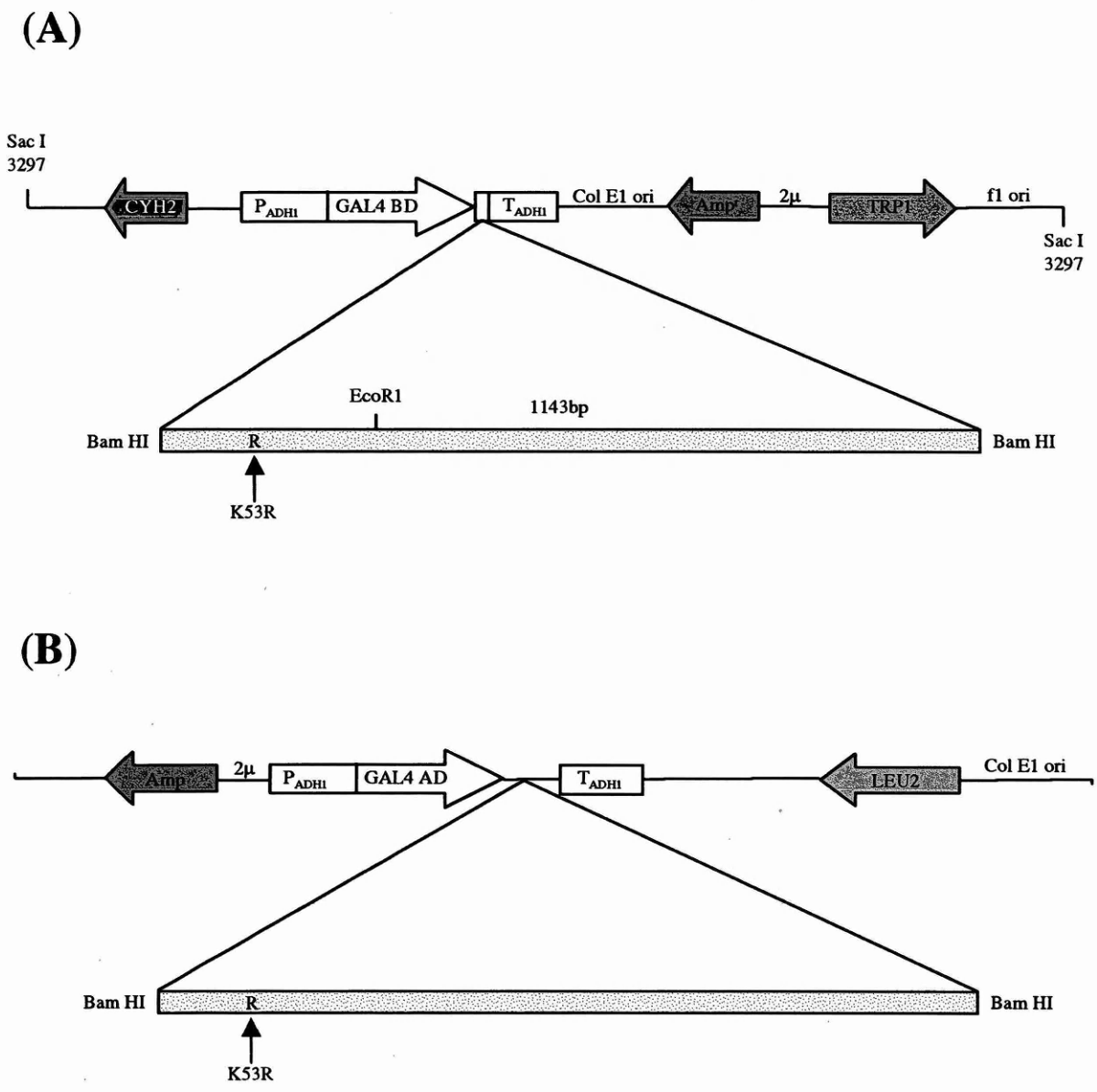

Figure 5.6: Construction of the GAL4 AD/p38 K53R fusion protein. **(A)** pAS2-1/GAL4BDp38K53R was digested with Bam HI and the insert was subcloned into Bam HI digested pGAD424 **(B).**

The GAL4 AD/p38K53R fusion protein was constructed by digesting pAS2-1/GAL4BDp38K53R with Bam HI and subcloning the fragment into the correct reading frame of pGAD424 (Figure 5.2A). Transformants were PCR screened to determine the correct orientation, using gene and vector specific oligonucleotide primers. A single clone in the correct orientation was designated pGAD424/GAL4ADp38K53R (Figure 5.6).

5.2.3 Validation of the amplified human leucocyte cDNA library

Prior to co-transformation of yeast HF7z cells with the human leucocyte cDNA library and the GAL4 fusion constructs the integrity of the amplified library was validated by PCR. The results of several PCR reactions in which integral members of the p38 MAPK signalling pathway are amplified are shown in Figure 5.7. MKK6B (Figure 5.7, *lane 4*), p38 (Figure 5.7, *lane 3*), ΔMAPKAPK-2 (Figure 5.7, *lane 5*) and Hsp27 (Figure 5.7, *lane 7*) were all represented and successfully amplified from the library cDNA, producing amplified fragments of the correct size (1143 bp, 1000 bp, 1100 bp and 630 bp respectively). The attempt to amplify full length MAPKAPK-2 was unsuccessful and should have produced an amplified fragment of 1240 bp (Figure 5.7, *lane 6*). However, for the reasons discussed in Chapter 3.3, in which the attempt to PCR full length MAPKAPK-2 from human PBMC cDNA was also unsuccessful, this result was not surprising. The result of this experiment confirmed that the full-length genes of several integral components of the p38 MAP kinase signalling pathway are represented in this library cDNA preparation.

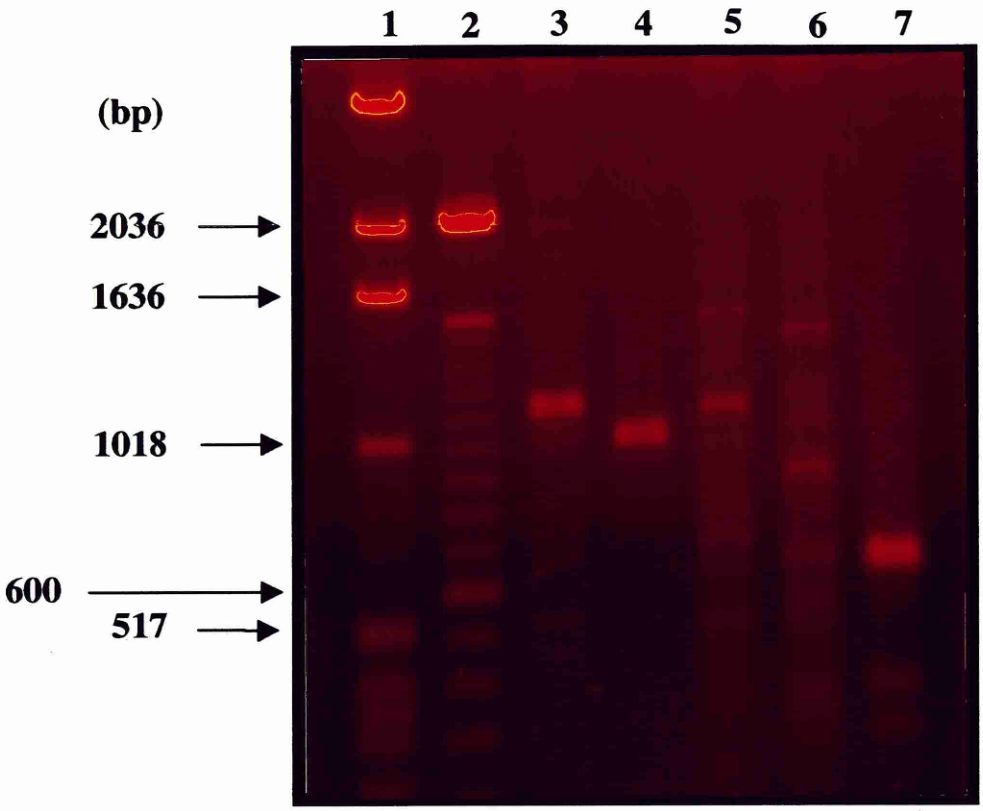

Figure 5.7: PCR analysis of the amplified human leucocyte Matchmaker cDNA library, demonstrating representation of several integral members of the p38 MAP kinase signalling pathway. The integrity of the amplified human leucocyte cDNA library was assessed by PCR amplification of relevant enzymes. Library cDNA (0.5 µg/ reaction) was used as template to amplify; p38 MAP kinase (***lane 3***), MKK6B (***lane 4***), ΔMAPKAPK-2 (***lane 5***) MAPKAPK-2 (***lane 6***), and Hsp27 (***lane 7***). ***lanes 1 and 2*** are 1 kb and 100 bp molecular weight markers respectively. 20 µl of a 50 µl PCR reaction was loaded and electrophoresed on a 1 % agarose gel.

5.2.4 Yeast phenotype verification and test for autonomous activation of the *HIS3* and *lacZ* reporter genes by the GAL4 BD fusion constructs

Prior to transforming the yeast strains with plasmid it was important to check the nutritional requirements of the HF7z and SFY526 yeast strains. Colonies from each were streaked onto synthetic dropout (SD) agar plates lacking either tryptophan (Trp^-), leucine (Leu^-) or histidine(His^-). The plates were then incubated at 30 °C and examined for growth after 3 days for HF7z and 4-5 days for SFY526. The results obtained are indicated in Table 5.3.

SD Medium	SFY526	HF7z
-Trp	-	-
-Leu	-	-
-His	-	-*

Table 5.2: Growth results of SFY526 and HF7z on various SD agar plates. The asterisk denotes that HF7z grows very slowly on SD/His^- plates.

To test for autonomous activation of the *HIS3* and *lacZ* reporter genes, by the GAL4 BD fusion proteins, the plasmids were separately transformed into yeast HF7z cells and plated onto SD/Trp^- agar plates. After incubation at 30°C for 3 days single colonies from each transformed plasmid were picked and resuspended in 20 µl of TE buffer. 10 µl of this suspension was spotted onto sterile filter paper overlayed on a SD/Trp^- agar plate and incubated for a further 3 days. The filters were lifted and assayed for β-gal activity as described in Chapter 2.5.4. The remaining 10 µl of the cell suspension was plated onto SD/His^- agar plates, which were incubated for 3 days at 30°C. None of the GAL4 BD fusion proteins autonomously activated the *lacZ*

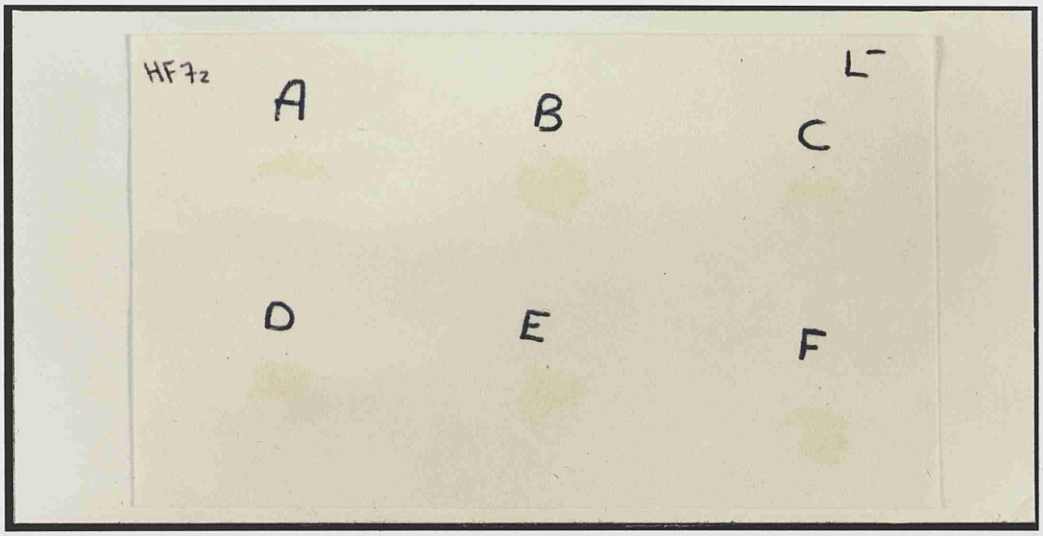

Figure 5.8: β-gal assays to test for autonomous activation of the *lacZ* reporter gene in yeast HF7z cells transformed with GAL4 BD fusion constructs. Competent HF7z cells were transformed with 0.5 μg of plasmid DNA and plated onto synthetic dropout (DO) medium, lacking tryptophan (Trp), SD/Trp$^-$. The plates were then incubated at 30°C for 3 days until colonies appeared. Single, well isolated colonies were picked and resuspended in sterile TE buffer and spotted onto sterile filter paper overlayed on SD/Trp$^-$ plates. After 48 hours incubation, the filter papers were lifted and β-galactosidase activity was determined by assaying the filters in Z buffer/X-gal solution for a maximum of 8 hours.

Expt.A: GAL4 BD/p38 K53R
Expt.B: GAL4 BD/ΔMAPKAPK-2 wt
Expt.C: GAL4 BD/ΔMAPKAPK-2 K93R
Expt.D: GAL4 BD/MKK6B
Expt.E: GAL4 BD/MAPKAPK-2 wt
Expt.F: GAL4 BD/MAPKAPK-2 K93R

reporter gene and no growth was observed with any of the transformed plasmids on SD/His$^-$ agar plates (Figure 5.8). In Figure 5.8, *Expts. B and C*, the autonomous activation results of truncated (Δ) MAPKAPK-2 wt and K93R GAL4 BD fusion proteins are shown. However, these constructs were not progressed any further in this study.

5.2.5 Activation of the *lacZ* reporter gene by interactions between GAL4 BD/MAPKAPK-2wt/K93R and GAL4 AD/p38 K53R fusion proteins

As discussed, the p38 K53R mutant was constructed as a GAL4 AD fusion protein to act as a control for a positive two-hybrid interaction when co-transformed with either MKK6B or MAPKAPK-2 GAL4 BD fusion proteins. Plasmids were co-transformed into yeast HF7z cells as described in Chapter 2.5.3 and plated onto SD/Trp$^-$/Leu$^-$ agar plates. Single isolated colonies were picked and assayed for β-gal activity (Figure 5.9).

As expected, co-transformation of the GAL4 AD/p38 K53R fusion protein with either the GAL4 BD/MAPKAPK-2wt or GAL4 BD/MAPKAPK-2 K93R fusion proteins produced a strong β-gal signal (Figure 5.9, *Expts. H and I respectively*). There was no visible signal when GAL4 AD/p38 K53R was co-transformed with the empty GAL4 BD fusion vector, pAS2-1, or when the wild type and kinase dead GAL4 BD/MAPKAPK-2 fusion proteins were co-transformed with empty GAL4 AD fusion vector (Figure 5.9, *Expts. G, J and K respectively*). Surprisingly, no positive β-gal signal was obtained when GAL4 AD/p38 K53R was co-transformed with GAL4 BD/MKK6B (Figure 5.9, *Expt. L*). There may be several reasons for the failure of p38 and MKK6B to interact and activate the *lacZ* reporter gene. One possible explanation

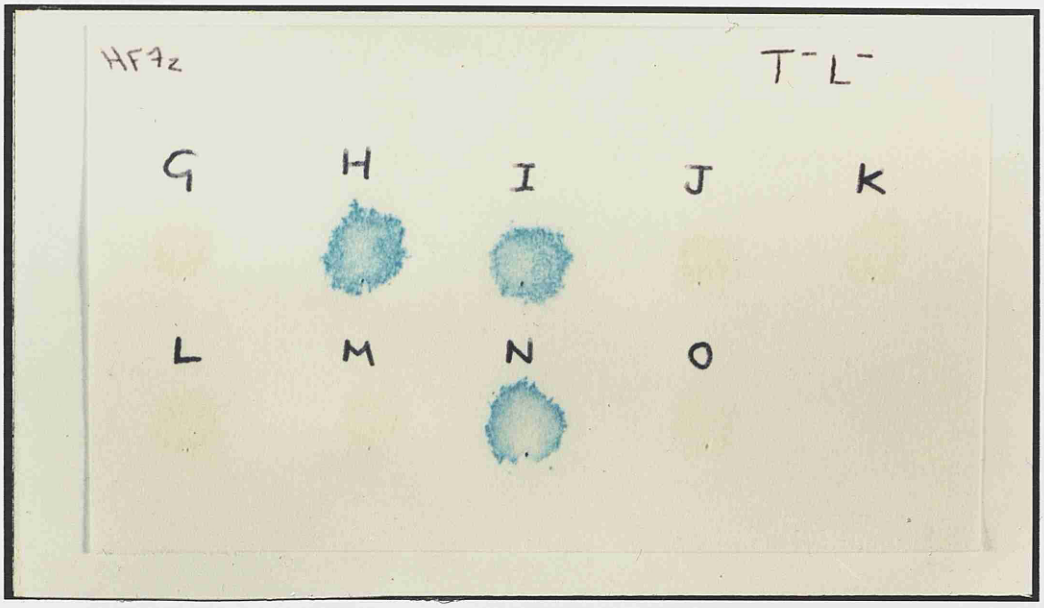

Figure 5.9: Positive control protein-protein interactions as determined by β-gal assays of co-transformed yeast HF7z cells. Competent HF7z cells were co-transformed with 0.5 µg of DNA from each plasmid and plated onto synthetic dropout (DO) medium, lacking tryptophan (Trp) and leucine (Leu),SD/Trp$^-$/Leu$^-$. The plates were then incubated at 30°C for 4-5 days until colonies appeared. Single, well isolated colonies were picked and resuspended in sterile TE buffer and spotted onto sterile filter paper overlayed on SD/Trp$^-$/Leu$^-$ plates. After 48 hours incubation, the filter papers were lifted and β-galactosidase activity was determined by assaying the filters in Z buffer/X-gal solution for a maximum of 8 hours.

Expt.G:	GAL4 AD/p38 K53R and GAL4 BD(empty vector)
Expt.H:	GAL4 AD/p38 K53R and GAL4 BD/MAPKAPK-2 wt
Expt.I:	GAL4 AD/p38 K53R and GAL4 BD/MAPKAPK-2 K93R
Expt.J:	GAL4 AD(empty vector) and GAL4 BD/MAPKAPK-2 wt
Expt.K:	GAL4 AD(empty vector) and GAL4 BD/MAPKAPK-2 K93R
Expt.L:	GAL4 AD/p38 K53R and GAL4 BD/MKK6B
Expt.M:	GAL4 AD(empty vector) and GAL4 BD/MKK6B
Expt.N:	pTD1 and pVA3 (positive control see Chapter 2, section 2.1.9)
Expt.O:	GAL4 AD(empty vector) and GAL4 BD (empty vector)

may be due to the lack of expression of the GAL4 BD/MKK6B fusion protein. To test this, transformed HF7z cells were lysed immunoblotted and probed with a murine anti-GAL4 BD monoclonal antibody. Figure 5.10 shows that the expression of GAL4 BD/MKK6B (~59 kDa) in yeast HF7z cells was clearly detectable.

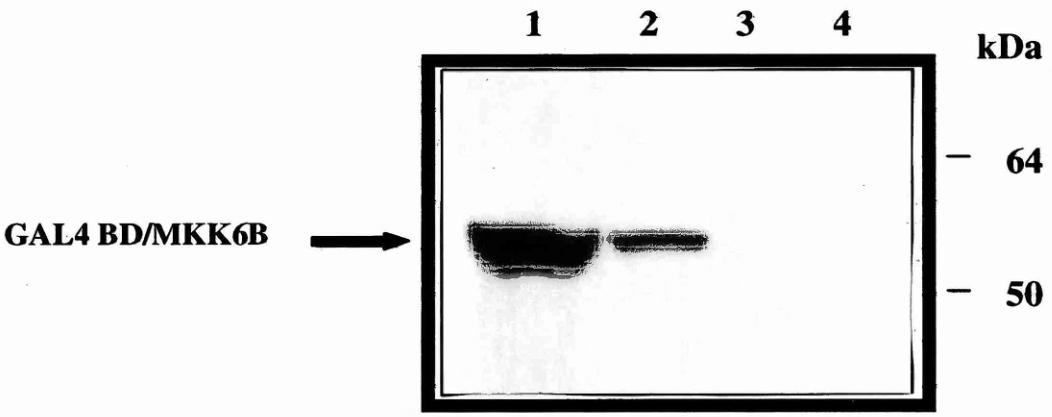

Figure 5.10: Expression of GAL4 BD/MKK6B in yeast HF7z cells. Transformed yeast cells were lysed and electrophoresed on a 4-20% Tris-glycine gel. The samples were immunoblotted and probed with an anti-GAL4 BD monoclonal antibody. **Lanes 1 & 2** indicate 40 µl and 10 µl loadings respectively of transformed cell lysates. **Lanes 3 & 4** represent equivalent loadings, 40 µl and 10 µl respectively, of untransformed cell lysates.

Another explanation could be that in yeast the proper post-translational modificatons required for native folding, or interactions of some mammalian proteins are not provided. This appears not to be the case because Zanke *et al.* (1996) demonstrated by two-hybrid interactions that MKK6 is able to interact with p38 wild type without the need of scaffold proteins. It maybe therefore that the success of a positive two-hybrid interaction may be determined more by the conformational changes imposed on a protein because of specific mutations, rather than any post-translational modifications

imposed by yeast. Because of its failure to interact with p38 K53R, the GAL4 BD/MKK6B fusion construct was not used in any further two-hybrid studies.

5.2.6 Two-hybrid screening of a human leucocyte cDNA library with MAPKAPK-2 K93R

Competent yeast HF7z cells were co-transformed with pAS2-1/GAL4BDMAPKAPK-2K93R and pGAD10/GAL4AD human leucocyte cDNA plasmids (500 µg each) as described in Chapter 2.5.3. The cells were plated onto SD/Trp$^-$/His$^-$/Leu$^-$ agar plates and incubated at 30°C for 8 days. In addition, to determine the efficiency of co-transformation, the cells were also plated onto SD/Leu$^-$/Trp$^-$ agar plates and incubated at 30°C. After 4 days the colonies were counted and the number of independent cDNA clones screened was determined. Seventy-six out of the 1.5 X 10^6 independent cDNA clones screened grew in the absence of histidine (His$^+$). Growth on histidine deficient medium alone may not reflect a true two-hybrid interaction. Activation of this reporter gene may occur for example due to the fortuitous cloning of HIS3 transcriptional activators or other activators that appear to require the presence of both types of hybrid, but are not dependent on interaction between the hybrid proteins. Consequently, screening for the expression of the second reporter gene (*lacZ*) is necessary.

His$^+$ co-transformants were picked, resuspended in 10 µl of TE buffer and gridded onto sterile filter paper overlayed on a SD/Trp$^-$/His$^-$/Leu$^-$ agar. After 48 hours the colonies were lifted and assayed for β-galactosidase activity. Thirty of the 76 His$^+$ co-transformants had detectable β-galactosidase activity after 8 hours incubation, albeit of varying intensities (Figure 5.11). Plasmids were recovered from the His$^+$, LacZ$^+$

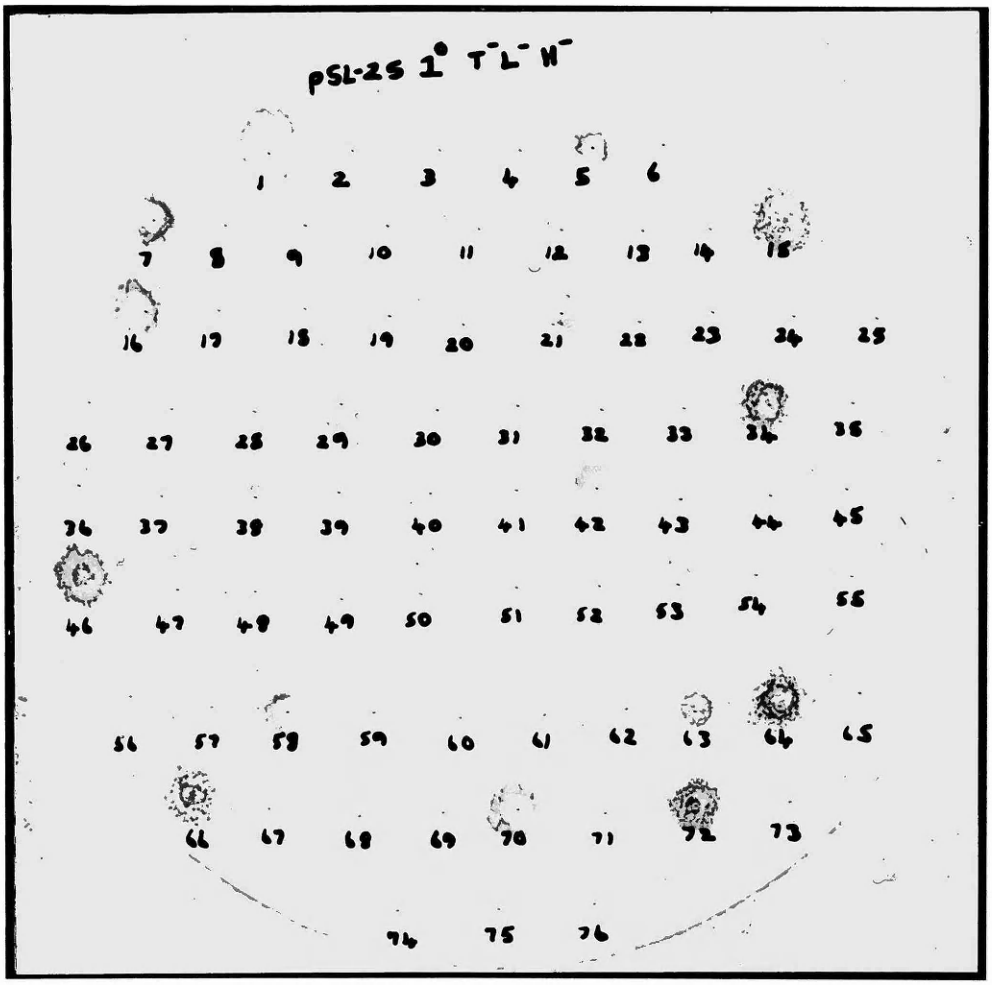

Figure 5.11: β-gal assay of the HIS⁺ co-transformants (putative MAPKAPK-2 K93R - interacting clones) isolated from a human leucocyte cDNA library screen. A human leucocyte cDNA library, pGAD10/library (500 μg), was simultaneously co-transformed with pAS2-1/MAPKAPK-2 K93R (500 μg) and plated out onto synthetic dropout (SD) medium, lacking tryptophan (Trp), leucine (Leu) and histidine (His), SD/Trp⁻/Leu⁻/His⁻.The plates were incubated at 30°C for 8 days and then examined for growth. Seventy six HIS⁺ colonies were picked, resuspended in sterile TE buffer and spotted onto sterile filter paper overlayed on SD/Trp⁻/Leu⁻/His⁻ agar. After 48 hours incubation at 30°C, the filter was lifted and assayed for *lacZ* reporter gene activity in Z buffer/Xgal solution for a maximum of 8 hours.

co-transformants and electroporated into *E.coli* HB101 cells. To select for the GAL4 AD/library component cells were plated onto SD/Leu$^-$, M9 minimal media containing ampicillin (50 μg/ml). Because transformed yeast cells may take up several plasmids, several *E.coli* colonies (10) transformed with plasmid isolated from each His$^+$, LacZ$^+$ yeast clone were PCR screened using pGAD10 vector specific oligonucleotides and the insert sizes were determined. Twenty-six out of the 30 His$^+$, LacZ$^+$ clones contained unique inserts. Plasmid DNA was prepared from each and sequenced at the 5' terminus with a specific oligonucleotide designed to bind complementary sequence in the GAL4 activation domain. The sequences were analysed using the NCBI BLAST nucleotide similarity search tool. Only two clones, pGAD10/AD1.1 and pGAD10/AD46.1, contained protein coding sequence that was correctly fused with the GAL4 activation domain. Both clones encoded partial, overlapping nucleotide sequences that shared substantial homology with the human homologue of polyhomeotic 2 (HPH2) protein (Gunster *et al.*, 1997). The remaining clones contained sequences of genomic DNA or cDNA sequences in the wrong reading frame. The high number of co-transformants that were HIS$^+$ and LacZ$^+$ positive and yet did not contain any coding sequence was of some concern. A possible explanation as to why unidentifiable or incorrectly fused cDNA messages appeared to activated the *HIS*$^+$ and *LacZ*$^+$ reporter genes is that the ADH terminator can sometimes act as cryptic promoter in yeast and initiate transcription in the reverse direction. These proteins are usually transcriptional activators which do not require the presence of the GAL4 AD in order to activate transcription of the reporter genes (Clontech, personal communication). However, plasmid isolated from these clones was not reconstituted, as described in Table 5.4, which would have subsequently identified many of these co-transformants as false positives.

5.2.7 Analysis of the HPH2-like clones, pGAD10/AD1.1 and pGAD10/AD46.1

Oligonucleotide sequencing primers were designed from the published sequence of the HPH2 gene (Gunster *et al.*, 1997). Both clones, pGAD10/AD1.1 and pGAD10/AD46.1, were sequenced in their entirety on both strands using gene and vector specific oligonucleotides. The sequencing results revealed that the longest clone, pGAD10/AD1.1, encoded a protein that was shorter than full the length HPH2 protein sequence by 138 amino acids at the N-terminus. In Figure 5.12 the amino acid f the two clones isolated in this study are shown aligned next to the published sequences of HPH2 and HPH1 (a closely related homologue of HPH2) (Gunster *et al.*, 1997). To avoid confusion in numbering, since HPH1 and HPH2 are different lengths, the amino acid residues in Figure 5.12 are numbered arbitrarily (1-300). From these alignments, it can be seen that the clones isolated in this study differed significantly from the published HPH2 sequence at three regions between amino acids 23-31, 141-171 and 202-337. The differences between the amino acid sequences at these regions were the result of a number of nucleotide deletions and insertions (nucleotide sequence not shown). The shorter clone, pGAD10/AD46.1 fused with the GAL4 activation domain at the start of the second variable region (141-171) and was identical to the sequence of pGAD10/AD1.1. To determine if the sequence changes in the isolated clones were authentic, HPH2-like was amplified from an independent cDNA library. Oligonucleotide primers, D5865 and C4047, were designed to the 5' and 3' terminal nucleotide sequences of pGAD10/AD1.1. A fragment of 900 bp was amplified from a human peripheral blood mononuclear cell (PBMC) cDNA library and cloned into pGEX-3X to generate the construct pGEX/GSTHPH2-like. Sequence analysis revealed that this clone contained exactly the same amino acid changes as those identified in pGAD10/AD1.1.

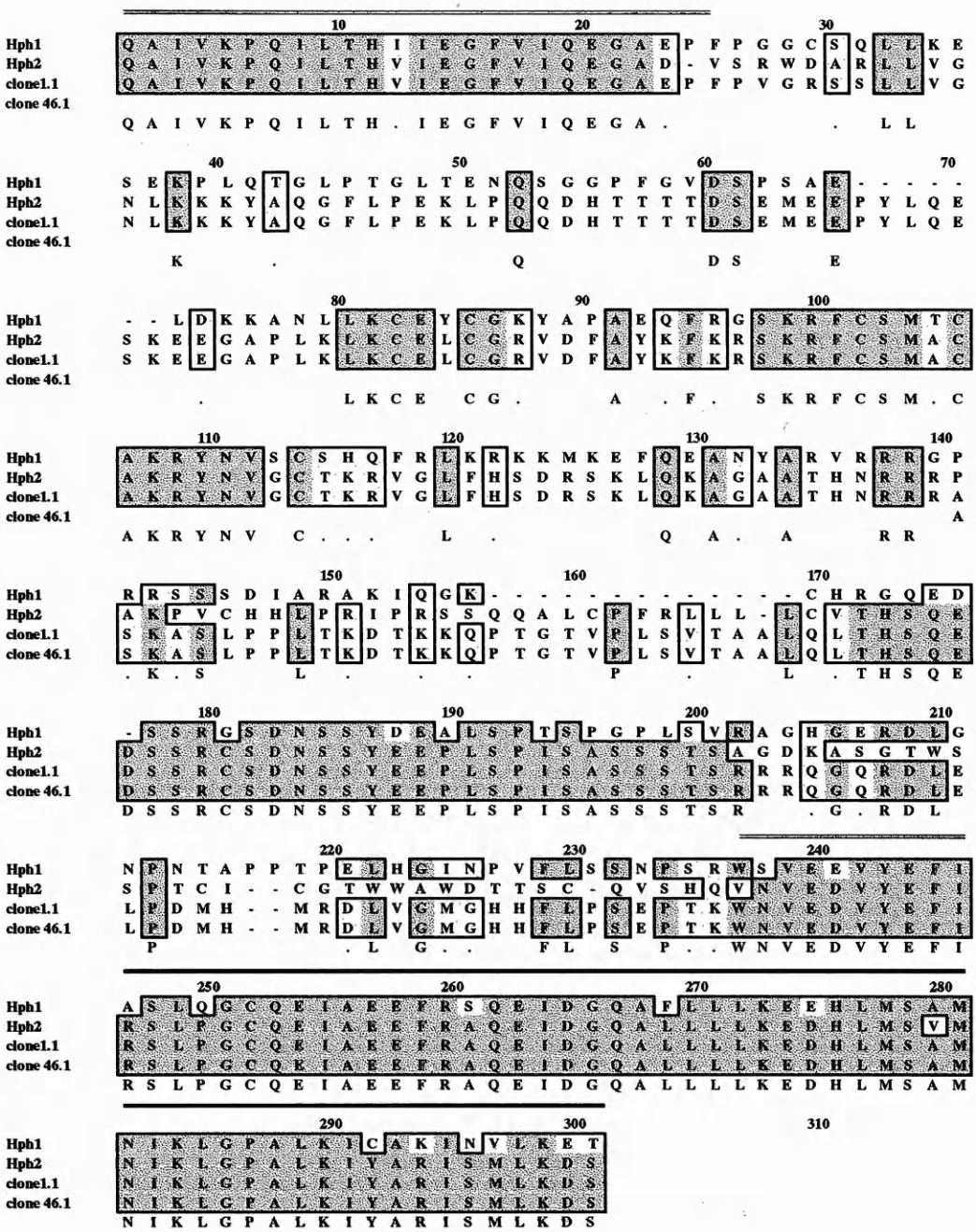

Figure 5.12: Partial sequence alignments of the published HPH1 and HPH2 amino acid sequences (Gunster *et al.*, 1997) against the sequences of the two clones pGAD10/AD1.1 and pGAD10/AD46.1 isolated in this study. The homology domain regions 1 (1-26) and 2 (237-301) are indicated by the bold lines

5.2.8 Reconstitution of the *HIS3* and *lacZ* reporter genes in HF7z cells

To determine whether or not the interaction between MAPKAPK-2 K93R and AD1.1 was a genuine two-hybrid interaction or a false positive interaction, HF7z cells were co-transformed with plasmids expressing the fusion proteins as described in Table 5.4. The co-transformed cells were plated onto a SD/Trp^-/Leu^- agar and assayed for β-galactosidase activity. HIS3 activity was determined by growth on SD/Trp^-/His^-/Leu^- agar plates.

Expt. No.	Test Purpose	Plasmid 1 (GAL4 BD/fusion)	Plasmid 2 (GAL4 AD/fusion)	Selection Medium	Expected β-gal Result
1	Confirm phenotype	BD/MAPKAPK-2 K93R	AD/1.1	$Leu^- Trp^-$	+
2	Check for autonomous activation	BD/No insert (pAS2-1)	AD/1.1	$Leu^- Trp^-$	-
3	Identify artifactual interactions	BD/ $p53_{(72-390)}$ (pVA3, see Chapter 2, section 2.1.8)	AD/1.1	$Leu^- Trp^-$	-
4	Positive control	BD/$p53_{(72-390)}$ (pVA3, see Chapter 2, section 2.1.8)	AD/largeT-Ag (pTD1, see Chapter 2, section 2.1.8)	$Leu^- Trp^-$	+
5	Positive control	BD/MAPKAPK-2 K93R	AD/p38 K53R	$Leu^- Trp^-$	+

Table 5.3: Reconstitution experiments in HF7z cells. To eliminate the possibility of a false positive interaction between MAPKAPK-2 K93R and AD1.1, the above co-transformations were carried out in yeast HF7z cells and assayed for β-gal activity (Figure 5.13).

The results of the β-galactosidase assays described above are shown in Figure 5.13. In addition, HF7z cells were also separately transformed with pGAD10/AD1.1 and the control plasmid pCL-1, encoding wild type full length GAL4 (see Chapter 2, section 2.1.9). The lack of β-galactosidase activity when HF7z cells are transformed with

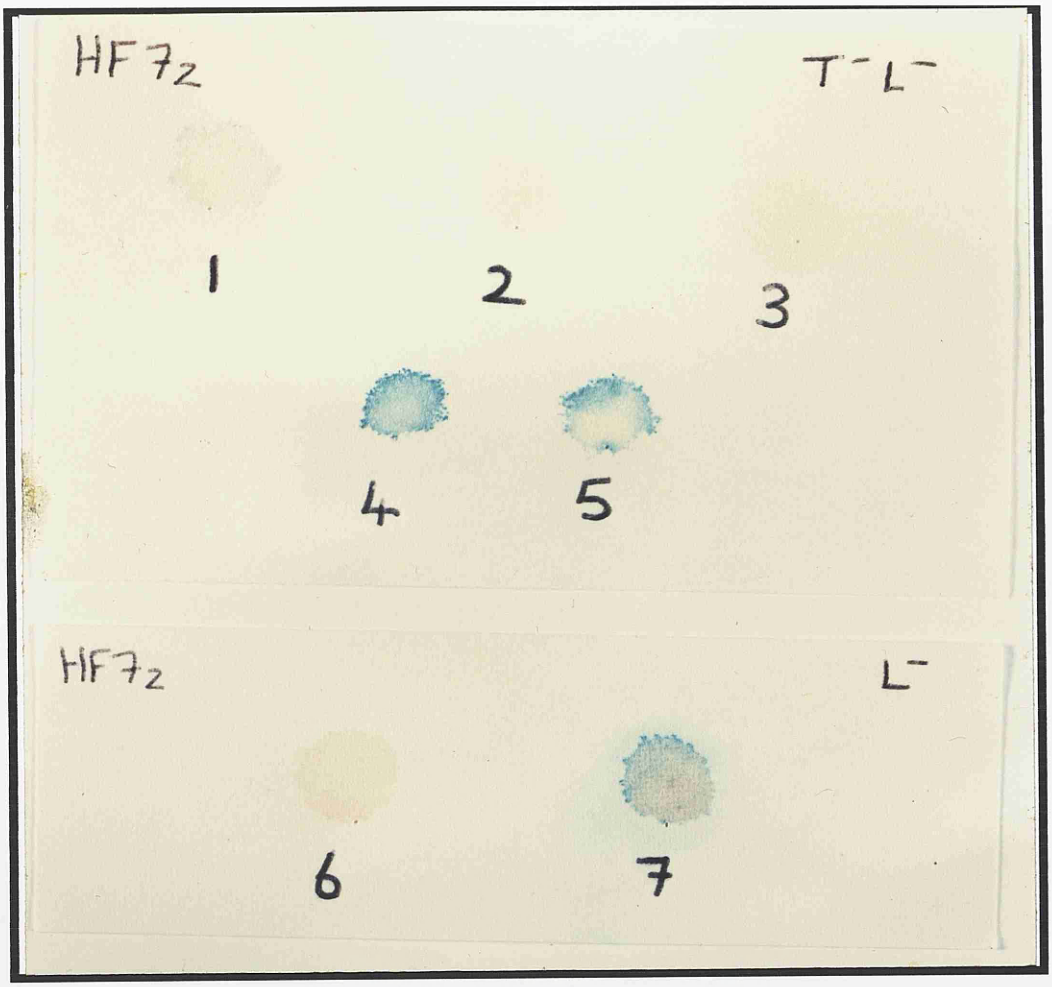

Figure 5.13: Reconstitution of the *lac Z* reporter gene by simultaneous co-transformation of pGAD10/AD1.1 (GAL4 AD/1.1) and pAS2-1/MAPKAPK-2 K93R into yeast HF7z cells. Competent HF7z cells were co-transformed with 0.5 µg of each plasmid and plated onto synthetic dropout (SD) medium, lacking tryptophan (Trp) and leucine (Leu), SD/Trp⁻/Leu⁻.The plates were incubated at 30°C for 4-5 days. Single, well isolated colonies were picked, resuspended in sterile TE and spotted onto sterile filter paper overlayed on SD/Trp⁻/Leu⁻ agar. After 48 hours incubation at 30°C, *lacZ* activity was determined by assaying the filters in Z buffer/X-gal solution for a maximum of 8 hours. In addition pGAD10/AD1.1 and pCL-1were separately transformed and plated onto SD/Leu⁻ agar.

Expt.1:	GAL4 AD/1.1 and GAL4 BD/MAPKAPK-2 K93R
Expt.2:	GAL4 AD/1.1 and pAS2-1 (empty vector)
Expt.3:	GAL4 AD/1.1 and pVA3
Expt.4:	pTD1 and pVA3 (positive control see Chapter 2, section 2.1.9)
Expt.5:	GAL4 AD/p38 K53R and GAL4 BD/MAPKAPK-2 K93R (positive control)
Expt.6:	GAL4 AD/1.1
Expt.7:	pCL-1(assay control see Chapter 2, section 2.1.9)

GAL4 AD/1.1 alone confirms the LacZ$^-$ phenotype, whilst full length GAL4 acts as a positive control for the β-gal assays (Figure 5.13, *Expts. 6 and 7 respectively*). Co-transformation of GAL4 AD/1.1 and GAL4 BD/MAPKAPK-2 K93R into HF7z cells produced a weak β-gal$^+$ signal, which began to appear after ~5 hours incubation (Figure 5.13, *Expt. 1*). The reactions were incubated for a total of 8 hours at room temperature (longer incubation periods can produce false positive signals). At the end of this incubation period there was no observed autonomous activation of the *lacZ* reporter gene by GAL4 AD/1.1 and no activation of the *lacZ* reporter gene due to artifactual interactions between GAL4 AD/1.1 and an unrelated control GAL4 BD fusion protein such as, BD/p53$_{(72\text{-}390)}$ (Figure 5.13, *Expt. 2 and 3 respectively*). The strong β-gal signal observed in Figure 5.13, *Expt. 4*, is the result of the interaction between the control proteins, GAL4 AD/SV40 large T-antigen$_{(84\text{-}708)}$ and GAL4 BD/murine p53$_{(72\text{-}390)}$, whilst the signal observed in Figure 5.13, *Expt. 5* represents the result of the interaction between GAL4 AD/p38 K53R and GAL4 BD/MAPKAPK-2 K93R.

Activation of the *HIS3* reporter gene was also achieved by co-transformation of GAL4 AD/1.1 and GAL4 BD/MAPKAPK-2 K93R into HF7z cells, as indicated by growth on histidine deficient media (Figure 5.14, *Sec^n A*). As expected HF7z cells co-transformed with the positive control plasmids encoding; GAL4 AD/p38 K53R and GAL4 BD/MAPKAPK-2 K93R or GAL4 AD/ SV40 large T-antigen$_{(84\text{-}708)}$ and GAL4 BD/murine p53$_{(72\text{-}390)}$ grew on SD/Trp$^-$/His$^-$/Leu$^-$ agar plates (Figure 5.14, *Sec^{ns} B and C respectively*), whilst, HF7z cells co-transformed with GAL4 AD empty vector and GAL4 BD empty vector or GAL4 AD/1.1 and GAL4 BD empty vector did not grow (Figure 5.14, *Sec^{ns} D and E respectively*).

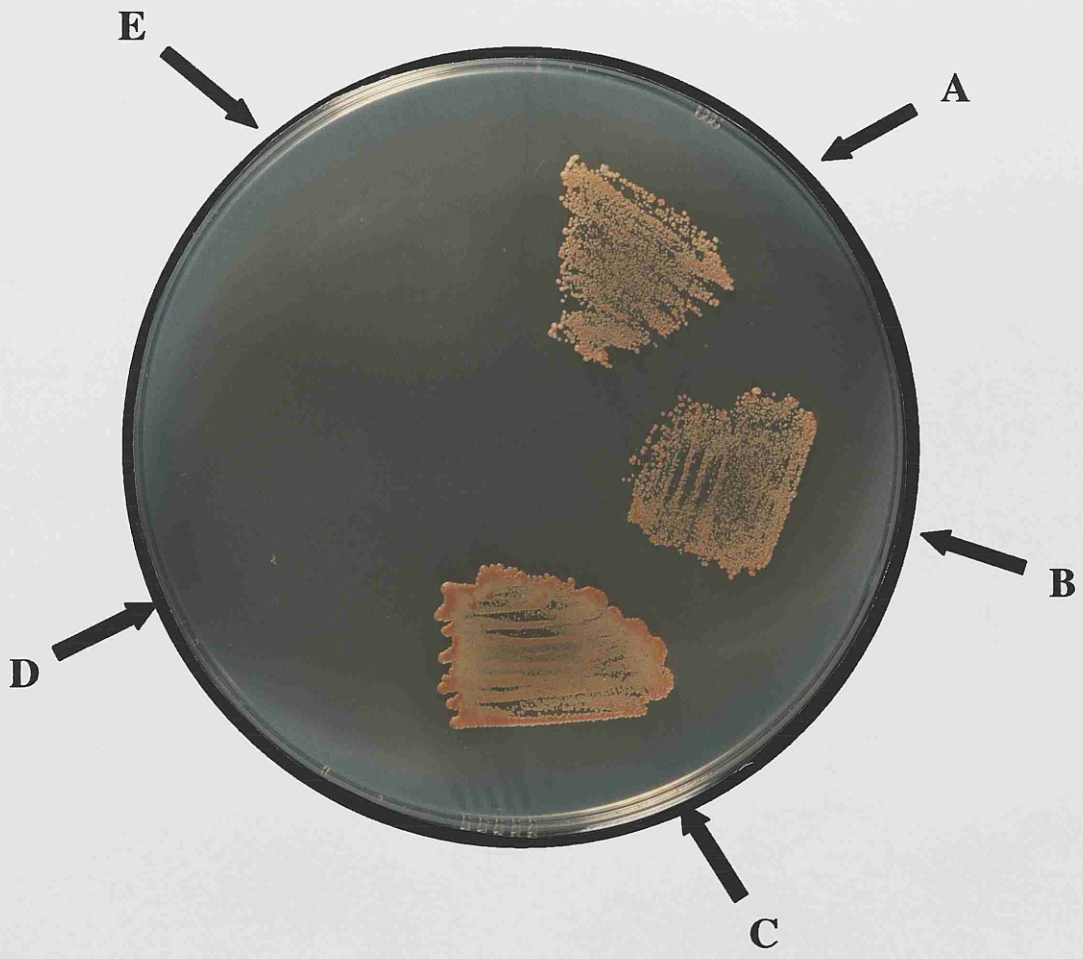

Figure 5.14: Reconstitution of the *HIS3* reporter gene by co-transformation of pGAD10/AD1.1 (GAL4 AD/1.1) and pAS2-1/MAPKAPK-2 K93R into yeast HF7z cells. Competent yeast cells were co-transformed with 0.5 µg of DNA from both plasmids and plated onto synthetic dropout (SD) medium lacking tryptophan (Trp) and leucine (Leu), SD/Trp$^-$/Leu$^-$.The plates were then incubated at 30°C for 4-5 days until colonies appeared. Single, well isolated colonies were picked, resuspended in sterile TE buffer and re-streaked onto SD medium also lacking histidine (His), SD/Trp$^-$/Leu$^-$/His$^-$. The plates were incubated at 30°C for 4-5 days. Growth after this period of time indicated *HIS3* reporter gene activity.

Section A: GAL4 AD/1.1 and GAL4 AD/MAPKAPK-2 K93R
Section B: GAL4 AD/p38 K53R and GAL4 BD/MAPKAPK-2 K93R
Section C: pTD1 and pVA3 (positive control see Chapter 2, section 2.1.9)
Section D: GAL4 AD (empty vector) and GAL4 BD (empty vector)
Section E: GAL4 AD/1.1 and GAL4 BD (empty vector)

5.2.9 Reconstitution and activation of the *lacZ* reporter gene in yeast SFY526 cells

As a further control to authenticate the interaction between AD1.1 and MAPKAPK-2 K93R, the proteins were co-transformed into yeast SFY526 cells (Harper *et al.*, 1993). As discussed in section 5.1.3, these cells contain a *lacZ* reporter gene under the control of a promoter that differs from the promoter of the *lacZ* reporter gene in HF7z cells (see Table 5.1). In HF7z cells the GAL4 binding elements are synthetically designed and the TATA box originates from the yeast cytochrome C1 (CYC1) gene. In contrast, SFY526 cells contain GAL4 binding and TATA sequences are derived from native GAL1 (Giniger *et al.*, 1985). Since these two promoters share only GAL4 binding elements and the rest of the promoters differ significantly, a 'true' positive two-hybrid interaction will activate the *lacZ* reporter gene in both of these yeast strains.

Co-transformation of GAL4 AD/1.1 and GAL4 BD/MAPKAPK-2 K93R into SFY526 cells resulted in the activation of the *lacZ* reporter gene as indicated by a positive β-galactosidase signal. The intensity of the β-gal signal in this yeast strain was much stronger than that obtained in HF7z cells (Figure 5.15, *Expt. 2*). This increase reflects the difference between the strengths of the two promoters of the *lacZ* reporter genes within these two strains. Co-transformation of SFY526 cells with GAL4 AD/1.1 and GAL4 BD empty vector did not result in the activation of *lacZ*, whilst co-transformation with plasmids expressing the positive control fusion proteins, GAL4 AD/p38 K53R and GAL4 BD/MAPKAPK-2 K93R, resulted in a strong β-gal signal (Figure 5.15, *Expt. 1 and 3 respectively*).

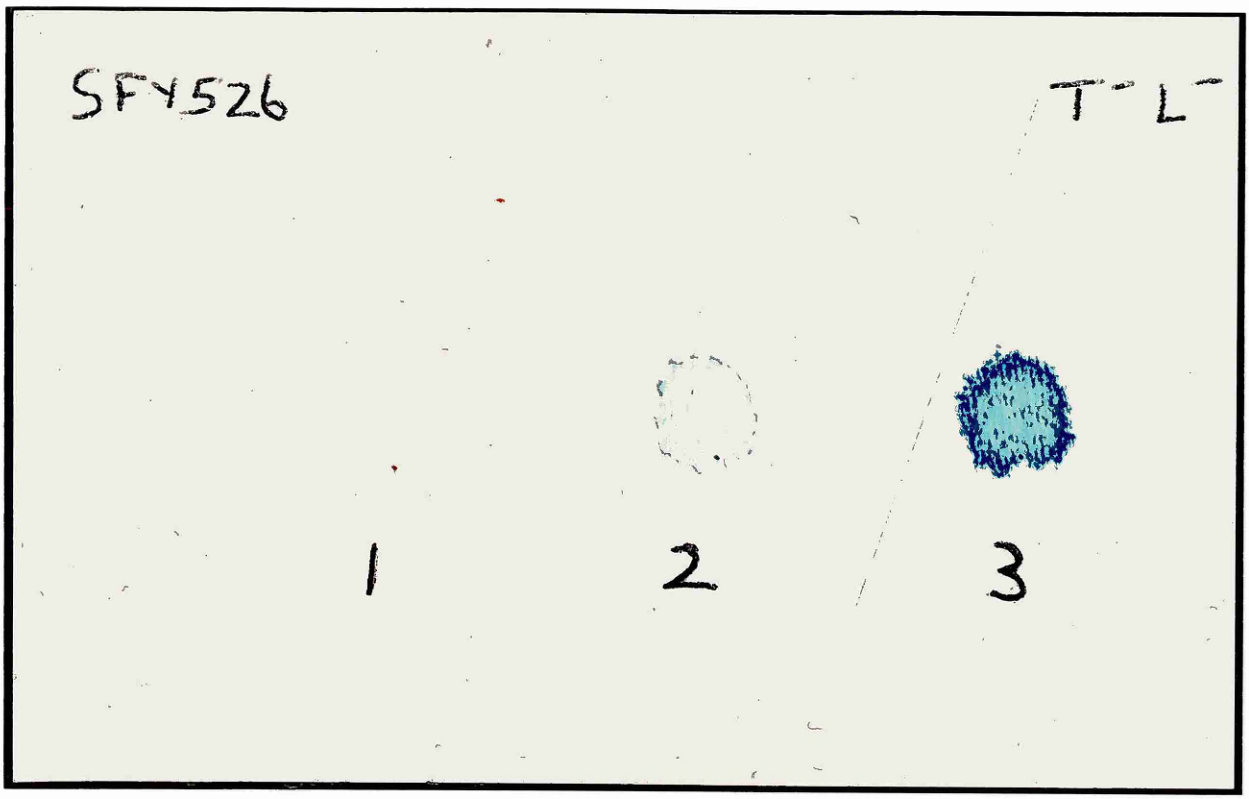

Figure 5.15: Reconstitution of the *lacZ* reporter gene by simultaneous co-transformation of pGAD10/AD1.1 (GAL4 AD/1.1) and pAS2-1/MAPKAPK-2 K93R into yeast SFY526 cells. Competent SFY526 cells were co-transformed with 0.5 µg of each plasmid and plated onto synthetic dropout (DO) medium, lacking tryptophan (Trp) and leucine (Leu), SD/Trp⁻/Leu⁻. The plates were then incubated at 30°C for 4-5 days until colonies appeared. Single, well isolated colonies were picked, resuspended in sterile TE buffer and spotted onto sterile filter paper overlayed on SD/-Trp/-Leu agar plates. After 48 hours incubation, *lacZ* activity was determined by assaying the filters in Z buffer/X-gal solution for a maximum of 8 hours.

Expt.1: GAL4 AD/1.1 and GAL4 BD (empty vector)
Expt.2: GAL4 AD/1.1 and GAL4 BD/MAPKAPK-2 K93R
Expt.3: GAL4 AD/p38 K53R and GAL4 BD/MAPKAPK-2 K93R (positive control)

5.3 Independent biochemical evaluation of the interaction between HPH2-like (AD1.1) and MAPKAPK-2 K93R

MAPKAPK-2 K93R and HPH2-like interacted and activated *HIS3* and *lacZ* reporter gene expression in both HF7z and SFY526 yeast strains. To further characterise and verify the interaction identified by two-hybrid methodology, co-immunoprecipitation of transiently expressed proteins and *in-vitro* immune complex kinase assays were carried out.

5.3.1 Expression of HPH2-like in HeLa cells and co-expression studies with MAPKAPK-2 K93R

To facilitate the detection of transiently expressed HPH2-like protein in HeLa cells, an N-terminal FLAG-epitope was incorporated by PCR amplification of pGAD10/AD1.1, using the oligonucleotides C4045 and C4047. The PCR fragment was digested with Hind III and Bam HI and cloned into pcDNA3. A single clone was sequenced in its entirety on both strands using vector and gene specific oligonucleotides and recorded as pcDNA3/FLAGHPH2-like. To test for expression, pcDNA3/FLAGHPH2-like was transiently transfected into HeLa cells and detected in cell lysates by immunoblotting using an anti-FLAG monoclonal antibody. FLAG-tagged HPH2-like expressed strongly in HeLa cells and migrated with an apparent molecular weight of ~40 kDa. (Figure 5.16, *lane 1*).

To confirm the association of HPH2-like and MAPKAPK-2 *in-vivo* HeLa cells were transiently co-transfected with pcDNA3/FLAGHPH2-like, pcDNA3/cMycMAPKAPK-2 K93R (see Chapter 3, section 3.2.7) and appropriate empty vector controls (Figure 5.16). FLAG-tagged p38 wt and the K53R mutant were

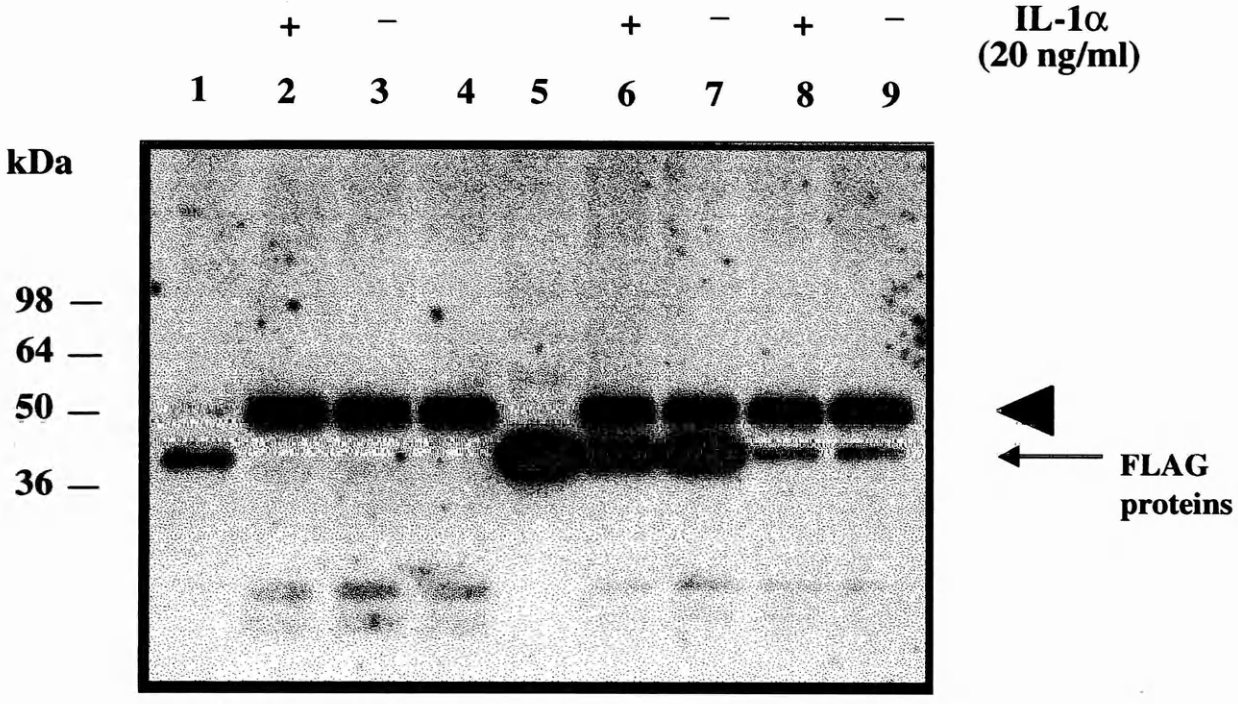

Figure 5.16: Co-immunoprecipitation of FLAG-tagged HPH2-like, p38wt and p38 K53R with cMyc-tagged MAPKAPK-2 K93R. HeLA cells were transiently co-transfected with 1.5 μg of DNA of each plasmid. After 48 hours the cells were stimulated with or without IL-1α (20 ng/ml) and incubated for a further 6 hours. The cells were then lysed in 1 ml of lysis buffer and cMyc-tagged MAPKAPK-2 K93R was immunoprecipitated using a rabbit anti-cMyc polyclonal antibody (5 μg/ml) complexed to Gammabind G sepharose beads. The beads were washed three times in lysis buffer, mixed with 50 μl of sample buffer and boiled for 5 minutes. Immunoprecipitated proteins were resolved by electrophoresis, transferred to nylon membrane and probed with a murine anti-FLAG monoclonal antibody (10 μg/ml). The proteins were visualised using a secondary antibody linked to HRP with enhanced chemiluminescence detection. The co-precipitated FLAG-tagged proteins are indicated by an *arrow*. The large *arrow head* indicates the heavy chain of the anti-cMyc antibody used for immunoprecipitation.

Lane 1:	HPH2-like HeLa cell lysate (control)
Lanes 2 and 3:	MAPKAPK-2 K93R and HPH2-like (+/- IL-1)
Lane 4:	MAPKAPK-2 K93R and pcDNA3 (empty vector)
Lanes 5:	p38wt HeLa cell lysate (control)
Lanes 6 and 7:	MAPKAPK-2 K93R and p38wt (+/- IL-1)
Lanes 8 and 9:	MAPKAPK-2 K93R and p38 K53R (+/- IL-1)

also co-transfected with cMyc-tagged MAPKAPK-2 K93R to act as positive controls. After 48 hrs the cells were treated with or without IL-1 (20 ng/ml) and incubated for a further 6 hours. Cells were lysed and MAPKAPK-2 K93R was immunoprecipitated with an anti-cMyc antibody (5 μg/ml). The immunoprecipitate was analysed by immunoblotting using an anti-FLAG antibody to detect co-precipitated FLAG-HPH2-like or FLAG-p38 (Figure 5.16). Immunoprecipitation of MAPKAP-2 K93R with an anti-cMyc antibody did not result in co-precipitation of HPH2-like in cells transfected with both cDNAs (Figure 5.16, *lanes 2 and 3*). Furthermore, stimulation with IL-1 (20 ng/ml) had no detectable influence on this interaction. As expected, p38 wt and the K53R mutant co-precipitated with MAPKAPK-2 K93R, but there was no observable difference between samples treated with or without IL-1 (Figure 5.16, *lanes 6, 7, 8 and 9 respectively*). However, there was a significant difference between the protein levels of p38 wt and p38 K53R detected. This difference may be due to the relative levels of expression, as demonstrated in Chapter 4, section 4.2.1, or alternatively it may represent a difference in the binding affinities of wild type and kinase dead p38 MAP kinase for MAPKAPK-2 K93R. These interactions appear to be unaffected by stimulation with IL-1. In Figure 5.16, *lanes 1 and 5* separately transfected controls of FLAG-HPH2-like and FLAG-p38 wt respectively are shown. *Lane 4* represents MAPKAPK-2 co-transfected with an empty vector control.

5.3.2 *In-vitro* phosphorylation of GST-HPH2-like by MAPKAPK-2

To determine if HPH2-like was as a substrate of MAPKAPK-2, *in-vitro* kinase assays were carried out. To facilitate this HPH2-like was sub-cloned into a GST-fusion vector (pGEX-3X), as described in section 5.2.7. Epicurian XL-1 blue *E.coli*

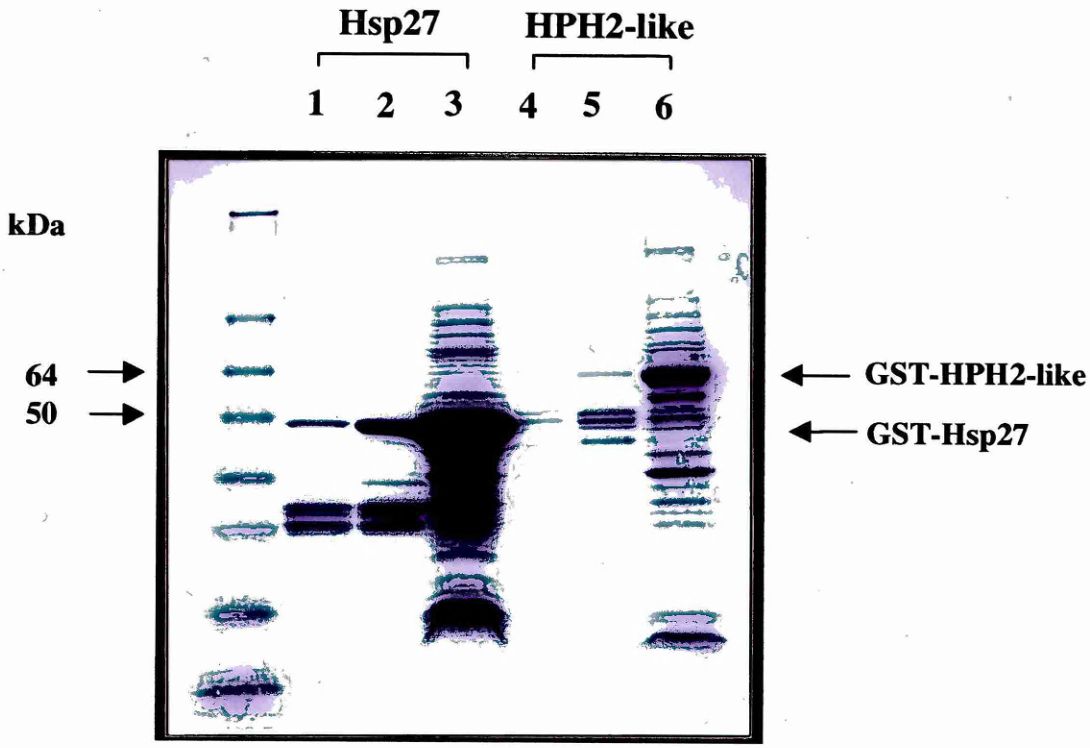

Figure 5.17: Purification of GST-Hsp27 and GST-HPH2-like. Epicurian XL-1 blue *E.coli* cells expressing GST-Hsp27 and GST-HPH2 were induced with IPTG (0.2 mM) for 4 hours and then lysed. GST-fusion proteins were purified using glutathione sepharose. **Lanes 1 and 2** represent 5 µl of GST-Hsp27 from two soluble glutathione fractions. **Lane 3** represents 5 µl from the insoluble GST-Hsp27 pellet. **Lanes 4 and 5** represent 5 µl of GST-HPH2-like from two soluble glutathione elutions **Lane 6** represents 5 µl from the insoluble GST-Hsp27 pellet.

transformed with GST-HPH2-like and GST-Hsp27 were induced with 0.2 mM isopropyl-β-D-thiogalactosidase (IPTG) for four hours at 30°C. The proteins were affinity purified using glutathione sepharose beads and examined by electrophoresis on a 4-20% Tris-glycine polyacrylamide gel and visualised by staining (Figure 5.17). GST-HPH2-like migrated with an apparent molecular mass of 65 kDa whilst GST-Hsp27 migrated with a mass of ~50 kDa (see Chapter 4, section 4.2.2). The relative expression level of GST-Hsp27, albeit very weak, was greater than GST-HPH2-like. However both proteins were predominantly insoluble in *E.coli*. To compare the phosphorylation of GST-HPH2-like with GST-Hsp27, *in-vitro* kinase assays were carried out using comparable amounts of substrate. Transiently expressed cMyc-tagged MAPKAPK-2wt was recovered from HeLa cells treated with or without NaCl (0.2 M) and incubated with purified GST-Hsp27 or GST-HPH2-like, as indicated in Figure 5.18. In this experiment HeLa cell lysates transfected with empty vector were also processed with or without the addition of precipitating antibody (Figure 5.18, *lanes 3, 4, 7 and 8*). In all cases GammaBind sepharose G was added to the samples.

As expected, the addition of 0.2 M NaCl to the cell culture medium significantly induced MAPKAPK-2 activity as observed by increased GST-Hsp27 phosphorylation. In the absence of NaCl, GST-Hsp27 was only very weakly phosphorylated and in the empty vector transfected cells (± anti-cMyc) no phosphorylation of GST-Hsp27 was observed. In the GST-HPH2 containing samples, NaCl induced kinase activity was also observed however, the apparent molecular mass of the phosphorylated product (50 kDa) did not correspond to the size (64 kDa) of GST-HPH2 (see Figure 5.17). The possibility of this being a phosphorylated breakdown product of GST-HPH2-like protein could not be dismissed. However, the

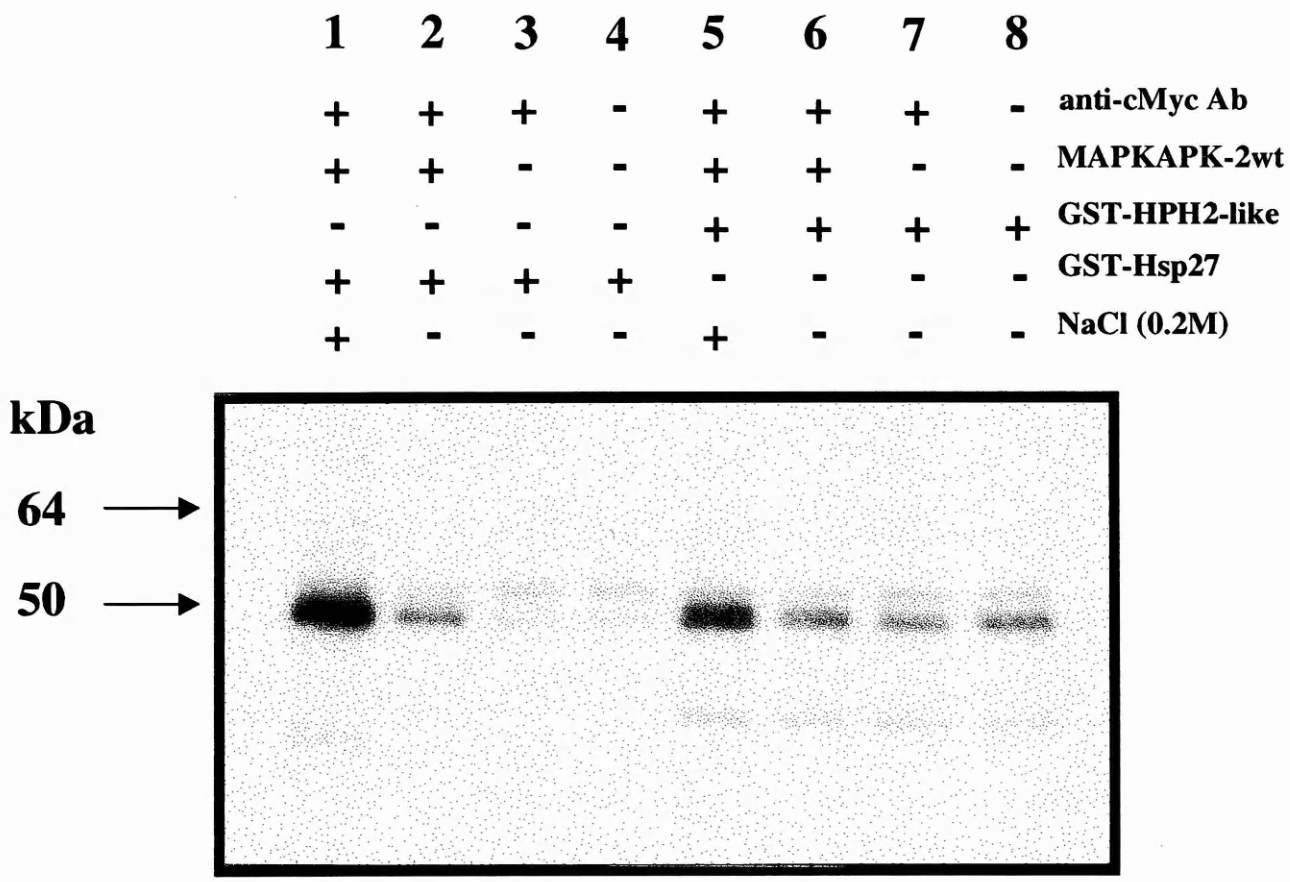

Figure 5.18: *In-vitro* phosphorylation of GST-Hsp27 and GST-HPH2-like by MAPKAPK-2. HeLa cells were transiently transfected with MAPKAPK-2 wt (***lanes 1,2, 5 and 6)*** or pcDNA3 empty vector. (***lanes 3,4, 7 and 8)***. Cells were incubated for 48 hours and then osmotically shocked with NaCl (0.2M) for 20 minutes prior to lysis. Epitope tagged MAPKAPK-2 wt was recovered by immunoprecipitation with an anti-cMyc antibody and incubated in an immune complex kinase assay with either GST-Hsp27 or GST-HPH2-like proteins.

assumption that the phosphorylation was MAPKAPK-2 dependent was inconclusive because the weakly phosphorylated breakdown product observed in the inactivated MAPKAPK-2 sample was also present in the samples devoid of any MAPKAPK-2 activity (Figure 5.18, *lanes 6, 7 and 8*). It therefore appears that the kinase activity observed in the GST-HPH2-like containing samples might be a consequence of other NaCl inducible HeLa cells kinases that are non-specifically bound to the sepharose beads. This assumption was supported by the finding that incubation of the same amount of GST-HPH2-like protein in a buffered kinase reaction without sepharose passed through HeLa cell lysate did not result in GST-HPH2-like phosphorylation (data not shown).

5.4 Discussion

In this chapter a human leucoctye cDNA library was screened with two integral components of the p38 MAP kinase signalling pathway, p38 K53R and MAPKAPK-2 K93R. Of these, only the MAPKAPK-2 K93R screen resulted in the identification of a novel putative two-hybrid interaction. From 1.5 x 10^6 human leucocytes clones screened, two clones that met all the specific criteria for binding to MAPKAPK-2 in yeast such as, activation of the *lacZ* and *HIS3* reporter genes in HF7z cells (see section 5.2.8) and activation of a modified second *lacZ* reporter gene in SFY526 cells, were isolated (see section 5.2.9). Both clones contained partial, overlapping cDNA sequences that shared substantial homology with the recently identified *human polyhomeotic 2 (HPH2)* gene (Gunster *et al.*, 1997).

HPH2 is the human homologue of the *Polyhomeotic (Ph)* gene, which belongs to the *Drosophila Polycomb (PcG)* group of genes that are part of the cellular memory

system responsible for the stable inheritance of gene activity (Franke *et al.*, 1992). PcG proteins form large multimeric, chromatin associated protein complexes. In there original study Gunster *et al* (1997) isolated HPH2 from a human leucocyte library by two-hybrid screening using Bmi1 as bait. Bmi1 is a murine oncogene that shares significant sequence homology with *Posterior sex combs (Psc).* As in Drosophila the vertebrate PcG proteins have been shown to be involved in the regulation of homeotic genes (van der Lugt *et al.*, 1996).

The amino acid sequence of the HPH2-like protein isolated in this study differed from the published sequence at three regions within the gene (Figure 5.12). Re-cloning and sequencing HPH2-like from an independent human peripheral blood mononuclear cell cDNA library authenticated these changes. Furthermore, the amino acid sequence of homology domain I of the clone isolated in this study shared more homology with the same domain from another closely related protein, HPH1, than did the clone isolated in the original study (Gunster *et al.*, 1997). Analysis of the nucleotide sequences from the two HPH2-like clones revealed that the published sequence contained several nucleotide deletions that altered the reading frame of the gene at the three regions identified.

Although the interaction between MAPKAPK-2 K93R and HPH2-like fulfilled all the criteria for binding within yeast, the two proteins did not show any kind of interaction when tested by two independent biochemical methods, co-expression in mammalian cells and *in-vitro* kinase assays. This raises the question as to whether the result is artifactual and that the interaction between MAPKAPK-2 K93R and HPH2-like in yeast is a false positive. False positives occur when interactions between different

proteins detected by the yeast two-hybrid system do not represent an in-vivo interaction in the cells in which these proteins are normally found (Fields and Sternglanz, 1994). Alternatively the interaction between MAPKAPK-2 K93R and HPH2-like may be genuine albeit very weak. Previous studies have used yeast two-hybrid technology to detect weak interactions undetectable by other physical methods such as co-immunoprecipitation (Li and Fields, 1993; Van Aelst *et al.*, 1993). Li *et al.* (1993) directly compared the sensitivity of the two-hybrid system to immunoprecipitation for the detection of weak interactions and demonstrated that the two-hybrid system could detect p53-largeT antigen interactions even with T antigen mutants that would no longer co-precipitate with p53. Thus, it is likely that transient or weak interactions, not stable in the *in-vitro* conditions of immunoprecipitation, lead to a transcriptional response *in-vivo* in yeast that activates the *lacZ* and *HIS3* reporter genes. It is clear from this study that if the interaction between MAPKAPK-2 is real then HPH2-like is not acting as a phosphorylated substrate since it was not phosphorylated *in-vitro* and in addition it does not contain any recognised MAPKAPK-2 phosphorylation motifs (Stokoe *et al.*, 1993). HPH2 is a nuclear chromatin-associated protein that forms large complexes with other largely unknown components (Gunster *et al.*, 1997). MAPKAPK-2 contains a putative nuclear localisation signal at it C-terminus (Stokoe *et al.*, 1993) and recent studies have demonstrated that in unstressed cells it is predominantly located in the nucleus and following activation it is translocated from the nucleus in a complex with p38 MAP kinase (Engel *et al.*, 1998; Ben-Levy *et al.*, 1998). Consequently, nuclear MAPKAPK-2 may be predominantly inactive and the possibility that MAPKAPK-2 and HPH2-like interact by binding to each other or as part of a larger complex in the nucleus can not be discounted.

Finally, although the two-hybrid system is a powerful technique for identifying proteins that bind to a protein of interest or to delineate residues or domains critical for interaction, the success of this technique may be dependent upon many factors such as authentic post-translational modifications within yeast. Also, when screening with enzymatically active proteins, such as protein kinases, success may be dependent upon whether the target protein has been mutated at any residues crucial for its biological activity, such as, the ATP binding or phosphorylation sites. In this study this was demonstrated by the failure of MKK6B to interact with p38 K53R and activate the *lacZ* reporter gene (see section 5.2.5) even though Zanke *et al.* (1996) had previously demonstrated a two-hybrid interaction with between MKK6 and p38 wild type. In addition to this, it also appears that even in successful two-hybrid screens there is no guarantee that in the same screen known interacting proteins will also be identified. For example when McLaughlin *et al.* (1996) identified MAPKAPK-3 using p38 D168A as bait, they did not isolate MAPKAPK-2 or MKK6. Likewise in this study using MAPKAPK-2 as bait we did not isolate p38 or Hsp27. This could reflect the cDNA message abundance within a given library however in this study both MKK6B and p38 MAP kinase cDNAs were detectable in the human leucocyte cDNA library prior to screening.

Chapter 6

Generation of HeLa cells stably overexpressing MAPKAPK-2 kinase dead and anti-sense RNA

6.1 Introduction

The varied biological properties of IL-1 are due to its ability to induce a wide variety of genes (see Chapter1, Table1.1). This induction may be a consequence of either increased gene transcription or increased mRNA stability (half-life) or both. Many of these genes are exquisitely sensitive to IL-1 and are induced only in inflammatory disease states. Of these, the increased expression of cyclooxygenase-2 (COX-2), phospholipase A_2 (PLA_2) and inducible nitric oxide synthase (iNOS) are some of the most dramatic and their metabolic products are potent pro-inflammatory mediators that prolong the biological effects of IL-1 long after activation (reviewed by Dinarello, 1996). Cytokines such as IL-8, which is a member of the chemokine protein family (Baggiolini, 1998) and IL-6 which initiates the hepatic acute phase response are also strongly induced by IL-1 (reviewed by Baumann and Gauldie, 1994).

In this chapter HeLa cells stably transfected with vectors overexpressing dominant negative MAPKAPK-2 (MAPKAPK-2 K93R) and MAPKAPK-2 anti-sense RNA were used to investigate the role of MAPKAPK-2 in IL-1 induced COX-2, IL-6 and IL-8 synthesis. Dominant negative and anti-sense methods to target and specifically

reduce endogenous kinase activities have previously been described in the ERK (p42/p44), JNK and p38 MAP kinase signalling pathways.

Pages *et al.* (1993) demonstrated by transiently transfecting p44 MAP kinase anti-sense and p42/44 MAP kinase mutants into fibroblasts that both MAP kinases are essential for growth factor stimulated proliferation. Of note in this study was that the anti-sense RNA had a more inhibitory effect on the endogenous kinase activity than the kinase dead mutants. This was shown to be due to the fact that the p44 MAP kinase anti-sense RNA inhibited the endogenous activities of both p42 and p44 MAP kinases. Krause *et al.* (1998) demonstrated that JNK is required in IL-1 induced IL-6 and IL-8 expression in KB cells (Krause *et al.*, 1998). Interestingly, in this study, although both methods reduced IL-6 and IL-8 induction the anti-sense effect was more pronounced and significantly only the anti-sense had an effect on endogenous JNK activity as determined by *in-vitro* kinase assays using GST-Jun as substrate.

Dominant negative studies have previously implicated components from the JNK and p38 MAP kinase pathways in the IL-1-induction of COX-2 (Guan *et al.*, 1998a; Guan *et al.*, 1998b). In these studies the efficiency of stably overexpressed JNK1 and p38 MAP kinase mutants on inhibiting endogenous kinase activities were assessed by immunoblotting with phospho-specific antibodies or by immune complex kinase assays. No attempts were made to look at the activities of any downstream substrates such as MAPKAPK-2. In this chapter evidence is presented suggesting a role for MAPKAPK-2 in IL-1 induced COX-2 synthesis. In addition the data presented also suggests that MAPKAPK-2 may also have role in IL-1 induced secondary pro-inflammatory cytokine production.

6.2 Results

6.2.1 Generation of stably transfected HeLa cells overexpressing MAPKAPK-2 K93R and MAPKAPK-2 anti-sense RNA

The vectors pcDNA3/cMycMAPKAPK-2K93R, pcDNA3/MAPKAPK-2 A/S (described in Chapter 3, sections 3.2.7 and 3.2.8) and pcDNA3 empty vector were stably transfected into HeLa cells as described in Chapter 2, section 2.3.4. Overexpression of the epitope-tagged MAPKAPK-2 K93R mutant was verified by western blotting using an anti-cMyc antibody. This detected an immunoreactive band with an apparent molecular weight of 50 kDa (Figure 6.4B), corresponding to the apparent molecular mass of the Hsp27 kinase reported by Freshney *et al.* (1994) and endogenous MAPKAPK-2 in human neutrophils (Krump *et al.*, 1997). To detect colonies overexpressing MAPKAPK-2 anti-sense RNA, RNA was isolated and RT-PCR, using oligonucleotides F6071 and F6070 designed to complementary sequences within the MAPKAPK-2 gene and to the c-Myc epitope respectively was carried out. F6071 and F6070 were designed to amplify a MAPKAPK-2 anti-sense fragment of ~640 bp. The integrity of mRNA purification and subsequent 1st-strand cDNA synthesis was verified using control GAPDH oligonucleotides. The RT-PCR result of an isolated MAPKAPK-2 anti-sense expressing clone, in comparison with the pcDNA3 transfected control cells is shown in Figure 6.1. The MAPKAPK-2 anti-sense specific oligonucleotides amplified a fragment of the expected size from the MAPKAPK-2 anti-sense transfected clone, whilst no signal was obtained from the pcDNA3 control (Figure 6.1, *lanes 1 and 2 respectively*). Both clones produced strong signals with the GAPDH oligonucleotides (Figure 6.1, *lanes 4 and 5 respectively*).

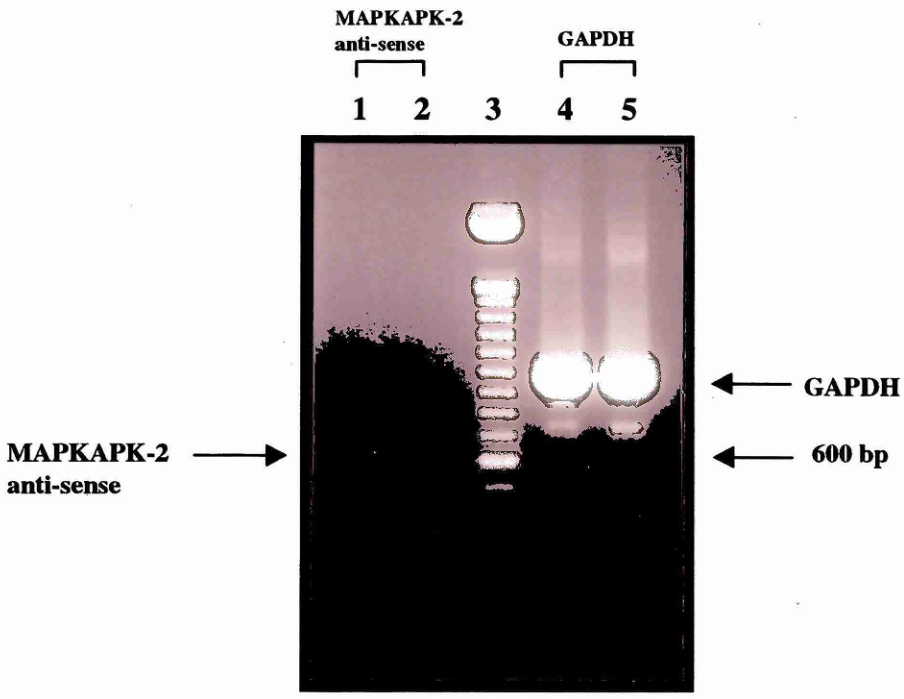

Figure 6.1: Confirmation of MAPKAPK-2 anti-sense overexpression by RT-PCR. RT-PCR was carried out using mRNA purified from G418 resistant HeLa colonies transfected with either pcDNA3/cMycMAPKAPK-2a A/S or pcDNA3 (empty vector). ***Lanes 1 and 2,*** represent amplifications of anti-sense and empty vector transfected clones respectively, using the oligonucleotides F6070 and F6071 (see text). ***Lanes 4 and 5,*** represent amplifications of anti-sense and empty vector transfected clones respectively using GAPDH specific oligonucleotides. ***Lane 3,*** 100 bp molecular weight marker.

To evaluate the effect of overexpressed anti-sense MAPKAPK-2 RNA on the level of endogenous MAPKAPK-2 protein, Western blots were carried out on cell lysate preparations (Figure 6.2). As discussed in Chapter 3, two isoforms of MAPKAPK-2, MAPKAPK-2a (Stokoe *et al.*, 1993) and MAPKAPK-2b (Zu *et al.*, 1994), generated by alternate splicing of the carboxy terminus exist, with the clone used in this study corresponding to the former. In addition, a closely related homologue, MAPKAPK-3, has been identified (McLaughlin e*t al.*, 1996). In Table 6.1 the anti-MAPKAPK-2a antibodies used in this study and the similarities between the respective epitope sequences of the two MAPKAPK-2 isoforms and MAPKAPK-3 are illustrated.

Antibody (conc.)	Host	Epitope	Result	Source
affinity purified anti-rabbit MAPKAPK-2 (1 µg/ml)	sheep	* * *MTSALATMRVDYEQIK* (residues 356-371)	see Fig.6.2E	UBI # 06-534
affinity purified anti-human MAPKAPK-2 (4 µg/ml)	rabbit	* * * * EDKERWEDVK*EEMTSAL* (residues 344-360)	see Fig.6.2B	Stressgen # KAP-MA015
affinity purified anti-human MAPKAPK-2 (1 µg/ml)	goat	* * * * * * * *LLLKRRKKARALEAAALA* (residues 382-399)	see Fig.6.2D	Santa Cruz # sc-6221
affinity purified anti-human MAPKAPK-2 (1 µg/ml)	rabbit	residues 2-66 (see Chapter 3, Fig. 3.8)	see Fig.6.2A	Santa Cruz # sc-7871
un-purified anti-human MAPKAPK-2 (1:1000)	rabbit	GST-ΔMAPKAPK-2 see Chapter 3, section 3.2.3	see Fig.6.2C	Kennedy Institute anti-p50

Table 6.1: List of polyclonal anti-MAPKAPK-2a antibodies used in this study. Where possible the epitope sequences from which the antibodies were raised are indicated. The residues are numbered with respect to the MAPKAPK-2/3 sequence alignments indicated in Figure 3.8, Chapter 3. Residues in italics represent sequence differences between MAPKAPK-2a and MAPKAPK-2b. Residues marked by an asterisk represent differences between MAPKAPK-2a and MAPKAPK-3.

HeLa cells expressing MAPKAPK-2 K93R and MAPKAPK-2 anti-sense RNA were solubilised in mammalian cell lysis buffer and 100 μg of cytosolic protein was resolved by electrophoresis on either a 4-20% or 10% SDS polyacrylamide gel and immobilised on nylon membrane (as described in Chapter 2, section 2.4.4). The membranes were then incubated overnight with each of the antibodies described in Table 6.1 at the concentrations indicated in parentheses. Proteins were visualised by chemiluminescence following incubation with the appropriate HRP-conjugated secondary antibody (1:5000).

In Figure 6.2, the results of immunoblotting with the antibodies illustrated in Table 6.1 are shown. Four of the five antibodies tested failed to detect a specific, immunoreactive band of the expected size (50 kDa) and significantly they also failed to detect an overexpressed product in the lysate from the dominant negative expressing cells (Figure 6.2A, B, C and E). However, the Santa Cruz antibody (#sc-6221) did detect a weak 50 kDa band from the dominant negative lysate which was absent in the control and anti-sense lysates (Figure 6.2D, *lane 3*). This antibody also reacted with several polypeptides within the 47-49 kDa molecular size range. In addition a faster band of approximately 42-43 kDa was also detected. Since the sequence of the immunogen used to raise this antibody is specific for MAPKAPK-2a and not MAPKAPK-2b, but does share some sequence similarity with MAPKAPK-3, it is possible that the faster 42-43 kDa could represent MAPKAPK-3 which has been reported to migrate in HL60 cells with an apparent molecular mass of 43 kDa (Sithanandam *et al.*, 1996). Alternatively, the products may be the result of non-specifically bound antibody.

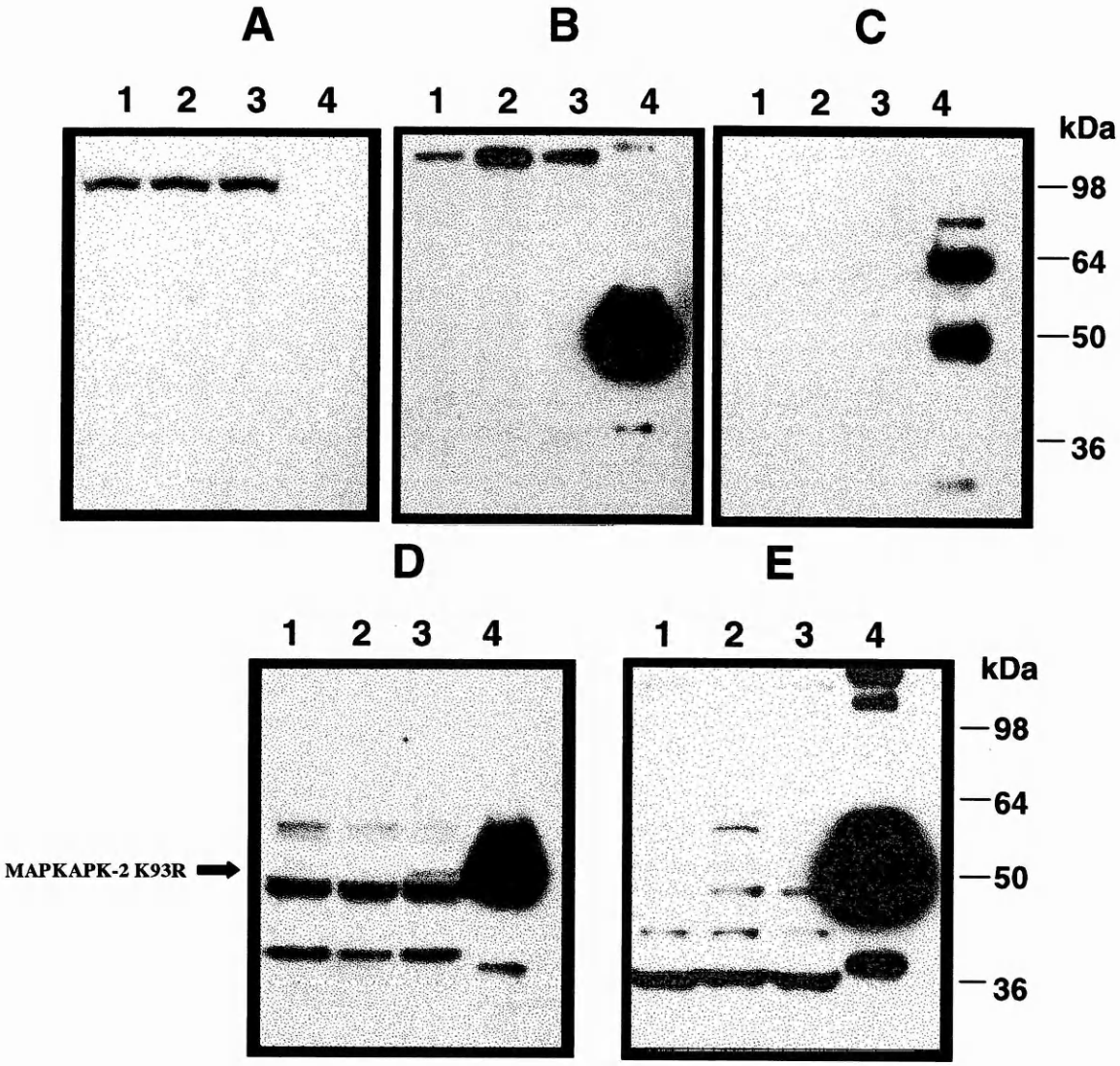

Figure 6.2: Comparison of commercial and non-commercial anti-MAPKAPK-2 antibodies to evaluate the effect of over-expressed MAPKAPK-2 anti-sense RNA on endogenous MAPKAPK-2 protein levels. 100 µg of cytosolic protein from the HeLa control cells (pcDNA3 transfected) (***lane1***) and cells stably expressing MAPKAPK-2 anti-sense RNA (***lane 2***) and MAPKAPK-2 K93R (***lane 3***) was resolved on a 4-20% SDS polyacrylamide gel and transferred to nylon membranes. These were then probed with five different MAPKAPK-2 antibodies (see Table 6.1); #sc-7871 (***A***), #KAP-MA015 (***B***), anti-p50 (***C***), #sc-6221 (***D***) and #06-534 (***E***). ***Lane 4*** represents a cleaved murine MAPKAPK-2 control. The position of the over-expressed 50 kDa recombinant protein detected by #sc-6221 (***6.2D, lane 3***) is indicated by an arrow.

With the exception of the N-terminally derived anti-human MAPKAPK-2 antibody, #sc-7871 (Figure 6.2A), all the remaining antibodies were able to detect the purified murine GST-cleaved MAPKAPK-2 control. The amino terminus of human MAPKAPK-2 is significantly different from its murine homologue, which would account for the failure of the N-terminally derived antibody to detect the murine recombinant control. In Figure 6.2C, *lane 4*, several larger bands are detected in the murine control sample. These are likely to represent partially or non-specifically cleaved murine GST-MAPKAPK-2 since the anti-MAPKAPK-2 antibody used in this experiment was raised against whole GST-MAPKAPK-$2_{40\text{-}400}$ protein.

To confirm that the weak 50 kDa band observed in Figure 6.2C, *lane 4* was a product of dominant negative MAPKAPK-2 mRNA overexpression, it was important to compare the mobility of this product to that of the epitope-tagged dominant negative mutant. The experiment was repeated and the samples were resolved on a 10% SDS polyacrylamide gel, immunoblotted and probed with the anti -MAPKAPK-2 antibody, #sc-6221, and an anti-cMyc antibody. A comparison of the results is shown in Figure 6.3. From this experiment it can be clearly seen that on a 10% gel, epitope-tagged MAPKAPK-2 K93R migrates as a doublet in which the upper band migrates with a molecular mass of 50 kDa and the lower band migrates with an apparent molecular mass of 48-49 kDa. This experiment was repeated several times and the relative amounts of the two bands varied between preparations, suggesting that the 48-49 kDa form is a proteolytic fragment. Significantly, the upper band migrated exactly with the weak 50 kDa band observed in Figure 6.2C, *lane 3*, whilst the lower band migrated with a molecular mass corresponding to the strongly expressed 47-49 kDa products

that were detected in all samples when probed with the anti-MAPKAPK-2 (#sc-6221) antibody.

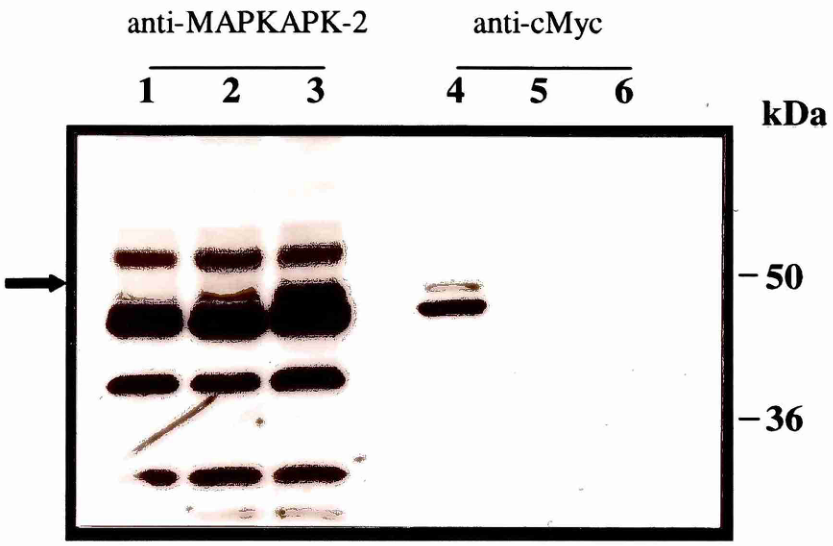

Figure 6.3: Comparison of the relative mobilities of the recombinant MAPKAPK-2 K93R proteins as detected using the anti-MAPKAPK-2 (#sc-6221) and anti-cMyc antibodies. 100 μg of cytosolic protein from HeLa control cells (pcDNA3 transfected) (***lanes 1 and 6***) and cells stably expressing MAPKAPK-2 anti-sense RNA (***lanes 2 and 5***) and MAPKAPK-2 K93R (***lanes 3 and 4***) was resolved on a 10% SDS polyacrylamide gel and transferred to nylon membranes. These were then probed with the anti-MAPKAPK-2 (#sc-6221) and an anti-cMyc antibody. The position of the overexpressed recombinant mutant detected by the anti-MAPKAPK-2 antibody is indicated by the arrow. Proteins were detected by chemiluminescence.

From the above results the effect of MAPKAPK-2 anti-sense expression upon endogenous MAPKAPK-2 levels could not be assessed by western blotting using the antibody reagents that were available at the time of this study. However, it was possible to detect the dominant negative mutant using one of the anti-MAPKAPK-2 antibodies, #sc-6221, showing that this antibody could detect MAPKAPK-2 when overexpressed. The observation that the recombinant epitope-tagged protein migrates

as a doublet as detected by the anti-cMyc antibody suggests that it is likely that endogenous MAPKAPK-2 protein will also be proteolytically degraded upon cell lysis. Consequently the failure of the anti-MAPKAPK-2 antibody to detect endogenous MAPKAPK-2 in the control and anti-sense expressing cells may be attributed to the strong non-specific 49 kDa band masking its presence.

6.2.2 Effect of MAPKAPK-2 K93R and MAPKAPK-2 anti-sense overexpression on IL-1 induced COX-2 protein production

In recent studies, the overexpression of dominant negative mutants or anti-sense RNA has successfully demonstrated a role for the p42/p44 MAP kinases in growth factor regulated cellular proliferation (Pages *et al.*, 1993), for SAPKβ in IL-1 induced expression of IL-6 and IL-8 in KB cells (Krause *et al.*, 1998) and for the JNK and p38 MAP kinase pathways in IL-1β induced COX-2 synthesis (Guan *et al.*, 1998a).

In this study a dominant negative approach was used to investigate the effect of MAPKAPK-2 on IL-1 induced COX-2 protein expression. Stably transfected cells were seeded into 6-well plates. Control cells (pcDNA3 transfected) were pre-treated with SB 203580 (1 μM) for 2 hours, after which time the cells were stimulated with IL-1α (20 ng/ml) for 8 hours as indicated in Figure 6.4. The cells were then lysed in equal volumes of buffer and analysed by immunoblotting with an anti-COX-2 antibody (Figure 6.4A). As expected, in the control cells pre-treated with SB 203580 the level of COX-2 protein was significantly reduced when compared with the DMSO treated control cells. This result demonstrates that p38 MAP kinase is involved in the regulation of IL-1α induced COX-2 synthesis and as reported by others this induction can be inhibited pharmacologically (Ridley *et al.*, 1997; Pouliot *et al.*, 1997; Guan *et*

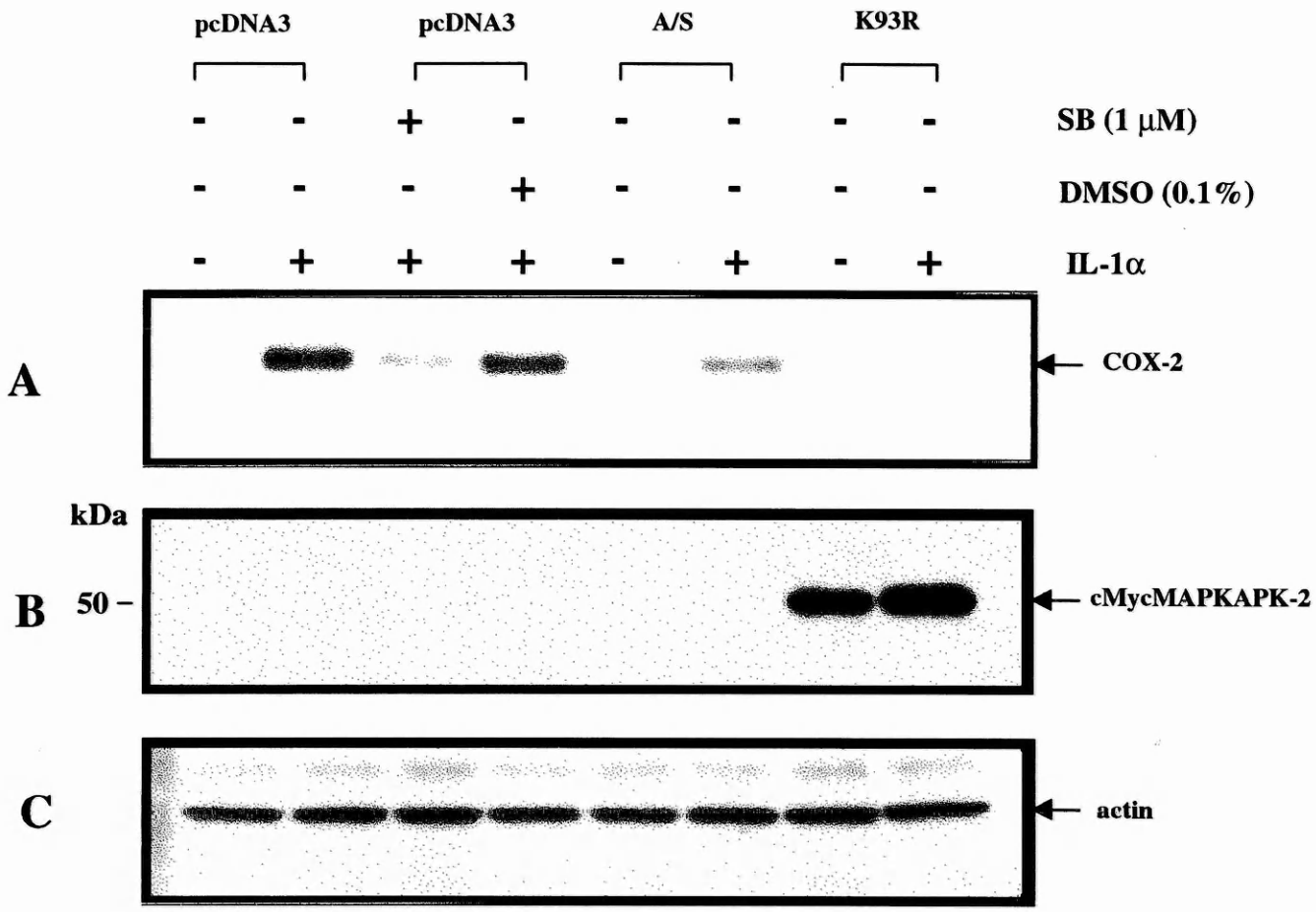

Figure 6.4: Effect of MAPKAPK-2 K93R and MAPKAPK-2 anti-sense RNA overexpression on IL-1 induced COX-2 induction. HeLa cells were stably transfected with pcDNA3/MAPKAPK-2a K93R, pcDNA3/MAPKAPK-2a A/S or pcDNA3 (empty vector). Cells were pre-treated with SB203580 (1 μM) for 2 hours and then stimulated with IL-1α (20 ng/ml) in the continuous presence of SB 203580 for 8 hours as indicated. Cells were lysed in 500 μl of lysis buffer and equal volumes of each sample were loaded onto Tris-glycine 4-20% polyacrylamide gel, resolved by electrophoresis and immunoblotted. ***Panel A,*** COX-2 protein induction was detected in response to IL-1α stimulation using an anti-COX-2 antibody. ***Panel B,*** epitope-tagged MAPKAPK-2 K93R over-expression was detected using an anti-cMyc antibody. ***Panel C,*** samples were probed with an anti-actin antibody to show comparable loadings.

al., 1997). Significantly, the induction of COX-2 by IL-1α was completely blocked by the dominant negative MAPKAPK-2 K93R mutant and to a lesser extent by the MAPKAPK-2 anti-sense RNA. Overexpression of the dominant negative MAPKAPK-2 mutant was confirmed by probing with an anti-cMyc antibody (Figure 6.4B). The degree of COX-2 inhibition caused by overexpression of MAPKAPK-2 anti-sense RNA was not as great as that observed in the cells pre-treated with SB 203580, but when compared to the control cells stimulated with IL-1α this reduction was significant. To ensure that the observed differences in COX-2 protein levels were real and not due to variations in sample loading, the samples were probed with an anti-actin antibody which is abundant and not induced by IL-1α. This result confirmed comparable loading (Figure 6.4C). Therefore the data presented here suggests that the COX-2 protein differences are most likely to be due to the overexpression of dominant negative MAPKAPK-2 K93R and MAPKAPK-2 anti-sense RNA.

6.2.3 Effect of MAPKAPK-2 K93R and MAPKAPK-2 anti-sense overexpression on prostaglandin E_2 production

To determine whether the reduced COX-2 protein levels correlated with decreased prostaglandin production, the amount of PGE_2 released into the overlaying culture medium was assayed using a competition based ELISA (described in Chapter 2, section 2.3.7). To demonstrate the role of p38 MAP kinase in PGE_2 synthesis, the pcDNA3 transfected control cells were pre-incubated with SB 203580 (1 μM) or DMSO for 2hours. The cells were then stimulated for 16 hours with IL-1α (20 ng/ml) as indicated in Figure 6.5. IL-1 activates cytoplasmic phospholipase A_2 ($cPLA_2$), which has also been proposed as a substrate of p38 MAP kinase (Borsch-Haubold *et*

al., 1997). However, the concentration of SB 203580 (1 μM) used in this study has previously been shown to have no effect upon arachidonate release from IL-1α-stimulated HeLa cells (Ridley *et al.*, 1998) or thromboxane release in collagen stimulated platelets (Saklatvala *et al.*, 1996) indicating that neither $cPLA_2$ or cyclooxygenase are directly inhibited by SB 203580 at this concentration.

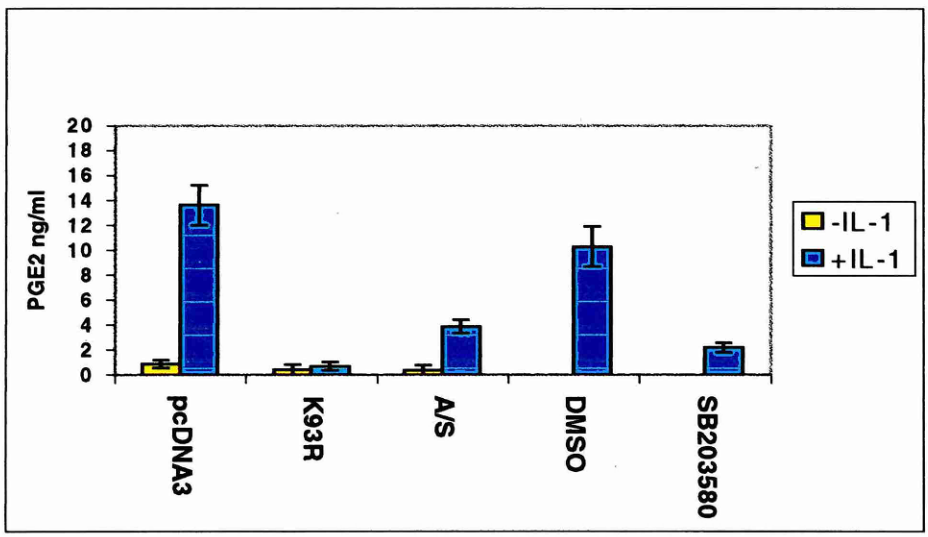

Figure 6.5: Inhibition of IL-1α induced prostaglandin E_2 (PGE_2) production in HeLa cells overexpressing dominant negative and anti-sense MAPKAPK-2 RNA. Control cells (pcDNA3 transfected) were also pre-incubated with SB 203580 (1μM) or DMSO (0.1%) for 2 hours followed by treatment with IL-1α (20 ng/ml) for 16 hours. The overlaying culture medium was removed and PGE_2 levels were assayed. No PGE_2 measurements in the absence of IL-1α were taken for the control cells treated with SB 203580 or DMSO. The above diagram is a representative of three experiments. Data points are mean +/-SD of triplicate readings.

IL-1 is a potent stimulant of prostaglandin production and as expected stimulation of the cells in the control reactions, pcDNA3 and pcDNA3+DMSO (annotated as DMSO in Figure 6.5), produced large amounts of PGE_2 (~13 and 10 ng/ml respectively). In contrast, the amounts of PGE_2 produced by stimulated cells overexpressing dominant negative MAPKAPK-2 (<1 ng/ml) and MAPKAPK-2 anti-sense RNA (~4 ng/ml)

were significantly less, indicating that in these cells IL-1α induced PGE_2 synthesis was severely impaired. In fact, PGE_2 induction in the stimulated dominant negative expressing cells was less than twice that of the unstimulated dominant negative expressing cells. This result reflected the level of COX-2 protein induced by IL-1α within these cells (Figure 6.4A). SB 203580 (1 μM) reduced the level of PGE_2 in the pcDNA3 transfected control cells by ~80%, which was comparable to the percentage inhibition (66%), at 1 μM SB 203580 in HeLa cells, observed by Ridley *et al.* (1998). No PGE_2 measurements were made for unstimulated pcDNA3 control cells with SB 203580 or DMSO. The relative trend of these data supported the differences in COX-2 protein levels as observed by antibody detection and confirmed that the inhibition of COX-2 protein synthesis correlated with decreased production of PGE_2 synthesis.

6.2.4 Effect of MAPKAPK-2 K93R and MAPKAPK-2 anti-sense overexpression on IL-1α induced COX-2 transcription

To investigate the mechanism by which the overexpression of dominant negative MAPKAPK-2 or MAPKAPK-2 anti-sense RNA may be inhibiting COX-2 protein synthesis, the level of COX-2 mRNA within these cells was examined by COX-2 RNAase protection assays. Cells ($1.5x10^6$) growing in 60 mm tissue culture plates were pre-treated with or without SB 203580 (1 μM) or DMSO (0.1%) for 2 hours and then stimulated for 8 hours with IL-1α (20 ng/ml) (see Figure 6.5). RPA assays using a 256 bp COX-2 riboprobe and a control GAPDH riboprobe were carried out as described in Chapter 2, section 2.2.15. The results were then analysed by autoradiography (Figure 6.6A) and quantified in a phosphorimager (Figure 6.6B). IL-1α treatment strongly induced COX-2 mRNA (10 fold increase) in the pcDNA3 control cells. SB 203580 (1 μM) inhibited IL-1α induction of COX-2 mRNA by

~62% which was in close agreement with the percentage inhibition (72%) of COX-2 mRNA in LPS-stimulated monocytes at the same concentration of inhibitor (Dean *et al.*, 1999). The addition of DMSO (0.1%) as a control for the inhibitor had no effect upon the level of induction. Overexpression of MAPKAPK-2 K93R and MAPKAPK-2 anti-sense RNA significantly inhibited the induction of COX-2 mRNA by IL-1α. As predicted from the IL-1α induced COX-2 protein levels (Figure 6.4A) overexpression of MAPKAPK-2 K93R dramatically reduced the level of COX-2 mRNA. In these cells the induced level of COX-2 mRNA was inhibited about 93% and there was also ~2-fold reduction in the basal or uninduced level of COX-2 mRNA when compared to the pcDNA3 control cells. MAPKAPK-2 anti-sense inhibited the IL-1α induced level of COX-2 mRNA by 86% when compared to the control cells. There was also a ~2-fold reduction in the basal level of COX-2 mRNA in these cells, which was comparable to the level of COX-2 mRNA in the MAPKAPK-2 K93R expressing cells. Interestingly, the IL-1α induced level of COX-2 mRNA from the anti-sense expressing cells was ~2.5- fold lower than from SB 203580 treated cells. This result differed from the observed levels of COX-2 protein between these samples in which pre-treatment with SB 203580 (1 μM) had a more pronounced effect on COX-2 protein inhibition. This discrepancy may be a result of experimental variation. The results obtained in this experiment clearly demonstrate that IL-1α induced COX-2 mRNA synthesis is inhibited by overexpressing MAPKAPK-2 K93R and MAPKAPK-2 anti-sense RNA and that this effect could be due to decreased transcription and/or reduced mRNA stability.

An attempt to look at the role of MAPKAPK-2 on COX-2 transcription by using a COX-2 reporter gene (described in Chapter 2, section 2.3.5) was carried out.

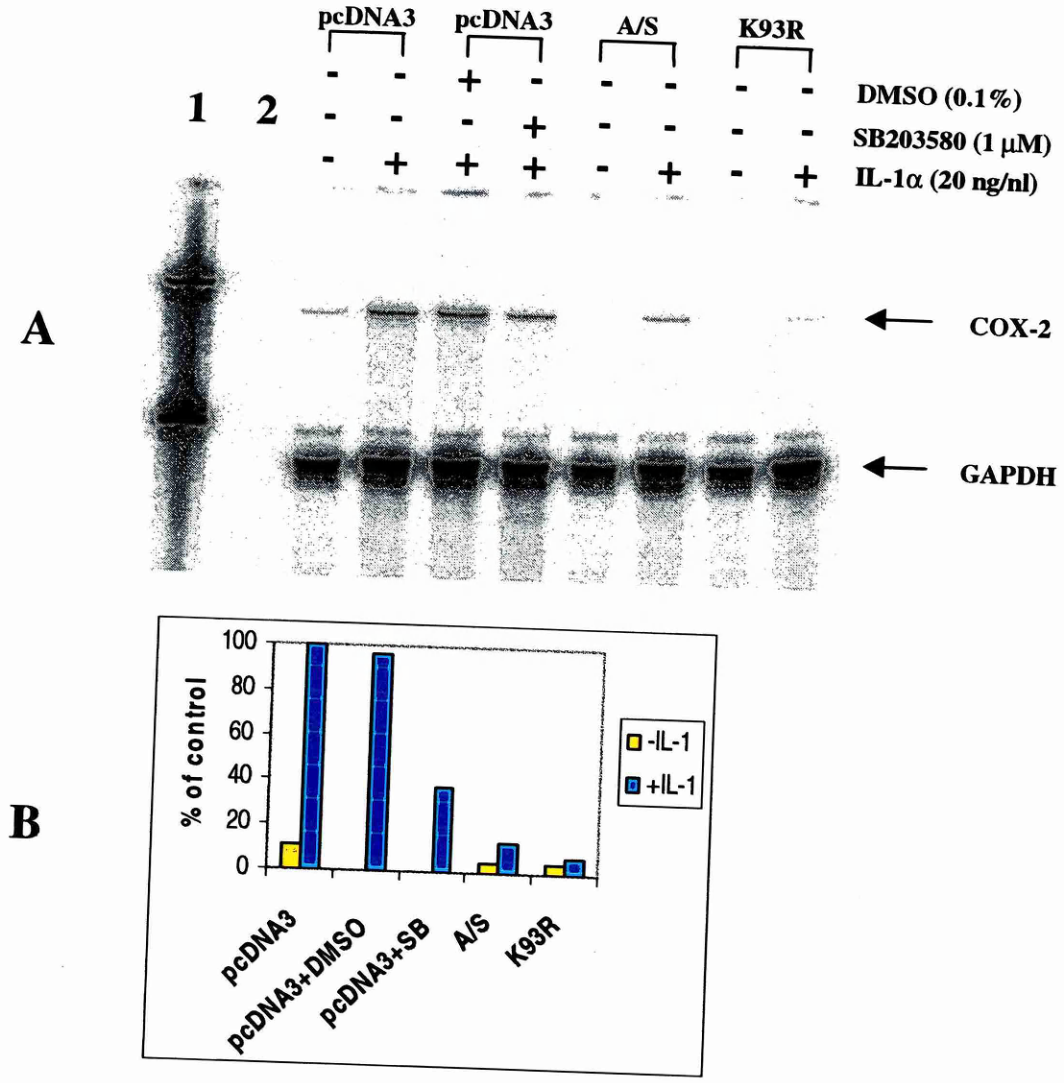

Figure 6.6: Effect of MAPKAPK-2 K93R and MAPKAPK-2 anti-sense RNA overexpression on IL-1α induced COX-2 mRNA synthesis in HeLa cells. Cells were pre-treated for 2 hours with 1 μM SB203580 or DMSO vehicle prior to stimulation with IL-1α for 8 hours (20 ng/ml). The cells were then lysed and RPA protection assays using COX-2 and GAPDH (internal control) riboprobes were carried out. Protected fragments were analysed and quantitated using a phosphorimager (**A**). COX-2 mRNA inhibition as a percentage of the stimulated pcDNA3 control cells is shown (**B**). ***Lane 1*** (***6.6A***) represents the control protected probe fragments, whilst ***lane 2*** represents the unprotected probe fragments.

However, IL-1α did not significantly increase the transcription (<2-fold) of a transiently transfected COX-2 luciferase reporter gene in the pcDNA3 control cells and therefore the MAPKAPK-2 K93R and anti-sense expressing cells were not transfected with this reporter plasmid. In contrast the transcription of an IL-1α responsive control plasmid containing an E-selectin minimal promoter was increased by ~500-fold in transiently transfected pcDNA3 control cells (Figure 6.7). The latter result served to confirm the integrity of the IL-1α signalling pathway within these cells after transfection.

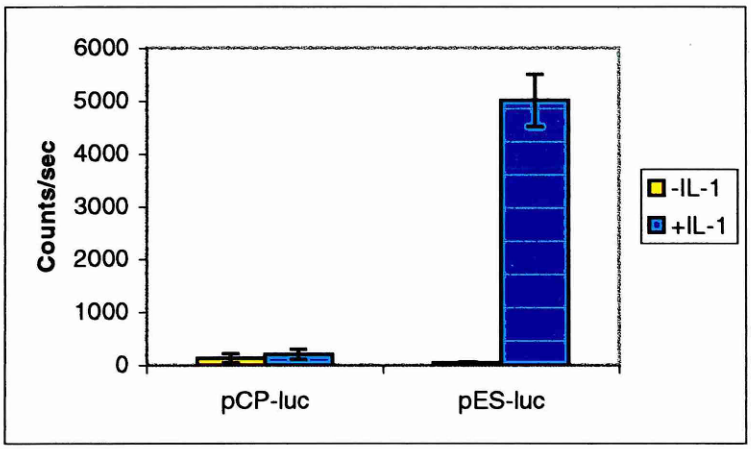

Figure 6.7: Effect of IL-1α stimulation on the induced transcription of a COX-2/luciferase reporter plasmid, CP(-2309/+37) pGL3b, in transiently transfected pcDNA3 control cells. Cells ($2x10^4$) were transiently transfected in 96 well plates with 50 ng of renilla luciferase* and 500 ng of a firefly luciferase reporter plasmid containing ~2300 bp of upstream COX-2 promoter sequence or a firefly luciferase reporter plasmid containing 170 bp of upstream E-selectin promoter sequence, ES (-170/+52) pGL3b. Cells were stimulated with IL-1α (20 ng/ml) for 8 hours and then assayed for luciferase. The above diagram is a representative of three experiments. Data points are mean +/-SD of triplicate readings, * -see text.

Thus IL-1α strongly induced COX-2 protein and mRNA in the pcDNA3 control cells (Figures 6.4B and 6.6 respectively) but did not significantly increase the transcription

of the COX-2 reporter gene (Figure 6.7). These results suggest that IL-1α induced COX-2 synthesis in HeLa cells is not due to increased transcriptional activity, but is mediated by post-transcriptional events, of which the stability of COX-2 mRNA has been previously described (Pouliot *et al.*, 1997; Dean *et al.*, 1999; Ridley *et al.*, 1998). Interestingly, in this experiment the rate of transcription of the control renilla luciferase vector, containing the hCMV promoter, increased following stimulation with IL-1 suggesting that this promoter is responsive to IL-1. As a consequence normalising the results between the unstimulated and stimulated samples was not possible, however, the relative counts for renilla luciferase between the unstimulated and stimulated samples from each transfection were similar.

6.2.5 Effect of MAPKAPK-2 K93R and MAPKAPK-2 anti-sense overexpression on Hsp27 phosphorylation *in-situ* and *in-vitro*

Hsp27 is a recognised physiological substrate of MAPKAPK-2 (Cuenda *et al.*, 1995). An investigation as to whether or not overexpressed MAPKAPK-2 K93R and MAPKAPK-2 anti-sense had a dominant negative effect and blocked IL-1α induced Hsp27 phosphorylation *in-situ* was carried out. Cells were seeded into 6-well tissue culture plates and labelled with [^{32}P]-orthophosphate as described in Chapter 2, section 2.4.6. As indicated in Figure 6.8, pcDNA transfected cells were pre-treated with or without SB 203580 (1μM) or DMSO (0.1%) for 2 hours prior to stimulation with IL-1α (20 ng/ml) for 20 minutes. Endogenous Hsp27 was immunoprecipitated as described in Chapter 2, section 2.4.1, using an anti-Hsp27 antibody. Samples were resolved by electrophoresis on a 4-20% SDS polyacrylamide gel, transferred to nylon membrane and analysed by autoradiography (Figure 6.8A and B). As expected SB 203580 (1 μM) significantly inhibited the IL-1 induced phosphorylation of

endogenous Hsp27 when compared to cells treated with DMSO vehicle. There was no significant inhibition of Hsp27 phosphorylation in cells overexpressing MAPKAPK-2 anti-sense RNA when compared to the pcDNA3 control cells and although a degree of inhibition was observed in the dominant negative expressing cells in this experiment, subsequent assays demonstrated that this was probably a result of experimental variation. These data suggest that overexpressing MAPKAPK-2 K93R and MAPKAPK-2 anti-sense is not sufficient to block the endogenous phosphorylation of Hsp27 and that other IL-1α induced Hsp27 kinases are likely to be present in HeLa cells. This assumption is supported by a recent study in which four major inducible Hsp27 kinases in HeLa cell lysates were identified. One was subsequently identified as PRAK, which in the same study was also identified as a substrate of p38 MAP kinase. A second was identified by western blot analysis as MAPKAPK-2 whilst the two remaining kinase activities were not identified (New *et al.*, 1998). In a separate study another p38 MAP kinase substrate, MAPKAPK-3, was identified and phosphorylated Hsp27 in-vivo (Sithanandam *et al.*, 1996; McLaughlin *et al.*, 1996). The effectiveness of SB 203580 (1 μM) at blocking endogenous Hsp27 phosphorylation is probably due to the fact that the known major inducible Hsp27 kinases are substrates of p38 MAP kinase. From these findings it is clear that Hsp27 can be phosphorylated by a number of known and unknown kinases and that overexpressing a mutant or anti-sense form of one of these kinases, MAPKAPK-2, is not by itself effective at blocking Hsp27 phosphorylation *in-situ*.

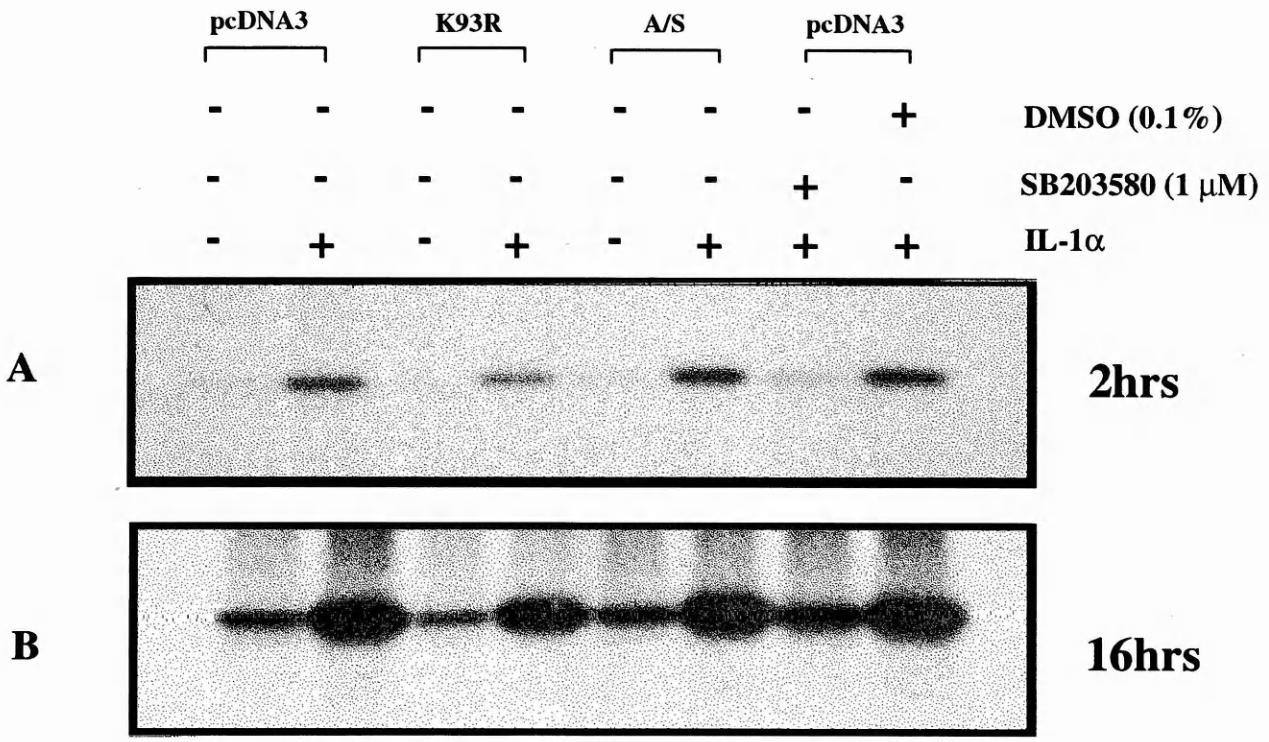

Figure 6.8: Effect of overexpressed MAPKAPK-2 K93R and MAPKAPK-2 anti-sense RNA (A/S) on inhibiting Hsp27 phosphorylation *in-situ*. Labelled cells (10^6) were incubated for 2 hours with or without SB203580 (1 μM) and DMSO vehicle prior to stimulation with IL-1α (20 ng/nl) for 20 minutes. Endogenous Hsp27 was immunoprecipitated from cell lysates, resolved by electrophoresis and transferred to nylon membrane. Hsp27phosphorylation was visualised by autoradiography. The images from two exposure times 2 hours **(A)** and 16 hours **(B)** are shown.

Next, to investigate whether overexpressed MAPKAPK-2 K93R or MAPKAPK-2 anti-sense RNA interfered with endogenous MAPKAPK-2 activation induced by IL-1 stimulation, *in-vitro* kinase assays using GST-Hsp27 as substrate were carried out. Cells (10^6) were seeded into 6-well tissue culture plates and pre-incubated, as indicated in Figure 6.8C, with or without SB 203580 (1 μM) or DMSO for 2 hours prior to stimulation with IL-1α (20 ng/ml). Cells were then lysed and endogenous and mutant MAPKAPK-2 enzymes were immunoprecipitated using two different anti-MAPKAPK-2 antibodies, #06-534 (Figure 6.9A) and #sc-6221 (Figure 6.9B). *In-vitro* kinase assays were carried out as described in Chapter 2, section 2.4.5. The samples were resolved by electrophoresis, transferred to nylon membrane and analysed by autoradiography (Figure 6.9A and B). As expected, in both experiments pre-incubation of the pcDNA3 control cells with SB 203580 (1 μM) completely inhibited GST-Hsp27 phosphorylation, indicating that endogenous MAPKAPK-2 activation by p38 MAP kinase was inhibited in these cells. However, a comparison of the results from both experiments indicated no significant difference in Hsp27 phosphorylation that could be attributed to overexpression of dominant negative MAPKAPK-2 or MAPKAPK-2 anti-sense RNA. This may be explained by the fact that the epitope sequences used to raise the two precipitating anti-MAPKAPK-2 antibodies, share homology with the Hsp27 kinase MAPKAPK-3 (see Table 6.1). These experiments suggest that overexpressed dominant negative MAPKAPK-2 or MAPKAPK-2 anti-sense RNA does not measurably interfere with the activation of endogenous MAPKAPK-2. However, it can not be ruled out that in these assays the activity of MAPKAPK-3 is also being measured and that this may mask any dominant negative effect on endogenous MAPKAPK-2 activity. Since, MAPKAPK-3 is activated upon

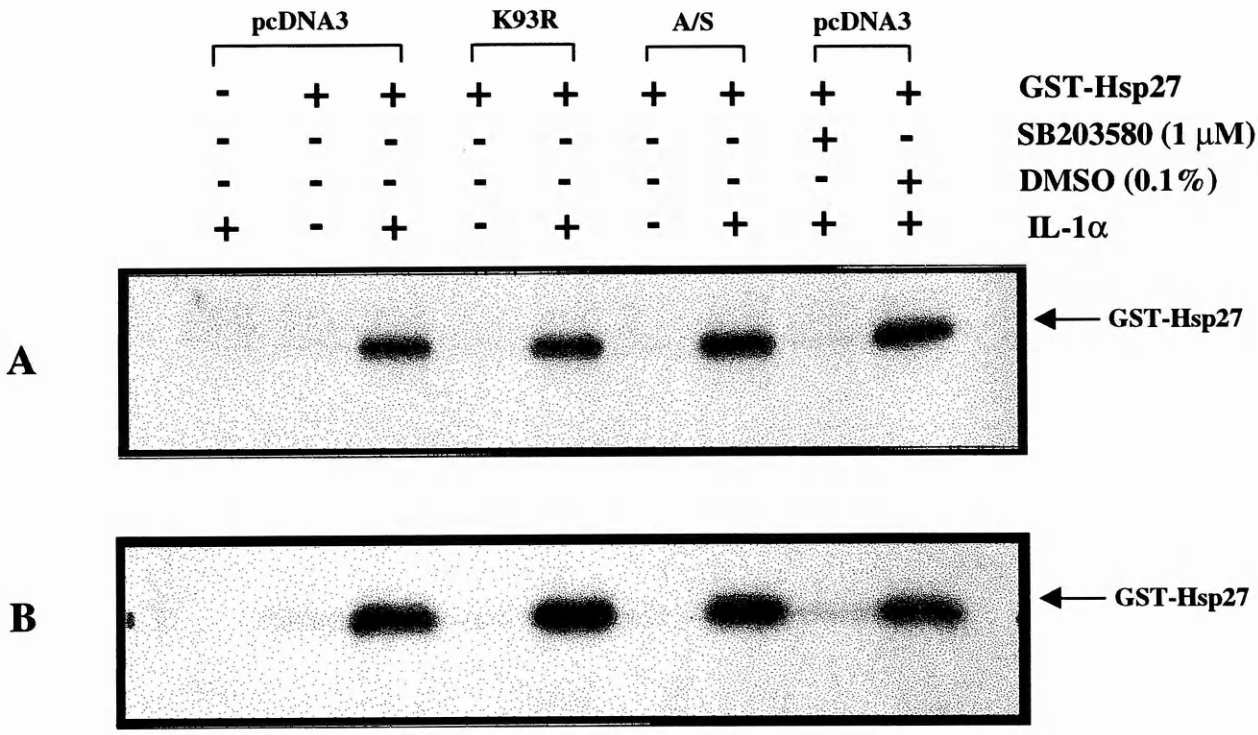

Figure 6.9: Effect of overexpressed MAPKAPK-2 K93R and MAPKAPK-2 anti-sense RNA (A/S) on endogenous MAPKAPK-2 activity. Cells (10^6) were incubated with or without SB 203580 (1 μM) or DMSO vehicle prior to stimulation with IL-1α (20 ng/ml) for 20 minutes. MAPKAPK-2 was immunoprecipitated with two different anti-MAPKAPK-2 antibodies #06-534 (**A**) and #sc-6221 (**B**) and incubated with GST-Hsp27 (3 μg) in an *in-vitro* kinase assay. Phosphorylated GST-Hsp27 was analysed by autoradiography.

phosphorylation by p38 MAPK pre-treatment with SB 203580 would inhibit any activity contributed by this enzyme in the kinase assays.

6.2.6 Effect of MAPKAPK-2 K93R and MAPKAPK-2 anti-sense overexpression on IL-1α induced IL-6 and IL-8 production

IL-6 and IL-8 are two important mediators induced by IL-1. Secreted IL-6 and IL-8 were assayed from the overlaying culture medium from cells pre-treated with or without SB 203580 (1 μM) or DMSO (0.1%) vehicle for 2 hours prior to stimulation with IL-1α (20 ng/ml) for 16 hours. Due to the variability of the levels of IL-1α induced IL-6 and IL-8 produced in this study, the results from four separate IL-6 (Figure 6.10) and IL-8 (Figure 6.11) assays are shown for discussion. As expected IL-1α induced the levels of both IL-6 and IL-8 in the pcDNA3 control cells and in the absence of IL-1α there was no significant production of either cytokine. Analysis of the IL-8 assay results revealed that SB 203580 caused partial inhibition in three out of four experiments when compared to the DMSO treated control cells. This results contrasts with that seen by Ridley *et al.* (1998) who reported that IL-1α had little or no effect on IL-8 production in human gingival fibroblasts and HUVEC cells. However, in a more recent report Suzuki *et al.* (2000) demonstrated that SB 203580 inhibited IL-1β and TNFα induced IL-8 production in a dose dependent manner, in rheumatoid synovial fibroblasts. Overexpression of MAPKAPK-2 anti-sense RNA had no significant inhibitory effect in three of the four experiments whilst the dominant negative MAPKAPK-2 mutant had no apparent inhibitory effect in all experiments.

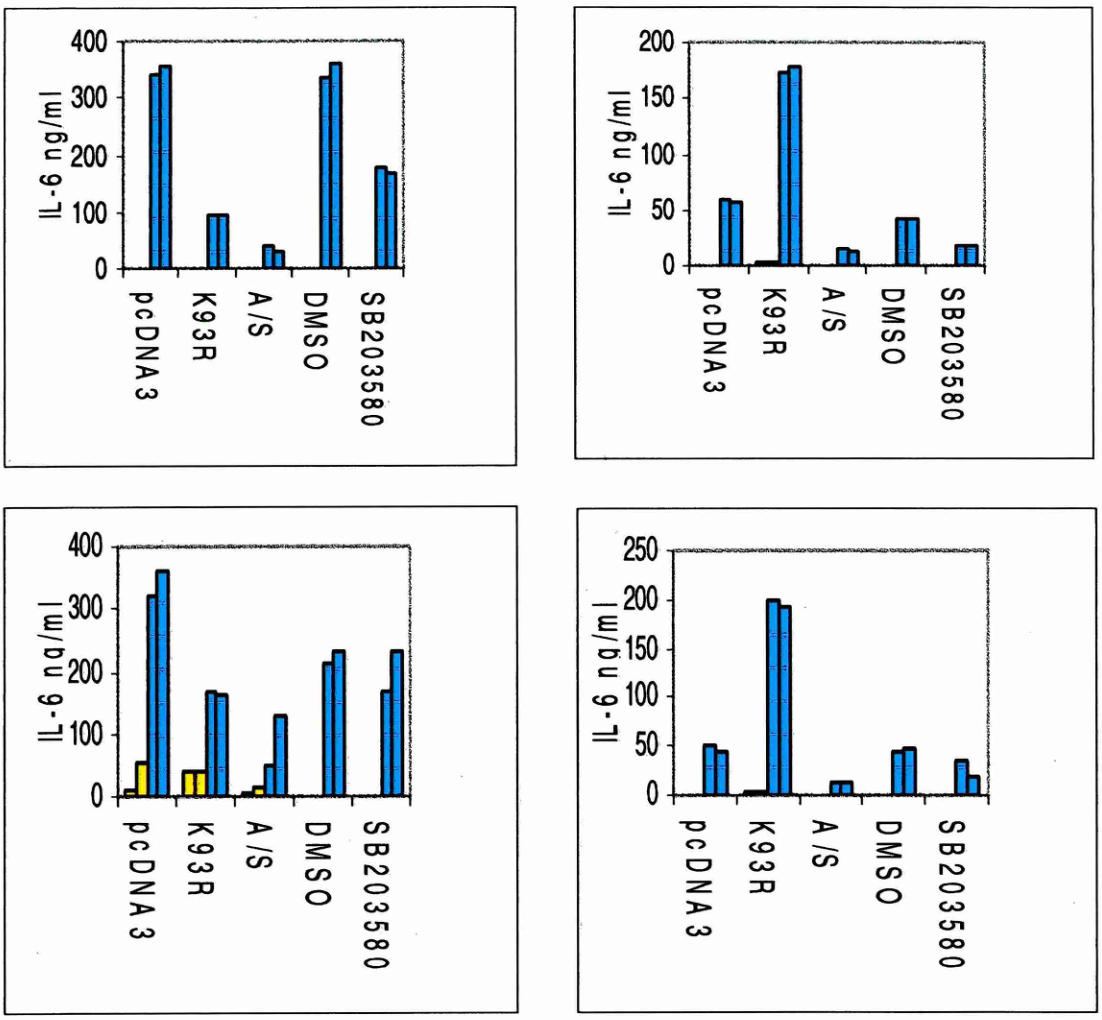

Figure 6.10: Effect of MAPKAPK-2 K93R and MAPKAPK-2 anti-sense RNA overexpression on IL-1α induced IL-6 secretion in HeLa cells. Cells were pre-treated for 2 hours with or without 1 μM SB203580 or DMSO vehicle prior to stimulation with IL-1α (20 ng/ml) for 16 hours. The overlaying culture medium was removed and assayed by specific IL-6 ELISA. IL-6 values were not determined for unstimulated DMSO or SB203580 samples. The above figure shows the results from duplicate samples from four separate experiments. Unstimulated □ , stimulated ■

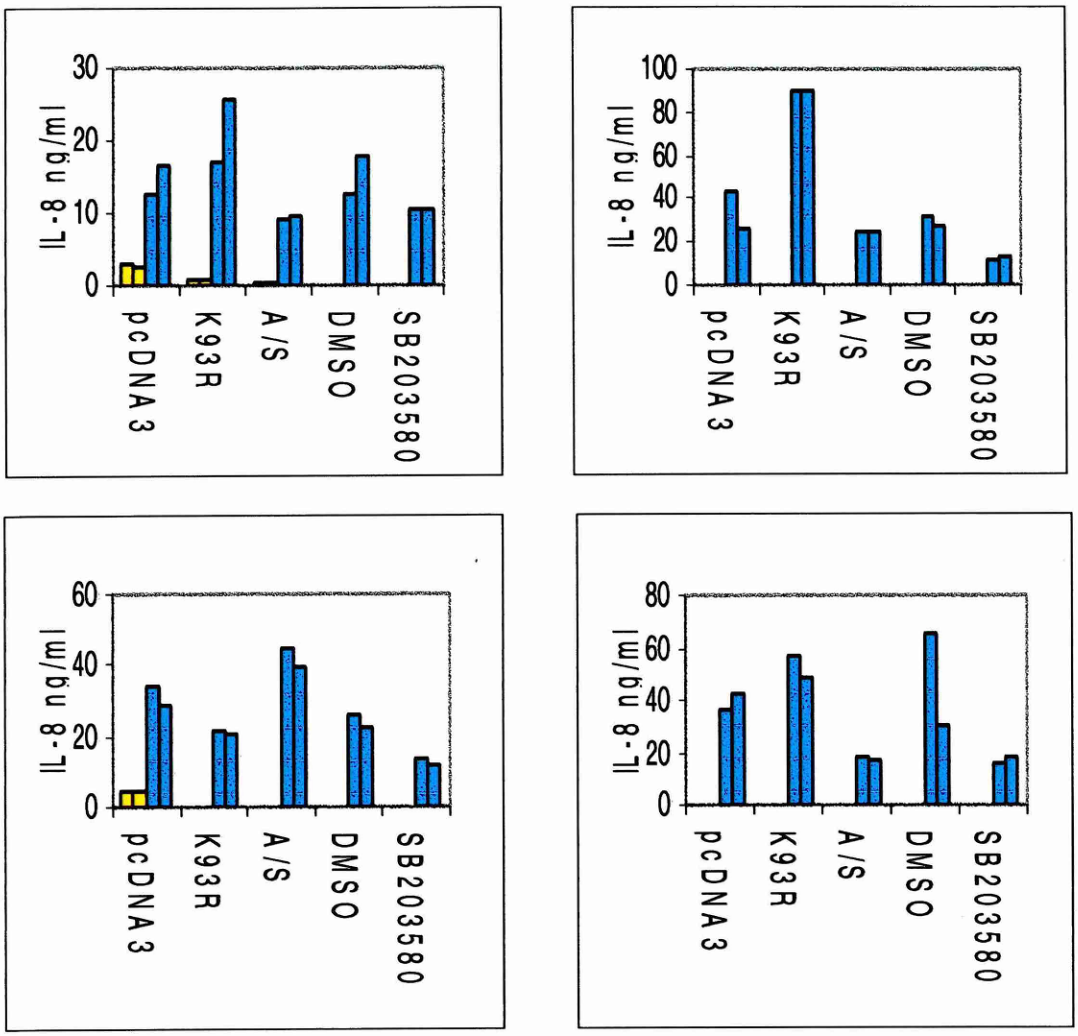

Figure 6.11: Effect of MAPKAPK-2 K93R and MAPKAPK-2 anti-sense RNA overexpression on IL-1α induced IL-8 secretion in HeLa cells. Cells were pre-treated for 2 hours with or without 1 μM SB203580 or DMSO vehicle prior to stimulation with IL-1α (20 ng/ml) for 16 hours. The overlaying culture medium was removed and assayed by specific IL-8 ELISA. IL-8 values were not determined for unstimulated DMSO or SB203580 samples. The above figure shows the results from duplicate samples from four separate experiments. Unstimulated □ , stimulated ■

SB 203580 has been shown by several workers to inhibit both TNF and IL-1 induced IL-6 production in several cell types (Ridley *et al.*, 1997; Miyazawa *et al.*, 1998; Suzuki *et al.*, 2000). In this study SB 203580 inhibited IL-1α induced IL-6 production in two of the four experiments when compared to the DMSO treated control cells. Significantly, overexpressed MAPKAPK-2 anti sense RNA dramatically reduced the levels of IL-6 in all experiments when compared to the pcDNA3 transfected control cells. In all cases this reduction was lower than that observed using SB 203580. The results from cells overexpressing dominant negative MAPKAPK-2 were slightly ambiguous. In two of the experiments elevated levels of IL-6 were observed, whilst in the other two experiments significant inhibitory effects were observed. As indicated above the high degree of variability observed in the production of IL-6 and IL-8 in these assays has made these results difficult to interpret. However, it is clear that HeLa cells overexpressing MAPKAPK-2 anti-sense RNA had a reproducible and significant inhibitory effect on IL-1α induced IL-6 when compared to the pcDNA3 transfected control cells.

6.3 Discussion

In this chapter evidence has been presented suggesting a role for MAPKAPK-2 in the regulation of IL-1α induced COX-2 synthesis. HeLa cells stably transfected with either a catalytically inactive MAPKAPK-2 mutant or a MAPKAPK-2 anti-sense RNA construct showed significant inhibition of IL-1α induced cyclooxygenase 2 (COX-2) protein synthesis and prostaglandin production. In both cases the inhibition of COX-2 protein correlated with an inhibition of COX-2 mRNA synthesis. In addition to the above findings overexpressed MAPKAPK-2 antisense RNA significantly inhibited IL-1α induced IL-6 production, suggesting a role for

MAPKAPK-2 in IL-1 induced cytokine production. Although it is possible that the results obtained from these cell lines are due to other genetic changes in other signalling pathways, the fact that these cell lines show Hsp27 phosphorylation in response to IL-1 confirms that the IL-1 receptor response is intact. In addition the fact that two independent approaches to modify the MAPKAPK-2 phenotype gave similar results on COX-2 synthesis suggests that a specific effect has been obtained

The exact mechanisms of inhibition by anti-sense and dominant negative mutants are unclear. Inhibition by anti-sense RNA is presumed to be due to decreased endogenous enzyme activity that is a consequence of reduced MAPKAPK-2 mRNA. By contrast the overexpressed MAPKAPK-2 K93R mutant may inhibit the function of endogenous MAPKAPK-2 by several different theoretical mechanisms such as; by binding to p38 MAP kinase and interfering with its activation by MKK6, by competing with endogenous enzyme for activation by p38 MAP kinase or by binding to downstream substrates and preventing their phosphorylation or subcellular targeting. From this we can speculate that MAPKAPK-2 anti-sense RNA affects IL-1α induced COX-2 and IL-6 synthesis by reducing the activity of endogenous MAPKAPK-2 on all downstream substrates involved in the regulation of these genes. In contrast, the MAPKAPK-2 mutant may differentially regulate the induction of these genes by binding specific downstream substrates of the endogenous enzyme. The conformational change imposed upon MAPKAPK-2 K93R as a result of the ATP binding site mutation may allow it to preferentially sequester and bind a downstream substrate that is specific for COX-2, therefore explaining the dramatic inhibition of induction of this gene.

The role of Hsp27 in pro-inflammatory cytokine signalling is unclear. Although not conclusive the data presented in this chapter suggests that Hsp27 is not involved in pro-inflammatory cytokine induced COX-2 and IL-6 synthesis. This notion is also supported by the finding that in L929 cells that lack Hsp25, the murine homologue of Hsp27, TNF signalling is unaffected, excluding a role of murine Hsp25 (Hsp27) in TNF action (Beyaert *et al.*, 1996).

Chapter 7

General Discussion

At the start of this thesis p38 MAP kinase had only recently been described (Han *et al.*, 1994). The link between p38 MAP kinase and the response of cells to pro-inflammatory cytokines was first established by Saklatvala and co-workers who showed that IL-1 activates a protein kinase cascade that results in the phosphorylation of the small heat shock protein, Hsp27, probably by MAPKAPK-2 (Freshney *et al.*, 1994). Subsequently workers at SmithKline Beecham showed that p38 MAPK was the target of a series of pyridinyl imidazole compounds which inhibited the production of pro-inflammatory cytokines (Lee *et al.*, 1994). As a consequence of these findings this project was undertaken with two inter-related aims. First, to try and identify additional novel enzyme components or interactions within the cytokine signalling pathway and second to examine the role of the p38 substrate MAPKAPK-2 in pro-inflammatory cytokine signalling. Using a PCR based strategy the enzymes described above were successfully cloned, mutated and epitope-tagged as described in Chapter 3. In Chapter 4, reconstitution experiments *in-vitro* confirmed loss of kinase activity in the recombinant p38 MAPK and MAPKAPK-2 enzymes, as a result of mutating the conserved lysine residues at their respective ATP binding sites. Following the successful outcome of these studies the enzymes were expressed as GAL4 binding domain fusion proteins and used as bait in a yeast two-hybrid screen. In Chapter 5, a novel protein interaction between MAPKAPK-2 and a human polyhomeotic 2-like protein (HPH2-like) is described.

Analysis of the HPH2-like protein revealed that there was no obvious connection with the p38 MAPK pathway and the significance of the interaction was unclear. It is interesting to note that in this study MAPKAPK-2 K93R did not detect p38 MAPK or Hsp27. In Chapter 6, the results form HeLa cells stably expressing dominant negative MAPKAPK-2 and MAPKAPK-2 anti-sense RNA suggest that MAPKAPK-2 is involved in IL-1α induced COX-2 synthesis and possibly IL-6 synthesis. Although not conclusive, evidence from these cell lines also suggests that Hsp27 is not involved in pro-inflammatory cytokine induced gene expression since its phosphorylation *in-situ* was not noticeably affected.

At the time of completion of this study evidence from MAPKAPK-2 knockout mice indicated that MAPKAPK-2 plays an important role in gene regulation (Kotylarov *et al.*, 1999). In these animals circulatory TNF levels were reduced by 90%. This was shown to be due to reduced protein and not decreased amounts of TNF mRNA. In addition these animals also had an increased resistance to LPS challenge. In contrast, Northern blot analysis of various cytokines in isolated spleen cells from LPS stimulated animals showed significantly reduced levels of IL-6 mRNA implying a role for MAPKAPK-2 in transcription or mRNA stability or both. In the MAPKAPK-$2^{-/-}$ mice the effect of MAPKAPK-2 on COX-2 was not examined. Consequently it would be interesting to test the IL-1α induced COX-2 response in, for example, fibroblasts isolated from these animals.

Although many unanswered questions have arisen from this work, the results provide a new focus for future studies. One important topic will be to identify the downstream substrates of MAPKAPK-2. Although yeast two-hybrid methodology was tested in this study, the failure to detect any known MAPKAPK-2 proteins indicate that the success of this technique may be determined by many factors, such as the choice of bait protein, conformation changes imposed by mutagenesis or the cDNA source. More recently proteomic studies have being used identify new proteins *in-situ*. This technique could be employed to look for phosphoprotein differences between the HeLa control and MAPKAPK-2 mutant cell lines. Current evidence using a tetracycline-controlled expression system in HeLa cells suggests MAPKAPK-2 may regulate gene synthesis in part by stabilising mRNA (Winzen *et al.*, 1999). In this report, constitutively active murine MAPKAPK-2 stabilised a β-globin reporter mRNA containing IL-8 3'-UTR sequences, whereas a dominant negative MAPKAPK-2 mutant interfered with MKK6 induced stabilisation. To search for novel downstream substrates of MAPKAPK-2 techniques such as the RNA-protein hybrid technology may be more successful than protein-protein interactions. This system allows the detection of interactions between known RNA bait for example, COX-2 or IL-6 and a potential RNA binding protein. Such studies may identify proteins involved in controlling pro-inflammatory cytokine induced gene synthesis and thus provide therapeutic opportunity for controlling inflammatory diseases.

References

Andersson, J., Bjork, L., Dinarello, C.A., Towbin, H., and Andersson, U. (1992). Lipopolysaccharide induces human interleukin-1 receptor antagonist and interleukin-1 production in the same cell. European Journal of Immunology *22*, 2617-2623.

Badger, A.M., Bradbeer, J.N., Votta, B., Lee, J.C., Adams, J.L., and Griswold, D.E. (1996). Pharmacological profile of SB 203580, a selective inhibitor of cytokine suppressive binding protein/p38 kinase, in animal models of arthritis, bone resorption, endotoxin shock and immune function. Journal of Pharmacology & Experimental Therapeutics *279*, 1453-1461.

Baggiolini, M. (1998). Chemokines and leukocyte traffic. Nature *392*, 565-568.

Bartel, P.L., Chien, C.-T., Sternglanz, R. & Fields, S. (1993a). Using the two-hybrid system to detect protein-protein interactions. In Cellular Interactions in Development: Apractical Approach., ed. Hartley, D.A. (Oxford University Press, Oxford) pp 153-179.

Baud, V., Liu, Z.G., Bennett, B., Suzuki, N., Xia, Y., and Karin, M. (1999). Signaling by proinflammatory cytokines: oligomerization of TRAF2 and TRAF6 is sufficient for JNK and IKK activation and target gene induction via an amino-terminal effector domain. Genes & Development *13*, 1297-1308.

Baumann, H. and Gauldie, J. (1994). The acute phase response [see comments]. [Review] [66 refs]. Immunology Today *15*, 74-80.

Ben-Levy, R., Leighton, I.A., Doza, Y.N., Attwood, P., Morrice, N., Marshall, C.J., and Cohen, P. (1995). Identification of novel phosphorylation sites required for activation of MAPKAP kinase-2. EMBO Journal *14*, 5920-5930.

Ben-Levy, R., Hooper, S., Wilson, R., Paterson, H.F., and Marshall, C.J. (1998). Nuclear export of the stress-activated protein kinase p38 mediated by its substrate MAPKAP kinase-2. [Review] [42 refs]. Current Biology *8*, 1049-1057.

Beyaert, R., Cuenda, A., Vanden Berghe, W., Plaisance, S., Lee, J.C., Haegeman, G, Cohen, P., and Fiers, W. (1996). The p38/RK mitogen-activated protein kinase pathway regulates interleukin-6 synthesis response to tumor necrosis factor. EMBO Journal *15*, 1914-1923.

Black, R.A., Rauch, C.T., Kozlosky, C.J., Peschon, J.J., Slack, J.L., Wolfson MF, Castner, B.J., Stocking, K.L., Reddy, P., Srinivasan, S., Nelson, N., Boiani N, Schooley, K.A., Gerhart, M., Davis, R., Fitzner, J.N., Johnson, R.S., Paxton RJ, March, C.J., and Cerretti, D.P. (1997). A metalloproteinase disintegrin that releases tumour-necrosis factor-alpha from cells. Nature *385*, 729-733.

Blumer, K.J. and Johnson, G.L. (1994). Diversity in function and regulation of MAP kinase pathways. [Review] [41 refs]. Trends in Biochemical Sciences *19*, 236-240.

Boldin, M.P., Goncharov, T.M., Goltsev, Y.V., and Wallach, D. (1996). Involvement of MACH, a novel MORT1/FADD-interacting protease, in Fas/APO-1- and TNF receptor-induced cell death. Cell *85*, 803-815.

Borsch-Haubold, A.G., Kramer, R.M., and Watson, S.P. (1997). Phosphorylation and activation of cytosolic phospholipase A2 by 38-kDa mitogen-activated protein kinase in collagen-stimulated human platelets. European Journal of Biochemistry *245*, 751-759.

Boulton, T.G., Yancopoulos, G.D., Gregory, J.S., Slaughter, C., Moomaw C, Hsu, J., and Cobb, M.H. (1990). An insulin-stimulated protein kinase similar to yeast kinases involved in cell cycle control. Science *249*, 64-67.

Boulton, T.G., Nye, S.H., Robbins, D.J., Ip, N.Y., Radziejewska, E., Morgenbesser, SD, DePinho, R.A., Panayotatos, N., Cobb, M.H., and Yancopoulos, G.D. (1991). ERKs: a family of protein-serine/threonine kinases that are activated and tyrosine phosphorylated in response to insulin and NGF. Cell *65*, 663-675.

Bresnihan, B., Alvaro-Gracia, J.M., Cobby, M., Doherty, M., Domljan, Z., Emery, P., Nuki, G., Pavelka, K., Rau, R., Rozman, B., Watt, I., Williams, B., Aitchison, R., McCabe, D., and Musikic, P. (1998). Treatment of rheumatoid arthritis with recombinant human interleukin-1 receptor antagonist [see comments]. Arthritis Rheum. *41*, 2196-2204.

Brewster, J.L., de Valoir, T., Dwyer, N.D., Winter, E., and Gustin, M.C. (1993). An osmosensing signal transduction pathway in yeast. Science *259*, 1760-1763.

Burns, K., Martinon, F., Esslinger, C., Pahl, H., Schneider, P., Bodmer JL, Di Marco, F., French, L., and Tschopp, J. (1998). MyD88, an adapter protein involved in interleukin-1 signaling. Journal of Biological Chemistry *273*, 12203-12209.

Cao, Z., Henzel, W.J., and Gao, X. (1996a). IRAK: a kinase associated with the interleukin-1 receptor. Science *271*, 1128-1131.

Cao, Z., Xiong, J., Takeuchi, M., Kurama, T., and Goeddel, D.V. (1996b). TRAF6 is a signal transducer for interleukin-1. Nature *383*, 443-446.

Caput, D., Beutler, B., Hartog, K., Thayer, R., Brown-Shimer, S., and Cerami, A. (1986). Identification of a common nucleotide sequence in the 3'-untranslated region of mRNA

molecules specifying inflammatory mediators. Proc. Natl. Acad. Sci. U. S. A. *83*, 1670-1674.

Carballo, E., Lai, W.S., and Blackshear, P.J. (1998). Feedback inhibition of macrophage tumor necrosis factor-alpha production by tristetraprolin. Science *281*, 1001-1005.

Carpentier, I., Declercq, W., Malinin, N.L., Wallach, D., Fiers, W, and Beyaert, R. (1998). TRAF2 plays a dual role in NF-kappaB-dependent gene activation by mediating the TNF-induced activation of p38 MAPK and IkappaB kinase pathways. FEBS Letters *425*, 195-198.

Carper, S.W., Rocheleau, T.A., and Storm, F.K. (1990). cDNA sequence of a human heat shock protein HSP27. Nucleic. Acids. Res. *18*, 6457

Carter, D.B., Deibel, M.R., Jr., Dunn, C.J., Tomich, C.S., Laborde, A.L., Slightom, J.L., Berger, A.E., Bienkowski, M.J., Sun, F.F., McEwan, R.N., and et al. (1990). Purification, cloning, expression and biological characterization of an interleukin-1 receptor antagonist protein [see comments]. Nature *344*, 633-638.

Cerretti, D.P., Kozlosky, C.J., Mosley, B., Nelson, N., Van Ness, K., Greenstreet, TA, March, C.J., Kronheim, S.R., Druck, T., Cannizzaro, L.A., and et al (1992). Molecular cloning of the interleukin-1 beta converting enzyme. Science *256*, 97-100.

Chen, C.Y., Xu, N., and Shyu, A.B. (1995). mRNA decay mediated by two distinct AU-rich elements from c-fos and granulocyte-macrophage colony-stimulating factor transcripts: different deadenylation kinetics and uncoupling from translation. Mol. Cell Biol. *15*, 5777-5788.

Chen, C.Y. and Shyu, A.B. (1994). Selective degradation of early-response-gene mRNAs: functional analyses of sequence features of the AU-rich elements. Mol. Cell Biol. *14*, 8471-8482.

Cheng, M., Zhen, E., Robinson, M.J., Ebert, D., and Goldsmith, E., Cobb MH. (1996). Characterization of a protein kinase that phosphorylates serine 189 of the mitogen-activated protein kinase homolog ERK3. Journal of Biological Chemistry *271*, 12057-12062.

Chinnaiyan, A.M., O'Rourke, K., Tewari, M., and Dixit, V.M. (1995). FADD, a novel death domain-containing protein, interacts with the death domain of Fas and initiates apoptosis. Cell *81*, 505-512.

Clerk, A. and Sugden, P.H. (1998). The p38-MAPK inhibitor, SB203580, inhibits cardiac stress-activated protein kinases/c-Jun N-terminal kinases (SAPKs/JNKs). FEBS Letters *426*, 93-96.

Colotta, F., Re, F., Muzio, M., Bertini, R., Polentarutti, N., Sironi, M., Giri, JG, Dower, S.K., Sims, J.E., and Mantovani, A. (1993). Interleukin-1 type II receptor: a decoy target for IL-1 that is regulated by IL-4. Science *261*, 472-475.

Crawley, J.B., Rawlinson, L., Lali, F.V., Page, T.H., Saklatvala, J., and Foxwell, B.M. (1997). T cell proliferation in response to interleukins 2 and 7 requires p38MAP kinase activation. Journal of Biological Chemistry *272*, 15023-15027.

Cuenda, A., Rouse, J., Doza, Y.N., Meier, R., Cohen, P., Gallagher, T.F., Young, PR, and Lee, J.C. (1995). SB 203580 is a specific inhibitor of a MAP kinase homologue which is stimulated by cellular stresses and interleukin-1. FEBS Letters *364*, 229-233.

Cuenda, A., Alonso, G., Morrice, N., Jones, M., Meier, R., Cohen, P., Nebreda, and AR. (1996). Purification and cDNA cloning of SAPKK3, the major activator of RK/p38 in stress- and cytokine-stimulated monocytes and epithelial cells. EMBO Journal *15*, 4156-4164.

Curtis, B.M., Widmer, M.B., deRoos, P., and Qwarnstrom, E.E. (1990). IL-1 and its receptor are translocated to the nucleus. Journal of Immunology *144*, 1295-1303.

de Laszlo, S.E., Visco, D., Agarwal, L., Chang, L., Chin, J., Croft G, Forsyth, A., Fletcher, D., Frantz, B., Hacker, C., Hanlon, W., Harper, C., Kostura, M., Li, B., Luell, S., MacCoss, M., Mantlo, N., O'Neill, E.A., Orevillo, C., Pang M, Parsons, J., Rolando, A., Sahly, Y., Sidler, K., O'Keefe, S.J., and et al. (1998). Pyrroles and other heterocycles as inhibitors of p38 kinase. Bioorganic & Medicinal Chemistry Letters *8*, 2689-2694.

Deak, M., Clifton, A.D., Lucocq, L.M., and Alessi, D.R. (1998). Mitogen- and stress-activated protein kinase-1 (MSK1) is directly activated by MAPK and SAPK2/p38, and may mediate activation of CREB. EMBO Journal *17*, 4426-4441.

Dean, J.L., Brook, M., Clark, A.R., and Saklatvala, J. (1999). p38 mitogen-activated protein kinase regulates cyclooxygenase-2 mRNA stability and transcription in lipopolysaccharide-treated human monocytes. Journal of Biological Chemistry *274*, 264-269.

Decoster, E., Vanhaesebroeck, B., Vandenabeele, P., and Grooten, J., Fiers W. (1995). Generation and biological characterization of membrane-bound, uncleavable murine tumor necrosis factor. Journal of Biological Chemistry *270*, 18473-18478.

DeMaria, C.T. and Brewer, G. (1996). AUF1 binding affinity to A+U-rich elements correlates with rapid mRNA degradation. J. Biol. Chem. *271*, 12179-12184.

Derijard, B., Hibi, M., Wu, I.H., Barrett, T., Su, B., Deng, T., Karin, M., Davis, and RJ. (1994). JNK1: a protein kinase stimulated by UV light and Ha-Ras that binds and phosphorylates the c-Jun activation domain. Cell *76*, 1025-1037.

Derijard, B., Raingeaud, J., Barrett, T., Wu, I.H., Han, J., Ulevitch, R.J., Davis, and RJ. (1995). Independent human MAP-kinase signal transduction pathways defined by MEK and MKK isoforms [published erratum appears in Science 1995 Jul 7;269(5220):17]. Science *267*, 682-685.

DeWitt, D. and Smith, W.L. (1995). Yes, but do they still get headaches? [published erratum appears in Cell 1996 Feb 23;84(4):following 650]. [Review] [16 refs]. Cell *83*, 345-348.

DeWitt, D.L. and Smith, W.L. (1988). Primary structure of prostaglandin G/H synthase from sheep vesicular gland determined from the complementary DNA sequence [published erratum appears in Proc Natl Acad Sci U S A 1988 Jul; 85(14):5056]. Proceedings of the National Academy of Sciences of the United States of America *85*, 1412-1416.

Dinarello, C.A. (1994). The interleukin-1 family: 10 years of discovery. [Review] [128 refs]. FASEB Journal *8*, 1314-1325.

Dinarello, C.A. (1996). Biologic basis for interleukin-1 in disease. [Review] [586 refs]. Blood *87*, 2095-2147.

Ebina, Y., Takahara, Y., Kishi, F., Nakazawa, A., and Brent, R. (1983). LexA protein is a repressor of the colicin E1 gene. Journal of Biological Chemistry *258*, 13258-13261.

Eck, M.J., Ultsch, M., Rinderknecht, E., de Vos, A.M., and Sprang, S.R. (1992). The structure of human lymphotoxin (tumor necrosis factor-beta) at 1.9-A resolution. J. Biol. Chem. *267*, 2119-2122.

Eder, J. (1997). Tumour necrosis factor alpha and interleukin 1 signalling: do MAPKK kinases connect it all?. [Review] [26 refs]. Trends in Pharmacological Sciences *18*, 319-322.

Eisenberg, S.P., Evans, R.J., Arend, W.P., Verderber, E., Brewer, MT, Hannum, C.H., and Thompson, R.C. (1990). Primary structure and functional expression from complementary DNA of a human interleukin-1 receptor antagonist. Nature *343*, 341-346.

Elliott, M.J., Maini, R.N., Feldmann, M., Kalden, J.R., Antoni, C., Smolen JS, Leeb, B., Breedveld, F.C., Macfarlane, J.D., Bijl, H., and et al (1994). Randomised double-blind comparison of chimeric monoclonal antibody to tumour necrosis factor alpha (cA2) versus placebo in rheumatoid arthritis. Lancet *344*, 1105-1110.

Elliott, M.J. and Maini, R.N. (1995). Anti-cytokine therapy in rheumatoid arthritis. [Review] [81 refs]. Baillieres Clinical Rheumatology *9*, 633-652.

Engel, K., Plath, K., and Gaestel, M. (1993). The MAP kinase-activated protein kinase 2 contains a proline-rich SH3-binding domain. FEBS Letters *336*, 143-147.

Engel, K., Schultz, H., Martin, F., Kotlyarov, A., Plath, K., Hahn, M., Heinemann, U., and Gaestel, M. (1995). Constitutive activation of mitogen-activated protein kinase-activated protein kinase 2 by mutation of phosphorylation sites and an A-helix motif. Journal of Biological Chemistry *270*, 27213-27221.

Engel, K., Kotlyarov, A., and Gaestel, M. (1998). Leptomycin B-sensitive nuclear export of MAPKAP kinase 2 is regulated by phosphorylation. EMBO Journal *17*, 3363-3371.

Estojak, J., Brent, R., and Golemis, E.A. (1995). Correlation of two-hybrid affinity data with in vitro measurements. Molecular & Cellular Biology *15*, 5820-5829.

Eyers, P.A., Craxton, M., Morrice, N., Cohen, P., and Goedert, M. (1998). Conversion of SB 203580-insensitive MAP kinase family members to drug-sensitive forms by a single amino-acid substitution. Chem. Biol. *5*, 321-328.

Feilotter, H.E., Hannon, G.J., Ruddell, C.J., and Beach, D. (1994). Construction of an improved host strain for two hybrid screening. Nucleic Acids Research *22*, 1502-1503.

Fields, S. and Song, O. (1989). A novel genetic system to detect protein-protein interactions. Nature *340*, 245-246.

Fields, S. and Sternglanz, R. (1994). The two-hybrid system: an assay for protein-protein interactions. [Review] [40 refs]. Trends in Genetics *10*, 286-292.

Finch, A., Holland, P., Cooper, J., Saklatvala, J., and Kracht, M. (1997). Selective activation of JNK/SAPK by interleukin-1 in rabbit liver is mediated by MKK7. FEBS Letters *418*, 144-148.

Foey, A.D., Parry, S.L., Williams, L.M., Feldmann, M., and Foxwell, B.M., Brennan FM. (1998). Regulation of monocyte IL-10 synthesis by endogenous IL-1 and TNF-alpha: role of the p38 and p42/44 mitogen-activated protein kinases. Journal of Immunology *160*, 920-928.

Franke, A., DeCamillis, M., Zink, D., Cheng, N., Brock, H.W., Paro, and R. (1992). Polycomb and polyhomeotic are constituents of a multimeric protein complex in chromatin of Drosophila melanogaster. EMBO Journal *11*, 2941-2950.

Frantz, B., Klatt, T., Pang, M., Parsons, J., Rolando, A., Williams H, Tocci, M.J., O'Keefe, S.J., and O'Neill, E.A. (1998). The activation state of p38 mitogen-activated

protein kinase determines the efficiency of ATP competition for pyridinylimidazole inhibitor binding. Biochemistry *37*, 13846-13853.

Freshney, N.W., Rawlinson, L., Guesdon, F., Jones, E., Cowley, S., Hsuan, J., and Saklatvala, J. (1994). Interleukin-1 activates a novel protein kinase cascade that results in the phosphorylation of Hsp27. Cell *78*, 1039-1049.

Frost, J.A., Xu, S., Hutchison, M.R., Marcus, S., and Cobb, M.H. (1996). Actions of Rho family small G proteins and p21-activated protein kinases on mitogen-activated protein kinase family members. Molecular & Cellular Biology *16*, 3707-3713.

Fukunaga, R. and Hunter, T. (1997). MNK1, a new MAP kinase-activated protein kinase, isolated by a novel expression screening method for identifying protein kinase substrates. EMBO Journal *16*, 1921-1933.

Gaestel, M., Gross, B., Benndorf, R., Strauss, M., Schunk, W.H., Kraft, R., Otto, A., Bohm, H., Stahl, J., and Drabsch, H. (1989). Molecular cloning, sequencing and expression in Escherichia coli of the 25-kDa growth-related protein of Ehrlich ascites tumor and its homology to mammalian stress proteins. Eur. J. Biochem. *179*, 209-213.

Galcheva-Gargova, Z., Derijard, B., Wu, I.H., and Davis, R.J. (1994). An osmosensing signal transduction pathway in mammalian cells. Science *265*, 806-808.

Garrington, T.P. and Johnson, G.L. (1999). Organization and regulation of mitogen-activated protein kinase signaling pathways. [Review] [58 refs]. Current Opinion in Cell Biology *11*, 211-218.

Gay, N.J. and Keith, F.J. (1991). Drosophila Toll and IL-1 receptor [letter]. Nature *351*, 355-356.

Gietz, D., St.Jean, A., Woods, R.A., and Schiestl, R.H. (1992). Improved method for high efficiency transformation of intact yeast cells. Nucleic Acids Research *20*, 1425

Giniger, E., Varnum, S.M., and Ptashne, M. (1985). Specific DNA binding of GAL4, a positive regulatory protein of yeast. Cell *40*, 767-774.

Giniger, E. and Ptashne, M. (1988). Cooperative DNA binding of the yeast transcriptional activator GAL4. Proceedings of the National Academy of Sciences of the United States of America *85*, 382-386.

Graves, L.M., Bornfeldt, K.E., Sidhu, J.S., Argast, G.M., Raines, E.W., Ross, R., Leslie, C.C., and Krebs, E.G. (1996). Platelet-derived growth factor stimulates protein kinase A through a mitogen-activated protein kinase-dependent pathway in human arterial smooth muscle cells. Journal of Biological Chemistry *271*, 505-511.

Greenfeder, S.A., Nunes, P., Kwee, L., Labow, M., and Chizzonite, R.A., Ju G. (1995). Molecular cloning and characterization of a second subunit of the interleukin 1 receptor complex. Journal of Biological Chemistry *270*, 13757-13765.

Grell, M. (1995). Tumor necrosis factor (TNF) receptors in cellular signaling of soluble and membrane-expressed TNF. J. Inflamm. *47*, 8-17.

Guan, Z., Baier, L.D., and Morrison, A.R. (1997). p38 mitogen-activated protein kinase down-regulates nitric oxide and up-regulates prostaglandin E2 biosynthesis stimulated by interleukin-1beta. Journal of Biological Chemistry *272*, 8083-8089.

Guan, Z., Buckman, S.Y., Miller, B.W., Springer, L.D., and Morrison, A.R. (1998a). Interleukin-1beta-induced cyclooxygenase-2 expression requires activation of both c-Jun NH2-terminal kinase and p38 MAPK signal pathways in rat renal mesangial cells. Journal of Biological Chemistry *273*, 28670-28676.

Guan, Z., Buckman, S.Y., Pentland, A.P., Templeton, D.J., Morrison, and AR. (1998b). Induction of cyclooxygenase-2 by the activated MEKK1 --> SEK1/MKK4 --> p38 mitogen-activated protein kinase pathway. Journal of Biological Chemistry *273*, 12901-12908.

Guesdon, F., Freshney, N., Waller, R.J., Rawlinson, L., and Saklatvala, J. (1993). Interleukin 1 and tumor necrosis factor stimulate two novel protein kinases that phosphorylate the heat shock protein hsp27 and beta-casein. Journal of Biological Chemistry *268*, 4236-4243.

Gum, R.J., McLaughlin, M.M., Kumar, S., Wang, Z., Bower, M.J., Lee, JC, Adams, J.L., Livi, G.P., Goldsmith, E.J., and Young, P.R. (1998). Acquisition of sensitivity of stress-activated protein kinases to the p38 inhibitor, SB 203580, by alteration of one or more amino acids within the ATP binding pocket. Journal of Biological Chemistry *273*, 15605-15610.

Gunster, M.J., Satijn, D.P., Hamer, K.M., den Blaauwen, J.L., de, Bruijn, D., Alkema, M.J., van Lohuizen, M., van Driel, R., and Otte, A.P. (1997). Identification and characterization of interactions between the vertebrate polycomb-group protein BMI1 and human homologs of polyhomeotic. Molecular & Cellular Biology *17*, 2326-2335.

Gupta, S., Campbell, D., Derijard, B., and Davis, R.J. (1995). Transcription factor ATF2 regulation by the JNK signal transduction pathway. Science *267*, 389-393.

Gupta, S., Barrett, T., Whitmarsh, A.J., Cavanagh, J., Sluss, H.K., Derijard B, and Davis, R.J. (1996). Selective interaction of JNK protein kinase isoforms with transcription factors. EMBO Journal *15*, 2760-2770.

Gupta, S. and Davis, R.J. (1994). MAP kinase binds to the NH2-terminal activation domain of c-Myc. FEBS Letters *353*, 281-285.

Guthrie, C. & Fink, G.R. (1991). Guide to yeast genetics and molecular biology. In Methods in Enzymology (Academic Press, San Diego) *194,* 1-932.

Habenicht, A.J., Goerig, M., Grulich, J., Rothe, D., Gronwald, R., Loth U, Schettler, G., Kommerell, B., and Ross, R. (1985). Human platelet-derived growth factor stimulates prostaglandin synthesis by activation and by rapid de novo synthesis of cyclooxygenase. Journal of Clinical Investigation *75*, 1381-1387.

Hall-Jackson, C.A., Goedert, M., Hedge, P., and Cohen, P. (1999). Effect of SB 203580 on the activity of c-Raf in vitro and in vivo. Oncogene *18*, 2047-2054.

Han, J., Thompson, P., and Beutler, B. (1990). Dexamethasone and pentoxifylline inhibit endotoxin-induced cachectin/tumor necrosis factor synthesis at separate points in the signaling pathway. J. Exp. Med. *172*, 391-394.

Han, J., Lee, J.D., Tobias, P.S., and Ulevitch, R.J. (1993). Endotoxin induces rapid protein tyrosine phosphorylation in 70Z/3 cells expressing CD14. Journal of Biological Chemistry *268*, 25009-25014.

Han, J., Lee, J.D., Bibbs, L., and Ulevitch, R.J. (1994). A MAP kinase targeted by endotoxin and hyperosmolarity in mammalian cells. Science *265*, 808-811.

Han, J., Lee, J.D., Jiang, Y., Li, Z., Feng, L., and Ulevitch, R.J. (1996). Characterization of the structure and function of a novel MAP kinase kinase (MKK6). Journal of Biological Chemistry *271*, 2886-2891.

Han, J., Jiang, Y., Li, Z., Kravchenko, V.V., and Ulevitch, R.J. (1997). Activation of the transcription factor MEF2C by the MAP kinase p38 in inflammation. Nature *386*, 296-299.

Han, J.W., Sadowski, H., Young, D.A., and Macara, I.G. (1990). Persistent induction of cyclooxygenase in p60v-src-transformed 3T3 fibroblasts. Proceedings of the National Academy of Sciences of the United States of America *87*, 3373-3377.

Hanks, S.K., Quinn, A.M., and Hunter, T. (1988). The protein kinase family: conserved features and deduced phylogeny of the catalytic domains. [Review] [119 refs]. Science *241*, 42-52.

Harper, J.W., Adami, G.R., Wei, N., Keyomarsi, K., and Elledge, S.J. (1993). The p21 Cdk-interacting protein Cip1 is a potent inhibitor of G1 cyclin-dependent kinases: Cell *75*, 805-816.

Hashimoto, S., Matsumoto, K., Gon, Y., Maruoka, S., Takeshita, I., Hayashi, S., Koura, T., Kujime, K., and Horie, T. (1999). p38 Mitogen-activated protein kinase regulates IL-8 expression in human pulmonary vascular endothelial cells. European Respiratory Journal *13*, 1357-1364.

Haskill, S., Martin, G., Van Le, L., Morris, J., Peace, A., Bigler, C.F., Jaffe, GJ, Hammerberg, C., Sporn, S.A., Fong, S., and et al. (1991). cDNA cloning of an intracellular form of the human interleukin 1 receptor antagonist associated with epithelium. Proceedings of the National Academy of Sciences of the United States of America *88*, 3681-3685.

Hazzalin, C.A., Cano, E., Cuenda, A., Barratt, M.J., Cohen, P., and Mahadevan, L.C. (1996). p38/RK is essential for stress-induced nuclear responses: JNK/SAPKs and c-Jun/ATF-2 phosphorylation are insufficient. Curr. Biol. *6*, 1028-1031.

Heslot, H. & Gaillardin, C., eds. (1992). Molecular Biology and Genetic Engineering of Yeasts, CRC Press, Inc.

Hickey, E., Brandon, S.E., Potter, R., Stein, G., Stein, J., and Weber, L.A. (1986). Sequence and organization of genes encoding the human 27 kDa heat shock protein [published erratum appears in Nucleic Acids Res 1986 Oct 24;14(20):8230]. Nucleic. Acids. Res. *14*, 4127-4145.

Hsu, H., Xiong, J., and Goeddel, D.V. (1995). The TNF receptor 1-associated protein TRADD signals cell death and NF-kappa B activation. Cell *81*, 495-504.

Hsu, H., Huang, J., Shu, H.B., Baichwal, V., and Goeddel, D.V. (1996). TNF-dependent recruitment of the protein kinase RIP to the TNF receptor-1 signaling complex. Immunity *4*, 387-396.

Huang, C.K., Zhan, L., Ai, Y., and Jongstra, J. (1997). LSP1 is the major substrate for mitogen-activated protein kinase-activated protein kinase 2 in human neutrophils. Journal of Biological Chemistry *272*, 17-19.

Huang, J., Gao, X., Li, S., and Cao, Z. (1997). Recruitment of IRAK to the interleukin 1 receptor complex requires interleukin 1 receptor accessory protein. Proceedings of the National Academy of Sciences of the United States of America *94*, 12829-12832.

Huguet, C., Crepieux, P., and Laudet, V. (1997). Rel/NF-kappa B transcription factors and I kappa B inhibitors: evolution from a unique common ancestor. Oncogene *15*, 2965-2974.

Isakson, P., Seibert, K., Masferrer, J., Salvemini, D., Lee, L., and Needleman, P. (1995). Discovery of a better aspirin. Adv. Prostaglandin. Thromboxane. Leukot. Res. *23:49-54*, 49-54.

Iwabuchi, K., Li, B., Bartel, P., and Fields, S. (1993). Use of the two-hybrid system to identify the domain of p53 involved in oligomerization. Oncogene *8*, 1693-1696.

Jacobson, A. and Peltz, S.W. (1996). Interrelationships of the pathways of mRNA decay and translation in eukaryotic cells. Annu. Rev. Biochem. *65:693-739*, 693-739.

Jakob, U., Gaestel, M., Engel, K., and Buchner, J. (1993). Small heat shock proteins are molecular chaperones. Journal of Biological Chemistry *268*, 1517-1520.

Janknecht, R., Ernst, W.H., Pingoud, V., and Nordheim, A. (1993). Activation of ternary complex factor Elk-1 by MAP kinases. EMBO J. *12*, 5097-5104.

Janknecht, R. and Hunter, T. (1997). Convergence of MAP kinase pathways on the ternary complex factor Sap-1a. EMBO Journal *16*, 1620-1627.

Jiang, Y., Chen, C., Li, Z., Guo, W., Gegner, J.A., Lin, S., and Han, J. (1996). Characterization of the structure and function of a new mitogen-activated protein kinase (p38beta). Journal of Biological Chemistry *271*, 17920-17926.

Johnston, M., Flick, J.S., and Pexton, T. (1994). Multiple mechanisms provide rapid and stringent glucose repression of GAL gene expression in Saccharomyces cerevisiae. Molecular & Cellular Biology *14*, 3834-3841.

Jones, E.Y., Stuart, D.I., and Walker, N.P. (1989). Structure of tumour necrosis factor. Nature *338*, 225-228.

Kaiser, P. and Auer, B. (1993). Rapid shuttle plasmid preparation from yeast cells by transfer to E. coli. Biotechniques *14*, 552

Karin, M. (1995). The regulation of AP-1 activity by mitogen-activated protein kinases. [Review] [54 refs]. Journal of Biological Chemistry *270*, 16483-16486.

Karin, M., Liu Zg, and Zandi, E. (1997). AP-1 function and regulation. [Review] [83 refs]. Current Opinion in Cell Biology *9*, 240-246.

Kato, K., Hasegawa, K., Goto, S., and Inaguma, Y. (1994). Dissociation as a result of phosphorylation of an aggregated form of the small stress protein, hsp27. Journal of Biological Chemistry *269*, 11274-11278.

Kaur, P., Welch, W.J., and Saklatvala, J. (1989). Interleukin 1 and tumour necrosis factor increase phosphorylation of the small heat shock protein. Effects in fibroblasts, Hep G2 and U937 cells. FEBS Letters *258*, 269-273.

Kawamori, T., Rao, C.V., Seibert, K., and Reddy, B.S. (1998). Chemopreventive activity of celecoxib, a specific cyclooxygenase-2 inhibitor, against colon carcinogenesis. Cancer Research *58*, 409-412.

Kobayashi, Y., Yamamoto, K., Saido, T., Kawasaki, H., Oppenheim, JJ, and Matsushima, K. (1990). Identification of calcium-activated neutral protease as a processing enzyme of human interleukin 1 alpha. Proceedings of the National Academy of Sciences of the United States of America *87*, 5548-5552.

Kotlyarov, A., Neininger, A., Schubert, C., Eckert, R., Birchmeier, C., Volk, H.D., and Gaestel, M. (1999). MAPKAP kinase 2 is essential for LPS-induced TNF-alpha biosynthesis [see comments]. Nat. Cell Biol. *1*, 94-97.

Kraemer, S.A., Meade, E.A., and DeWitt, D.L. (1992). Prostaglandin endoperoxide synthase gene structure: identification of the transcriptional start site and 5'-flanking regulatory sequences. Archives of Biochemistry & Biophysics *293*, 391-400.

Krause, A., Holtmann, H., Eickemeier, S., Winzen, R., Szamel, M., Resch K, Saklatvala, J., and Kracht, M. (1998). Stress-activated protein kinase/Jun N-terminal kinase is required for interleukin (IL)-1-induced IL-6 and IL-8 gene expression in the human epidermal carcinoma cell line KB. Journal of Biological Chemistry *273*, 23681-23689.

Krump, E., Sanghera, J.S., Pelech, S.L., Furuya, W., and Grinstein, S. (1997). Chemotactic peptide N-formyl-met-leu-phe activation of p38 mitogen-activated protein kinase (MAPK) and MAPK-activated protein kinase-2 in human neutrophils. Journal of Biological Chemistry *272*, 937-944.

Kujubu, D.A., Fletcher, B.S., Varnum, B.C., Lim, R.W., and Herschman, H.R. (1991). TIS10, a phorbol ester tumor promoter-inducible mRNA from Swiss 3T3 cells, encodes a novel prostaglandin synthase/cyclooxygenase homologue. Journal of Biological Chemistry *266*, 12866-12872.

Kumar, S., McLaughlin, M.M., McDonnell, P.C., Lee, J.C., Livi, G.P., and Young, P.R. (1995). Human mitogen-activated protein kinase CSBP1, but not CSBP2, complements a hog1 deletion in yeast. Journal of Biological Chemistry *270*, 29043-29046.

Kumar, S., McDonnell, P.C., Gum, R.J., Hand, A.T., Lee, J.C., and Young, P.R. (1997). Novel homologues of CSBP/p38 MAP kinase: activation, substrate specificity and sensitivity to inhibition by pyridinyl imidazoles. Biochemical & Biophysical Research Communications *235*, 533-538.

Kyriakis, J.M., Banerjee, P., Nikolakaki, E., Dai, T., Rubie, E.A., Ahmad, M.F., Avruch, J., and Woodgett, J.R. (1994). The stress-activated protein kinase subfamily of c-Jun kinases. Nature *369*, 156-160.

Kyriakis, J.M. and Avruch, J. (1990). pp54 microtubule-associated protein 2 kinase. A novel serine/threonine protein kinase regulated by phosphorylation and stimulated by poly-L-lysine. Journal of Biological Chemistry *265*, 17355-17363.

Landry, J., Lambert, H., Zhou, M., Lavoie, J.N., Hickey, E., Weber, L.A., and Anderson, C.W. (1992). Human HSP27 is phosphorylated at serines 78 and 82 by heat shock and mitogen-activated kinases that recognize the same amino acid motif as S6 kinase II. J. Biol. Chem. *267*, 794-803.

Laneuville, O., Breuer, D.K., DeWitt, D.L., Hla, T., and Funk, C.D., Smith WL. (1994). Differential inhibition of human prostaglandin endoperoxide H synthases-1 and -2 by nonsteroidal anti-inflammatory drugs. Journal of Pharmacology & Experimental Therapeutics *271*, 927-934.

Larochelle, S. and Suter, B. (1995). The Drosophila melanogaster homolog of the mammalian MAPK-activated protein kinase-2 (MAPKAPK-2) lacks a proline-rich N-terminus. Gene *163*, 209-214.

Lavoie, J., Chretien, P., and Landry, J. (1990). Sequence of the Chinese hamster small heat shock protein HSP27. Nucleic. Acids. Res. *18*, 1637

Lavoie, J.N., Hickey, E., Weber, L.A., and Landry, J. (1993). Modulation of actin microfilament dynamics and fluid phase pinocytosis by phosphorylation of heat shock protein 27. Journal of Biological Chemistry *268*, 24210-24214.

Lee, J.C., Badger, A.M., Griswold, D.E., Dunnington, D., Truneh, A., Votta B, White, J.R., Young, P.R., and Bender, P.E. (1993). Bicyclic imidazoles as a novel class of cytokine biosynthesis inhibitors. [Review] [79 refs]. Annals of the New York Academy of Sciences *696*, 149-170.

Lee, J.C., Laydon, J.T., McDonnell, P.C., Gallagher, T.F., Kumar, S., Green, D., McNulty, D., Blumenthal, M.J., Heys, J.R., Landvatter, S.W., and et al. (1994). A protein kinase involved in the regulation of inflammatory cytokine biosynthesis. Nature *372*, 739-746.

Lemaitre, B., Nicolas, E., Michaut, L., Reichhart, J.M., and Hoffmann, J.A. (1996). The dorsoventral regulatory gene cassette spatzle/Toll/cactus controls the potent antifungal response in Drosophila adults. Cell *86*, 973-983.

Li, B. and Fields, S. (1993). Identification of mutations in p53 that affect its binding to SV40 large T antigen by using the yeast two-hybrid system. FASEB Journal *7*, 957-963.

Li, Z., Jiang, Y., Ulevitch, R.J., and Han, J. (1996). The primary structure of p38 gamma: a new member of p38 group of MAP kinases. Biochemical & Biophysical Research Communications *228*, 334-340.

Lin, A., Minden, A., Martinetto, H., Claret, F.X., Lange-Carter, C., Mercurio, F., Johnson, G.L., and Karin, M. (1995). Identification of a dual specificity kinase that activates the Jun kinases and p38-Mpk2. Science *268*, 286-290.

Lin, L.L., Wartmann, M., Lin, A.Y., Knopf, J.L., Seth A, and Davis, R.J. (1993). cPLA2 is phosphorylated and activated by MAP kinase. Cell *72*, 269-278.

Lipsky, P.E. and Isakson, P.C. (1997). Outcome of specific COX-2 inhibition in rheumatoid arthritis. [Review] [21 refs]. Journal of Rheumatology *24 Suppl 49*, 9-14.

Lisnock, J., Tebben, A., Frantz, B., O'Neill, E.A., Croft, G., O'Keefe SJ, Li, B., Hacker, C., de Laszlo, S., Smith, A., Libby, B., Liverton, N., Hermes J, and LoGrasso, P. (1998). Molecular basis for p38 protein kinase inhibitor specificity [published erratum appears in Biochemistry 1999 Mar 16;38(11): 3456]. Biochemistry *37*, 16573-16581.

Liu, Y., Guyton, K.Z., Gorospe, M., Xu, Q., Kokkonen, G.C., Mock, YD, Roth, G.S., and Holbrook, N.J. (1996). Age-related decline in mitogen-activated protein kinase activity in epidermal growth factor-stimulated rat hepatocytes. Journal of Biological Chemistry *271*, 3604-3607.

Loetscher, H., Schlaeger, E.J., Lahm, H.W., Pan, Y.C., Lesslauer, W., and Brockhaus, M. (1990). Purification and partial amino acid sequence analysis of two distinct tumor necrosis factor receptors from HL60 cells. Journal of Biological Chemistry *265*, 20131-20138.

Loll, P.J., Picot, D., and Garavito, R.M. (1995). The structural basis of aspirin activity inferred from the crystal structure of inactivated prostaglandin H2 synthase [see comments]. Nature Structural Biology *2*, 637-643.

Lopata, M.A., Cleveland, D.W., and Sollner-Webb, B. (1984). High level transient expression of a chloramphenicol acetyl transferase gene by DEAE-dextran mediated DNA transfection coupled with a dimethyl sulfoxide or glycerol shock treatment. Nucleic Acids Research *12*, 5707-5717.

Ludwig, S., Engel, K., Hoffmeyer, A., Sithanandam, G., Neufeld, B., Palm, D., Gaestel, M., and Rapp, U.R. (1996). 3pK, a novel mitogen-activated protein (MAP) kinase-activated protein kinase, is targeted by three MAP kinase pathways. Molecular & Cellular Biology *16*, 6687-6697.

Maier, J.A., Hla, T., and Maciag, T. (1990). Cyclooxygenase is an immediate-early gene induced by interleukin-1 in human endothelial cells. Journal of Biological Chemistry *265*, 10805-10808.

Malinin, N.L., Boldin, M.P., Kovalenko, A.V., and Wallach, D. (1997). MAP3K-related kinase involved in NF-kappaB induction by TNF, CD95 and IL-1. Nature *385*, 540-544.

Mancilla, J., Ikejima, T., and Dinarello, C.A. (1992). Glycosylation of the interleukin-1 receptor type I is required for optimal binding of interleukin-1. Lymphokine & Cytokine Research *11*, 197-205.

Marais, R., Wynne, J., and Treisman, R. (1993). The SRF accessory protein Elk-1 contains a growth factor-regulated transcriptional activation domain. Cell *73*, 381-393.

March, C.J., Mosley, B., Larsen, A., Cerretti, D.P., Braedt, G., Price V, Gillis, S., Henney, C.S., Kronheim, S.R., Grabstein, K., and et al (1985). Cloning, sequence and expression of two distinct human interleukin-1 complementary DNAs. Nature *315*, 641-647.

Marnett, L.J. (1992). Aspirin and the potential role of prostaglandins in colon cancer. [Review] [311 refs]. Cancer Research *52*, 5575-5589.

Marsters, S.A., Frutkin, A.D., Simpson, N.J., and Fendly, B.M., Ashkenazi A. (1992). Identification of cysteine-rich domains of the type 1 tumor necrosis factor receptor involved in ligand binding. Journal of Biological Chemistry *267*, 5747-5750.

Matsushima, K. and Oppenheim, J.J. (1989). Interleukin 8 and MCAF: novel inflammatory cytokines inducible by IL 1 and TNF. [Review] [50 refs]. Cytokine *1*, 2-13.

McLaughlin, M.M., Kumar, S., McDonnell, P.C., Van Horn, S., Lee, J.C., Livi, G.P., and Young, P.R. (1996). Identification of mitogen-activated protein (MAP) kinase-activated protein kinase-3, a novel substrate of CSBP p38 MAP kinase. Journal of Biological Chemistry *271*, 8488-8492.

McMahan, C.J., Slack, J.L., Mosley, B., Cosman, D., Lupton, S.D., Brunton LL, Grubin, C.E., Wignall, J.M., Jenkins, N.A., Brannan, C.I., and et al. (1991). A novel IL-1 receptor, cloned from B cells by mammalian expression, is expressed in many cell types. EMBO Journal *10*, 2821-2832.

Medvedev, A.E., Sundan, A., and Espevik, T. (1994). Involvement of the tumor necrosis factor receptor p75 in mediating cytotoxicity and gene regulating activities. European Journal of Immunology *24*, 2842-2849.

Meier, R., Rouse, J., Cuenda, A., Nebreda, A.R., and Cohen, P. (1996). Cellular stresses and cytokines activate multiple mitogen-activated-protein kinase kinase homologues in PC12 and KB cells. European Journal of Biochemistry *236*, 796-805.

Miyasaka, N., Sato, K., Goto, M., Sasano, M., Natsuyama, M., Inoue K, and Nishioka, K. (1988). Augmented interleukin-1 production and HLA-DR expression in the synovium of rheumatoid arthritis patients. Possible involvement in joint destruction. Arthritis & Rheumatism *31*, 480-486.

Miyazawa, K., Mori, A., Miyata, H., Akahane, M., and Ajisawa, Y., Okudaira H. (1998). Regulation of interleukin-1beta-induced interleukin-6 gene expression in human fibroblast-like synoviocytes by p38 mitogen-activated protein kinase. Journal of Biological Chemistry *273*, 24832-24838.

Moriguchi, T., Kuroyanagi, N., Yamaguchi, K., Gotoh, Y., Irie, K., Kano, T., Shirakabe, K., Muro, Y., Shibuya, H., Matsumoto, K., Nishida, E., and Hagiwara, M. (1996). A

novel kinase cascade mediated by mitogen-activated protein kinase kinase 6 and MKK3. Journal of Biological Chemistry *271*, 13675-13679.

Moriguchi, T., Toyoshima, F., Masuyama, N., Hanafusa, H., Gotoh, Y, and Nishida, E. (1997). A novel SAPK/JNK kinase, MKK7, stimulated by TNFalpha and cellular stresses. EMBO Journal *16*, 7045-7053.

Moss, M.L., Jin, S.L., Milla, M.E., Bickett, D.M., Burkhart, W., Carter HL, Chen, W.J., Clay, W.C., Didsbury, J.R., Hassler, D., Hoffman, C.R., Kost, TA, Lambert, M.H., Leesnitzer, M.A., McCauley, P., McGeehan, G., Mitchell, J., Moyer M, Pahel, G., Rocque, W., Overton, L.K., Schoenen, F., Seaton, T., Su, J.L., Becherer JD, and et al (1997). Cloning of a disintegrin metalloproteinase that processes precursor tumour-necrosis factor-alpha [published erratum appears in Nature 1997 Apr 17;386(6626):738]. Nature *385*, 733-736.

Muzio, M., Polentarutti, N., Sironi, M., Poli, G., De Gioia, L., Introna, M., Mantovani, A., and Colotta, F. (1995). Cloning and characterization of a new isoform of the interleukin 1 receptor antagonist. Journal of Experimental Medicine *182*, 623-628.

Natoli, G., Costanzo, A., Ianni, A., Templeton, D.J., Woodgett, J.R., Balsano, C., and Levrero, M. (1997). Activation of SAPK/JNK by TNF receptor 1 through a noncytotoxic TRAF2-dependent pathway. Science *275*, 200-203.

New, L., Jiang, Y., Zhao, M., Liu, K., Zhu, W., Flood, L.J., Kato, Y, Parry, G.C., and Han, J. (1998). PRAK, a novel protein kinase regulated by the p38 MAP kinase. EMBO Journal *17*, 3372-3384.

Newton, R., Seybold, J., Liu, S.F., and Barnes, P.J. (1997). Alternate COX-2 transcripts are differentially regulated: implications for post-transcriptional control. Biochem. Biophys. Res. Commun. *234*, 85-89.

Ninomiya-Tsuji, J., Kishimoto, K., Hiyama, A., Inoue, J., and Cao, Z., Matsumoto K. (1999). The kinase TAK1 can activate the NIK-I kappaB as well as the MAP kinase cascade in the IL-1 signalling pathway. Nature *398*, 252-256.

O'Neill, L.A. and Greene, C. (1998). Signal transduction pathways activated by the IL-1 receptor family: ancient signaling machinery in mammals, insects, and plants. [Review] [53 refs]. Journal of Leukocyte Biology *63*, 650-657.

Okusawa, S., Gelfand, J.A., Ikejima, T., Connolly, R.J., Dinarello, and CA. (1988). Interleukin 1 induces a shock-like state in rabbits. Synergism with tumor necrosis factor and the effect of cyclooxygenase inhibition. Journal of Clinical Investigation *81*, 1162-1172.

Pages, G., Lenormand, P., L'Allemain, G., Chambard, J.C., Meloche, S, and Pouyssegur, J. (1993). Mitogen-activated protein kinases p42mapk and p44mapk are required for fibroblast proliferation. Proceedings of the National Academy of Sciences of the United States of America *90*, 8319-8323.

Peng, X., Angelastro, J.M., and Greene, L.A. (1996). Tyrosine phosphorylation of extracellular signal-regulated protein kinase 4 in response to growth factors. Journal of Neurochemistry *66*, 1191-1197.

Penning, T.D., Talley, J.J., Bertenshaw, S.R., Carter, J.S., Collins, P.W., Docter, S., Graneto, M.J., Lee, L.F., Malecha, J.W., Miyashiro, J.M., Rogers, R.S., Rogier, D.J., Yu, S.S., AndersonGD, Burton, E.G., Cogburn, J.N., Gregory, S.A., Koboldt, C.M., Perkins, W.E., Seibert, K., Veenhuizen, A.W., Zhang, Y.Y., and Isakson, P.C. (1997). Synthesis and biological evaluation of the 1,5-diarylpyrazole class of cyclooxygenase-2 inhibitors: identification of 4-[5-(4-methylphenyl)-3-(trifluoromethyl)-1H-pyrazol-1-yl]benze nesulfonamide (SC-58635, celecoxib). J. Med. Chem. *40*, 1347-1365.

Pietersma, A., Tilly, B.C., Gaestel, M., de Jong, N., Lee, J.C., Koster, J.F., and Sluiter, W. (1997). p38 mitogen activated protein kinase regulates endothelial VCAM-1 expression at the post-transcriptional level. Biochemical & Biophysical Research Communications *230*, 44-48.

Pouliot, M., Baillargeon, J., Lee, J.C., Cleland, L.G., and James, M.J. (1997). Inhibition of prostaglandin endoperoxide synthase-2 expression in stimulated human monocytes by inhibitors of p38 mitogen-activated protein kinase. Journal of Immunology *158*, 4930-4937.

Price, M.A., Cruzalegui, F.H., and Treisman, R. (1996). The p38 and ERK MAP kinase pathways cooperate to activate Ternary Complex Factors and c-fos transcription in response to UV light. EMBO Journal *15*, 6552-6563.

Proost, P., Wuyts, A., and van Damme, J. (1996). The role of chemokines in inflammation. [Review] [116 refs]. International Journal of Clinical & Laboratory Research *26*, 211-223.

Raingeaud, J., Gupta, S., Rogers, J.S., Dickens, M., Han, J., Ulevitch, R.J., and Davis, R.J. (1995). Pro-inflammatory cytokines and environmental stress cause p38 mitogen-activated protein kinase activation by dual phosphorylation on tyrosine and threonine. Journal of Biological Chemistry *270*, 7420-7426.

Raingeaud, J., Whitmarsh, A.J., Barrett, T., Derijard, B., and Davis, R.J. (1996). MKK3- and MKK6-regulated gene expression is mediated by the p38 mitogen-activated protein kinase signal transduction pathway. Molecular & Cellular Biology *16*, 1247-1255.

Rajagopalan, L.E. and Malter, J.S. (1994). Modulation of granulocyte-macrophage colony-stimulating factor mRNA stability in vitro by the adenosine-uridine binding factor. J. Biol. Chem. *269*, 23882-23888.

Rao, C.V., Rivenson, A., Simi, B., Zang, E., Kelloff, G., Steele, V, and Reddy, B.S. (1995). Chemoprevention of colon carcinogenesis by sulindac, a nonsteroidal anti-inflammatory agent. Cancer Research *55*, 1464-1472.

Regnier, C.H., Song, H.Y., Gao, X., Goeddel, D.V., Cao, Z., and Rothe, M. (1997). Identification and characterization of an IkappaB kinase. Cell *90*, 373-383.

Reitz, D.B., Li, J.J., Norton, M.B., Reinhard, E.J., Collins, J.T., Anderson, G.D., Gregory, S.A., Koboldt, C.M., Perkins, W.E., and Seibert, K. (1994). Selective cyclooxygenase inhibitors: novel 1,2-diarylcyclopentenes are potent and orally active COX-2 inhibitors. J. Med. Chem. *37*, 3878-3881.

Ridley, S.H., Sarsfield, S.J., Lee, J.C., Bigg, H.F., Cawston, T.E., Taylor, D.J., DeWitt, D.L., and Saklatvala, J. (1997). Actions of IL-1 are selectively controlled by p38 mitogen-activated protein kinase: regulation of prostaglandin H synthase-2, metalloproteinases, and IL-6 at different levels. Journal of Immunology *158*, 3165-3173.

Ridley, S.H., Dean, J.L., Sarsfield, S.J., Brook, M., Clark, A.R., and Saklatvala, J. (1998). A p38 MAP kinase inhibitor regulates stability of interleukin-1-induced cyclooxygenase-2 mRNA. FEBS Letters *439*, 75-80.

Rincon, M., Enslen, H., Raingeaud, J., Recht, M., Zapton, T., Su, M.S., Penix, L.A., Davis, R.J., and Flavell, R.A. (1998). Interferon-gamma expression by Th1 effector T cells mediated by the p38 MAP kinase signaling pathway. EMBO Journal *17*, 2817-2829.

Ristimaki, A., Narko, K., and Hla, T. (1996). Down-regulation of cytokine-induced cyclo-oxygenase-2 transcript isoforms by dexamethasone: evidence for post-transcriptional regulation. Biochem. J. *318*, 325-331.

Rogalla, T., Ehrnsperger, M., Preville, X., Kotlyarov, A., Lutsch G, Ducasse, C., Paul, C., Wieske, M., Arrigo, A.P., Buchner, J., and Gaestel, M. (1999). Regulation of Hsp27 oligomerization, chaperone function, and protective activity against oxidative stress/tumor necrosis factor alpha by phosphorylation. Journal of Biological Chemistry *274*, 18947-18956.

Rothe, M., Wong, S.C., Henzel, W.J., and Goeddel, D.V. (1994). A novel family of putative signal transducers associated with the cytoplasmic domain of the 75 kDa tumor necrosis factor receptor. Cell *78*, 681-692.

Rouse, J., Cohen, P., Trigon, S., Morange, M., Alonso-Llamazares, A., Zamanillo, D, Hunt, T., and Nebreda, A.R. (1994). A novel kinase cascade triggered by stress and heat shock that stimulates MAPKAP kinase-2 and phosphorylation of the small heat shock proteins. Cell *78*, 1027-1037.

Saklatvala, J., Rawlinson, L.M., Marshall, C.J., and Kracht, M. (1993). Interleukin 1 and tumour necrosis factor activate the mitogen-activated protein (MAP) kinase kinase in cultured cells. FEBS Letters *334*, 189-192.

Saklatvala, J., Rawlinson, L., Waller, R.J., Sarsfield, S., Lee, J.C., Morton, L.F., Barnes, M.J., and Farndale, R.W. (1996). Role for p38 mitogen-activated protein kinase in platelet aggregation caused by collagen or a thromboxane analogue. Journal of Biological Chemistry *271*, 6586-6589.

Sanchez, I., Hughes, R.T., Mayer, B.J., Yee, K., Woodgett, J.R., Avruch, J., Kyriakis, J.M., and Zon, L.I. (1994). Role of SAPK/ERK kinase-1 in the stress-activated pathway regulating transcription factor c-Jun. Nature *372*, 794-798.

Scapigliati, G., Ghiara, P., Bartalini, M., and Tagliabue, A., Boraschi D. (1989). Differential binding of IL-1 alpha and IL-1 beta to receptors on B and T cells. FEBS Letters *243*, 394-398.

Seibert, K., Zhang, Y., Leahy, K., Hauser, S., Masferrer, J., Perkins W, Lee, L., and Isakson, P. (1994). Pharmacological and biochemical demonstration of the role of cyclooxygenase 2 in inflammation and pain. Proceedings of the National Academy of Sciences of the United States of America *91*, 12013-12017.

Shapiro, L. and Dinarello, C.A. (1995). Osmotic regulation of cytokine synthesis in vitro. Proceedings of the National Academy of Sciences of the United States of America *92*, 12230-12234.

Shibuya, H., Yamaguchi, K., Shirakabe, K., Tonegawa, A., Gotoh, Y., Ueno, N., Irie, K., Nishida, E., and Matsumoto, K. (1996). TAB1: an activator of the TAK1 MAPKKK in TGF-beta signal transduction. Science *272*, 1179-1182.

Sims, J.E., Acres, R.B., Grubin, C.E., McMahan, C.J., Wignall, J.M., March CJ, and Dower, S.K. (1989). Cloning the interleukin 1 receptor from human T cells. Proceedings of the National Academy of Sciences of the United States of America *86*, 8946-8950.

Sirois, J. and Richards, J.S. (1992). Purification and characterization of a novel, distinct isoform of prostaglandin endoperoxide synthase induced by human chorionic gonadotropin in granulosa cells of rat preovulatory follicles. Journal of Biological Chemistry *267*, 6382-6388.

Sithanandam, G., Latif, F., Duh, F.M., Bernal, R., Smola, U., Li, H., Kuzmin, I., Wixler, V., Geil, L., and Shrestha, S. (1996). 3pK, a new mitogen-activated protein kinase-activated protein kinase located in the small cell lung cancer tumor suppressor gene region [published erratum appears in Mol Cell Biol 1996 Apr; 16(4):1880]. Molecular & Cellular Biology *16*, 868-876.

Smith, C.A., Davis, T., Anderson, D., Solam, L., Beckmann, M.P., Jerzy R, Dower, S.K., Cosman, D., and Goodwin, R.G. (1990). A receptor for tumor necrosis factor defines an unusual family of cellular and viral proteins. Science *248*, 1019-1023.

Smith, J.W., 2d, Urba, W.J., Curti, B.D., Elwood, L.J., Steis, R.G., Janik JE, Sharfman, W.H., Miller, L.L., Fenton, R.G., Conlon, K.C., and et al. (1992). The toxic and hematologic effects of interleukin-1 alpha administered in a phase I trial to patients with advanced malignancies. Journal of Clinical Oncology *10*, 1141-1152.

Smith, W.L., Meade, E.A., and DeWitt, D.L. (1994). Interactions of PGH synthase isozymes-1 and -2 with NSAIDs. [Review] [39 refs]. Annals of the New York Academy of Sciences *744*, 50-57.

Smith, W.L., Garavito, R.M., and DeWitt, D.L. (1996). Prostaglandin endoperoxide H synthases (cyclooxygenases)-1 and -2. [Review] [75 refs]. Journal of Biological Chemistry *271*, 33157-33160.

Smith, W.L. and DeWitt, D.L. (1995). Biochemistry of prostaglandin endoperoxide H synthase-1 and synthase-2 and their differential susceptibility to nonsteroidal anti-inflammatory drugs. [Review] [126 refs]. Seminars in Nephrology *15*, 179-194.

Smith, W.L. and DeWitt, D.L. (1996). Prostaglandin endoperoxide H synthases-1 and -2. [Review] [221 refs]. Advances in Immunology *62*, 167-215.

Stevenson, F.T., Bursten, S.L., Fanton, C., Locksley, R.M., and Lovett, D.H. (1993). The 31-kDa precursor of interleukin 1 alpha is myristoylated on specific lysines within the 16-kDa N-terminal propiece. Proceedings of the National Academy of Sciences of the United States of America *90*, 7245-7249.

Stokoe, D., Campbell, D.G., Nakielny, S., Hidaka, H., Leevers, S.J., Marshall, C., and Cohen, P. (1992). MAPKAP kinase-2; a novel protein kinase activated by mitogen-activated protein kinase. EMBO Journal *11*, 3985-3994.

Stokoe, D., Caudwell, B., Cohen, P.T., and Cohen, P. (1993). The substrate specificity and structure of mitogen-activated protein (MAP) kinase-activated protein kinase-2. Biochemical Journal *296*, 843-849.

Sturgill, T.W. and Wu, J. (1991). Recent progress in characterization of protein kinase cascades for phosphorylation of ribosomal protein S6. [Review] [68 refs]. Biochimica et Biophysica Acta *1092*, 350-357.

Suzuki, M., Tetsuka, T., Yoshida, S., Watanabe, N., Kobayashi, M., Matsui, N., and Okamoto, T. (2000). The role of p38 mitogen-activated protein kinase in IL-6 and IL-8 production from the TNF-α- or IL-1β-stimulated rheumatoid synovial fibroblasts. FEBS Letters *465*, 23-27.

Tan, Y., Rouse, J., Zhang, A., Cariati, S., Cohen, P., and Comb, M.J. (1996). FGF and stress regulate CREB and ATF-1 via a pathway involving p38 MAP kinase and MAPKAP kinase-2. EMBO Journal *15*, 4629-4642.

Tartaglia, L.A., Ayres, T.M., Wong, G.H., and Goeddel, D.V. (1993a). A novel domain within the 55 kd TNF receptor signals cell death. Cell *74*, 845-853.

Tartaglia, L.A., Goeddel, D.V., Reynolds, C., Figari, I.S., Weber, RF, Fendly, B.M., and Palladino, M.A., Jr. (1993b). Stimulation of human T-cell proliferation by specific activation of the 75-kDa tumor necrosis factor receptor. Journal of Immunology *151*, 4637-4641.

Thornberry, N.A., Bull, H.G., Calaycay, J.R., Chapman, K.T., Howard, A.D., Kostura, MJ, Miller, D.K., Molineaux, S.M., Weidner, J.R., Aunins, J., and et al. (1992). A novel heterodimeric cysteine protease is required for interleukin-1 beta processing in monocytes. Nature *356*, 768-774.

Tibbles, L.A., Ing, Y.L., Kiefer, F., Chan, J., Iscove, N., Woodgett JR, and Lassam, N.J. (1996). MLK-3 activates the SAPK/JNK and p38/RK pathways via SEK1 and MKK3/6. EMBO Journal *15*, 7026-7035.

Tong, L., Pav, S., White, D.M., Rogers, S., Crane, K.M., Cywin, C.L., Brown, M.L., and Pargellis, C.A. (1997). A highly specific inhibitor of human p38 MAP kinase binds in the ATP pocket. Nature Structural Biology *4*, 311-316.

Tournier, C., Whitmarsh, A.J., Cavanagh, J., Barrett, T., Davis, and RJ. (1997). Mitogen-activated protein kinase kinase 7 is an activator of the c-Jun NH2-terminal kinase. Proceedings of the National Academy of Sciences of the United States of America *94*, 7337-7342.

Tredget, E.E., Yu, Y.M., Zhong, S., Burini, R., Okusawa, S., Gelfand JA, Dinarello, C.A., Young, V.R., and Burke, J.F. (1988). Role of interleukin 1 and tumor necrosis factor on energy metabolism in rabbits. American Journal of Physiology *255*, E760-8.

Van Aelst, L., Barr, M., Marcus, S., Polverino, A, and Wigler, M. (1993). Complex formation between RAS and RAF and other protein kinases. Proceedings of the National Academy of Sciences of the United States of America *90*, 6213-6217.

van den Berg, W.B., Joosten, L.A., Helsen, M., and van de Loo, F.A. (1994). Amelioration of established murine collagen-induced arthritis with anti-IL-1 treatment. Clin. Exp. Immunol. *95*, 237-243.

van der Lugt, N.M., Alkema, M, Berns, A., and Deschamps, J. (1996). The Polycomb-group homolog Bmi-1 is a regulator of murine Hox gene expression. Mechanisms of Development *58*, 153-164.

van Dullemen, H.M., van, Deventer, S.J., Hommes, D.W., Bijl, H.A., Jansen, J., Tytgat, G.N., and Woody, J. (1995). Treatment of Crohn's disease with anti-tumor necrosis factor chimeric monoclonal antibody (cA2). Gastroenterology *109*, 129-135.

Vannier, E. and Dinarello, C.A. (1993). Histamine enhances interleukin (IL)-1-induced IL-1 gene expression and protein synthesis via H2 receptors in peripheral blood mononuclear cells. Comparison with IL-1 receptor antagonist. Journal of Clinical Investigation *92*, 281-287.

Vannier, E. and Dinarello, C.A. (1994). Histamine enhances interleukin (IL)-1-induced IL-6 gene expression and protein synthesis via H2 receptors in peripheral blood mononuclear cells. Journal of Biological Chemistry *269*, 9952-9956.

Vilcek, J. and Lee, T.H. (1991). Tumor necrosis factor. New insights into the molecular mechanisms of its multiple actions. [Review] [99 refs]. Journal of Biological Chemistry *266*, 7313-7316.

Volpe, F., Clatworthy, J., Kaptein, A., Maschera, B., Griffin, AM, and Ray, K. (1997). The IL1 receptor accessory protein is responsible for the recruitment of the interleukin-1 receptor associated kinase to the IL1/IL1 receptor I complex. FEBS Letters *419*, 41-44.

Wang, B., Kondo, S., Shivji, G.M., Fujisawa, H., Mak, T.W., Sauder, and DN. (1996). Tumour necrosis factor receptor II (p75) signalling is required for the migration of Langerhans' cells. Immunology *88*, 284-288.

Wang, X.Z. and Ron, D. (1996). Stress-induced phosphorylation and activation of the transcription factor CHOP (GADD153) by p38 MAP Kinase. Science *272*, 1347-1349.

Wang, Z., Harkins, P.C., Ulevitch, R.J., Han, J., and Cobb, M.H., Goldsmith EJ. (1997). The structure of mitogen-activated protein kinase p38 at 2.1-A resolution. Proceedings of the National Academy of Sciences of the United States of America *94*, 2327-2332.

Wang, Z., Canagarajah, B.J., Boehm, J.C., Kassisa, S., Cobb, M.H., Young PR, Abdel-Meguid, S., Adams, J.L., and Goldsmith, E.J. (1998). Structural basis of inhibitor selectivity in MAP kinases. Structure *6*, 1117-1128.

Waskiewicz, A.J., Flynn, A., Proud, C.G., and Cooper, J.A. (1997). Mitogen-activated protein kinases activate the serine/threonine kinases Mnk1 and Mnk2. EMBO Journal *16*, 1909-1920.

Waskiewicz, A.J. and Cooper, J.A. (1995). Mitogen and stress response pathways: MAP kinase cascades and phosphatase regulation in mammals and yeast. [Review] [79 refs]. Current Opinion in Cell Biology *7*, 798-805.

Watanabe, N. and Kobayashi, Y. (1994). Selective release of a processed form of interleukin 1 alpha. Cytokine *6*, 597-601.

Wesche, H., Henzel, W.J., Shillinglaw, W., Li, S., and Cao, Z. (1997a). MyD88: an adapter that recruits IRAK to the IL-1 receptor complex. Immunity *7*, 837-847.

Wesche, H., Korherr, C., Kracht, M., Falk, W., Resch, K., Martin, and MU. (1997b). The interleukin-1 receptor accessory protein (IL-1RAcP) is essential for IL-1-induced activation of interleukin-1 receptor-associated kinase (IRAK) and stress-activated protein kinases (SAP kinases). Journal of Biological Chemistry *272*, 7727-7731.

Whittle, N., Adair, J., Lloyd, C., Jenkins, L., Devine, J., Schlom J, Raubitschek, A., Colcher, D., and Bodmer, M. (1987). Expression in COS cells of a mouse-human chimaeric B72.3 antibody. Protein Engineering *1*, 499-505.

Williams, R.O., Feldmann, M., and Maini, R.N. (1992). Anti-tumor necrosis factor ameliorates joint disease in murine collagen-induced arthritis. Proc. Natl. Acad. Sci. U. S. A. *89*, 9784-9788.

Wilson, K.P., Fitzgibbon, M.J., Caron, P.R., Griffith, J.P., Chen, W., McCaffrey, P.G., Chambers, S.P., and Su, M.S. (1996). Crystal structure of p38 mitogen-activated protein kinase. Journal of Biological Chemistry *271*, 27696-27700.

Wilson, K.P., McCaffrey, P.G., Hsiao, K., Pazhanisamy, S., Galullo, V, Bemis, G.W., Fitzgibbon, M.J., Caron, P.R., Murcko, M.A., and Su, M.S. (1997). The structural basis for the specificity of pyridinylimidazole inhibitors of p38 MAP kinase. Chemistry & Biology *4*, 423-431.

Winzen, R., Kracht, M., Ritter, B., Wilhelm, A., Chen, C.Y., Shyu, A.B., Muller, M., Gaestel, M., Resch, K., and Holtmann, H. (1999). The p38 MAP kinase pathway signals for cytokine-induced mRNA stabilization via MAP kinase-activated protein kinase 2 and an AU-rich region-targeted mechanism. EMBO J. *18*, 4969-4980.

Xie, W.L., Chipman, J.G., Robertson, D.L., Erikson, R.L., Simmons, and DL. (1991). Expression of a mitogen-responsive gene encoding prostaglandin synthase is regulated by

mRNA splicing. Proceedings of the National Academy of Sciences of the United States of America *88*, 2692-2696.

Yang, S.H., Whitmarsh, A.J., Davis, R.J., and Sharrocks, A.D. (1998). Differential targeting of MAP kinases to the ETS-domain transcription factor Elk-1. EMBO Journal *17*, 1740-1749.

Yao, Z., Diener, K., Wang, X.S., Zukowski, M., Matsumoto, G., Zhou, G, Mo, R., Sasaki, T., Nishina, H., Hui, C.C., Tan, T.H., Woodgett, J.P., Penninger, and JM. (1997). Activation of stress-activated protein kinases/c-Jun N-terminal protein kinases (SAPKs/JNKs) by a novel mitogen-activated protein kinase kinase. Journal of Biological Chemistry *272*, 32378-32383.

Yoccum, R.R. (1987). The GAL1, 7 and 10 upstream activator sequences are not enhancers. Biological Research on Industrial Yeasts.Vol.3, Stewart, G., Klein, R. & Hiebsch, R., Ed., CRC Press, Boca Raton, Fl; page 61.

Zanke, B.W., Rubie, E.A., Winnett, E., Chan, J., Randall, S., Parsons, M., Boudreau, K., McInnis, M., Yan, M., Templeton, D.J., and Woodgett, J.R. (1996). Mammalian mitogen-activated protein kinase pathways are regulated through formation of specific kinase-activator complexes. Journal of Biological Chemistry *271*, 29876-29881.

Zhang, F., Strand, A., Robbins, D., Cobb, M.H., and Goldsmith, E.J. (1994). Atomic structure of the MAP kinase ERK2 at 2.3 A resolution [see comments]. Nature *367*, 704-711.

Zu, Y.L., Wu, F., Gilchrist, A., Ai, Y., Labadia, M.E., and Huang, C.K. (1994). The primary structure of a human MAP kinase activated protein kinase 2. Biochemical & Biophysical Research Communications *200*, 1118-1124.

Zu, Y.L., Ai, Y., Gilchrist, A., Maulik, N., Watras, J., Sha'afi, R.I., Das, D.K., and Huang, C.K. (1997). High expression and activation of MAP kinase-activated protein kinase 2 in cardiac muscle cells. Journal of Molecular & Cellular Cardiology *29*, 2159-2168.